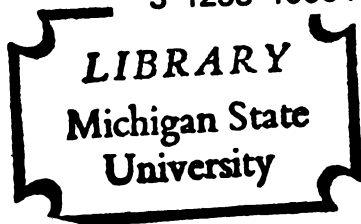




THESI



3 1293 10064 2770



This is to certify that the

thesis entitled

AMONIA SORPTION AND DRYING MODEL
IN A FIXED-BED GRAIN DRYING SYSTEM

presented by

RONG-CHING HSIEH

has been accepted towards fulfillment
of the requirements for

Ph. D. degree in Agricultural
Engineering

Major professor

Date November 8, 1979



OVERDUE FINES ARE 25¢ PER DAY
PER ITEM

Return to book drop to remove
this checkout from your record.

AMMONIA SORPTION AND DRYING MODEL
IN A FIXED-BED GRAIN DRYING SYSTEM

By

Rong-Ching Hsieh

A DISSERTATION

Submitted to
Michigan State University
in partial fulfillment of the requirements
for the degree of

DOCTOR OF PHILOSOPHY

Department of Agricultural Engineering

1979

ABSTRACT

AMMONIA SORPTION AND DRYING MODEL IN A FIXED-BED GRAIN DRYING SYSTEM

By

Rong-Ching Hsieh

One of the alternative energy-saving methods in drying grain is to apply a chemical as a grain preservative when the grain is drying slowly. Recent studies have shown that various chemicals such as ammonia, propionic acid, acetic acid, methylene bis-propionate, formalin and sulfur dioxide can serve as fungicidal agents.

A computer simulation model has been developed for the ammonia drying system of a fixed bed of grain. The model is based on the theoretical analysis of heat and mass transfer. Mass balances are made on the air and on the corn resulting in four independent differential equations. The fifth equation for the temperature was derived by combining the two independent heat balance equations in the air and in the grain by assuming that the grain and the air temperatures are equal.

Several crucial parameters in the ammonia drying simulation are unknown. The following estimated values were obtained by analyzing closely related systems: (1) the heat of ammonia adsorption in corn: 35.4 KJ/mole-NH₃, (2) the convective heat transfer coefficient (h,w/mk) in a fixed-bed system: $2.3278 G_a^{0.49}$, when $G_a < 2400 \text{ kg/hr/m}^2$, (3) the mass transfer coefficient between the grain and the ammonia: $1.156 \times 10^{-6} \text{ h}$,

and (4) the amount of fixed ammonia (residual) in the corn: 30 percent of the free ammonia content.

The equilibrium ammonia content in corn is a function of the grain moisture content and temperature. The ammonia sorption isotherms were established by assuming the water portion in corn to be the active component in adsorbing ammonia. A semi-empirical equation has been developed for the ammonia sorption isotherms at low ammonia concentrations (less than 20 percent, d.b.).

The five-equation model was solved numerically by finite differences. The simulation model was tested for its numerical accuracy by comparing it with the predicted results at extremely small computing time increment and depth interval. An acceptable combination of the computing time increment of 1 hour and the computing depth interval of 15.24 cm (0.5 ft) was established. The selection of appropriate grid sizes was based on the analysis of the computational error compared to the true numerical solution and the central processor time required by the computer.

An experimental bin test of ammonia grain drying was performed to verify the simulation model. The corn was dried with ambient air from 25.6 to 15.6 percent (w.b.) moisture in 72 days and 16 hours of fan operation at $1.43 \text{ cm}^2/\text{m}^2$ (1 cfm/bu) at a grain depth of 1.83 m (6 ft). The final corn sample showed no unacceptable grain spoilage. The total amount of anhydrous ammonia applied was 18.3 kg (0.8 percent d.b.). Satisfactory agreement between the experimental and the predicted results was found. The energy requirement in this ammonia grain drying experiment was 3696 kJ/kg-water removed which is an energy saving of over 50 percent comparing with the high-temperature drying (7500

kJ/kg-water).

A series of sensitivity tests on several important parameters was performed to determine their significance on the ammonia sorption rates. A significant increase in the ammonia adsorption rate was predicted when the grain moisture content is higher and the grain is treated at a lower temperature. A higher airflow rate and, consequently, a larger mass transfer coefficient also resulted in a higher adsorption rate.

This investigation has established the general grain drying simulation model using fungicidal chemicals. The general model can easily be made specific to simulate the treatment of a certain type of grain with a specific fungicidal chemical by specifying the relevant property parameters.

Approved

F. W. Becker - Dickson

Major Professor

11/9/79

Approved

Fubach H. Juter

Department Chairman

To :

My Parents : Pin-Ho and Tsai-Lian Hsieh

My family : Suewei and Chanlee

and

The People of TAIWAN

ACKNOWLEDGMENTS

The author would like to express sincere gratitude to Dr. Fredrick W. Bakker-Arkema, the best advisor I have ever known, for his inspiring guidance during the course of this study and for serving as the major professor.

Appreciation is extended to Dr. J. V. Beck (Mechanical Engineering), Dr. A. M. Pearson (Food Science and Human Nutrition), Dr. D. R. Heldman (Agricultural Engineering) and Dr. E. B. Bagley (North Regional Research Laboratory of USDA) for serving as guidance committee members. Sincere thanks to all the friendly and helpful researchers of the NRRL, USDA at Peoria, Illinois for their generous cooperation.

Special thanks is expressed to Ms. S. L. Cuppett, an experienced technician at the Department of Food Science and Human Nutrition, for her excellent performance in the chemical analyses.

The financial support by the Michigan Energy Administration and the Michigan State University is very much appreciated.

Deep gratitude is expressed to his wife, Suewei, for her encouragement and support during the course of the study, and to the newborn, Chanlee, for her unbelievable cooperation.

Finally, thanks to Mrs. Susan Vincent for her extraordinary diligence in typing this manuscript.

TABLE OF CONTENTS

	Page
List of Tables	vi
List of Figures	vii
List of Symbols	xiii
 Chapters	
1. Introduction	1
1. Corn Production in Michigan.	1
2. Corn Drying Practices.	2
3. Natural Air Drying	5
4. Molding and Aflatoxin Production	6
5. Application of Ammonia in Grain Preservation and Detoxification	8
6. Objectives	11
2. Literature Review.	13
1. Fixed-Bed Grain Drying Systems	13
1-A. Natural Air and Low-Temperature Drying Systems	14
1-B. Energy Source of Low-Temperature Drying.	15
1-C. Fixed-Bed Computer Models.	16
2. Ammonia Preservation and Detoxification.	17
2-A. Chemical Preservation.	17
2-B. Ammonia Preservation and Detoxification.	18
3. Mold Growth and Aflatoxin.	20
3-A. Mold Growth in Corn.	21
3-B. Aflatoxin Contamination in Grain	22
3-B.1. Aflatoxin in Corn Before Harvest	22
3-B.2. Aflatoxin in Corn during Storage	24
3-B.3. Bright Greenish-Yellow Fluorescence and Aflatoxins	26
3-C. Detection and Determination of Aflatoxin in Corn	27
3-D. Detoxification of Aflatoxin.	31
4. Experimental Results from North Regional Research Laboratory (NRRL) of USDA.	32
4-A. The Diffusion of Ammonia in Corn	33
4-B. The Fungicidal Effects of Ammonia.	34
4-C. The Closed-System Ammoniation.	36

Chapters	Page	
2.	4-D. Influence of Ammonia and Moisture Levels on the Detoxification of Aflatoxin B ₁	36
	4-E. Long-Term Preservation of High-Moisture Grain	38
	4-F. The Composition Changes of Ammonia-Treated Corn	44
3.	Ammonia Sorption Isotherms.	49
1.	Introduction.	49
2.	Adsorption and Diffusion Models	49
	2-A. The External Diffusion Models-Diffusion in Fluid.	50
	2-B. The Surface Adsorption Models	51
	2-C. The Internal Diffusion Models-Diffusion in Solid.	55
3.	Production and the Properties of Ammonia.	56
	3-A. Energy Required in Ammonia Production	56
	3-B. Physical Properties of Ammonia.	57
	3-C. Vapor Pressure of Ammonia	59
	3-C.1. Vapor Pressure of Liquid Ammonia.	59
	3-C.2. Partial Pressure of Ammonia in Aqueous Solution.	59
4.	Adsorption and Desorption of Ammonia in Corn.	62
	4-A. Classification of Sorption Isotherms.	62
	4-B. Equilibrium Ammonia Content in Aqueous Solution	64
	4-C. Equilibrium Ammonia Content in Corn	68
	4-D. Hysteresis and Residuals.	69
	4-D.1. Hysteresis.	71
	4-D.2. Residuals	72
	4-D.3. The Combined Effects of Hysteresis and Residuals on the Desorption Process	74
	4-E. Proposed Sorption Isotherms in the Ammonia-Corn System at Low Ammonia Pressures	78
4.	General Sorption and Drying Models in a Fixed-Bed System.	80
1.	Introduction.	80
2.	General Fixed-Bed Sorption Models	83
	2-A. The Transport Mechanism	83
	2-B. The Equations of Transport.	84
	2-C. The External Transport Equation	85
	2-D. The Pore Diffusion Equations.	86
	2-E. The Internal Diffusion Equations.	87
3.	The Local-Equilibrium Theory.	89
	3-A. Local-Equilibrium Transport Equations	89
	3-B. The Break-Through Curve	91
4.	The Thomas Solution of Break-Through Curves	95
5.	Design of an Ammonia Adsorption and Drying Experiment	101
1.	The Grain -- Yellow Corn.	101
2.	Experimental System	102
	2-A. The Bin Structure	102

Chapters	Page
5.	2-B. The Fan 102
	2-C. The Ammonia Application System. 104
	2-C.1. Ammonia Tank. 104
	2-C.2. Ammonia Flow Controlling System 104
	2-C.3. Temperature Recording System. 105
3.	Sampling Systems. 106
	3-A. Grain Sampling. 106
	3-B. Air Sampling. 106
4.	Weather Conditions During the Experiment. 109
5.	Timetable of Fan Operation and Ammonia Application. . . . 111
	5-A. Part I. Trial Period (11/13/78-1/10/79) 111
	5-B. Part II. Constant Rate Periods (4/4/79-4/24/79) . . 115
6.	Procedures of Sample Analyses 118
	6-A. Determination of Free Ammonia (Black, 1978) 118
	6-B. Determination of Total Ammonia (Black, 1978). . . . 118
	6-C. Determination of Mold Count (Speck, 1976) 119
6.	Development of a Simulation Model for Ammonia Adsorption in Fixed-Bed Drying Systems 121
	1. Introduction. 121
	2. Assumptions 123
	3. Derivation of Model Equations 126
	3-A. Mass Balance of Ammonia in Bulk Stream. 128
	3-B. Mass Balance of Water Vapor in Bulk Stream. . . . 131
	3-C. Ammonia Sorption Rate in Corn 132
	3-D. Changes of Moisture Content in Corn Kernel -- Thin-layer Drying Equations 134
	3-E. Enthalpy Balance of the Bulk Air Stream 135
	3-F. Enthalpy Balance in Corn. 137
	3-G. The Model Equations 140
	4. The Combined Temperature Equation 141
	5. Heat and Mass Transfer Coefficient for Forced Convection through Packed Beds. 142
	5-A. Forced Convection for a Single Sphere 142
	5-B. Evaluation of Heat Transfer Coefficients in Packed Beds. 144
	5-C. Estimation of Mass-Transfer Coefficients at Low Mass-Transfer Rates. 146
	5-C.1. Ratio of Mass and Heat Transfer Coefficients. 146
	5-C.2. Estimation of the Mass Diffusivity. 147
	6. Dry Matter Decomposition. 149
	7. Equilibrium Moisture Content. 153
	8. The Finite Difference Method. 155
	8-A. Finite Difference Formulation 155
	8-B. Solution of Finite Difference Equations 156
	8-C. Temperature Condensation Simulator. 159
	9. The Flowcharts. 161

Chapters	Page
7. Results and Discussion.	170
1. Introduction.	170
2. Definition of the Standard Conditions	171
3. The Accuracy Tests of the Ammonia Sorption and Drying Model.	172
3-A. The Accuracy of the Average Ammonia Concentrations.	172
3-B. The Ammonia Concentration Profiles in the Air as Influenced by the Computing Scheme	181
3-C. The Selection of a Proper Combination of the Operating Time and Depth Increments	181
4. The Ammonia Breakthrough Characteristics.	186
4-A. The Adsorption Concentration Profiles	186
4-B. The Desorption Concentration Profiles	190
4-C. The Ammonia Adsorption and Desorption Rates	193
4-D. The Breakthrough Curves	196
5. The Sensitivity Tests of the Important Parameters	196
5-A. The Initial Grain Moisture Content.	199
5-B. The Initial Grain Temperature	203
5-C. The Airflow Rate.	206
5-D. The Ratio of the Mass-Heat Transfer Coefficients.	207
5-E. The Inlet Ammonia Concentrations.	213
5-F. The Division Factor	219
6. Experimental Verification of the Ammonia Sorption and Drying Model.	222
6-A. The Ammonia Concentration in the Air during Adsorption	222
6-B. The Ammonia Concentration in the Air during Desorption	225
6-C. Comparison of the Experimental and Predicted Ammonia Concentration Profiles.	228
6-D. Comparison of the Experimental and Predicted Grain Moisture Contents and Temperatures.	239
6-E. The Experimental Results of Mold Contamination.	246
6-F. Energy Consumption in Ammonia Grain Drying.	248
8. Conclusions	251
9. Suggestions for Future Research	253
Appendices	255
A. Unit Conversions.	255
B. Fortran Listing of the Ammonia Sorption and Drying Model.	257
Bibliography	266

LIST OF TABLES

Table	Page
1.1. Acreage, production, and value of corn for grain in Michigan, 1975-1978	2
1.2. The percentages of various drying techniques in some Midwestern states in recent years.	4
1.3. The percentages of shelled corn dried artificially by various dryer types in Michigan	4
2.1. Aflatoxin incidence in corn (Shotwell, 1977)	25
2.2. Screening methods using minicolumns.	29
2.3. Effects of ammonia on inhibiting bacteria and mold growth and the relationship between free ammonia and the amount of ammonia added (data taken from Peplinski et al., 1975).	41
2.4. Chemical analysis of the stored corn (Peplinski et al., 1975).	45
2.5. Chemical analysis of corn removed from storage by layers (Peplinski et al., 1975).	46
3.1. Physical properties of ammonia	58
3.2. Partial pressures of ammonia over aqueous solution of ammonia (from Liley and Gambill, 1973)	61
3.3. Values of parameters in isotherm model for ammonia solution at 1 atm : $y=Ax^B$ and corresponding correlation coefficients at different temperatures	66
6.1. The mechanical damage multipliers.	152
7.1. Relative percentage errors in the computation of average ammonia concentrations in the air and in corn after 2 hours of ammoniation using various computing time and depth intervals compared to the true numerical results extrapolated at $\Delta t=0$ and $\Delta z=0$	177

LIST OF FIGURES

Figures	Page
1.1. Environmental limits and optima for growth and development of microorganisms, insects, and mites associated with stored grain and its products (Sinha and Muir, 1973).	7
1.2. The use and prices of anhydrous ammonia in the U.S. in recent years based on 1967.	10
2.1. Diffusion of free ammonia from whole corn into water at room temperature (Lancaster et al., 1974)	35
2.2. The initial application of ammonia eliminated or reduced all microorganisms (Bothast et al., 1975).	35
2.3. Effects of ammonia content and corn moisture level on the inactivation of aflatoxin B ₁ (from Brekke et al., 1975)	37
2.4. Effects of temperature on the inactivation of aflatoxin B ₁ in corn (data taken from Brekke et al., 1975).	39
2.5. The amount of ammonia residual in corn as related to the cumulative amount of ammonia added (data taken from Nofsinger et al., 1976).	43
3.1. Types of generalized BET adsorption isotherm	54
3.2. The vapor pressure of ammonia as a function of temperature.	60
3.3. Ammonia isotherm curves in ammonia-water system at 1 atm	63
3.4. Five types of classical adsorption isotherms classified by Braunauer, Emmett and Teller (1938)	66
3.5. Ammonia isotherm curves in ammonia-water system at low concentration.	67
3.6. Ammonia isotherms of shelled corn for different moisture content at 4.4°C	70

Figure	Page
3.7. "Scanning" of the hysteresis loop in the adsorption of water by titania gel.	73
3.8. Proposed model for the ammonia adsorption and desorption process in an "ink bottle" pore	76
3.9. The proposed general adsorption and desorption isotherm curves of the ammonia-corn system for the entire pressure range	77
4.1. The adsorption wave (Treybal, 1968).	92
4.2. Influence of mass transfer coefficient on the adsorption and desorption concentration waves.	93
4.3. Breakthrough curves for carbon dioxide on solid carbon using bulk flow rate of 4.26 cm/s (Weyde and Wicke, 1940).	98
4.4. Function used in the Thomas' (1944) solution	98
5.1. The experimental ammonia sorption and drying system.	103
5.2. The position of a 10-compartment grain sampler in the grain bin during sampling.	107
5.3. The average ambient air temperature, relative humidity and the measured average grain temperatures for the first part of experiment	110
5.4. The average air temperatures, relative humidities and the measured average grain temperatures for the second part of experiment.	112
5.5. The timetable for ammonia application and the ambient air temperature in the first part of the experiment.	114
5.6. The timetable for ammonia application and the ambient air temperature in the second part of the experiment	116
6.1. The graphical presentation of the control volume in a grain drying bin in the simulation model	129
6.2. Graphical presentation of the condensation simulator	160
6.3. The flowchart presentation of the main program ADSFIX.	163
6.4. The computing and print time scheme in the main program ADSFIX.	166
6.5. The flowchart presentation of the subroutine ADSPT	167

Figure	Page
6.6. The flowchart presentation for the subroutine ADSPT1 — ammonia sorption at the first inner node in the first computing time interval.	169
7.1. Influence of computing time increment on the average ammonia concentration in the air	173
7.2. Influence of computing time increment on the average free ammonia content in corn	175
7.3. Influence of the computing depth interval on the estimation of average ammonia concentrations which are obtained by extrapolating at zero computing time increment	176
7.4. Influence of computing depth interval on the average ammonia concentration in the air	179
7.5. Influence of computing depth interval on the average free ammonia content in corn	180
7.6. Influence of computing time increment on the ammonia concentration profile in the air using $\Delta z=3.05$ cm after 2 hours of ammoniation	182
7.7. Influence of computing time increment on the ammonia concentration profile in the air using $\Delta z=15.24$ cm after 2 hours of ammoniation	183
7.8. Influence of computing time increment on the ammonia concentration profile in the air using $\Delta z=30.48$ cm after 2 hours of ammoniation	184
7.9. The concentration profile of ammonia in the air at different times (in hours)	187
7.10. The concentration profile of free ammonia in corn at different times (in hours)	188
7.11. The desorption profile of ammonia in the air at different times (in hours)	191
7.12. The desorption profile of free ammonia in corn at different times (in hours)	192
7.13. Ammonia adsorption rate at different grain levels.	194
7.14. Ammonia desorption rate at different grain levels.	195
7.15. Influence of grain depth on the breakthrough curve under standard conditions.	197

Figure	Page
7.16. Influence of grain depth on the desorption break-through curve under standard conditions.	198
7.17. Influence of initial grain moisture content on the ammonia concentrations	200
7.18. Influence of grain moisture content on the ammonia concentration profile in the air after 3 hours of ammoniation.	201
7.19. Influence of grain moisture content on the free ammonia concentration profile in corn after 3 hours of ammoniation	202
7.20. Influence of initial grain temperature on the ammonia concentration in the air	204
7.21. Influence of the initial grain temperature on the average free ammonia content in corn	205
7.22. Influence of airflow rate (cm/m^2) on the ammonia concentration profile in the air after 3 hours of ammoniation.	208
7.23. Influence of the airflow rate (cm/m^2) on the average ammonia concentration in the air	209
7.24. Influence of the airflow rate (cm/m^2) on the free ammonia content in corn.	210
7.25. Influence of the ratio of mass/heat transfer coefficients on the free ammonia profile in corn after 3 hours of ammoniation	212
7.26. Influence of the ratio of mass/heat transfer coefficients on the average ammonia concentration in the air and in the corn.	214
7.27. Ammonia concentration profile in the air at different inlet ammonia concentrations in the air after 3 hours of ammoniation	215
7.28. Fraction of ammonia lost in the exhaust air at different ammonia inlet levels	217
7.29. Free ammonia concentration profile in the corn at different inlet ammonia concentrations after 3 hours of ammoniation	218
7.30. Ammonia concentration profile in the air using different computing schemes after 2 hours of ammoniation . .	220

Figure	Page
7.31. Average ammonia concentrations in the air and in the corn using different computing schemes	221
7.32. Comparison of the predicted and the experimental values of the ammonia concentration in the air in the ammonia adsorption test.	224
7.33. Comparison of the predicted and the experimental ammonia concentration profile in the air in the ammonia adsorption test.	226
7.34. The measured grain temperature, moisture content and free ammonia content at the start of the ammonia desorption test.	227
7.35. Comparison of the predicted and the experimental values of the ammonia concentration in the air in the ammonia desorption test.	229
7.36. Comparison of the predicted and the experimental values of the ammonia concentration profile in the air in the ammonia desorption test	230
7.37. Comparison of the predicted and the experimental values of ammonia concentrations at the 10th hour in the second part of experiment	232
7.38. Comparison of the predicted and the experimental values of ammonia concentrations at the 22nd hour in the second part of experiment	233
7.39. Comparison of the predicted and the experimental values of ammonia concentrations at the 140th hour in the second part of experiment	235
7.40. Comparison of the predicted and the experimental values of ammonia concentrations at the 161st hour in the second part of experiment	236
7.41. Comparison of the predicted and the experimental values of ammonia concentrations at the 242nd hour in the second part of experiment	237
7.42. Comparison of the predicted and the experimental values of ammonia concentrations at the 262nd hour in the second part of experiment	238
7.43. Comparison of the predicted and the experimental values of the grain moisture content and temperature at the 13th hour of experiment	241

Figure	Page
7.44. Comparison of the predicted and the experimental values of the grain moisture content and temperature at the 392nd hour of experiment.	242
7.45. Comparison of the predicted and the experimental values of the grain moisture content and temperature at the 1447th hour of experiment	244
7.46. Comparison of the predicted and the experimental values of the grain moisture content and temperature at the 1744th hour of experiment	245
7.47. The relationship between the average mold count, average grain moisture content and the grain temperature throughout the entire ammonia corn drying process.	247
7.48. The variation of mold counts at different levels and times in the bin throughout the entire ammonia corn drying process	249

LIST OF SYMBOLS

A	Size parameter in Equation 3.11
a	Specific surface area, m^2/m^3
B	Shape factor in Equation 3.11
C	Concentration of adsorbate in fluid, mole/m^3
c	Specific heat, $\text{J}/\text{kg}^\circ\text{C}$
c_l	Specific heat of liquid ammonia, $\text{J}/\text{kg}^\circ\text{C}$
c_g	Specific heat of ammonia gas, $\text{J}/\text{kg}^\circ\text{C}$
c_{pa}	Apparent specific heat of bulk air stream, $\text{J}/\text{kg}^\circ\text{C}$
c_{pp}	Apparent specific heat of the product, $\text{J}/\text{kg}^\circ\text{C}$
D	Diffusion coefficient, m^2/hr
d_p	Particle diameter, m
G_a	Airflow rate, $\text{kg}/\text{hr}/\text{m}^2$
H	Absolute humidity, $\text{kg-H}_2\text{O}/\text{kg-dry air}$
H'	Parameter defined in Equation 4.32
h	Heat transfer coefficient, $\text{W}/\text{hr}/\text{m}^2$
H_{ad}	Heat of ammonia adsorption, J/kg
h_{fg}	Latent heat of evaporation of water, J/kg
h_m	Mass transfer coefficient, $\text{kg}/\text{hr}/\text{m}^2$
I_n	Modified Bessel function of order n of the first kind
J	A function defined in Equation 4.36
j_H	Colburn factor
K	Equilibrium reaction constant

k	Thermal conductivity, W/hr/m
K_A	Ratio of rate constants, k_a/k_d in Equation 3.4
k_f	Fluid-phase mass transfer coefficient, cm/hr
K_h	Ratio of the mass/heat transfer coefficients, $\text{kg}^\circ\text{C}/\text{J}$
K_L	Constant used in Equation 3.5
L	Latent heat, J/kg
M	Grain moisture content, decimal
m	Number of layers of the adsorbate
M_A	The ammonia multiplier
M_D	The mechanical damage multiplier
M_M	The moisture multiplier
M_T	The temperature multiplier
M_e	Equilibrium moisture content, d.b.
MR	The moisture ratio
N	Rate of ammonia accumulation, $\text{kg}/\text{m}^3/\text{hr}$
n	Dimensionless distance defined in Equation 4.33
Nu	Nusselt number
p	Partial pressure of adsorbable component of gas, mm Hg
p_s	Saturated vapor pressure, mm Hg
Pr	Prandtl number
q	Concentration of the adsorbate in solid, mole/kg
q_m	Saturated adsorbate concentration, g/mole
Q_s	Site interaction energy of adsorption, J
Q_1	Total heat of adsorption of the monolayer, J
R	Separation factor in Equation 4.11
R'	Universal gas constant, 1.987 cal/mole K
r	Radius

Re	Reynolds number
rh	Relative humidity
S	Cross section area in the bin, m^2
Sc	Schmidt number
St	Stanton number
T	Temperature, °C or K
t	Time, hr
t	The elapsed time, hr
T_r	Parameter defined in Equation 4.34
t_b	The breakthrough time, hr
t_e	Equivalent storage time at the reference conditions, hr
T_f	Film temperature, °C
T_w	Wall temperature, °C
v	Velocity, m/hr
X	Concentration of fluid in fluid, dimensionless
x_1	Ammonia concentration in the air, kg-NH ₃ /kg-dry air
x_2	Ammonia concentration in corn, d.b.
x_2^*	Equilibrium ammonia content in corn, d.b.
x_{2f}^*	Equilibrium free ammonia content in corn, d.b.
x_{2m}	Saturated ammonia concentration in corn, d.b.
x_{2R}	Fixed-ammonia content in corn, d.b.
Y	Adsorbate concentration in solid, dimensionless
y	Adsorbate concentration in adsorbent, dimensionless
z	Position, grain depth, m
α	Thermal diffusivity, m^2/hr
α_D	Mass diffusivity, m^2/hr
δ	Fraction of residuals based on x_{2f}^*

ϵ	Void fraction
κ	Kinetic mass transfer coefficient, cm/hr in Equation 4.30
θ	Grain temperature, °C
θ_a	Fraction of solid surface area covered by adsorbate
ρ	Density, kg/m ³
μ	Viscosity, kg/m/hr
ψ	Correction factor in Equation 4.11

Subscripts

a	dry air
B	bulk phase
g	gas
l	liquid
m	saturation in solid phase
p	product
s	solid
v	vapor
w	liquid water
f	fluid phase
o	inlet
∞	in the bulk fluid

Superscripts

*	equilibrium
'	reference condition
°	initial

CHAPTER 1
INTRODUCTION

1. Corn Production in Michigan

Corn, the biggest cash crop in Michigan, has earned 13.5 percent of the cash received from marketings of all agricultural commodities in 1977 (Fedewa and Pscodna, 1979). The production of corn for grain in Michigan surged to a record high of 197.20 million bushels in 1977, 28 percent larger than the 1976 crop. The year 1977 also reached a record high average yield, 85.0 bushels per acre, in Michigan. Nevertheless, the national average yield for corn in the U.S. was 90.8 bushels per acre in 1977. The high Michigan yield is partly due to the warm and dry weather in the spring of 1977 which permitted unusually early planting of corn; additional rains in late June and early July helped corn (Fedewa and Pscodna, 1978, 1979).

The production of corn for grain in Michigan ranked ninth in the U.S. in both 1977 and 1978 crops and accounted for 3.0 percent in 1977 and 2.6 percent in 1978 of the total U.S. production (Fedewa and Pscodna, 1978, 1979). The harvested acreage, production and value of corn for grain in Michigan in recent years are shown in Table 1.1. The dramatic increase in corn production is due to the record high yield since the increase in harvested acreage was only about 4 percent compared to 1976. Total grain corn production in 1978, while 8 percent lower than the record high in 1977, was 18 percent higher than the 1976 crop. The

yield in 1978, however, was 5 percent below that of 1977.

The disposition of the grain corn produced in Michigan in 1978 (182.25 million bu) was about 30 percent used on the farm where it is grown and the rest is sold to the market.

Table 1.1. Acreage, production, and value of corn for grain in Michigan, 1975-1978.

Year	Harvested Acreage (1000 acre)	Production		Unit price Received (\$)	Value of Production (\$1000)
		Bu/acre	Total (Million bu)		
1978	2250	81.0	182.25	2.05	373,613
1977	2320	85.0	197.20	1.92	378,624
1976	2230	69.0	153.87	2.04	313,895
1975	2090	80.0	167.20	2.35	392,920

Source: Fedewa and Pscodna, Michigan Agricultural Statistics, 1979.

2. Corn Drying Practices

Foster (1976) indicated that field shelling of corn increased from 2 percent of the total crop in 1956 to 85 percent by 1975 in the central U.S. corn belt (Indiana, Illinois, and Iowa). In the same period, the amount of corn artificially dried increased from 14 to 72 percent of the total crop. Corn can be dried naturally in the field or during storage or it can be dried artificially on-farm and off-farm. The percentages of these drying techniques for some Midwestern states in recent years are shown in Table 1.2. There is a sharp decrease of corn dried naturally in the field or during storage in 1977 (25.1 percent) compared to that in 1975 (45.3 percent). On the other hand, the percentage of corn dried artificially on the farm increased from 51.0 percent in 1975 to 72.5 percent in 1977. Other Midwestern states

showed the same trend but the changes are not as large as in Michigan.

The increase in the use of on-farm artificial grain drying implies that more fuel is needed at the farmstead. Bakker-Arkema et al. (1974) stated that over 60 percent of the energy required to produce corn on the farm is used for artificial drying. The major types of fuel are propane and natural gas. In 1977, a total of 74.9 percent of the corn produced in Michigan was dried artificially and 88.1 percent of the total energy for corn drying was from propane with a small percentage of natural gas (3.7 percent) and fuel oil (4.5 percent). Since propane became the predominant drying fuel in the mid-1950s (Brooker et al., 1978), the use of propane by farmers in the Corn Belt to dry grain has doubled in the past 10 years (Wheeler, 1976). A significant rise in the drying costs of corn is due to the rising cost of propane gas which has been the major source of energy on the farm for drying.

The distribution of various dryer types used for drying shelled corn artificially in Michigan in recent years is shown in Table 1.3. Corn dried at the elevator is, at the present time, mostly dried in continuous crossflow dryers. There has been an increasing tendency for farmers to employ high temperature rapid batch dryers rather than slower and more risky bin-drying systems. The percentage of corn dried with natural air has decreased to a minimal level in 1977. Part of the reason was due to the unusual wet weather in the fall of 1977. Some corn was left standing in the field and harvested the next spring (Fedewa and Pscodna, 1978). As a result, the energy use for drying corn per unit weight also increased rapidly in 1977.

Table 1.2. The percentages of various drying techniques in some Midwestern states in recent years.

State	Dried naturally in field or during storage			Dried artificially								
				On-farm			Off-farm					
	1974	1975	1976	1977	1974	1975	1976	1977	1974	1975	1976	1977
MICHIGAN	40.2	45.3	-	25.1	57.0	51.0	-	72.5	2.8	3.7	-	2.4
Illinois	21.0	33.5	13.0	-	77.5	65.0	85.0	-	1.5	1.5	2.0	-
Indiana	12.0	12.2	11.8	10.7	86.3	87.2	86.6	87.4	1.7	0.6	1.6	1.9
Iowa	37.5	30.6	29.3	29.3	60.2	68.4	68.9	68.6	2.3	1.0	1.8	2.1
Wisconsin	39.7	45.3	44.8	-	57.3	52.0	52.9	-	3.0	2.7	2.3	-

Source: Fedewa et al. (1978), and Kenyon et al. (1976).

Table 1.3. The percentages of shelled corn dried artificially by various dryer types in Michigan in recent years.

	1974	1975	1977
Continuousflow	45.7	39.5	40.4
Batch	38.3	48.1	50.7
Bin	14.3	9.2	8.4
Natural air	1.7	3.2	0.5

Source: Fedewa et al., 1978.

3. Natural Air Drying

Ambient air drying has been described by Foster (1953) and by Shove and Andrew (1968). A discouraging problem associated with the ambient air drying is the microbial growth at warm harvest temperatures. Hodges (1970) cooled bins of field-shelled corn in periods of 2, 4, and 8 days. Mold growth observation indicated that corn with 26 to 28 percent moisture content and 21 to 32°C initial temperature should be cooled to about 4.5°C in two days. Shove (1974) reported that the drying potential of ambient air is relatively high during warm days of early harvest. However, the allowable drying time for corn without deterioration is short.

The most important and decisive factors in the success of ambient drying of high-moisture corn are the weather conditions and the airflow rate. Foster (1953) recommended an airflow rate of $3.3 \text{ m}^3/\text{min}/\text{ton}$ (3 cfm/bu) as adequate to dry shelled corn from 25 to 15.5 percent (w.b.) moisture content in moderate fall weather. Shove (1976) recommended the same airflow rate for 26 percent moisture corn. Lower airflows, 2.1 to $2.9 \text{ m}^3/\text{min}/\text{ton}$ (1.9 to 2.6 cfm/bu) can be used in ambient air corn drying without spoilage if an "extender", such as chemical preservative, is used (Nofsinger et al., 1978). The use of extenders permits low-temperature drying systems to be successful over a wider range of conditions. Furthermore, the drying operation is dependent on the weather and a slow drying process free of unacceptable grain deterioration can be assured.

Low-temperature drying has been defined by Shove (1973) as a system in which the drying air temperature is in the range of -1 to 10°C (30-50°F). In this temperature range, various *Penicillium* and

Aspergillus species are able to grow and play an important role in the deterioration of aerated moist corn (Thompson, 1972; Tuite et al., 1970; Sinha and Muir, 1973; Felkel et al., 1978).

4. Molding and Aflatoxin Production

The microbial growth that causes spoilage of grain is affected by: (1) the moisture content of grain, (2) storage temperature, (3) oxygen to CO₂ ratio in the voids, (4) degree of mechanical damage, (5) insect infestation, (6) fungal contamination, and (7) time of storage.

Generally, a higher moisture in the grain, a higher storage temperature, a higher oxygen content, and a higher degree of mechanical damage favor the growth of microorganisms and enhance the rate of spoilage. Sinha and Muir (1973) stated that mold growth occurs between 40 and 60 days in grain at 14.5 to 17.0 percent m.c. and 12 to 15°C and between 20 and 30 days in grain with 18 to 19 percent m.c. at that temperature.

A collection of the ranges of temperatures at which organisms grow are shown in Figure 1.1, which was compiled by Sinha and Muir (1973) from various sources. The bold lines represent optimum temperatures for growth and multiplication of organisms which includes molds, bacteria, insects and mites. In general, microorganisms can survive and duplicate at temperature and humidity ranges wider than those for insects and mites. At temperatures around 27°C, numerous species will grow under suitable relative humidities. Since living organisms can only survive and multiply within certain relative humidity ranges (which, in general, are close to 80 or 90 percent), controlling the relative humidity by lowering the moisture content of the stored grain is an effective method of preventing spoilage.

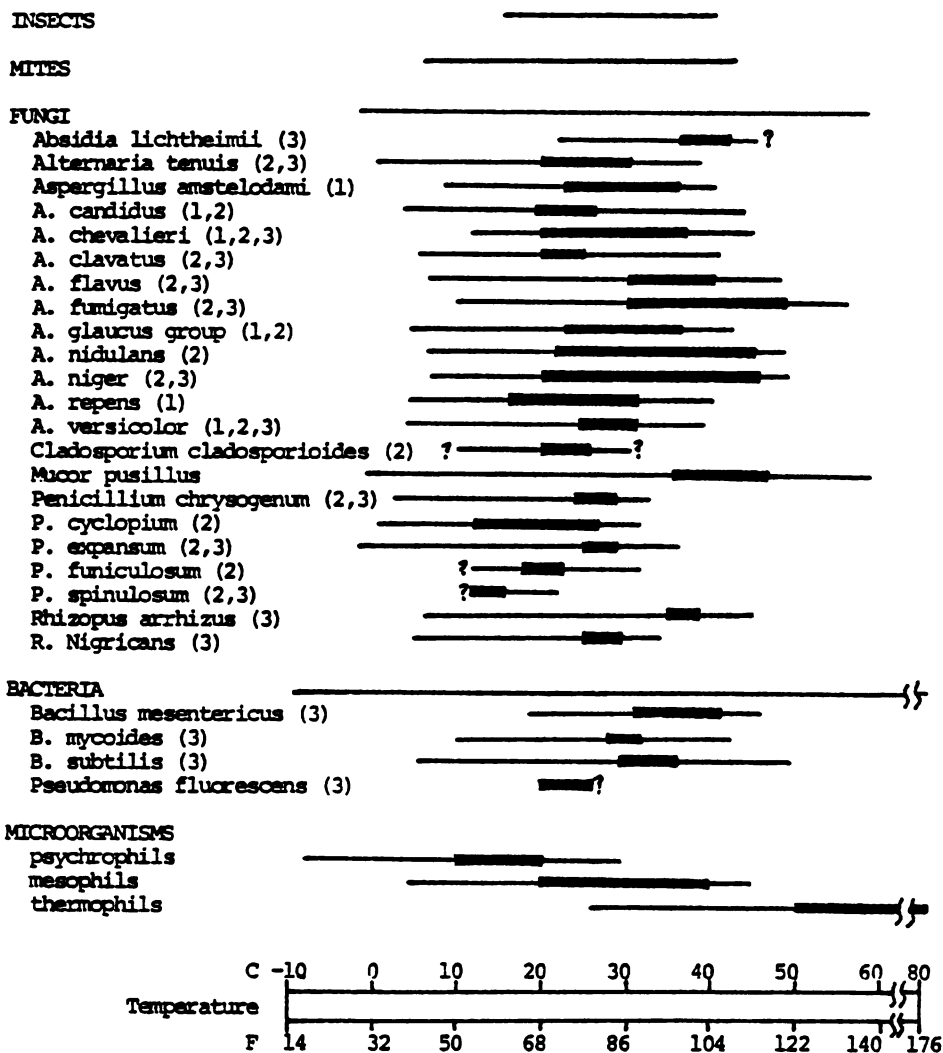


Figure 1.1. Environmental limits and optima for growth and development of microorganisms, insects, and mites associated with stored grain and its products (Sinha and Muir, 1973)
 Subscripts: 1-xerophyte, develop at RH below 80% ; 2-mesophyte, develop at RH range 80-90% ; 3-hydrophyte, develop at RH above 90%.

The degree of grain deterioration is commonly expressed as dry matter loss which is measured by the carbon dioxide production (Steele, 1967). The permissible storage time was suggested by Steele et al. (1969) as having a maximum dry matter loss of 0.5 percent for field-shelled corn.

Certain microorganisms can produce toxins when they are allowed to grow under proper environmental conditions. The occurrence of aflatoxin in corn flared up the attention of researchers in all related areas. The aflatoxin is known to be very toxic and carcinogenic. Numerous studies of aflatoxin naturally occurring in corn have been made since the early 1960s. The USDA launched several intensive surveys of corn produced in the Corn Belt and some southern states between 1970 and 1975. It was found that the potential for aflatoxin contamination does exist in improperly handled corn.

Aflatoxin contamination is a problem in a number of agricultural products. Among those reported to have been contaminated are: peanuts, Brazil nuts, almonds, walnuts, pecans, filberts, cottonseed, seed oil, legumes, peppers, dried fruit, wine, dairy products as well as wheat, sorghum, oats, rice and corn (Stoloff, 1976).

Aflatoxin can be produced on corn by widely distributed strains of two common molds: (1) *Aspergillus flavus* and (2) *A. parasiticus*. The toxin's dietary effect upon poultry can result in poor growth, increased mortality and poor feed conversion.

5. Application of Ammonia in Grain Preservation and Detoxification

It is impossible to store cereal grains at normal harvest temperatures for an extended period of time without drying grains to a moisture level low enough to avoid fungal growth.

With the rising costs and uncertain supply of fuels, the drying costs of cereal grains increase rapidly. Alternative methods of grain drying which consume less energy have been investigated recently. It is generally believed that slower drying techniques use less energy in removing a unit weight of water from the grain. One of the alternative methods is to use chemicals as grain preservatives while the grain is drying slowly. Recent studies have shown that various chemicals, such as ammonia, volatile fatty acids, propionic acid, methylene bispropionate (MBP), formalin and sulfur dioxide, can serve as grain preservatives or antifungal agents when applied to high-moisture grains (Bothast et al., 1975; Hall et al., 1974; Herting and Drury, 1974; Vandergraft et al., 1975; Sauer et al., 1975; Peplinski et al., 1978; Eckhoff et al., 1978). Application of ammonia has been reported in connection with the preservation and detoxification of high-moisture grain (Bothast et al., 1975; Lancaster et al., 1974; Lancaster et al., 1975; Brekke et al., 1975; Peplinski et al., 1978; Nofsinger et al., 1976), the preservation of high-moisture forage (Knapp et al., 1974) and as a nonprotein nitrogen source to give silage a superior feeding value (Huber, 1975; Huber et al., 1973).

The use of anhydrous ammonia and the prices paid for it by farmers in recent years in the U.S. are shown in Figure 1.2. The average price of anhydrous ammonia reached a record high of \$238/ton in 1975 and has dropped since then. In 1978, the average price was \$172/ton, or 7.8¢/lb of anhydrous ammonia.

The use of ammonia as a preservative in high moisture corn has been exempted from the requirement of a tolerance level (Federal Register, Vol. 43, No. 234, 1978). The ammonia-treated corn can only be used as

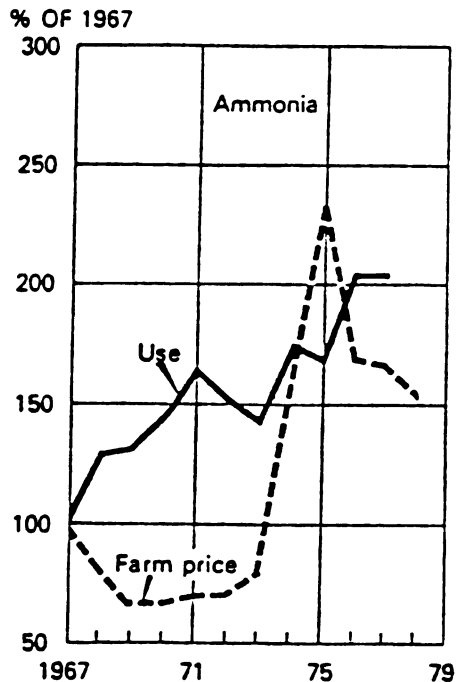


Figure 1.2. The use and prices of anhydrous ammonia in the U.S. in recent years based on 1967. Source: Fedewa and Pscodna (1979).

animal feed. This proposal was submitted by the U.S. Department of Agriculture and approved by the Environmental Protection Agency (EPA). The USDA claimed that "this use of ammonia on corn as a preservative would permit farmers to store and dry the corn without resorting to propane or natural gas to quickly reduce moisture levels. The trickle ammonia process for corn preservation would contribute significant savings to growers in energy consumption and costs." The fungicide ammonia is exempted from the requirements of a tolerance when used after harvest on the raw agricultural commodities including grapefruit, lemons, oranges and corn grain (amended in Part 180, Subpart D, Section 180.1003, Federal Food, Drug and Cosmetic Act, Food and Drug Administration, 1978).

This research effort was intended to work in cooperation with researchers in the North Regional Research Laboratory (NRRL) of USDA

at Peoria, Illinois. A large amount of effort has been performed by a group of researchers including microbiologists, toxicologists, chemists, agricultural engineers, and cereal grain scientists in recent years. Their contributions have been many especially in the areas of identifying the importance of aflatoxin contamination in grains, especially corn; surveying the occurrence of aflatoxin in corn in the Corn Belt and some southern states; comparing the fungicidal effects of several possible chemicals as grain preservatives; identifying ammonia as an inhibitor of bacteria and fungi; and, finally, carrying out several practical-scale field tests of ammonia grain drying.

While reviewing the results generated at NRRL, it becomes obvious that a systematic engineering analysis in the area of ammonia preservation and drying processes has not yet been made. This investigation will focus on the analysis of the behavior of ammonia (or any other chemical) in a fixed-bed of corn (or any other grain) in the ambient air drying of high-moisture grain.

6. Objectives

1. To demonstrate mathematically (using computer modeling techniques) the application of ammonia in the natural air grain drying system.

2. To predict the behavior of anhydrous ammonia in the storage and drying system of cereal grains. The investigated ammonia characteristics include both the inhibitory effects of ammonia towards bacteria and fungi growth and the ammonia concentration and temperature distributions of the air and the grain in the drying bin over the entire conditioning/drying process.

3. To generalize the numerical prediction model of ammonia-corn sorption systems for the application of other chemicals on high-moisture grains other than shelled corn.

4. To evaluate the research efforts performed at the North Regional Research Laboratory of USDA on ammonia preservation, detoxification, and drying.

5. To perform a bin test on ammonia grain drying in order to verify the prediction model.

6. To perform the sensitivity and accuracy tests of the developed ammonia sorption and drying models and compare with the experimental results of model bin tests in this investigation.

CHAPTER 2
LITERATURE REVIEW

1. Fixed-Bed Grain Drying Systems

A fixed-bed drying process of grains is usually performed in a bin system. A basic bin structure provides a controllable environment to physical, chemical, and biological changes in grain and an isolated system from rodent and insect damage and contamination of fungi and bacteria. The drying rate in a bin of grain depends on many factors, e.g. airflow rate, weather conditions, heated air temperature, initial grain conditions — temperature, moisture, BCFM (broken corn and foreign material), and time. It is possible to investigate the influence of these factors by setting up models and equations which describe the entire system.

The first serious attempt to model deep-bed grain drying was performed by Hukill (1954). He related the moisture ratio of grain with time under different drying conditions. A series of so-called "bulk drying curves", which can be expressed analytically, were drawn to determine the approximate moisture content at any grain depth in a fixed-bed drying system at any time after drying was started. The curves are considered rough estimates since it was assumed that moisture ratio of a thin layer of grain decreases proportional to the drying time while laboratory tests of thin-layer drying have shown that the drying rate is a function of the kernel moisture content.

1-A. Natural Air and Low-Temperature Drying Systems

Bloome (1969) first developed a computational model of drying shelled corn with ambient air. Flood et al. (1972) simulated a natural air drying system for corn using: (1) the thin-layer drying equation of Sabbah (1968), (2) the rewetting equation developed by del Giudice (1959), and (3) the equilibrium moisture content equation of Thompson's (1968). The criterion for successful drying were described as the dry matter loss of less than 0.5 percent at the end of drying when the average grain moistures were below 15.5 percent wet basis. The airflow rate was 50 cfm/ft².

The importance of stored grain temperature in a bin was emphasized and a simulation model was developed by Yaciuk et al. (1975). This simulation model is different from the existing models by considering (1) wind velocity and (2) type of bin-wall material. Heats of respiration of seeds and other organisms were assumed negligible, thus the model can only simulate sound and relatively dry (14.5 percent m.c.) grain.

Aldis and Foster (1977) modeled the moisture changes in grain exposed to ambient air during grain handling. They concluded that small amounts of moisture transfer from warm air to cold grain can occur in short time periods during handling. However, the moisture condensed on the grain surface may be sufficient for rapid mold growth. The amount of moisture adsorbed by grain during aeration and bin filling were calculated using del Giudice's (1959) empirical rewetting equation and a theoretical equation based on a combined diffusion, adsorption mechanism developed by Park et al. (1974).

Two major problems encountered in natural air and low-temperature drying are: (1) overdrying on the bottom layers, and (2) high airflow rate is required for early harvested high moisture corn (Pierce and Thompson, 1978). One way of preventing overdrying on the bottom is to remove the dry grain from the bottom. Roberts et al. (1975) dried a full bin of grain with a recirculator to sweep dry grain from the bottom and spread on the top of the grain mass. This drying technique is known as in-bin counterflow drying. If the rate at which the grain is removed from the bottom of the bin is equal to the rate at which the drying zone moves through the bed, the drying front remains at the bottom of the bin and overdrying is prevented. To prevent the rewetting of dry grain placed on the top of grain mass, the dry grain can be transferred to another aeration bin instead.

It is difficult to design a natural air drying system, which guarantees successful drying, without overdesigning it. The determination of minimum airflow requirements is critical. The idea of using a stirrer in a bin to increase the airflow and reduce the moisture gradient throughout the bin was studied by Williams et al. (1978). They concluded that using a larger than recommended fan on an unstirred bin appreciably decreases drying time with only a slight increase in operating and fixed costs. The additional cost of a stirring device cannot be justified. Nevertheless, using a bigger fan will worsen the overdrying problem which can be easily prevented by a stirrer.

1-B. Energy Source of Low-Temperature Drying

Zink et al. (1978) investigated various heat energy options for low-temperature drying. The most widely used heat sources for low-temperature drying are liquid propane gas and electrical heat, both

of which have the benefit of low capital investment. Alternative heat sources from solar collectors, heat pump and cob gasifier, were analyzed and compared for their economics and practicability.

Solar energy can be utilized in different manners (Lai and Aldis, 1978) in low-temperature grain drying systems: (1) direct solar heated air, (2) silica gel dehumidified air and (3) phase change material heated air. Compared with natural air drying system, no distinct difference on grain qualities and no significant energy savings were observed.

1-C. Fixed-Bed Computer Models

The first modern study on deep-bed grain drying using computer simulation techniques for solving model equations was published by Boyce (1965). Shortly afterwards, two concurrent grain drying modeling attempts were started: one was conducted by Thompson et al. (1968) and the other one was conducted by Bakker-Arkema et al. (1966) at Michigan State University (MSU).

Thompson's model is empirical in nature while the MSU model started with theoretical analysis and differential equations (Brooker et al., 1974). The effects of a number of parameters, such as airflow rate, surface heat and mass transfer coefficients, inlet air conditions, porosity and thermal properties of grain, on the rate of cooling in a deep bed of biological products were investigated using a three-equation analysis (Bakker-Arkema and Bickert, 1967).

The drying of a bed of grain-dough particle was analyzed with a combination of three-equation analysis during constant-rate drying period and the four-equation model during the falling-rate drying period (Farmer and Bakker-Arkema, 1970). The four-equation MSU fixed-bed grain drying model was solved numerically and the computer code of

the four basic equations on heat and mass transfer of grain drying was published by Bakker-Arkema et al. (1974). This MSU model was found too sophisticated to simulate long drying periods because it requires excessive computer time. A number of simplified deep-bed grain drying models have been used in the simulation of solar grain drying by making modifications in the basic MSU model in order to simulate long-period, low-temperature drying (Bakker-Arkema et al., 1977).

A literature review of fixed-bed heat and mass transfer problems was presented by Bakker-Arkema et al. (1978). The fixed-bed models will be discussed in Chapter 4.

2. Ammonia Preservation and Detoxification

2-A. Chemical Preservation

The method of chemical preservation has long been used to store high moisture corn for animal feed. Propionic acid and acetic acids were found effective in controlling mold growth in high moisture grain (Young et al., 1970; Goering and Gordon, 1973; Sauer, 1973). The pH value on the surface of acid-treated corn is lowered to about 4.5 (Hall et al., 1974). The chemical-treated grain is only good for feed grain because of the brown-colored embryos due to chemical reaction and consequently the grain grade was lowered. The viability of chemical-treated grain is drastically reduced.

Sauer and Burroughs (1974) tested the effectiveness of several chemicals as a grain mold inhibitor. Of the various organic acids and their salts, propionic acid was found to be the most effective and consistent mold inhibitor for high moisture corn (18 to 24 percent, w.b.). Isobutyric, acetic and formic acids followed in order. Salts of acids were less effective. The efficacy of methylene bis-propionate (MBP)

was equal to or slightly better than propionic acid when applied to corn harvested at 23 and 29 percent moisture content (Sauer et al., 1975). Corn of 23 percent moisture showed no sign of spoilage after 8 months storage with 0.7 percent (by weight) of MBP and 0.9 percent for 29 percent moisture corn.

Recently, sulfur dioxide has been investigated as a possible alternative chemical to supplement ambient air drying of high-moisture corn (Eckhoff et al., 1978). Sulfur dioxide is readily available and is one of the most extensively used food additives. It is used as a fungicide for the preservation of fruits, vegetables, meat, fish, and alcoholic beverages (Schroeter, 1966). The "trickle" (intermittent injection) process was also used in the sulfur dioxide tests of grain preservation. Sulfur dioxide was proved to be able to control microbial growth effectively during aeration and drying of high-moisture corn with no apparent decrease in grain quality.

2-B. Ammonia Preservation and Detoxification

Ammonia was found to be one of the more effective reagents for practical treatment of contaminated cottonseed and peanut meals by the researchers at the Southern and the Western Regional Research Centers (Marsi et al., 1969). It was later learned (Bothast et al., 1973) that ammonia kills most molds in the corn very rapidly and also destroys bacteria. A group of researchers at the North Regional Research Laboratory of USDA at Peoria, Illinois, have conducted a series of ammonia preservation and detoxification tests (Lancaster et al., 1974; Bothast et al., 1975; Lancaster et al., 1975; Brekke et al., 1975; Peplinski et al., 1975; and Nofsinger et al., 1976).

Ammonia has highly visible effects on treated corn; the pericarp starts yellowing immediately after the treatment. The entire kernel slowly turns brown. The browning of ammonia-treated corn is similar to the reaction of an aldose (a sugar) with an amine through a series of browning reaction to produce pigmented compounds (Lancaster et al., 1974). Methods have been developed for determining "free" ammonia (part of the ammonia surrounding corn kernels in the pores of the kernel surface, and the ammonia dissolved in corn, but still in the form of ammonia) and the total ammonia content of the treated corn. It is believed that free ammonia is responsible for fungicidal activity.

A microbiological study of the secondary fungal growth in chemically treated corn (Bothast et al., 1975) showed that the predominant molds after 30 days of treatments of various chemicals were different: *Scopulariopsis brevicaulis* predominated on ammonia treated corn; *Mucorales* and species of *Monascus*, *Penicillium*, *Fusarium*, and *Aspergillus flavus*, as well as *A. fumigatus*, were found in ammonia isobutyrate-treated corn. *A. flavus* was the predominant mold infecting isobutyric acid and propionic-acetic acid treated corn. The organic acids were better than ammonia and ammonia-isobutyrate only in controlling bacteria growth. However, late development of *A. flavus* on corn treated with organic acids indicated the possibility of aflatoxin contamination. Bothast et al. (1975) endorsed ammonia as a grain preservative based on the above reason and economic, nutritional advantages.

Research activities at the Peoria Laboratory have recently concentrated on the ammonia preservation of high-moisture corn. Lancaster et al. (1975) treated shelled corn with anhydrous ammonia-air mixtures (or called ammonia-laden air). The first attempt to theorize the ammonia

treatment was performed by Lancaster et al. (1975) after the potential role of ammonia as a grain preservative had been determined. Simple transport and diffusion mechanisms for isothermal conditions were proposed.

Aqua ammonia has been proved to be very effective in inactivating the toxin produced in naturally contaminated corn (Brekke et al., 1975). A high dose (1.5 to 2 percent by weight) of ammonia, applied either in anhydrous or aqueous form, can very effectively detoxify the aflatoxin in contaminated corn. In another preservation test (Peplinski et al., 1975) of high moisture corn with ammonia to control microbial deterioration, ammonia destroyed all molds, lowered bacteria counts for up to four months and modified some chemical and physical properties of the corn stored 410 days at ambient temperatures ranging from 16 to 39°C.

Natural air drying of high moisture corn was first supplemented with an intermittent application of anhydrous ammonia (0.009-0.09 percent d.b.) in a 14.2 ton (560 bu) bin (Nofsinger et al., 1976). The airflow was 1.8 cfm/ton (1.6 cfm/bu) and the moisture content was reduced from 23.2 to 17.7 percent during the first 56 days. The ambient air drying was extended as long as six months without spoilage.

3. Mold Growth and Aflatoxin

Stoloff (1976) presented a thorough review on the worldwide occurrence of mycotoxins in foods and feed. The year 1960 divides the descriptive phase of mycotoxin investigation from the analytical one. It was the first time in history that a group of fluorescent compounds were extracted from toxic meals, and *Aspergillus flavus* was isolated from a toxic meal (Sargent and Carnaghan, 1963). When the toxic meal was shown to be capable of producing cancer in liver (Dickens and Jones, 1963),

it stimulated intensive investigations of the isolated compounds now called aflatoxin.

3-A. Mold Growth in Corn

Invasion by fungi is affected by the amount of spore inoculum in the field, stresses on the plant, invertebrate infections, damage by other fungi, plant resistance, mechanical damage, mineral nutrition of the plant, and temperature (Hesseltine, 1976). Grain is exposed to mechanical damage and mold inoculum during harvest. After harvest mold growth depends on the handling and storage conditions.

The occurrence of *Aspergillus flavus* and *A. parasiticus* in corn in the field was reported as early as 1920 in Texas (Taubenhaus, 1920). Levels of infection of *A. flavus* in corn kernels before harvest in the order 0.02 to 0.09 percent (Tuite, 1961) and 0.4 percent (Tuite and Caldwell, 1971) were reported in Indiana. The predominant types of mold found in samples of corn meal belonged to the genera *Penicillium*, *Aspergillus*, *Fusarium*, and *Mucor* (Bullerman et al., 1975). *A. flavus* produced aflatoxin B₁ and B₂ in sterile moistened corn meal, but not in unsterilized meal containing a mixed flora. This shows that when toxic molds are growing in competition with other microorganisms, toxins are not produced under all conditions. Corn kernels from insect damaged ears were reported to have a considerable higher incidence of *A. flavus* and other toxin-producing fungi (Fennell et al., 1975). It was also found that insect damage of corn increases the probability of toxin contamination before harvest (Lillehoj et al., 1975A, 1976B; Hesseltine et al., 1976) and several investigations have implicated insect damage as a critical factor in the establishment of *A. flavus* infection in developing corn (Lillehoj et al., 1975B, 1975C; Hesseltine et al., 1976;

Fennell et al., 1975).

3-B. Aflatoxin Contamination in Grain

Aflatoxin contamination is a problem in a number of agricultural products. The factors influencing mold growth and toxin formation can be classified into three major categories (Hesseltine, 1976): (1) physical: moisture content, temperature, relative humidity, mechanical damage, blending of grain, hot spots, and time; (2) chemical: CO₂ and O₂ content in stored environment, nature of the substrate, mineral nutrition and chemical treatment; and (3) biological: plant stress, fungus infection, microbiological ecosystem, etc. The effects of the above factors act as multiples and interact dynamically.

Hayes et al. (1966) claimed that aflatoxin is not formed until at least 48 hours after spore germination. This delay means that corn, with a moisture level optimal for the growth of *A. flavus*, will not be dangerous even when heavily inoculated, if the corn can be dried to below 13 percent moisture content within 48 hours. However, it is widely recognized nowadays that the corn at 15.5 percent is low enough for long time storage.

3-B.1. Aflatoxin in Corn Before Harvest

Aflatoxin has been found in the field in corn samples at all stages of development and maturity (Anderson et al., 1975). Stressed growing conditions, such as a dense plant population or reduced fertilization, appear to have a positive influence on the incidence of aflatoxin contamination.

Aflatoxin contamination in corn before harvest has been reported by Lillehoj et al. (1976B, 1977) and Fennell et al. (1975, 1977). *A. flavus*

was generally associated with insect activity. *A. flavus* infected seed and the characteristic kernel fluorescence were related to the occurrence of aflatoxin in corn samples. Fungal-contaminated kernels exhibited two types of fluorescence: (1) bright greenish-yellow fluorescence (BGYF) in the germ margin, or (2) intense yellow fluorescence throughout the endosperm. About one-half of the samples exhibited BGYF in the cracked fraction. Seventeen percent contained detectable levels (2 ppb) of toxins in a survey of 1975 corn crop from Iowa (Lillehoj et al., 1977). These observations demonstrate that extensive *A. flavus* infection and aflatoxin production occur in corn before harvest.

It was not until recently that the significance of *A. flavus* contamination in corn before harvest was realized. In 1973, corn from a region of South Carolina was collected at harvest to determine field occurrence of *A. flavus* and aflatoxin (Lillehoj et al., 1975B). Thirty-two percent of the 297 samples contained aflatoxin at levels exceeding 20 ppb [this is the present Food and Drug Administration guideline for the maximum amount of toxin tolerable in animal feed (Stoloff, 1972)]. In an effort to determine the origin of the inoculum responsible for *A. flavus* infection of corn before harvest, silks and insects from developing and mature ears of corn from several locations were examined for the presence of the fungus (Fennell et al., 1977). Insects showed a relatively uniform presence of *A. flavus* ranging from 1.7 to 3.1 percent of insects from various locations in the Midwestern states. Overall, 52 percent of *A. flavus* isolates from silk and 32 percent of those from insects produced aflatoxin in a qualitative test.

3-B.2. Aflatoxin in Corn during Storage

Samples from a mycotoxin contaminated hot spot in a bin of corn in central Illinois were analyzed (Shotwell et al., 1975D). It was not fully understood that even in grain lots contaminated with *A. flavus* mycelia, aflatoxin-free kernels occurred adjacent to highly contaminated kernels. In no kernel were both aflatoxin and zearalenone detected. This variation on levels of aflatoxin contamination in individual corn kernels made it necessary to take large samples when estimating the average aflatoxin content of a bulk quantity of corn. Sampling of a small quantity for the determination of aflatoxin contamination has to be done very carefully (Bothast et al., 1976).

In order to determine the distribution of toxin among product fractions, a dry milling test of corn was performed (Brekke et al., 1975C). The aflatoxin level was found to be the lowest in the grits and highest in the germ, hull, or degermer fines.

Present grading factors do not reflect the consequences of aflatoxin contaminated samples. In a survey of white corn under loan (Shotwell et al., 1975A), the toxin content was found to be related to grade with a low correlation coefficient based on geometric means: 0.29 for aflatoxin B₁ and 0.27 for aflatoxin B₂.

To determine the possibility and incidence of aflatoxin contamination in corn, a series of surveys were performed by the North Regional Research Center of USDA, Food and Drug Administration and private industries (Table 2.1). The survey, made from 1964 until 1975, covers all the major corn-producing areas in the U.S. Although the situation is not alarming in the Corn Belt, it is becoming a serious problem in the southern states of the U.S. According to a survey by the FDA on

Table 2.1. Aflatoxin incidence in corn (Shotwell, 1977).

Year	Agency surveying	Origin samples	Types samples and source	Number of samples assayed	Percent samples with indicated level toxin (ppb)			
					ND	<20	20-49	50-100
1964-1965	MRRC	Corn Belt(1)	Grain inspection AMS	1311	98	2	<0.1	
1965	Met. milling industry	Corn Belt(2)	Corn received by industry	372	97	3		
1967	MRRC	Corn Belt(1)	Grain inspection AMS	283	98	1	1	
1968-1969	MRRC	Export cargo(3)	Grain inspection AMS	293	97	2	1	
1969-1970	MRRC	South(4)	Grain inspection AMS	60	65	13	5	8
1971	MRRC	Southeast Missouri(5)	Stored ASCS white corn	1283	68	18	7	4
1972	FDA	Corn Belt(6)	Elevator and food processing plants	223	98	2		
1973	MRRC	South Carolina(7)	Field-freshly harvested	297	49	19	17	8
1973	FDA	Corn Belt(8)	Farm and country elevator	169	98	2		
1973	FDA	South(8)*	Farm and country elevator	146	64	22	7	4
1975	MRRC	Iowa(9)	Field-freshly harvested	214	83	15	1	<1

* includes Southeast, Appalachia, Southeast MO, KY, TN, OK, TX, and CA.

References:

1. Shotwell et al., 1969, 1970.
2. Watson and Yahl, 1971.
3. Shotwell et al., 1971.
4. Shotwell et al., 1973.
5. Shotwell et al., 1975A.
6. Eppley et al., 1974.
7. Lillehoj et al., 1975B.
8. Stoloff et al., 1976.
9. Lillehoj et al., 1977.

aflatoxin and zearalenone in 1973 (Stoloff et al., 1976) of the crop corn stored on farms and in country elevators, aflatoxin contamination was most frequently encountered in the Southeast-Appalachia area with a 34 percent incidence of marketable corn with detectable aflatoxins (Table 2.1).

Aflatoxin in corn seems to be a worldwide problem. Limited surveys showed a high incidence and high level of aflatoxin contamination in corn samples from some African and Asian countries (Stoloff, 1976).

3-B.3. Bright Greenish-Yellow Fluorescence and Aflatoxins

Bright greenish-yellow fluorescence (BGYF) has been reported in cotton balls infected with *A. flavus* (Marsh et al., 1955). A positive correlation between aflatoxin and the occurrence of BGYF (Marsh et al., 1969) was reported. A similar fluorescence was detected in corn by Shotwell et al. (1972) and Fennell et al. (1973). Shotwell et al. (1972) suggested using long-wave ultraviolet light (365 nm wavelength) to detect BGYF with subsequent chemical analysis for aflatoxin. Preliminary evidence indicated a good correlation between BGYF and aflatoxin in the commercial corn (Fennell et al., 1973).

The relationship between fluorescences and the types of fungus in corn during storage has been investigated (Rambo et al., 1975). Two yellow dent hybrids were inoculated with *A. flavus* and *A. parasiticus* and stored in static and aerated systems. Two types of fluorescence, bright greenish-yellow (BGYF) and blue white (BWF) fluorescence, were observed. The *A. parasiticus* inoculated grain had more BWF than BGYF fluorescence, whereas corn inoculated with *A. flavus* had similar amounts of both types. The correlation between the incidence of either the BGYF or BWF and aflatoxins in individual kernels was 74-80 percent for

A. parasiticus (a good aflatoxin producer), but very low (5.0–6.2 percent) for *A. flavus* (a poor aflatoxin producer) (Rambo et al., 1975). Aflatoxin also occurred in 6.7 and 19.6 percent of the nonfluorescing kernels examined. Although some fungi-produced compounds in corn with other colors of fluorescence are not associated with aflatoxin, the substance responsible for the BGYF flow in corn is not aflatoxin but a substance often produced by the mold that also makes the toxin (USDA, 1977). Fluorescence, therefore, should be interpreted as a warning that more definite tests are required.

3-C. Detection and Determination of Aflatoxin in Corn

A number of analytical methods have been developed for the detection and determination of aflatoxin. These methods vary in purpose and complexity. Mycotoxins do not occur uniformly in contaminated corn; only a single highly-contaminated corn kernel may show contamination in an entire bulk of clean grain.

Methods for aflatoxin analysis in corn can be divided into three categories (Shotwell, 1977):

- (1) **Rapid Presumptive Tests:** to locate lots of corn that may contain mycotoxin by visual test of fluorescences under an ultraviolet lamp. Although numbers of BGY fluorescing particles are related to the level of aflatoxin, the BGY fluorescent test cannot be used to determine levels of toxin (Lillehoj et al., 1973; Shotwell et al., 1975C). A field method for the detection of aflatoxin based on this presumptive test has been proposed by Hunt et al. (1976). Samples with kernels exhibiting BGYF under high intensity black light were tested for aflatoxin content using Velasco's (1972) rapid florisil column method.

- (2) Screening Procedures: to detect the presence or absence of aflatoxin at a predetermined level. A small glass column (i.e. the minicolumn) containing appropriate adsorbents (e.g. florisil or silica gel) can be used as a quick screening procedure. The test requires 0.3 to 1 hour. The screening procedure has been adopted as the official first action by the Association of Official Analytical Chemists (AOAC, 1975) for the detection of aflatoxin in corn, peanuts, peanut butter, peanut meal, cottonseed meal, mixed feeds, and pistachio nuts (Romer and Campbell, 1976).

Romer (1975) described a screening method of detecting the total aflatoxins (B_1 , B_2 , G_1 , and G_2) in mixed feeds, grains, nuts and fruit products in samples containing as little as 5 to 15 ppb. A practical screening test was defined as having the following characteristics: (1) short time of analysis, about 30 minutes, (2) equipment, simple and inexpensive, (3) capability of being performed by an unskilled personnel, (4) low cost, (5) reasonable accuracy, (6) sensitivity of better than 20 ppb, and (7) suitability for analysis of mixed feeds and feed ingredients.

Holaday first developed the minicolumn screening procedure for peanuts and has since published an improved procedure (Holaday and Lansden, 1975). Shotwell and Stubblefield (1973) presented three screening methods for the determination of aflatoxin in corn. All three methods involve minicolumn chromatography of partially purified extracts. These studies were followed by a number of research reports on screening with the aid of minicolumns (Table 2.2). Detection limits of minicolumns range from 1 to 10 ppb aflatoxin. The reasonable accuracy and short throughput

Table 2.2. Screening methods using minicolumns* .

Reference	STEP					Detection limit(ppb)
	Extraction	Precipitation	Concentration	Minicolumn adsorbent	Minicolumn development	
Velasco (1972)	Aceton:water 85:15(v/v)	Ferric gel	Evaporation	Florisil	Decending	5
Shannon (1973)	Aceton:water 85:15(v/v)	Ammonium sulfate	Liquid-liquid transfer	Silica gel	Ascending	10
Pon (1973)	Acetonitrile: water 80:20 (v/v)	Lead acetate	Liquid-liquid transfer	Silica gel	Ascending	10
Barabolek (1974)	Acetone:water 85:15(v/v)	Ammonium sulfate	Evaporation	Florisil	Decending	1
Holaday (1975)	Methanol:water 80:20(v/v)	Zinc acetate	Liquid-liquid transfer	Florisil	Decending	2
Thomas (1975)	Methanol:water 60:40(v/v)	Cupric carbonate	Liquid-liquid transfer	Silica gel	Ascending	2

* previously compiled by Shotwell, 1977.

period have made the screening methods suitable for field use.

A rapid field method for the detection of aflatoxin contaminated corn has been developed (Shotwell et al., 1975B). The results were compared with laboratory quantitative and thin-layer chromatographic methods. No significant differences were found. Shotwell et al. (1976) devised another rapid screening test using minicolumns and chromatographic analysis for aflatoxins to be performed at the corn elevator level. Presence of aflatoxin in corn sample results in blue fluorescent band at top of florisil layer that can be identified by comparison with a standard column free of aflatoxin. The method detects total aflatoxin level of 20 ppb or higher.

- (3) Quantitative Methods: to determine the type and amount of aflatoxins. These procedures are usually lengthy (about 3 hours), complex and unsuited for field use. However, they can detect the amount of aflatoxins as low as 1 to 3 ppb, the lowest detectable level. The procedure recommended by the Association of Official Analytical Chemists (AOAC, 1975) and the American Association of Cereal Chemists (AACC, 1975) is the so-called CB (Contaminants Branch) method (Sec. 26.044-26.047, AOAC Official Method of Analysis, 12th edition).

Seitz and Mohr (1976) described a method extended from a simple screening test for the quantitation of aflatoxins in corn. The method is claimed to be faster, easier, and less expensive than the CB method and the results are similar. High-pressure liquid chromatography (HPLC) is used for the separation and quantitative identification of aflatoxins B₁, B₂, G₁, and G₂

with good resolution and high sensitivity, 1 to 2 ppb of each aflatoxin.

The chemical confirmation of the identity of aflatoxin is by the derivative formation method (AOAC, 1970) which the chemical derivatives of aflatoxins are formed directly on the thin-layer chromatographic plate. This simple rapid method for the confirmation of aflatoxin B₁ was developed by Przybylski (1975). The "Przybylski derivative procedure" has been shown to give good results and can be performed easily (Stack and Pohland, 1975).

3-D. Detoxification of Aflatoxin

The problems associated with the proposed methods of detoxifying aflatoxin-contaminated agricultural commodities have been reviewed by Goldblatt (1969). The toxicity and carcinogenicity of aflatoxin were investigated by Wogan (1973) and stated that aflatoxin B₁ has two functional groups, the dihydrofurofuran segment and the lactone-pentanone ring system, responsible for B₁ biological activity. To investigate the reaction of weak bases, such as ammonia, with aflatoxin, radiolabeled-C¹⁴ aflatoxin B₁ were added to corn grain flour (Beckwith et al., 1975). Low levels of ammonia as ammonia hydroxide ($\leq 2\text{g NH}_3/100\text{g}$ flour) caused irreversible binding of B₁ to corn flour components. It was further established that the binding is preferentially with the major protein fraction and water-soluble portion of the corn (Vesonder et al., 1975). Cucullu et al. (1976) proposed a series of chemical reactions for the ammoniation of aflatoxin B₁ to produce D₁ (M.W. 286) and a compound with M.W. 206.

In a laboratory test of corn samples inoculated with *A. flavus*, it was found that both ammonia (2 percent by wt.) and propionic acid

(1 percent by wt.) reduce mold growth and subsequent aflatoxin and ochratoxin formation. Both ammonia and propionic acid remained effective in inhibiting mold growth and aflatoxin production for 19 and 29 weeks, respectively (Vandegraft et al., 1975). Beckwith et al. (1976) investigated some chemical methods for detoxifying aflatoxins in foods and feeds and found that ammoniation at ambient temperatures decomposes and inactivates aflatoxins.

Aflatoxins in grain artificially inoculated were found to be destroyed in a continuous fermentation process and by-product isolation (Dam et al., 1977). The results indicated a loss of aflatoxins after fermentation of slightly greater than 60 percent of the original aflatoxin level. Further alkaline extraction treatments involved in the isolation of protein concentrate led to a destruction of total aflatoxins in excess of 90 percent. The destruction of aflatoxin have happened due to the alkaline (NaOH) extraction procedure during the process.

Besides chemical detoxification, some physical methods have been investigated. Roasting aflatoxin-contaminated corn was found to reduce aflatoxin levels (Shannon and Shotwell, 1975; Peplinski et al., 1975). Physical separation methods involving dry cleaning, wet cleaning, and hand separation of aflatoxin-contaminated grain were not successful (Brekke et al., 1975B) in lowering the aflatoxin content of the naturally contaminated corn.

4. Experimental Results from North Regional Research Laboratory (NRRL) of USDA

The results were generated from various tests on ammonia detoxification, ammonia preservation, and ammonia-assisted ambient air drying. The composition analysis of the ammonia-treated samples gives very

important clues on the actual chemical reaction between the grain components and ammonia. The experimental results presented in this section were closely related to the behaviors of ammonia in various ammonia treatment processes.

4-A. The Diffusion of Ammonia in Corn

Lancaster et al. (1974) proposed that "since the ammonia molecule is the same order of size as the water molecule, its rate should be similar at an equivalent driving force ". However, the molecular size alone cannot be taken to compare the diffusion rates. The ammonia molecule has stronger affinity towards the water molecule than the water molecule to itself as indicated by the relative mass diffusivities (Sec. 5-C.2., Chapter 5).

The diffusion of free ammonia from whole corn into water at room temperature is a slow process. The times needed for diffusion of free ammonia from the corn kernel are shown in Figure 2.1. It takes about six hours to extract 95 percent of free ammonia from the corn kernels. Results in Figure 2.1 roughly indicate the ammonia diffusion rate in the corn kernel despite the test is a soaking process. The fact of slow rates of ammonia diffusion in the corn kernel is evident and a slower rate of ammonia application will lose less ammonia in the exhaust air.

In another test by Lancaster et al. (1974) to investigate the time required to equilibrate ammonia treated and untreated corn, it was found that ammonia took about 20 times (about four days) longer to reach equilibrium than between corn and water in a stagnant situation. The long equilibration time indicates the difficulties of losing free ammonia from the corn kernels. Nevertheless, this test does demonstrate

that a homogeneous sample can be obtained from mixing ammonia-treated and ammonia-free samples.

In order to investigate the ammonia adsorption capability of low-moisture corn, a sample of 2.7 kg of corn at 12 percent m.c. (w.b.) was placed in a glass column and 7 percent of ammonia was added slowly with no escape of ammonia over a period of two days. The amount of free ammonia was 3.8 percent. Thus, the residuals constitute about 45.7 percent of the total ammonia added. It is also shown that the fixed ammonia content (or residuals) in corn increases with increasing temperature and time.

In a series of ammonia detoxification tests using aqua ammonia for corn samples adjusted to various moisture levels (Brekke et al., 1975), the percentages of ammonia with respect to the total ammonia added were determined. The results indicate that at ammonia addition levels of 1.5 percent and above, the free ammonia values level off at about 2/3 of the ammonia added when samples are held 14 days at 25°C. The lower the amount of total ammonia added, the lower the percentage of free ammonia is when the total ammonia level is below 1.5 percent.

4-B. The Fungicidal Effects of Ammonia

High moisture corn (27 percent) was treated with 0.48 percent ammonia applied as a 22 percent aqueous solution in a gas-tight tower silo (Harvestore System) containing 52.8 m³ of corn (Bothast et al., 1975). With the initial application of ammonia, all microorganisms were either eliminated or reduced significantly as shown in Figure 2.2.

It was suspected that the initial heating was a result of ammonia adsorption and the subsequent heating was due to the respiration of the developing microorganisms. After 30 days of storage, the free ammonia

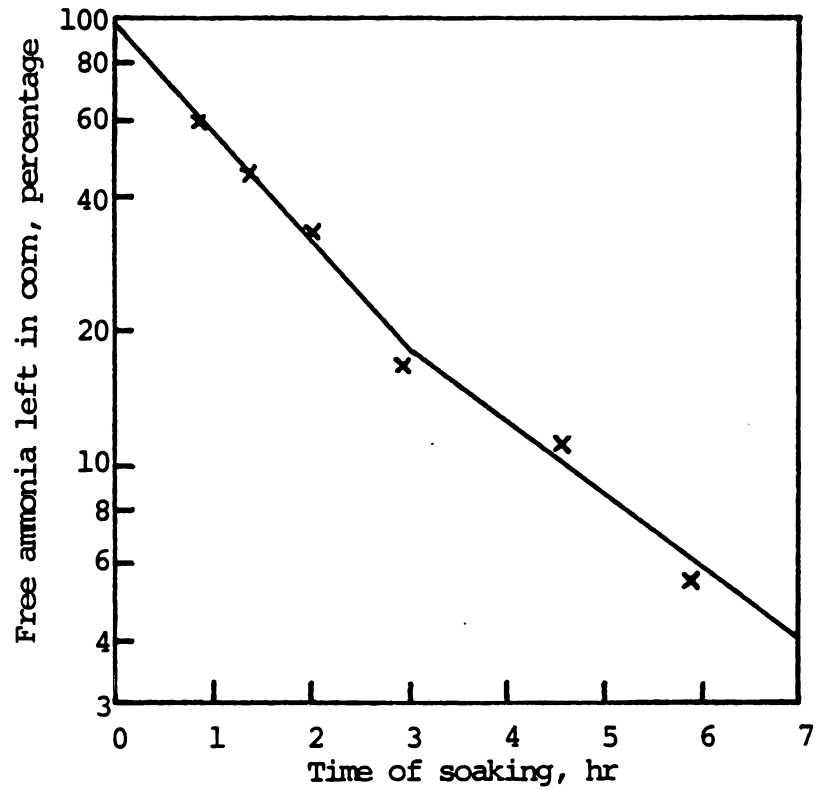


Figure 2.1. Diffusion of free ammonia from whole corn into water at room temperature (Lancaster et al., 1974).

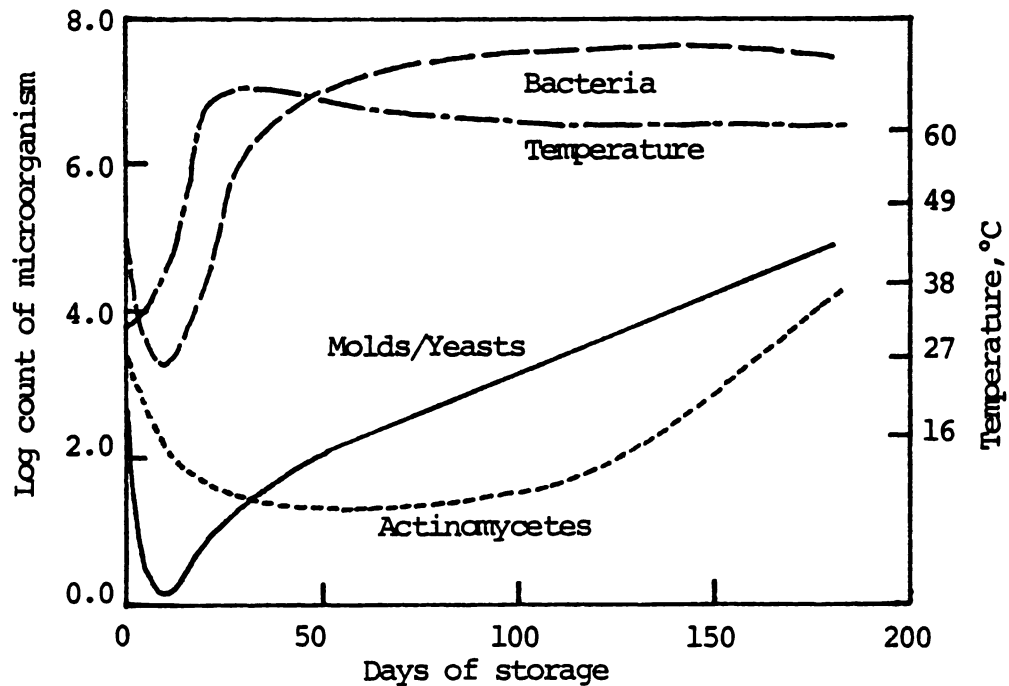


Figure 2.2. The initial application of ammonia eliminated or reduced all microorganisms (Bothast et al., 1975).

disappeared and the grain moisture migrated. Loss of fungicidal properties of the ammonia was evidenced by the increasing fungal and actinomycete populations after the first 10 days of storage.

4-C. The Closed-System Ammoniation

In a recycle gas-phase treatment of 17 and 26 percent moisture corn (Lancaster et al., 1975), 2.3 kg of shelled yellow dent corn was treated with ammonia in air in a glass column (6.9 cm I.D. x 114 cm long). The airflow through the column was 0.56 cmm/m³ (0.6 cfm/bu). The inlet ammonia concentration was 16.2 percent for the 17 percent moisture corn. The total amount of ammonia applied was equal to 2.5 percent within a three-hour period. For 26 percent moisture corn, 11.8 percent of inlet ammonia in the air was added over a 1 1/4-hour period. The total amount of ammonia applied is equal to 0.75 percent.

Lancaster et al. (1975) stated that localized adsorption of a quantity of ammonia equal to five percent in the corn can raise the corn temperature by 39°C in a stagnant and isolated system. The heating of corn during the application of anhydrous ammonia is fast and temporary in contrast to the slow temperature rise due to microbial growth observed during the subsequent storage period.

4-D. Influence of Ammonia and Moisture Levels on the Detoxification of Aflatoxin B₁

The influence of ammonia and moisture levels on the inactivation of aflatoxin B₁ was considered by Brekke et al. (1975). The samples were held for 14 days at 25°C after the treatment of aqua ammonia at different ammonia content levels. The pronounced effect of corn moisture on the inactivation of aflatoxin B₁ with ammonia is shown in Figure 2.3.

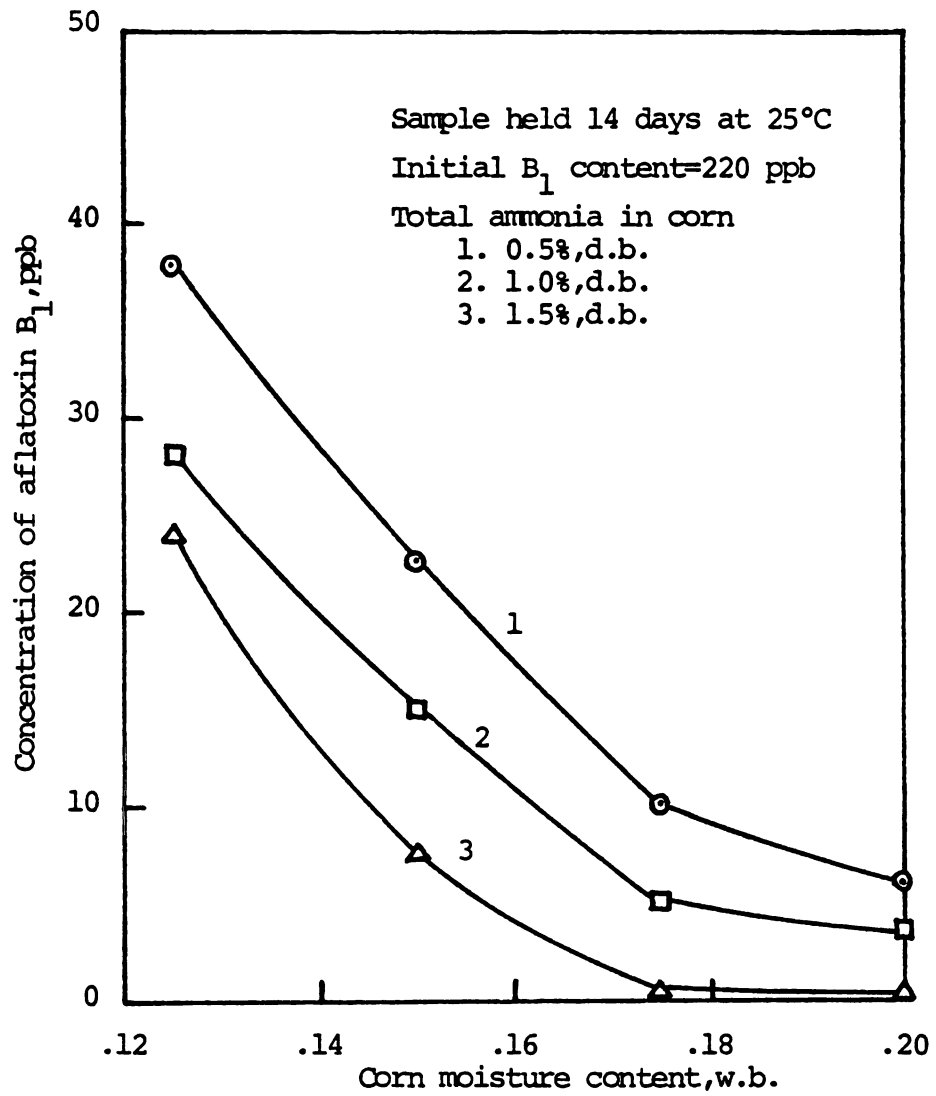


Figure 2.3. Effects of ammonia content and corn moisture level on the inactivation of aflatoxin B₁ (from Brekke et al., 1975).

The inactivation is much more effective when the corn is treated at higher moistures. At moisture contents above 17 percent, aflatoxin B₁ is almost completely inactivated when treated with 1.5 percent ammonia.

It can be concluded from the results in Figure 2.3 that treating lower-moisture corn requires a higher dosage of ammonia in order to reach the same degree of inactivation of aflatoxin B₁. The reason is that high-moisture corn is capable of dissolving more free ammonia which is the primary element for aflatoxin inactivation.

In another ammonia detoxification test of artificially contaminated (1000 ppb) corn samples (Brekke et al., 1975), the effectiveness of detoxification was found to be temperature dependent as shown in Figure 2.4. At higher temperatures, shorter periods of ammonia treatment were needed because of higher ammonia diffusion rate and higher chemical reaction rate between the aflatoxin and ammonia. Furthermore, less ammonia was needed at higher temperatures to have the same inactivation effect on aflatoxin B₁.

4-E. Long-Term Preservation of High-Moisture Grain

Although a high dosage of ammonia (1.5 percent) is frequently used in the detoxification process, the required amount of ammonia is much lower (0.5 percent) for the purpose of preserving freshly harvested high-moisture corn free from spoilage (Nofsinger et al., 1976).

In a long-term preservation test of high-moisture grain (Peplinski et al., 1975), ammoniation destroyed all molds, lowered bacteria counts for up to four months, and modified some chemical and physical properties of the treated corn. During a 14-month storage test of 4036 kg (158 bu) of 23 percent (w.b.) moisture corn treated initially with 1.02 percent aqua ammonia (in 19.2 percent solution, weight basis), the moisture

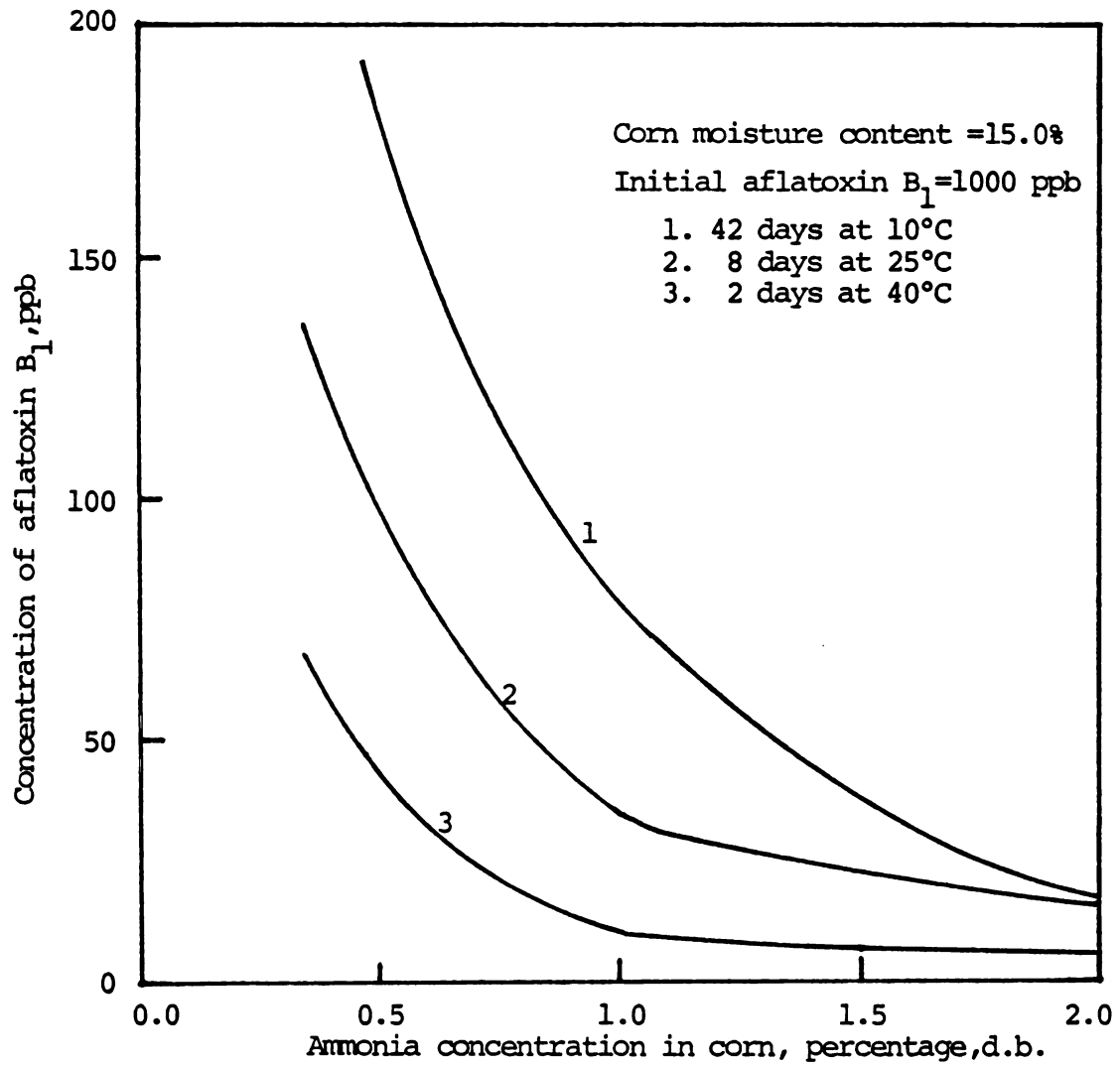


Figure 2.4. Effects of temperature on the inactivation of aflatoxin B₁ in corn (data taken from Brekke et al., 1975).

content of corn was increased to 28 percent. A 1.12-Kw (1.5-hp) centrifugal blower recycled the ammonia-air mixture. The mixture was recycled for periods of 1.5 to 25 hours at a flow rate of $1.8 \text{ cm}/\text{m}^3$. In total, an amount of 3.04 percent of ammonia was added to the corn in aqua and anhydrous form.

The relationships between the amount of ammonia applied, the average free ammonia content, the bacteria, and the mold counts are shown in Table 2.3 throughout the entire treatment. Molds were almost completely wiped out by ammonia after the first treatment of 1.02 percent ammonia. The bacteria counts were also reduced significantly due to the presence of ammonia.

The relationship between the free ammonia content and the bacteria count did indicate a general trend of lower bacteria count for the grain with higher free ammonia content (Peplinski et al., 1975). A limited correlation between bacteria and free ammonia shows that a minimum level of 0.50 percent free ammonia in the corn is necessary to keep bacteria below 100,000 per gram of corn.

In another ammonia-supplemented ambient drying test of high-moisture corn conducted by Nofsinger et al. (1976), 14.2 tons (560 bu) of 23.2 percent m.c. (w.b.) corn was dried with ambient air and ammonia preservation over six months without corn spoilage. The fan was rated 1/3 hp (248 W) and the airflow was $1.8 \text{ cm}/\text{ton}$ ($1.6 \text{ cfm}/\text{bu}$). The corn was dried to 17.7 percent in 56 days during which the fan operated 44 days. Anhydrous ammonia was applied intermittently. The ammonia application rate was much higher in the beginning of the drying process; about one-half of the total 42.9 kg ammonia was applied in the first three days and more than 75 percent of the total ammonia was applied in the first

Table 2.3. Effects of ammonia on inhibiting bacteria and mold growth and the relationship between free ammonia and the amount of ammonia added (data taken from Peplinski et al., 1975).

Day	Ammonia applied (%d.b.)	Average free ammonia (%d.b.)	Bacteria count (m.o./g)	Mold count (m.o./g)	Average corn MC (%w.b.)
0	1.02	0	2,000,000	630,000	23.0 28.0*
1	0	-	3,000	ND**	-
3	0	0.69	-	-	28.0
7	0	-	1,000	ND	-
13	0	0.25	-	-	27.0
26	0	0.13	-	-	26.3
28	0.26	-	-	-	-
32	0	0.29	410,000	ND	26.7
45	0	0.22	22,000	ND	27.0
60	0	0.09	1,030,000	30	27.3
67	0.51	-	-	-	-
69	0	0.42	-	-	27.0
98	0	0.28	182,000	ND	27.7
111	0.51	-	-	-	-
146	0	0.50	173,000	ND	28.0
166	0	0.37	114,000	ND	26.3
235	0	0.25	80,000	ND	27.7
242	0.26	-	-	-	-
276	0	0.19	902,000	ND	24.7
297	0.48	-	-	-	-
355	0	-	33,000	ND	-
410	0	0.27	-	-	20.3

* The moisture increase is due to the addition of aqua ammonia.

** ND = none detected

twelve days of ambient air drying. The air temperature varied from about 20 to -5°C and the relative humidity from 60 to 90 percent throughout the drying operation.

The maximum ammonia flow rate was 0.36 g/(hr.kg). The relationship between the total amount of ammonia actually picked up by corn and the cumulative ammonia added is shown in Figure 2.5. An appreciable amount of ammonia was lost in the exhaust air. The amount of ammonia remained in the corn consists of free and fixed ammonia during ammonia treatment. However, the portion of free ammonia will become either lost in the air or a part of fixed ammonia after an extended period of aeration.

Surface-sterilized corn kernels were tested for mold and bacteria growth during ammonia application. Mold counts were reduced from 6100 to 16 propagules/g and mold-infected kernels were reduced from 92 to 14 percent. Molds increased slightly thereafter but were effectively controlled by the presence of ammonia.

In contrast, bacteria counts increased from 2.4×10^4 to 1.6×10^7 /g during the first seven days of storage because of favorable growing temperature and humidity. The bacteria growth then leveled off and the subsequent growth was limited since the corn moisture level was reduced and unfavorable to microbial growth.

The amount of residual ammonia in the corn was found to be about 40 percent of the cumulative ammonia added in another ammonia grain drying test performed by Nofsinger et al. (1977) using typical farm-size bins. The largest retention of ammonia and lowest mold infection were detected near the bottom of the bin.

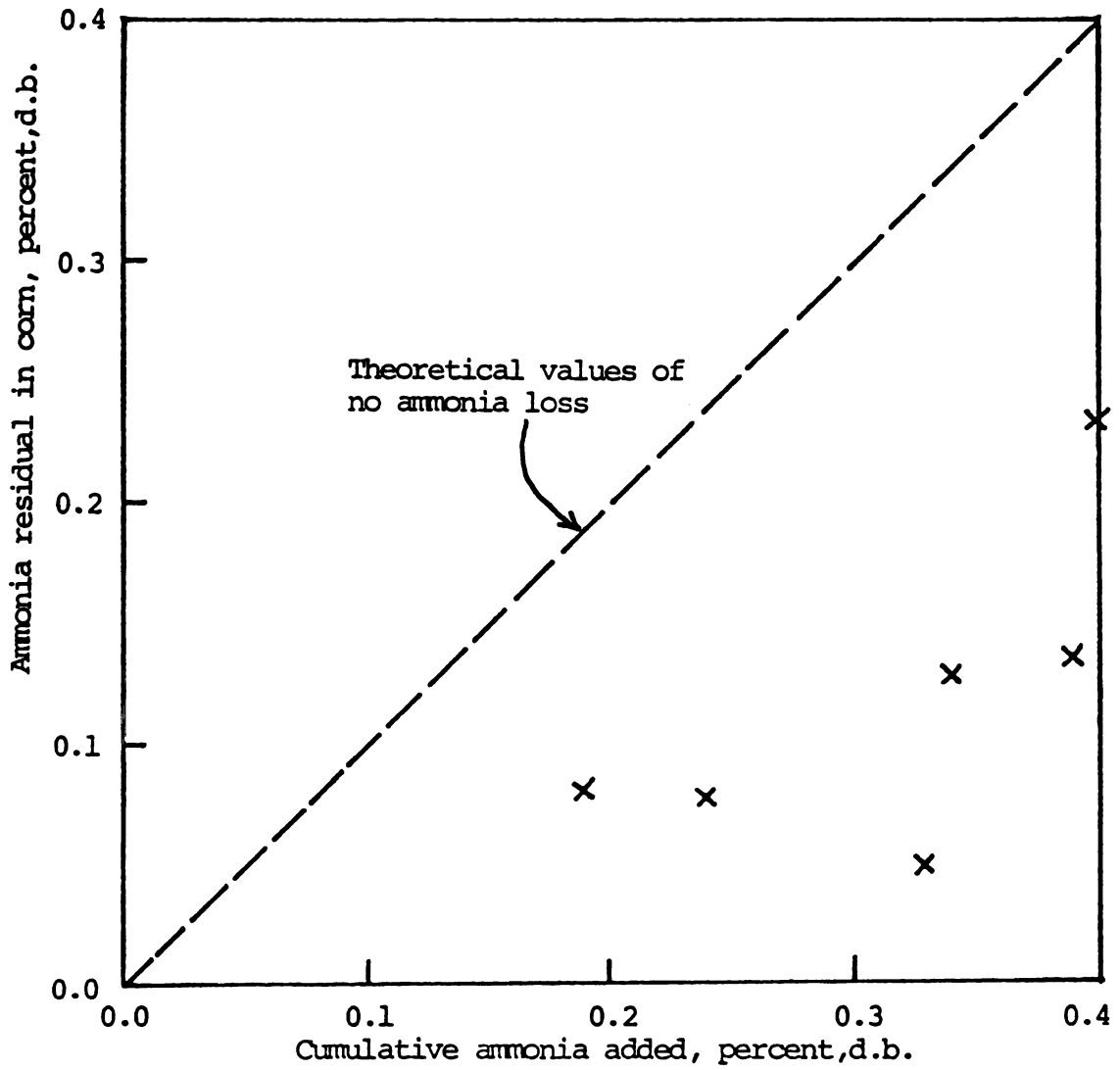


Figure 2.5. The amount of ammonia residual in corn as related to the cumulative amount of ammonia added (data taken from Nofsinger et al., 1976).

4-F. The Composition Changes of Ammonia-Treated Corn

The chemical changes of stored corn treated with ammonia during a 14-month storage test were analyzed by Peplinski et al. (1975). The percentage changes of the major components in corn are shown in Table 2.4.

The total nitrogen content in the corn increased from 1.5 to 2.1 percent which is about the same amount of increase for ammoniacal nitrogen. Among the 21.4 kg of ammonia adsorbed by the grain eventually, total ammonia (ammoniacal nitrogen) accounted for 74.3 percent (15.9 kg) of the total nitrogen increase. The rest 5.5 kg of ammonia applied reacted with corn components to form other than ammoniacal compounds which is evidenced by the increase in soluble solids from 6.5 to 9.5 percent. Analyses of the solid residues indicated that the chemical reaction products accounted for the change in soluble solids.

The decrease in extracted fat content is almost entirely due to the decrease in linoleic acid ($C_{18}H_{32}O_2$, an unsaturated fatty acid with two double bonds) content. Four unknown compounds ranging from 0.9 to 8.0 percent of the total fatty acid composition developed during the ammonia treatment due to the degradation of linoleic acid. The reduction of non-reducing sugars from 2.9 to 1.3 percent indicates microbial growth and respiration.

At the end of the 410 days storage test, the corn was removed in six separate layers. Excluding higher-moisture corn adhering to the bin walls, 90 percent of the corn was removed with moisture contents ranging from 15 to 24 percent. The chemical composition of each layer of corn is shown in Table 2.5. The free ammonia content, higher toward the top of the bin, averaged 0.2 percent while the total nitrogen content averaged 2.2 percent.

Table 2.4. Chemical analysis of the stored corn (Peplinski et al., 1975).

Day	Total nitrogen (%d.b.)	Total ammonia (%d.b.)	Fat extracted (%d.b.)	Linoleic acid* (%d.b.)	Starch (%d.b.)	Non-reducing sugars (%d.b.)	Ash (%d.b.)	Soluble solids (%d.b.)
0	1.5	0	4.5	61.0	71.0	2.9	1.3	6.5
3	1.8	0.2	4.2	43.0	70.0	2.7	1.3	7.5
13	1.8	0.3	3.5	35.0	71.0	2.2	1.3	6.3
26	1.9	0.3	3.5	27.0	71.0	2.0	1.3	6.5
32	2.0	0.3	3.2	24.0	70.0	2.5	1.3	6.5
45	2.0	0.4	3.1	23.0	71.0	2.3	1.3	6.9
98	2.1	0.4	2.8	19.0	75.0	1.3	1.4	7.6
146	2.0	0.4	2.9	16.0	73.0	1.4	1.4	7.2
166	-	0.4	2.7	16.0	73.0	-	1.4	8.2
235	1.9	0.4	2.5	16.0	69.0	1.1	1.4	9.5
276	2.1	0.4	2.6	16.0	73.0	1.0	1.5	9.3
410	2.1	0.5	2.4	17.0	73.0	1.3	1.3	9.5

* as percent of extracted fat.

Table 2.5. Chemical analysis of corn removed from storage by layers* (Peplinski et al., 1975).

Layer	Moisture content (%w.b.)	Free ammonia (%d.b.)	Total nitrogen (%d.b.)	Fat extracted (%d.b.)	Linoleic acid** (%d.b.)	Starch (%d.b.)	Non-reducing sugars (%d.b.)	Ash (%d.b.)	Soluble solids (%d.b.)
top	23.0	0.3	2.1	2.0	12.0	74.0	1.4	1.1	13.0
2	24.0	0.3	2.3	2.1	11.0	74.0	1.6	1.4	12.0
3	22.0	0.2	2.3	2.2	12.0	74.0	1.6	1.4	12.0
4	20.0	0.2	2.2	2.2	14.0	74.0	1.8	1.4	11.0
5	17.0	0.2	2.2	2.3	15.0	74.0	1.7	1.4	9.0
bottom	15.0	0.1	2.1	2.7	21.0	75.0	1.8	1.4	7.0
Weighted average	20.0	0.2	2.2	2.3	15.0	74.0	1.7	1.4	10.0

* excluding the high-moisture corn adhering to the bin wall.

** as percent of extracted fat.

The general trend of variations in the chemical compositions of different layers is as follows: 1. The fat and linoleic acid increased while the soluble solids content decreased toward the bin bottom. This is an indication of more chemical reactions happening between ammonia and corn components toward the bin top than the bottom. This is due to the more ammonia dissolved in the grain in the bin top as a result of the higher grain moisture content. 2. The non-reducing sugar (sucrose) content increased toward the bin bottom. This is a sign of more microbial activity in the top layers as was expected. 3. Starch and ash contents did not vary significantly in the grain samples throughout the bin.

The following practical information has been summarized from the above experimental results which have assisted this investigation:

1. The fungicidal effects of ammonia towards molds, bacteria, and aflatoxins have been verified.
2. Practical-scale tests of the ammonia treatment for high-moisture corn have been performed and were proved to be feasible, practical, and economical.
3. The total ammonia in corn consists of the free ammonia and the fixed ammonia; the fixed ammonia content was found to be about 30 to 50 percent of the total ammonia depending on the rapidity and the amount of ammonia application.
4. The composition analysis of the ammonia-treated corn has verified the existence and the amount of residuals — the fixed ammonia.
5. The amount of ammonia required in a long-time preservation and drying test of corn is about 0.5 percent d.b. (based

on the weight of dry corn).

6. The amount of ammonia required for the detoxification of a batch of aflatoxin-contaminated corn is about 1.5 to 3.0 percent d.b.
7. Only an aeration fan which delivers around 1 to 2 cmm/ton is required in the ammonia-assisted ambient air drying and the ammonia treatment permits several months to dry the corn to 15.5 percent w.b. without spoilage.
8. The trickle (intermittent injection) ammonia application process requires a high dosage in the beginning to completely inactivate the initial contamination of microorganisms.

Nevertheless, it was found that some important aspects were ignored. The following information is essential in analyzing the ammonia grain drying system but is lacking in the above experimental results:

1. the ammonia sorption isotherm which is necessary in describing the steady state sorption characteristics;
2. the dynamic movement of ammonia in the grain bin, i.e. the ammonia concentration changes with time and position;
3. a systematic analysis of the influence of important parameters, such as the mass transfer coefficient, airflow rate, inlet ammonia concentration, grain moisture content, temperature, etc., on the ammonia sorption processes.

The result of a systematic analysis will not only identify the important parameters in the system but also establish the basis of a prediction model.

CHAPTER 3

AMMONIA SORPTION ISOTHEIRMS

1. Introduction

In order to investigate the behavior of ammonia in a fixed bed of biological products, such as grains, the mass transfer processes of ammonia between the moving air stream and the fixed bed of grain must be analyzed. The ammonia sorption in a fixed bed of corn is a dynamic process. The proposed model is deterministic (without random variables). In analyzing a dynamic process, a steady-state system is frequently first investigated. In the steady-state system, all the parameters are independent of time and the system is studied under equilibrium conditions. The curve of ammonia sorption behavior at constant temperature is called the Ammonia Sorption Isotherm.

2. Adsorption and Diffusion Models

Adsorption results from the field force at the surface of the solid (adsorbent) which attracts gas molecules (adsorbate) and are in turn adhered to the solid. The force of attraction could come from physical (van der Waal's type) or chemical means.

The process of adsorption has important applications in drying, purification, separation, catalysis, waste treatment and many other chemical processes. The adsorption system in the ammonia grain drying system consists of corn (the adsorbent) and ammonia gas (the adsorbate). In general, the majority of large scale commercial applications of

adsorption involves nonisothermal adsorption of multicomponent mixtures in fixed or fluidized beds. The ammonia grain drying system is one example of an adsorption application in agriculture. Strictly speaking, in most agricultural crop drying systems, treating a fixed bed of corn with ammonia-air mixture is an example of the adsorption process. The process involves nonisothermal sorptions of multicomponent mixtures of ammonia, moisture, and dry air.

The rate expressions of sorption processes have been classified into three groups: (1) external diffusion, (2) surface adsorption, and (3) internal diffusion. The sorption process consists of numerous different processes; the rate at which an adsorbent takes up adsorbate can be limited by any or all of the above models.

2-A. The External Diffusion Models-Diffusion in Fluid

The external diffusion model describes the concentration gradient existing within the bulk stream of the fluid phase and the transport mechanism of the ammonia to the external surface of corn. The overall rate of adsorption depends on the diffusion velocity of ammonia from the bulk stream to the vicinity of the corn surface and on the rate of adsorption of ammonia at the surface layer of the corn. The external diffusion model is usually expressed by Fick's diffusion equation:

$$\frac{\partial C}{\partial t} = D \nabla^2 C \quad (3.1)$$

where C is the concentration of adsorbate, t is the time, and D is the diffusion coefficient.

Equation (3.1) is a form of Fick's second law and is analogous to the transient heat conduction equation. The solution of this equation involves prescribed boundary conditions and numerical techniques,

such as finite differences, finite element methods, etc.

In the external diffusion model it is assumed that the rate of surface adsorption is so rapid that there is solely diffusion control. The ammonia adsorption isotherm defines the boundary condition. Nevertheless, the mathematical model defined by the diffusion law and the boundary condition mentioned above poses a very complex problem, since the model equation (Equation 3.1) involves two independent variables and second order differential term(s). It is usually simplified to the "film diffusion model" by defining a simple mass transfer equation to describe the external diffusion of adsorbate from the bulk stream to the outer surface of the solid:

$$\frac{dq}{dt} = k_f a (C - C_\infty) \quad (3.2)$$

where q is the adsorbate content in solid, a is the specific (external) surface area of solid particles, and k_f is the fluid-phase mass transfer coefficient. The driving force for mass transfer is defined by the concentration difference across an effective "film" resistance surrounding the particle between the fluid at the surface (C) and the bulk fluid (C_∞). The mass transfer coefficient k_f is a function of fluid velocity, viscosity, density, the diffusivity of adsorbate in the fluid, and the size and shape of the solid particles.

2-B. The Surface Adsorption Models

The surface adsorption model describes the mass transfer on the solid surfaces. Solid adsorbents have a limited total internal surface area on which adsorbate can be adsorbed.

The theory of the adsorption rate on an active surface was first derived by Langmuir (1918) who equated the rate of capture of molecules

from the gas to the rate of escape of molecules from the surface under equilibrium conditions:

$$k_a p(1-\theta_a) = k_d \theta_a \quad (3.3)$$

where k_a and k_d are the rate constants for adsorption and desorption, θ_a is the fraction of surface area covered by adsorbed molecules, and p is the partial pressure of the adsorbate molecules. Solving for θ_a and letting $K_A = k_a/k_d$,

$$\theta_a = \frac{K_A p}{1+K_A p} \quad (3.4)$$

In the case of ammonia adsorption in corn, the equilibrium concentration of ammonia in corn (x_2^*) at any concentration of ammonia in the air (x_1) can be expressed using the above equation:

$$x_2^* = \frac{x_{2m} x_1}{K_L + x_1} \quad (3.5)$$

where,

$$x_2^* = \theta_a \cdot x_{2m}$$

$$x_1 = p/p_s$$

$$K_L = 1/K_A p_s$$

$$p_s = \text{saturated ammonia pressure}$$

The capacity of the solid phase onto which adsorbate can be adsorbed (x_{2m}) refers to the total coverage of active sites on the solid surface where the adsorption solely occurs. However, in the ammonia adsorption process in corn, the only active component in corn absorbing ammonia is assumed to be water. The water portion is believed to be distributed evenly within the entire corn kernel. Thus, the following assumptions must be proposed in order to use the Langmuir monolayer surface adsorption

isotherm for the ammonia-corn system:

- 1) The individual corn kernel is small enough that the internal ammonia concentration gradient can be neglected, or, the ammonia in corn at any moment is rapidly equilibrated and evenly distributed. In other words, all the active sites of corn in adsorbing ammonia are located on the surface.
- 2) All the other components besides water in corn absorb a negligible amount of ammonia through physical adsorption or chemisorption.

The Langmuir isotherm describes the processes of ion exchange, active carbon adsorption, etc., since these processes obviously fall in the category of surface adsorption. Nevertheless, the sorption processes of ammonia or water in most biological products cannot be explained satisfactorily by the Langmuir monolayer isotherm alone. In dealing with the sorption of water vapor in food products, the BET equation (Brunauer, Emmett, and Teller, 1938) is frequently used. The BET equation allows multilayer adsorption on the solid surface.

$$\frac{x_2^*}{x_{2m}} = \frac{c_1 x_1}{(1 - x_1) [1 + (c_1 - 1)x_1]} \quad (3.6)$$

A simplified expression for the constant c_1 is:

$$c_1 = \exp (Q_s/R'T) \quad (3.7)$$

where,

Q_s = site interaction energy of adsorption = $Q_1 - L$,

Q_1 = total heat of adsorption of the monolayer,

L = latent heat of evaporation of adsorbate at temperature T ,

T = absolute temperature, and

R' = universal gas constant.

Q_1 may be estimated by the heat of solution of ammonia in water, 8480 cal/mole and the latent heat of evaporation, L , of ammonia is 4889 cal/mole at 15.6°C.

In certain cases when the number of layers is limited to a finite number n , the BET treatment leads to the modified equation:

$$\frac{x_2^*}{x_{2m}} = \frac{c_1 x_1}{1 - x_1} \cdot \frac{1 - (m+1) x_1^m + m x_1^{m+1}}{1 + (c_1 - 1)x_1 - c_1 x_1^{m+1}} \quad (3.8)$$

Equation 3.8 represents the general BET equation which includes special cases such as the Langmuir isotherm (Equation 3.5) by letting $m = 1$, and the standard BET equation (Equation 3.6) by putting $m = \infty$. These two extreme sorption isotherm types are shown in Figure 3.1.

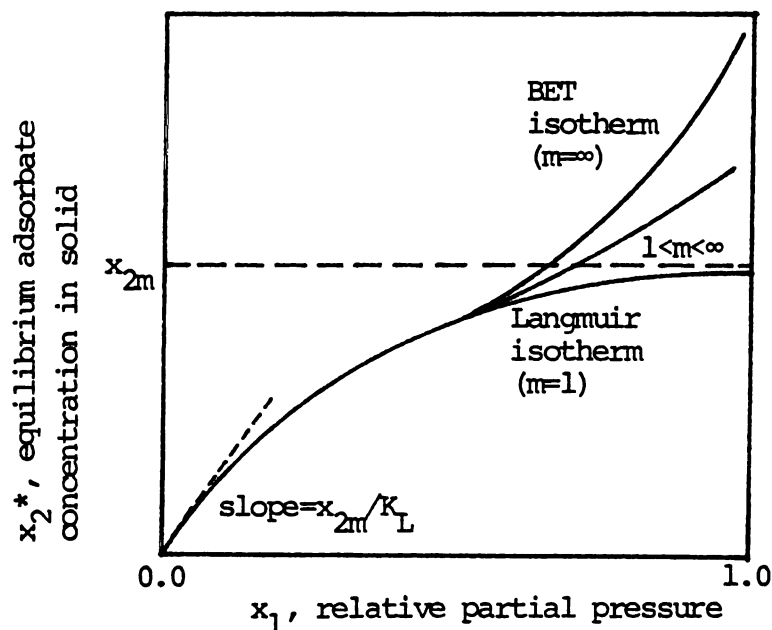


Figure 3.1. Types of generalized BET adsorption isotherm.

At low relative partial pressures of adsorbate in a fluid stream, the sorption behavior has negligible difference for Langmuir and BET equations since they are still in the monolayer adsorption region. Therefore, it is not necessary to differentiate these models if the

ammonia concentration in the air is low.

2-C. The Internal Diffusion Models—Diffusion in Solid

The internal diffusion process involves the transport of adsorbate to the interior of the adsorbent through one of the following mechanisms:

- 1) gaseous diffusion through the pore structures, e.g. pores, crevices, capillaries, cracks, and checks, in a porous adsorbent, or
- 2) surface diffusion along the solid surfaces of the pores in a porous adsorbent, or
- 3) solid diffusion through the homogeneous, permeable, non-porous adsorbent.

Adsorbents are usually classified as porous and non-porous depending on the effective radii of the pores. The effective radii of the largest variety of adsorbent pores (macropores) exceed 1000\AA , the effective radii of intermediate pores ranges from 18 to 1000\AA and those of the smallest variety of pores (micropores) ranges from 5 to 10\AA (Dubinin, 1972). As the pore size diminishes, the "porous" material becomes non-porous.

Diffusion in porous materials may occur by one or more of the following three mechanisms (Sherwood, 1975):

- 1) Ordinary or bulk diffusion: prevails as the pores are large in relation to the mean free path* of the molecules of adsorbate. The process is recognized as an ordinary diffusion within the gas contained in the pores. The resistance to diffusion along the pores is due primarily to molecular collisions. Hence, the resistance

* "Mean free path" is important in kinetic theory, and means the average distance a molecule travels between collisions with each other. The mean free path of ammonia is 441\AA at 0°C and 1 atmosphere (Moore, 1965).

of the pore walls may be neglected and the diffusion coefficient will be independent of the pore radius. The diffusion coefficients values range between $1.0 \text{ cm}^2/\text{sec}$ for gaseous and 10^{-4} to $10^{-5} \text{ cm}^2/\text{sec}$ for liquids (Wheeler, 1951). For gaseous, the diffusion coefficient is inversely proportional to the pressure and is proportional to $T^{1.5}$ or $T^{1.75}$ (Smith, 1970; Karger et al., 1973). The rate equations proposed by some researchers have been thoroughly reviewed by Park (1974).

- 2) Knudsen diffusion: occurs when the pore sizes are small compared to the mean free path of the gas molecules. The molecules collide much more frequently with the pore walls than with each other. A molecule travels within the pores by a series of "random flights" interrupted by collisions with the pore wall and adsorption by the pore walls.
- 3) Surface diffusion: occurs when the diffusion species are adsorbed by the solids. The equilibrium surface concentration increases with concentration in the gas. So the surface layer tends to develop a concentration gradient in the solid in the same sign and direction as the concentration gradient of the gas in the pore. If the rate of surface diffusion is not the limiting factor or if the size of particle is small enough, the concentration gradient in the solid can be neglected.

3. Production and the Properties of Ammonia

3-A. Energy Required in Ammonia Production

Anhydrous ammonia is being produced industrially from natural gas through a series of high temperature chemical reactions. The energy

requirement of the production of one ton of anhydrous ammonia is (Faith et al., 1975):

<u>Input</u>	<u>Quantity</u>	<u>Energy Equivalent/ton</u>
Natural Gas (92% methane)	736 m ³	2.719 x 10 ¹⁰ J
Fuel Gas (for driving compressors)	0.594 m ³	2.321 x 10 ¹⁰ J
Electricity	108 Kw hr	3.888 x 10 ⁸ J
<hr/> Total:		5.079 x 10 ¹⁰ J/ton

The total energy input for the production of one ton of anhydrous ammonia amounts to about 5.079 x 10¹⁰ J/ton, or 5.598 x 10⁷ J/kg-ammonia (24067 Btu/lb-ammonia).

3-B. Physical Properties of Ammonia

Ammonia is colorless and has a pungent odor. The physical properties of ammonia are listed in Table 3.1. From the solubility of ammonia in water and the density of ammonia gas, it is known that liquid water is able to absorb over 600 times its volume of ammonia gas at 0°C, one atmosphere. The toxicity limit is the concentration of ammonia to which workers may be exposed without harmful effects. The ammonia concentrations of 20 to 50 ppm in the air can be detected by smell. At high concentrations (above 700 ppm) of ammonia can cause severe irritations to the eyes, bleeding and swollen eyelids. Without immediate medical treatment, partial or complete loss of vision may occur.

Moist skin is mildly irritated when a concentration of one percent of bulk air is reached in the atmosphere. Liquid anhydrous ammonia in contact with the skin will cause severe burns and frostbite due to

Table 3.1. Physical properties of ammonia*.

Molecular weight	17.03
Specific volume (at 21°C, 1 atm)	1411 ml/g (22.6 ft ³ /lb)
Boiling point (at 1 atm)	-33.4°C (-28.1°F)
Freezing point (at 1 atm)	-77.7°C (-107.9°F)
Density, Gas (at 0°C, 1 atm)	0.00077 g/ml
Liquid (at b.p.)	0.674 g/ml
Viscosity, Gas (at 0°C, 1 atm)	0.00918 centipoise
Flammability limits in air	15-28 percent (by volume)
Heat of vaporization (at b.p.)	327.4 cal/g
Heat capacity, Gas (at 25°C, 1 atm)	
C _p	0.516 cal/g°C
C _v	0.407 cal/g°C
Ratio of C _p /C _v	1.269
Vapor pressure (at 21°C)	7.867 x 10 ⁴ N/m ²
	(114.1 psig)
Solubility in water (at 0°C, 1 atm)	47.3 g/100 g water
Thermal conductivity, Gas (at	
0°C, 1 atm)	0.02184 W/m K
Specific gravity, Gas (at 0°C, 1 atm) ..	0.597
Toxicity limit (Threshold limit value).	25 ppm

* From LINDE, Product Information, Union Carbide, specialty gases and equipment (1977).

the rapid evaporation of ammonia from the skin surface.

Although ammonia is a non-flammable gas when contained in a tank with liquid phase, it can be ignited in air at concentrations of 15 to 28 percent by volume, when sparked. Workers handling ammonia should wear a face shield in addition to the normal safety equipment. It is also recommended that anyone working with anhydrous ammonia carry a small spray bottle of water as a first aid to flush and protect the eyes.

3-C. Vapor Pressure of Ammonia

3-C.1. Vapor Pressure of Liquid Ammonia

The vapor pressure of liquid ammonia in a container as a function of temperature is shown in Figure 3.2. The ammonia vapor pressure is increased exponentially with temperature. At higher temperatures, the vapor pressure increases significantly. Thus, keeping the ammonia tank covered or sheltered while it is left in the field is very important in preventing overheating of the tank by direct sunlight.

3-C.2. Partial Pressure of Ammonia in Aqueous Solution

The partial pressures of ammonia over an aqueous solution of ammonia are listed in Table 3.2. The units for ammonia concentration both in the air and in the solution are expressed in accordance with those of the water vapor adsorption isotherm. The ammonia concentration in the air is expressed as the volume percentage at one atmosphere based on the bulk stream total volume. However, as a matter of consistency and simplicity in the model equations and computer implementation, the ammonia concentration in the air is expressed on the basis of volume percentage per dry air volume.

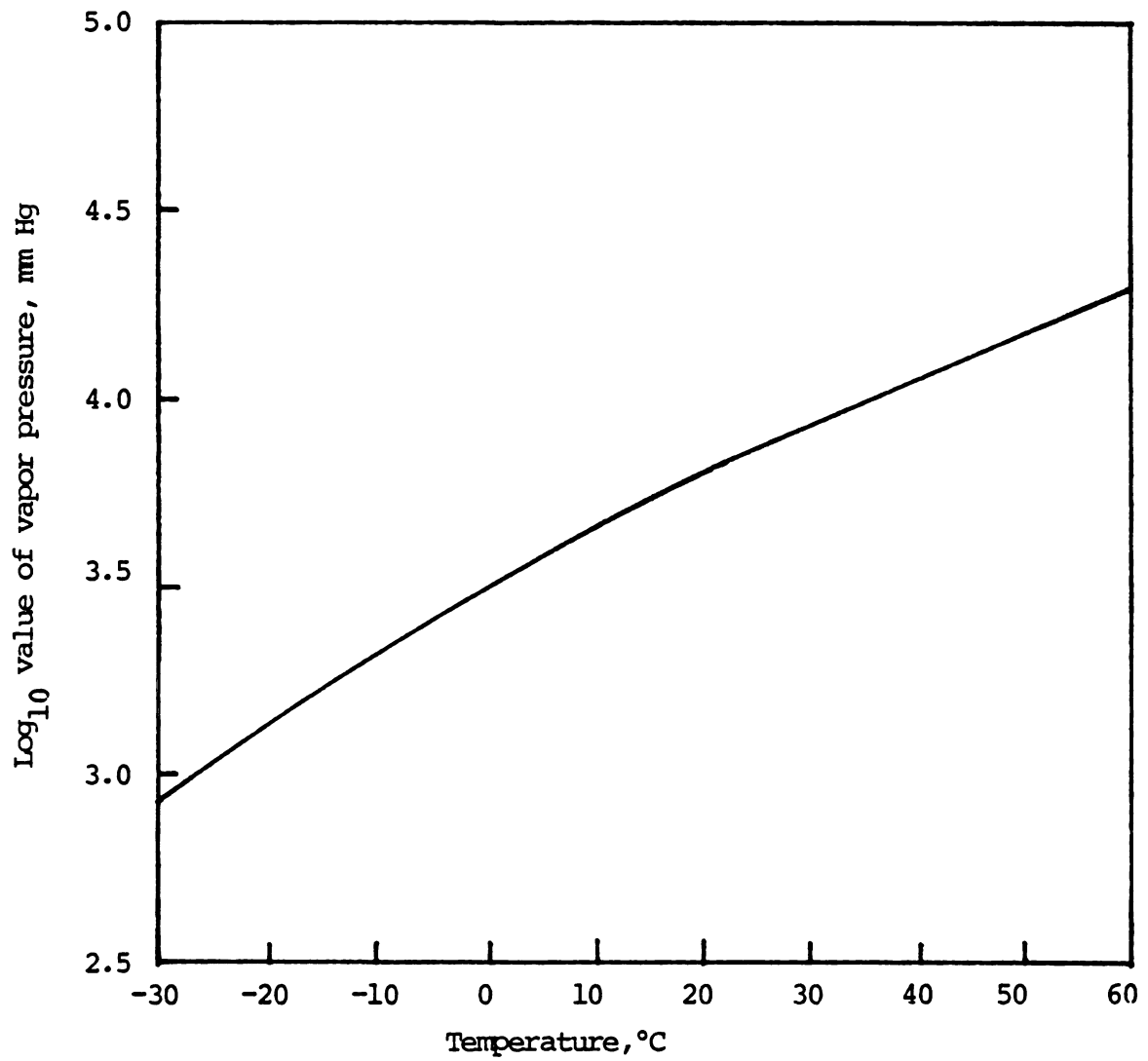


Figure 3.2. The vapor pressure of ammonia as a function of temperature.

Table 3-2. Partial pressures of ammonia over aqueous solution of ammonia (from Liley and Gambill, 1973).

Ammonia concentration in the solution ¹	Ammonia concentration in the air at 1 atm ²						
	(ml-NH ₃ / 100 ml-bulk stream)						
	0°C	4.4°C	10°C	15.6°C	21.1°C	26.7°C	32.2°C
4.74	1.77	2.25	3.20	4.22	5.65	7.08	9.25
9.50	3.54	4.49	6.06	8.10	10.34	13.47	17.15
14.29	6.12	7.76	10.21	13.61	17.69	22.73	28.92
19.10	10.27	13.06	17.22	21.84	29.12	37.08	46.82
23.94	18.17	21.50	28.31	36.47	46.75	59.13	74.10
28.81	29.06	34.91	45.11	57.70	73.22	92.00	114.04
33.71	44.50	54.30	69.68	88.87	111.12	138.06	-----
38.64	60.76	81.52	103.70	130.31	-----	-----	-----
43.59	96.15	116.63	-----	-----	-----	-----	-----
48.57	131.74	-----	-----	-----	-----	-----	-----

1. Units for ammonia concentration in the solution are in weight percentages, g-NH₃ / 100 g-water.
2. The values of ammonia concentration in the air were originally shown as psia by Liley and Gambill (1973).

Isotherms for ammonia solution at one atmosphere are plotted in Figure 3.3. Due to the characteristics of the saturation of ammonia in aqueous solution, the isotherm curves for ammonia solution resemble Langmuir isotherms even though they are not certainly related. At higher temperatures, the same partial pressure of ammonia in the air will dissolve a less amount of ammonia in water under equilibrium conditions since the solubility of ammonia in water is smaller at higher temperatures.

4. Adsorption and Desorption of Ammonia in Corn

4-A. Classification of Sorption Isotherms

The amount of adsorbate adsorbed (y) per unit mass of adsorbent depends on the equilibrium partial pressure of the adsorbate (p), the temperature (T), and the nature of the gas (g) and solid (s):

$$y = f(p, T, g, s) \quad (3.9)$$

In general, the sorption system is investigated under constant temperature (i.e. isothermal) and under the assumption that the properties and state of gas and solid do not vary significantly, Equation 3.9 simplifies to:

$$y = f(p)_{T,g,s} \quad (3.10)$$

if the gas is below its critical temperature* throughout the temperature ranges considered. In other words, there is no phase change due to temperature changes alone. The following equation is most commonly referred to as the adsorption isotherm equation:

* For ammonia gas (NH_3), the critical temperature is 405.6 K (Moore, 1965), which is well above the temperature range considered here.

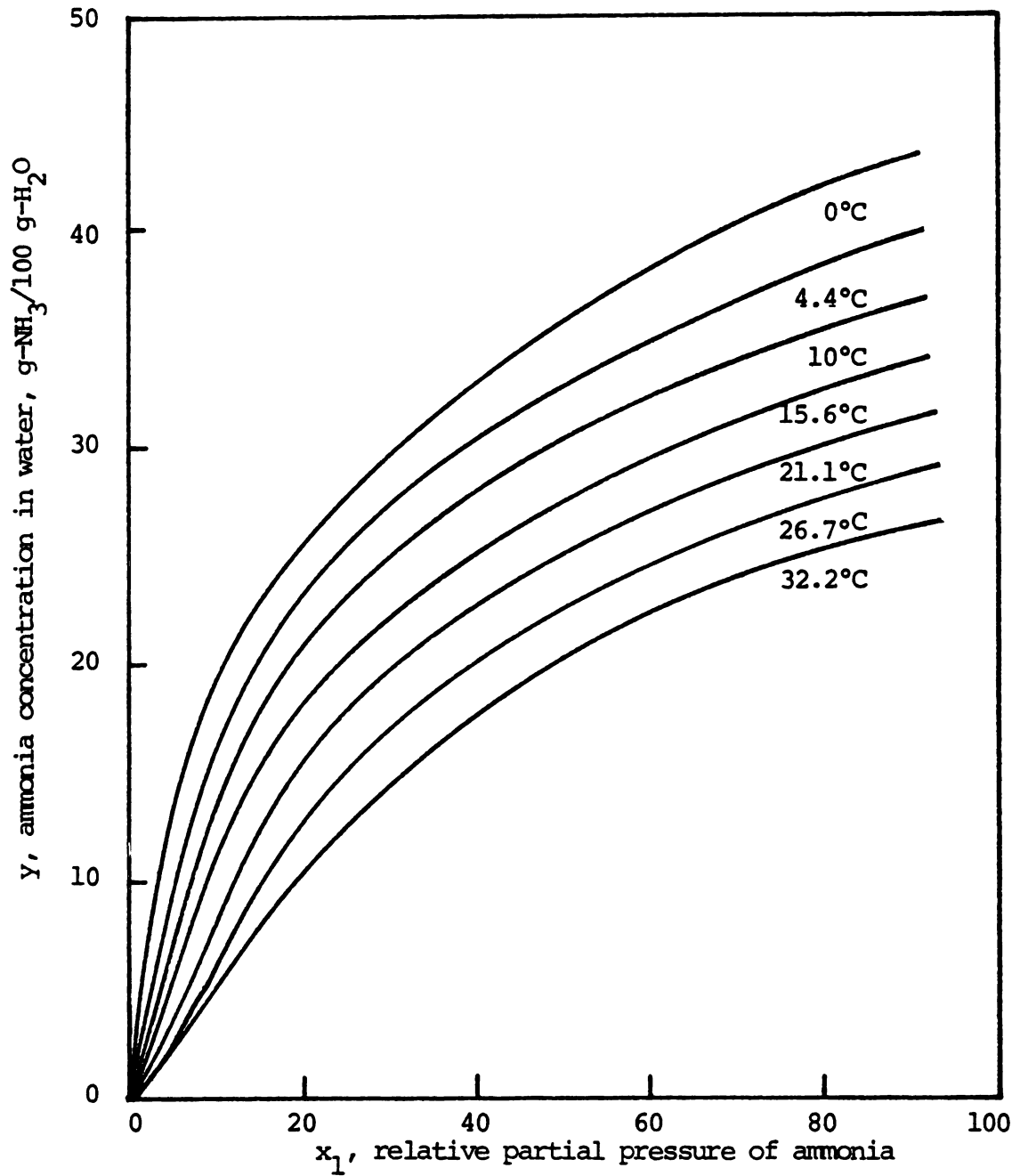


Figure 3.3. Ammonia isotherm curves in ammonia-water system at 1 atm.

$$y = f(x)_{T,g,s}$$

where $x = p/p_0$ is the relative partial pressure and p_0 is the saturation vapor pressure of the adsorbate.

Most of the adsorption isotherms resulted from physical adsorption and reported in the literature have been classified into five types by Brunauer, Emmett, and Teller (BET) (1938) as shown in Figure 3.4. Type I is the Langmuir adsorption isotherm which is interpreted as a monolayer adsorption phenomenon. The S-shaped Type II is the well known BET isotherm for multilayer adsorption. Physical interpretations of Types II, III, IV, and V were presented by Brunauer, Deming, Deming, and Teller (1940). Types II and III resemble Types IV and V respectively except when the relative pressure approaches 1.0, the adsorption in Types II and III increases sharply and in some cases approaches $x = 1.0$ line asymptotically whereas the adsorption in Types IV and V levels off and approaches maxima.

Not all the isotherm curves can be classified into the above five classical types. As a matter of fact, many of the isotherms encountered in practice also show a further upward turn (denoted by the dotted lines in Figure 3.4) as the saturation vapor pressure is approached (Gregg and Sing, 1967).

4-B. Equilibrium Ammonia Content in Aqueous Solution

The equilibrium ammonia content curves in aqueous solution at temperatures ranging from 0 to 32.2°C are shown in Figure 3.3. Although the sorption isotherm curves in a liquid solution cannot be classified in the category of the five adsorption isotherms mentioned above, the ammonia isotherm in aqueous solution can be investigated as an adsorption

isotherm in solids if the water portion in the solid adsorbent be considered the primary "sites" of ammonia adsorption.

Judging from the shape of isotherm curves in Figure 3.3 at different temperatures, they look like isotherm curves in Type I Langmuir monolayer adsorption at lower temperatures and Type V at higher temperatures. Both types I and V possess a saturation value but differ at lower relative pressure ranges. Strictly speaking, isotherm curves in Figure 3.3 are not purely physical adsorption isotherms and they have no direct relationships with the (surface) adsorption in the solid. Nevertheless, satisfactory explanations can be stated indirectly if one would relate ammonia in aqueous solution to the ammonia in water-containing corn. An analog is existed between the saturation characteristics of gas ammonia in an aqueous solution under certain pressure and the saturation of active surface sites of adsorption for a porous medium.

In the practical application of ammonia treatment for grains, the concentrations of ammonia in the air seldom exceed 20 percent of the saturated partial pressure of ammonia. Thus only the lower portion of the ammonia isotherm curves will be studied in this investigation. This part of the ammonia isotherms in aqueous solution at one atmosphere is shown in Figure 3.5. It is difficult to categorize the isotherm curves in Figure 3.5 in a specific type among the five classical isotherm types. A new model is proposed to incorporate the lower portions of curves at different temperatures in one model equation. A geometric equation has excellent correlation (Table 3.3) for lower concentrations of ammonia in the air:

$$y = A(T) x^{B(T)} \quad (3.11)$$

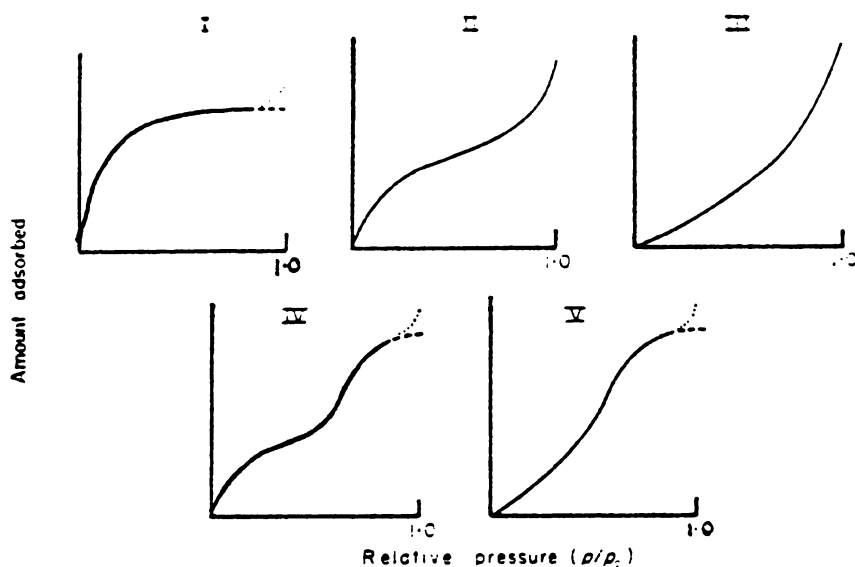


Figure 3-4. Five types of classical adsorption isotherms classified by Braunauer, Emmett and Teller (1938).

Table 3-3. Values of parameters in isotherm model for ammonia solution at 1 atm : $y = Ax^B$ and corresponding correlation coefficients at different temperatures.

Temperatures (°C)	A	B	Correlation
0.0	1.897	1.048	.9985
4.4	1.533	1.032	.9989
10.0	1.204	1.011	.9992
15.6	.964	.993	.9993
21.1	.833	.983	.9998
26.7	.686	.966	.9999
32.2	.569	.950	.9999

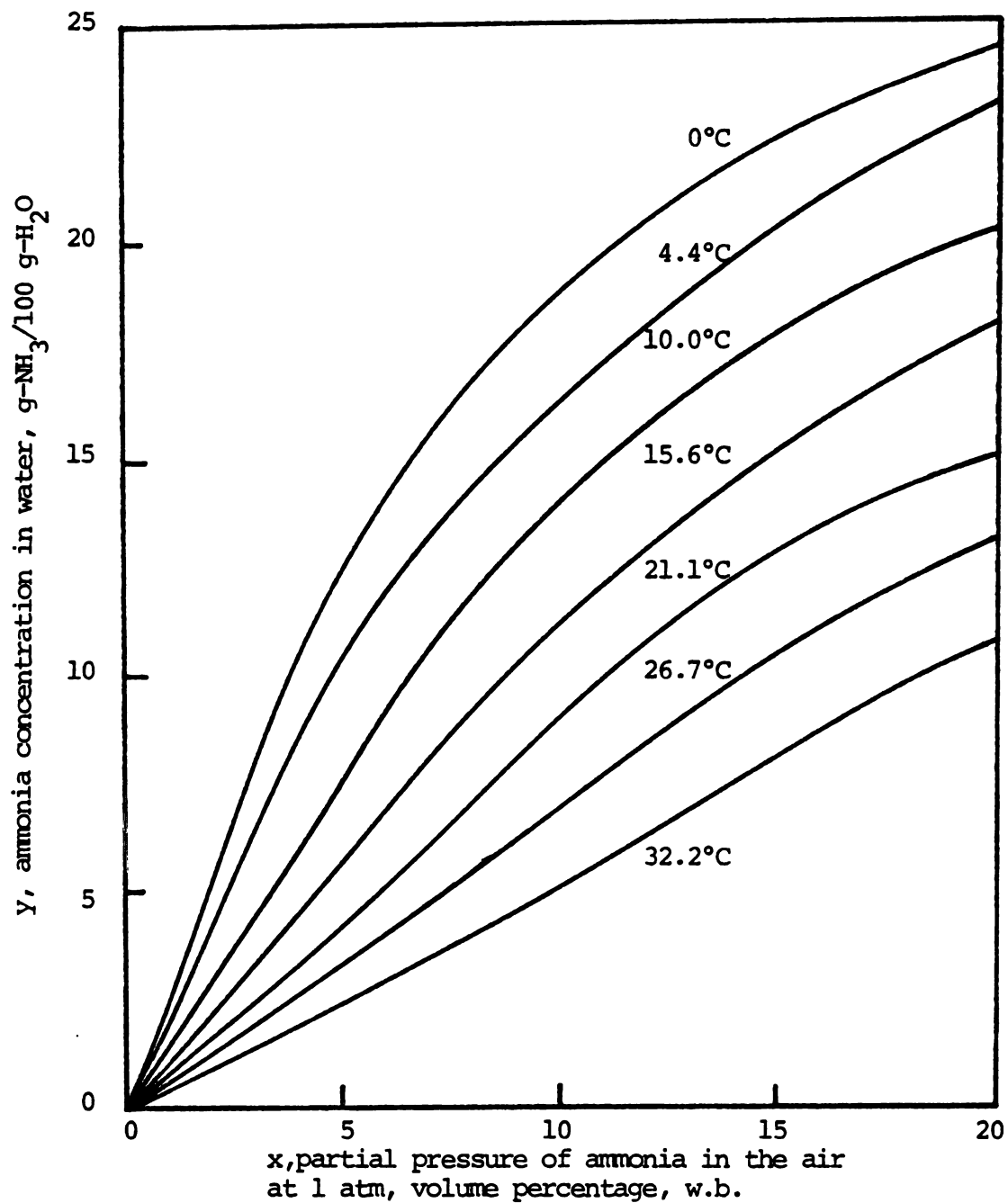


Figure 3.5. Ammonia isotherm curves in ammonia-water system at low concentrations.

where,

y = percentage ammonia concentration in aqueous solution,

$g - \text{NH}_3 / 100 g - \text{H}_2\text{O}$

x = percentage ammonia concentration in the air,

$\text{ml} - \text{NH}_3 / 100 \text{ ml} - \text{bulk stream}$

A = size parameter, function of temperature

B = shape factor, function of temperature

The value of A defines the "height" of an isotherm curve (lower temperature curves have larger A values). The shape factor B defines the concave or convex shape of the isotherm curve. The functions of A and B are solved with high correlation coefficients by plotting them against temperature:

$$A(T) = 108.0 (1.8 T + 32)^{-1.155} \quad (3.12a)$$

$$B(T) = 1.0442 - 2.974 \times 10^{-3} T \quad (3.12b)$$

The final equation for the ammonia isotherm is:

$$y = A(T) x^{B(T)} \quad (3.13)$$

for $0^\circ\text{C} < T < 32.2^\circ\text{C}$ and $x \leq 20$.

4-C. Equilibrium Ammonia Content in Corn

Based on the isotherm model for aqueous ammonia solution (Equation 3.13), the isotherm equation for ammonia in corn was developed based on the following assumptions:

- 1) The only active component in corn responsible for ammonia adsorption is the water portion of the grain.
- 2) All the water, which can be removed in the standard oven-heating moisture content determination method (103°C , 72 hours for corn),

has the same capability of absorbing ammonia (no matter in what form the water exists).

The ammonia concentration in corn can be expressed as:

$$x_2^* = y M_{db} \quad (3.14)$$

where,

x_2^* = percentage ammonia concentration in corn, dry basis

M_{db} = moisture content of corn, dry basis, decimal.

The isotherm equation for ammonia in corn at low relative pressures can then be obtained by substituting Equation 3.13 into Equation 3.14:

$$x_2^* = M_{db} A(T) x^{B(T)} \quad (3.15)$$

for cereal grains at temperatures between 0 and 32.2°C. An example of the isotherm curves for corn at different moisture contents at 4.4°C is shown in Figure 3.6. The figure demonstrates the influence of moisture content and ammonia pressure on the ammonia concentration in shelled corn.

Equation 3.15 is semi-empirical. The data for ammonia concentration in aqueous solutions and the ammonia partial pressures has been tabulated by Liley and Gambill (1973) from several sources. The ammonia isotherms for corn are derived based on these empirical results and the assumptions described previously.

4-D. Hysteresis and Residuals

When the multilayer adsorption on the surface of a non-porous solid (Types II and III) becomes indefinitely thick, it is a sign of condensation. If, however, the solid adsorbent is porous, the thickness of the adsorbed layer on the internal surfaces of the pores is limited by the width of the pores. The shape of the isotherm is modified

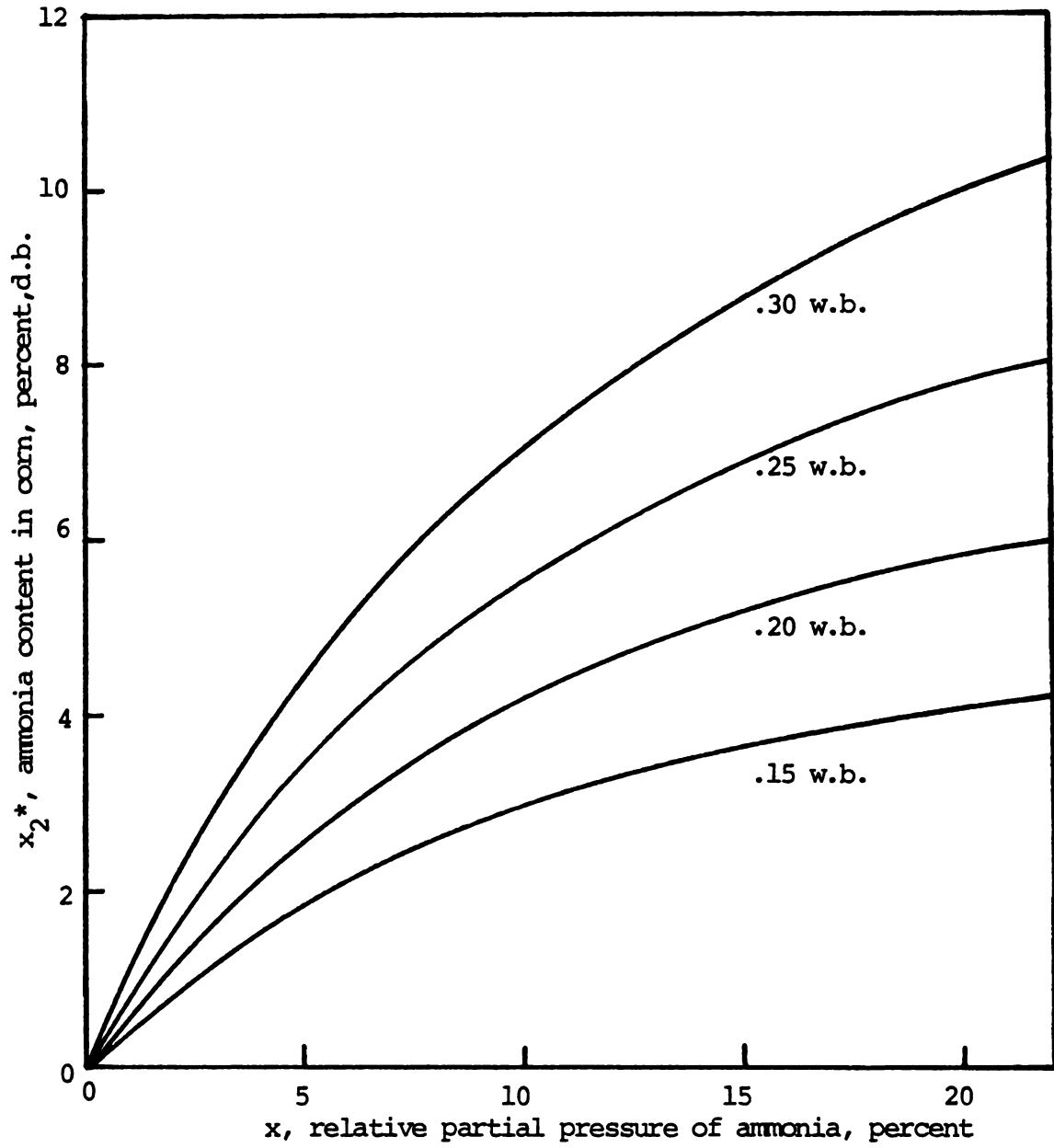


Figure 3.6. Ammonia isotherms of shelled corn for different moisture content at 4.4°C.

correspondingly: a Type II changes to a Type IV isotherm and a Type III to a Type V isotherm. The specific surface and the pore size distribution of the porous adsorbent can thus be determined by considering isotherm Type IV and Type V characteristics (Gregg and Sing, 1967). Hysteresis is one phenomenon of porous adsorbents closely related to the size and configuration of pores.

4-D.1. Hysteresis

The hysteresis loop happens when there are two values of concentration of adsorbate in the solid (x_2^*) for any given value of relative partial pressure of the adsorbate (x). The value of x_2^* is always higher for the desorption than for the adsorption branch in portion of the sorption isotherm curves.

The cause for hysteresis has been hypothesized as a capillary condensation phenomenon in "ink bottle" shaped pores by Kraemer (1931), McBain (1935) and others (Rao, 1941; Katz, 1949). When the desorption branch is traversed, evaporation cannot occur according to the adsorption curve since the neck of the pore is blocked by a meniscus which can only be evaporated at lower pressures depending on the contact angle in the meniscus; the entire pore then empties at once. It is a common practice for most researchers to assume the adsorption, rather than the desorption, branch to represent equilibrium (Gregg and Sing, 1967). The degree of departure of the desorption curve from the adsorption curve under equilibrium conditions for a given temperature depends on the pore size, distribution, and characteristics.

The "ink bottle" hypothesis has led to the investigation of the so-called scanning phenomenon of the hysteresis loop (Rao, 1941). It was established that the loop may be crossed by moving from the

adsorption to the desorption branch but not vice versa. The results in Figure 3.7a show the crossing of loops on the desorption curves when the desorptions happened at different pressures. As the pressure was increased during the desorption process, readsorption occurred and followed different paths under different pressures within the hysteresis loop. The readsorption paths do not cross each other as shown in Figure 3.7b.

4-D.2. Residuals

In a purely physical adsorption model for porous biological products, the chemical reactions between the adsorbate and the components in the solid adsorbent are not considered. However, in the case of ammonia treatment for corn, browning of ammonia-treated corn has been reported (Lancaster et al., 1975). The browning reaction is similar to that of the browning of aged corn where it is interpreted as an example of the classical nonenzymatic browning reaction (Reynolds, 1963).

The browning reaction involves the reaction between an aldose (a sugar) and an amine through a series of chemical transformations producing pigmented and sometimes highly flavored compounds. Certain kinds of nitrogen containing compounds, such as guanidine and pyridine, may be formed by the browning reaction of corn with ammonia (Lancaster et al., 1975).

The chemical reactions and their reaction mechanisms between ammonia and certain corn components are not fully understood. It has been known that the ammonia "adsorbed" by corn (referred to as the total ammonia) contains both volatile (free) and nonvolatile (fixed) ammonia. Free ammonia is water extractable and the amount can be easily determined by a titration method. The gaseous ammonia diffuses

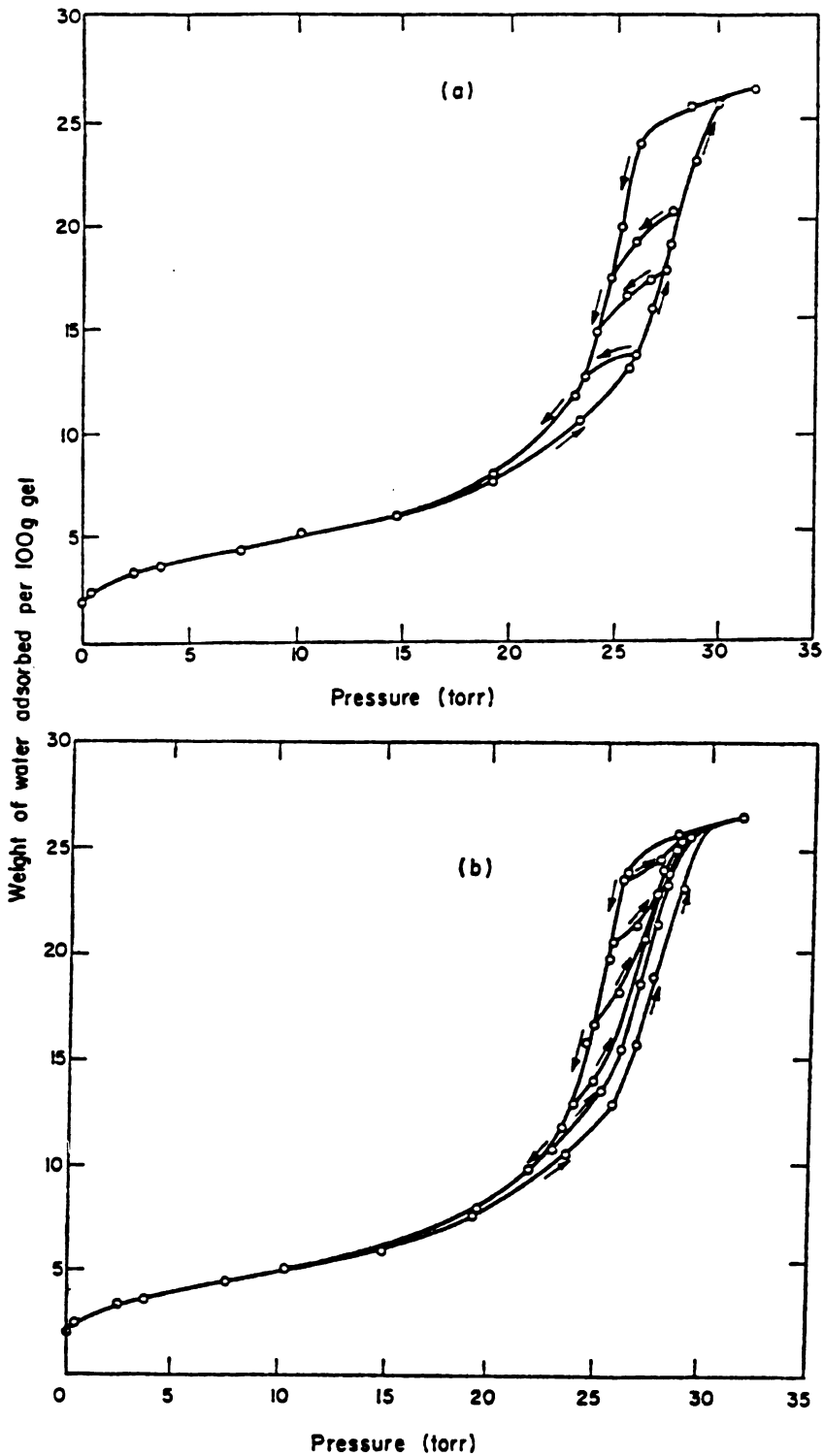


Figure 3.7. "Scanning" of the hysteresis loop in the adsorption of water by titania gel. The loop may be crossed by moving from the adsorption to the desorption branch, but not vice versa (Rao, 1941).

into the pores of corn surface which composes most of the free ammonia and will eventually become either fixed or lost.

During the desorption process of ammonia-treated corn, only the free ammonia portion is removed. The free ammonia in the pores and on the surfaces of corn is being dissolved in the water portion of corn. The free ammonia, in the pores and in the corn, reacts chemically with certain corn components continuously and becomes the fixed ammonia and is referred to as "residuals". The residuals are dynamic quantities and they are temperature and concentration dependent.

4-D.3. The Combined Effects of Hysteresis and Residuals on the Desorption Process

Experimental results of the desorption of ammonia in corn are not available in the literature. Thus the formulation of a desorption isotherm has to be based on certain assumptions:

- 1) Corn is a porous medium and the sorption of ammonia displays hysteresis above certain ammonia partial pressures in the air.
- 2) The chemical reactions between corn components and ammonia consume ammonia in an irreversible manner; the reactions may take place both on the pore walls and in the solid.
- 3) The free ammonia in the pores is considered the adsorbed ammonia which is dissolving into and reacting continuously with water and other components in the corn.
- 4) The fixed ammonia (or residual) is counted as part of the total ammonia adsorbed in the corn but only the free ammonia is responsible for the physical adsorption and desorption processes.
- 5) The amount of residual is assumed to be a known and fixed percentage of the highest free ammonia concentration (x_{2f}^*) the solid

ever possessed.

The proposed adsorption and desorption models for ammonia in a pore on the corn surface are shown graphically in Figure 3.8. The corresponding isotherm curves are shown in Figure 3.9 where the approximate positions corresponding to the intermediate steps in adsorption and desorption are indicated.

The adsorption of ammonia in an ammonia-free "ink bottle" pore (A1) at low pressures starts with an even coverage of free ammonia on the pore wall (A2). The free ammonia on the pore surface builds up and at the same time is dissolving into the water portion of solid corn as free ammonia. Meanwhile, the dynamic processes of chemical reaction between free ammonia and certain corn components both on the pore wall and in the solid are progressing. As the above processes continue, the depth of the deposit of free ammonia becomes deeper (A3). More free ammonia is dissolving into the solid. The entire pore volume is finally filled with adsorbed free ammonia (A4) and saturation is reached.

As the ammonia pressure in the air is reduced, the originally saturated pore (D1) starts losing free ammonia. The bottle neck of the pore resists evaporation of free ammonia in the pore (D2). The solution of free ammonia from the pore to the solid is stopped and may revert its direction -- the free ammonia in the solid may enter the pore again due to reduced pressure. The "ink bottle" is suddenly emptied at once (D3) when the partial pressure of ammonia is low enough. There is a very small amount of free ammonia in the pore then; the free ammonia in the solid starts evaporating into the pore and leaving the pore.

The equilibrium amount of the free ammonia in the solid depends on the partial pressure of ammonia in the air. At the end of desorption

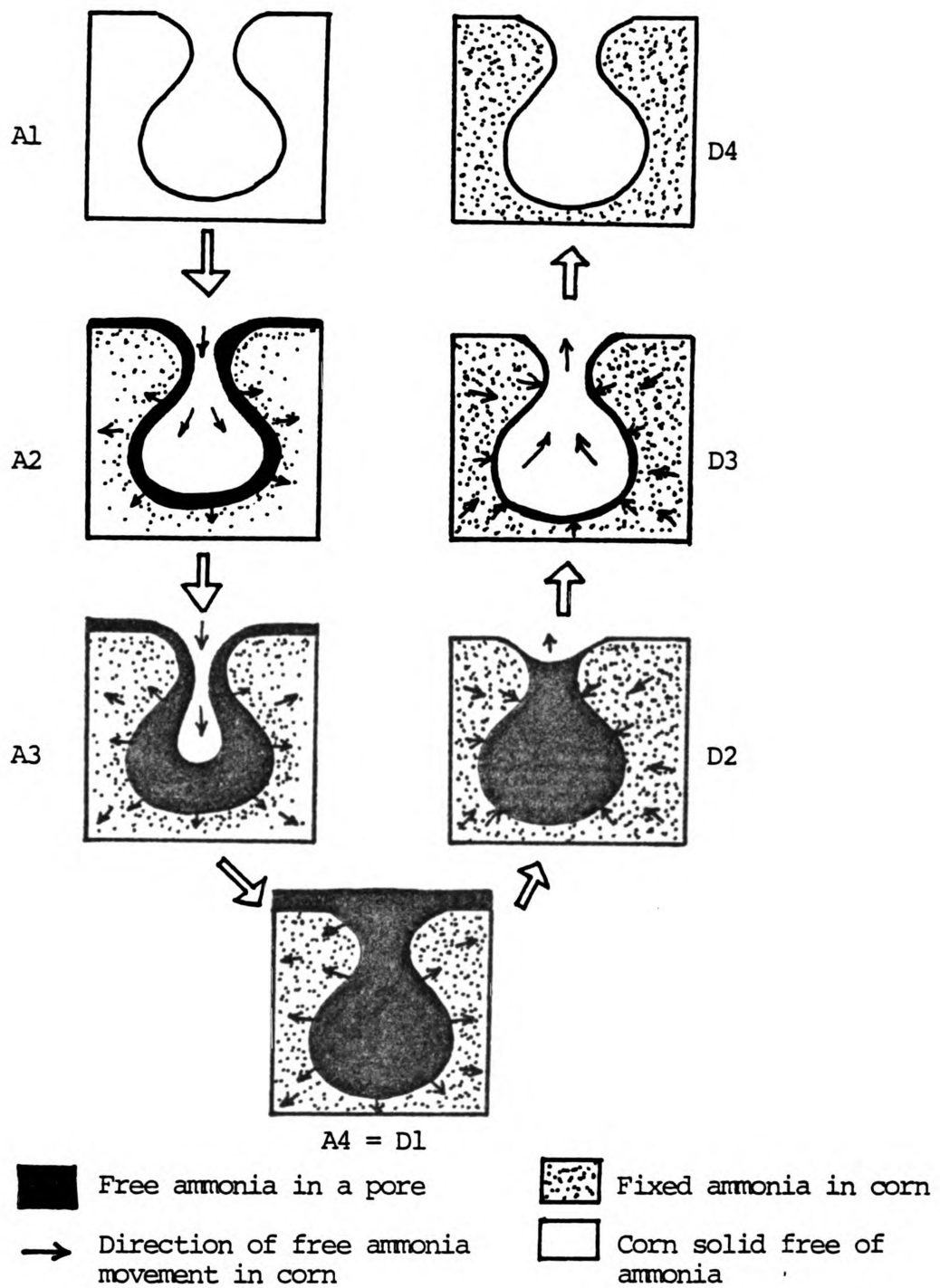


Figure 3.8. Proposed model for the ammonia adsorption and desorption process in an "ink bottle" pore.

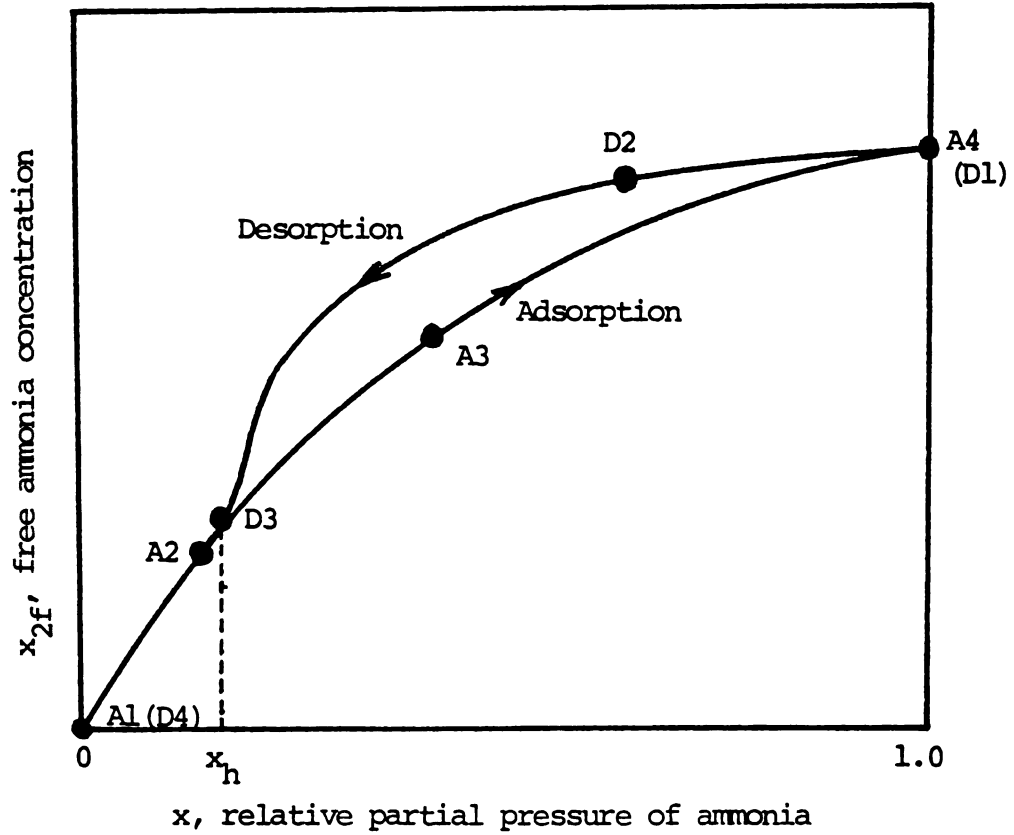


Figure 3.9. The proposed general adsorption and desorption isotherm curves of the ammonia-corn system for the entire pressure range. Approximate positions of the relative intermediate steps are indicated in accordance with those in Figure 3.8.

process, as the ammonia supply is completely stopped, there is no free ammonia in the entire system under equilibrium. However, the fixed ammonia (residual) is accumulated in the solid and becomes a permanent part of the solid (D4).

Due to the variations of size and shape of the pores and other adsorption sites, e.g. tip of corn, cracks, etc., the sorption process is not exactly the same for all the adsorption sites. Therefore, the changes shown in Figure 3.9 for the adsorption and desorption processes are not as dramatic as those in Figure 3.8.

The effect of hysteresis is not seen until the ammonia concentration in the air reaches a certain level x_h (Figure 3.9) when some pores start being filled up. Since the residual is a dynamic quantity and cannot be indicated on the sorption isotherm curve, residuals do not play a direct role in the ammonia sorption isotherms which are purely physical adsorption and desorption processes. However, the equilibrium amount of residuals does depend on the free ammonia concentration.

4-E. Proposed Sorption Isotherms in the Ammonia-Corn System at Low Ammonia Pressures

In the previous discussion, the partial pressure range of ammonia in the air varied from 0 to 1 atmosphere. As was mentioned previously (Section 4-B), in the practical applications of ammonia in grain drying in a fixed-bed system, the inlet concentrations of ammonia in the air seldom exceed 20 percent. Equation 3.15 for the equilibrium ammonia content in corn may be applied to the adsorption in this pressure range. It has been shown by Ngoddy (1969) that at relative pressure of 20 percent, the adsorption of water vapor on corn is still monolayer

for moisture isotherms. Thus one would assume that the hysteresis loop does not exist below the ammonia concentration of 20 percent in the air. Thus the effect of hysteresis can be neglected.

Therefore, the adsorption and desorption isotherms for the ammonia-corn system at lower ammonia pressures are identical. The adsorbed amount of ammonia in the solid for these physical adsorption processes refers to the free ammonia content only. The isotherm equation for free ammonia in corn at lower ammonia pressure x can thus be expressed as:

$$x_{2f}^* = M_{db} A(T) x^{B(T)} \quad (3.16)$$

According to assumption 5 (Section 4-D.3) the equilibrium ammonia residual value (x_{2R}) is a known and fixed fraction (δ) of the maximum free ammonia concentration in corn (x_{2f}^*). The value of δ is dependent on the temperature, relative partial pressure of ammonia (x) in the air, and the length of time the adsorbent is exposed to the ammonia pressures. If a rapid equilibrium state would be reached in practical dynamic problems, δ is only a function of temperature. In the ambient air drying system, which is the case in this investigation, the temperature changes will not be too big to influence δ significantly, δ can be assumed to be constant. The value of δ can be determined experimentally.

The total ammonia in corn (x_2^*) can be expressed as the summation of free ammonia and fixed ammonia (residuals):

$$x_2^* = x_{2f}^* + x_{2R} = (1+\delta) x_{2f}^* \quad (3.17)$$

In the physical sorption processes, only the free ammonia content, x_{2f}^* , is considered while the ammonia depletion due to chemical reactions is lumped in the residuals term, x_{2R} .

CHAPTER 4

GENERAL SORPTION AND DRYING MODELS IN A FIXED-BED SYSTEM

1. Introduction

Grain drying in a fixed-bed system is a batch drying process. The grain drying in a bin implies several different drying systems, among them are natural air drying, low-temperature drying, layer drying, solar heated air drying, dehydrated air drying, etc. Although the fixed-bed drying systems are different in performance, they can be described by the same simulation equations.

The proposed model equations for a fixed bed grain drying system have been part of the results of a series of grain drying simulation research efforts performed at Michigan State University (MSU) by Bakker-Arkema and Bickert (1966, 1967) and Bakker-Arkema et al. (1968, 1970, 1974, 1977, 1978). The following assumptions have been made in the development of the MSU grain dryer models (Brooker et al., 1974):

- 1) no appreciable volume shrinkage occurs during the drying process,
- 2) the temperature gradients within the individual particle are negligible,
- 3) the particle-to-particle conduction is negligible,
- 4) the airflow in the bin is plug-flow,
- 5) the $\partial T/\partial t$ and $\partial H/\partial t$ terms are negligible compared to the $\partial T/\partial z$ and $\partial H/\partial z$ terms,
- 6) the bin walls are adiabatic with negligible heat capacity,

- 7) the heat capacities of the drying air and the grain are constant during short time period, and
- 8) the equilibrium moisture isotherm and thin-layer drying equations are known for the grain to be dried.

Based on heat and mass balances and above assumptions, the fixed-bed drying model equations are written as (Bakker-Arkema et al., 1974):

$$\frac{\partial T}{\partial z} = \frac{-h a}{G_a c_a + G_a c_v H} (T-\theta) \quad (4.1)$$

$$\frac{\partial \theta}{\partial z} = \frac{h a}{\rho_p c_p + \rho_p c_w M} (T-\theta) - \frac{h_{fg} + c_v (T-\theta)}{\rho_p c_p + \rho_p c_w M} G_a \frac{\partial H}{\partial z} \quad (4.2)$$

$$\frac{\partial H}{\partial z} = - \frac{\rho_p \partial M}{G_a \partial t} \quad (4.3)$$

$$\frac{\partial M}{\partial t} = \text{an appropriate thin-layer drying equation} \quad (4.4)$$

The appropriate thin-layer equation can be chosen for the proper grain and air temperature, humidity, and grain moisture ranges.

There are four unknowns in the above model equations: air temperature (T), grain temperature (θ), absolute humidity (H), and grain moisture content (M). Accordingly, the above four equations must be independent in order to solve them. The best way to solve these simultaneous differential equations with variable coefficients is by numerical methods and digital computers.

According to the CRC Handbook (1976), the term "adsorption" is defined as the condensation of gases, liquids, or dissolved substances on the surfaces of solids. Sorption, as defined by Vermeulen et al. (1973), involves "contacting a free fluid phase (gas or liquid) with a rigid and durable particulate phase which has the property of selectively taking up and storing one or more solute species originally

contained in the fluid". Furthermore, in general sorption processes, "it is usually necessary to recover the solute or to purify and reuse the sorbent, and then conditions for desorption must also exist". Fixed-bed adsorption processes are applied in the areas of chromatography, ion exchange, heterogeneous catalysis, and other separation processes in chemical engineering. To formulate the theory of fixed-bed phenomena requires the knowledge of phase equilibria and interphase mass transfer rates. The fluid-solid equilibria have been discussed in the previous chapter for ammonia-corn systems. Interphase mass transfer rates and other sorption characteristics will be the subject of this chapter.

Ammonia drying systems differ from ordinary sorption processes in the following aspects (summarized from the previous chapter):

- 1) In an ammonia drying system, the solids (corn) not only adsorb ammonia on the surface and in the pores but also diffuse the adsorbed ammonia into the solid, and
- 2) the adsorbed ammonia reacts with the solid (corn) components, at relatively low temperatures (e.g. ambient temperatures), chemically to form residuals which are not regenerable.

Adsorption usually refers to the physical adsorption process of a gas-solid system. Adsorption may occur through a chemical bonding between the adsorbed gas and solid on the adsorbing surface at temperatures usually higher than 204°C (Vermeulen et al., 1973); it is then termed Chemisorption. The residuals formed in the ammonia-corn system are apparently not the result of chemisorption since the corn temperature is far below 204°C (400°F) throughout the ambient air drying processes.

2. General Fixed-Bed Sorption Models

2-A. The Transport Mechanism

The mechanism of transport consists of several distinctly different steps with each step contributing to the overall performance of the mass transfer process (Vermeulen et al., 1973):

- 1) Mass transfer from the fluid phase to the external surfaces of the solid particles.
- 2) Pore diffusion in the fluid phase within the particles.
- 3) Reaction at the phase boundary of fluid and solid.
- 4) Internal diffusion in the solid.

In general, systems with a high total solute concentration in the fluid phase are more likely to have the mass transfer rates controlled by the internal diffusion (Step 4) while systems with a low total fluid-phase concentration are more likely to be controlled by fluid external diffusion (Step 1) or pore diffusion (Step 2). The reaction at the phase boundary of fluid and solid (Step 3) exerts small resistance to the mass transfer since this process is usually very fast (Vermeulen et al., 1973). The boundary resistance is also independent of the solute concentrations since the concentration effects are mostly described by Steps 1, 2, and 4.

The major difference between pore diffusion (Step 2) and internal diffusion (Step 4) is that they happened in different phases: pore diffusion occurs when the adsorbate is still in the fluid phase while internal diffusion occurs when the adsorbate has penetrated into the solid. The two steps are separated by a phase transition step (Step 3). For non-porous adsorbents, only mechanism 1-3-4 dominates since there is negligible pore diffusion process. Mechanisms 1-2-3 and 1-3-4 both

may happen in parallel in porous adsorbents with the faster one of the two controls the rate of sorption. Mechanism 1-2-3 dominates when the rate of internal diffusion in the solid is low while mechanism 1-3-4 controls when the rate of pore diffusion in the fluid phase is slow.

2-B. The Equations of Transport

The fixed-bed sorption models are usually analyzed by describing the mass balances within a control volume of bed. Assume a fixed-bed system with constant cross sectional area perpendicular to the direction of airflow which is plug-type. The packed material has a void volume fraction of ϵ and the bulk density of ρ_B . A mass balance within the control volume on the fluid and solid phases results in the following transport equation (Sherwood, 1975):

$$\epsilon \frac{\partial C}{\partial t} + \rho_B \frac{\partial q}{\partial t} + \epsilon v \frac{\partial C}{\partial t} = 0 \quad (4.5)$$

where C and q are fluid and solid concentrations of adsorbate in moles per volume and moles per weight units, respectively. The interstitial fluid velocity is expressed as v and thus ϵv becomes the superficial velocity in an empty tube. Equation 4.5 must be coupled with another equation describing the adsorption rate in the solid phase. The adsorption is assumed to be driven by a driving force function $F(C, q)$ and the rate equation can be written as

$$\rho_B \frac{\partial q}{\partial t} = h_m a F(C, q) \quad (4.6)$$

where h_m is the overall mass transfer coefficient and a is the specific surface area. The driving force function can be expressed in several forms depending on the dominating transport mechanism.

As it was mentioned in Section 2-A that the reaction at the phase boundary (Step 3) is not controlling; the mass transfer rate of mechanism 1-2-3 depends primarily on the mass transport in the fluid side. The driving force function is thus a function of the fluid concentration alone (Section 2-C). However, the pore concentration of adsorbate in the fluid is usually expressed by the equilibrium relationships with contacting solids and thus the driving force can be expressed by the adsorbate concentration in the solid phase. Pore diffusion will be discussed further in Section 2-D. The slower mass transfer rate of Steps 1 and 2 determines the overall mass transfer rate.

For mechanism 1-3-4, the driving force for Step 1 is a function of fluid concentration while it is a function of the adsorbate concentration in the solid alone for Step 4. Again, the slower rate of Steps 1 and 4 defines the mass transfer rate for mechanism 1-3-4.

2-C. The External Transport Equation

The rate of mass transport in a solid can be expressed in terms of the concentration difference in the fluid phase if the transport rate is assumed to be controlled by external diffusion (Step 1) (Sherwood, 1975):

$$\rho_B \frac{\partial q}{\partial t} = k_f a (C - C^*) \quad (4.7)$$

where C^* is the interface concentration in the fluid in equilibrium with the outer surface of the solid. The fluid-phase mass transfer coefficient, k_f , which carries the units of cm/hr, may be determined by general mass transfer correlations (Vermeulen, 1958; Wilke and Hougen, 1945) and expressed in terms of the fluid properties and the effective particle diameter.

The mass transfer coefficient was determined by Wilke and Hougen (1945) for packed-bed operations under linear-flow gas-solid contact conditions:

$$k_f = \frac{10.9 \epsilon v(1-\epsilon)}{a d_p} \left(\frac{D_f}{d_p \epsilon v} \right)^{0.51} \left(\frac{D_f \rho_f}{\mu_f} \right)^{0.16} \quad (4.9)$$

where d_p is the particle diameter; ϵv is the superficial velocity or volumetric flow rate of fluid per unit area of superficial cross sectional area; D_f is the fluid-phase diffusivity; and ρ_f and μ_f are the density and viscosity of the fluid respectively.

2-D. The Pore Diffusion Equations

The diffusion rate of adsorbate in the fluid-filled pores inside the particles for spherical-shaped pores with an internal radius r can be expressed as:

$$\rho_B \frac{\partial q}{\partial t} = D_{\text{pore}} (1-\epsilon) \left(\frac{\partial^2 C^*}{\partial r^2} + \frac{2}{r} \frac{\partial C^*}{\partial r} \right) \quad (4.10)$$

where the pore concentration C^* is determined by the equilibrium relationship with the contacting solid. The pore diffusivity, D_{pore} (cm^2/hr), has been solved and summarized for various gases and liquids by Satterfield (1970) as a function of the internal porosity of the particle, the average pore radius, the tortuosity (or, winding, twisting) and the temperature in the pore.

The major disadvantage of the above pore diffusion equation in the difficulties in the numerical integration of second order differential equation with a commonly-encountered solution stability* problem. Vermeulen and Quilia (1970) expressed the pore diffusion equation by a

* The stability problem in the solution of differential equations using numerical integration has been discussed in detail by Nogotov (1978).

modified driving force approximation involving the overall particle concentrations:

$$\frac{dq}{dt} = \psi_{\text{pore}} k_{\text{pore}} a \frac{q^* - q}{[1 + (R-1)q/q^*]^{1/2}} \quad (4.11)$$

with

$$k_{\text{pore}} a = \frac{60 D_{\text{pore}}}{d_p^2} (1 - \epsilon) \quad (4.12)$$

where R is the separation factor defined by Vermeulen and Hiester (1954) as $\frac{X(1-Y)}{Y(1-X)}$ in describing the shape of the isotherm curves and X , Y are dimensionless concentrations referred to some reference concentrations C^* and q^* , i.e. $X = C/C^*$, $Y = q/q^*$. The separation factor for the Langmuir adsorption is a constant while other isotherm curves are expressed by variable separation factors. For the pore diffusion case, R is equal to $(1-Y^*)/Y^*$ at $X = 0.5$. The term ψ_p is a correction factor and equal to $0.548/(1-0.452R^{1/2})$ for $R < 1$.

2-E. The Internal Diffusion Equations

The solid-phase diffusion equation expresses the concentration gradient of adsorbate existed within each individual solid particle. The solid phase is assumed to be homogeneous, isotropic, and permeable. For spherical particles the rate of internal diffusion can be expressed by the Fick's second law of diffusion as follows:

$$\frac{\partial Y}{\partial t} = D_p \left(\frac{\partial^2 Y}{\partial r^2} + \frac{2}{r} \frac{\partial Y}{\partial r} \right) \quad (4.13)$$

where D_p is the diffusivity of solid particles and Y is the dimensionless solid-phase concentration at an internal radius r and time t .

The theoretical Equation 4.13 is similar to Equation 4.10 and is difficult to solve. Solution of Equation 4.13 not only solves the concentration of adsorbate in the solid as a function of time but

also shows the concentration gradient within the particle which is sometimes trivial for small particles or for a macroscopic system. Thus, Equation 4.13 is often approximated by the linear-driving-force equation of Glueckauf (1955):

$$\frac{dq}{dt} = \psi_p k_p a (q^* - q) \quad (4.14)$$

where q is the average concentration for the entire particle. The specific area a^\dagger can be expressed as $6(1-\epsilon)/d_p$. The mass transfer coefficient k_p has units of cm/hr and was recommended by Vermeulen et al. (1973) as:

$$k_p a = \frac{60 D_p}{d_p^2} \quad , \text{ or} \quad (4.15)$$

$$k_p = \frac{10 D_p}{(1-\epsilon) d_p} \quad (4.16)$$

Equation 4.16 is obtained by substituting $a = 6(1-\epsilon)/d_p$ into Equation 4.15. The correction factor ψ_p which partly corrects the linear driving force approximation is obtained from the slope of curves of the particle uptake vs. time with Equation 4.14 at $Y = 0.5$ (Hall, 1966). The value of ψ_p was estimated from:

$$\psi_p = 0.894 / (1 - 0.106 R^{1/4}) \quad , \text{ for } R < 1 \quad (4.17)$$

$$\psi_p \approx 1 \quad , \text{ for } R > 1$$

Vermeulen (1953) proposed a quadratic-driving-force equation which better approximates the behavior of the theoretical equation (Equation 4.13) than the linear-driving-force equation (Equation 4.14). The quadratic equation is:

$$\dagger \quad a = \frac{\text{area}}{\text{volume}} = \frac{\pi d_p^2}{\frac{1}{6} \pi d_p^3 / (1-\epsilon)} = \frac{6(1-\epsilon)}{d_p}$$

$$\frac{dY}{dt} = \psi_q k_p a \frac{Y^{*2} - Y^2}{2Y} \quad (4.18)$$

where

$$\psi_q = 0.590 (1 - 0.410 R^{1/2}) \quad , \text{ when } R < 1; = 1, \text{ when } R > 1 \quad (4.19)$$

and $R = X^*/(1-X^*)$ at $Y^* = 0.5$

3. The Local-Equilibrium Theory

The equations for the different stages within the sorption transport mechanism have been described in the previous section. The solution of these transport equations requires the knowledge of the isotherm equation and the dynamic behavior of a number of parameters such as the mass transfer coefficient and the product properties. Perhaps the most difficult parameter to determine is the mass transfer coefficient which has to be calibrated for each experiment under a set of specified conditions in order to be consistent to the results from the experimental determinations which are sometimes tedious and time-consuming. A good estimation of the mass transfer coefficient under a particular set of experimental conditions can be obtained from a carefully designed and performed experiment.

3-A. Local-Equilibrium Transport Equations

Consider the case when the mass transfer into and out of the solids have negligible resistance, i.e. mass transfer coefficient is infinite, then "local equilibrium" exists at all time and positions between the solid particles and adjacent fluid. Therefore, q may be replaced by q^* in Equations 4.5 and 4.6 where q^* is a function of the fluid concentration, $q^* = f(C)$, as specified by the isotherm equations. The mass balance equation (Equation 4.5) in the gas-solid sorption system is then simplified to the following equation (Sherwood, 1975):

$$\left[1 + \frac{\rho_B}{\epsilon} f'(C) \right] \frac{\partial C}{\partial t} + v \frac{\partial C}{\partial x} = 0 \quad (4.20)$$

where f' represents the first time derivative of the function. The solution of C is not straightforward since a variable coefficient $f'(C)$ is involved. The term x in this chapter refers to the bed position.

If a solution $C(x,t)$ exists and has been solved, an additional equation involving the partial derivatives of C can be formulated according to the "method of characteristics" (Aris and Amundson, 1973):

$$\left(\frac{\partial C}{\partial t} \right) dt + \left(\frac{\partial C}{\partial x} \right) dx = dC \quad (4.21)$$

The solution is expressed by two equations for $(\partial C/\partial t)$ and $(\partial C/\partial x)$:

$$\frac{\partial C}{\partial t} = \frac{v dC}{g(C) dx - v dt} \quad (4.22a)$$

$$\frac{\partial C}{\partial x} = \frac{g(C) dC}{g(C) dx - v dt} \quad (4.22b)$$

where,

$$g(C) = 1 + f'(C) \rho_B / \epsilon \quad (4.22c)$$

Certain characteristic directions in the xt plane (dx/dt) will make the denominator equal to zero. The numerator, and accordingly dC must also be zero if the solutions are to be finite. Therefore, C is constant along the "characteristic lines" (Sherwood, 1975) which are expressed as:

$$\frac{dx}{dt} = \frac{v}{g(C)} \quad (4.23)$$

Since C is a constant, the slopes of the characteristic lines (dx/dt) are also constant. Thus, the characteristic lines are straight lines on the xt plane. An example of this graphical presentation for the solution of a fixed-bed adsorption and desorption problem is presented by Sherwood (1975) using the Langmuir isotherm.

The slope of characteristic lines implies an important property in a fixed-bed system: the speed of penetration. The penetration property is described by the concentration wave velocity, dx/dt , which is the velocity of the initial concentration wave front moving through a packed bed.

3-B. The Break-Through Curve

In order to investigate the break-through characteristics of an adsorption wave, consider a column adsorber (i.e. a deep bed of adsorbent) and a solution containing a strongly adsorbed solute at concentration C_0 as shown in Figure 4.1. As the adsorbent is at first contact with the solution, the solid adsorbs solute very rapidly; very little solute is left in the solution. The effluent concentration of solute is practically zero until the adsorption zone starts breaking through -- C_0 is the break point. After the break point, the concentration of solute in effluent rises very rapidly until the adsorption zone almost reaches the exit of the bed (C_d). The concentration of solute in the effluent becomes saturated to the input concentration asymptotically. The break-through characteristics are usually investigated using constant input adsorption process. The steepness of the break-through curve depends on the sharpness of the adsorption zone in the packed bed which is in turn influenced by the solution feed rate, packed-bed properties, mass transfer rate, etc.

The adsorption and desorption curves derived from the local-equilibrium theory are shown as solid line segments in Figure 4.2. During the time required for the wave to emerge from the bed of depth x , the total amount of solute flowing into the bed is $C_0 v t$; none flows out. The amount of accumulated solute in the bed is $\epsilon C_0 x + \rho_B q_0^* x$.

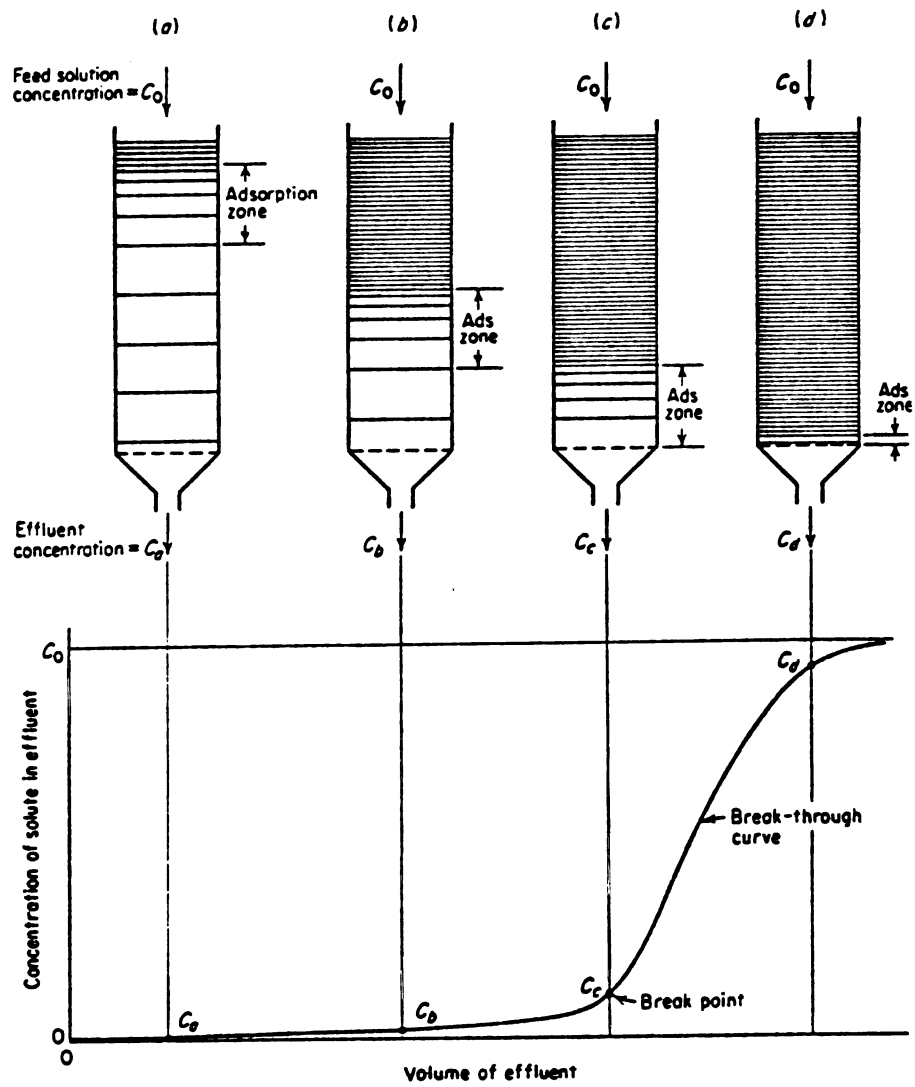


Figure 4.1. The adsorption wave (Treybal, 1968).

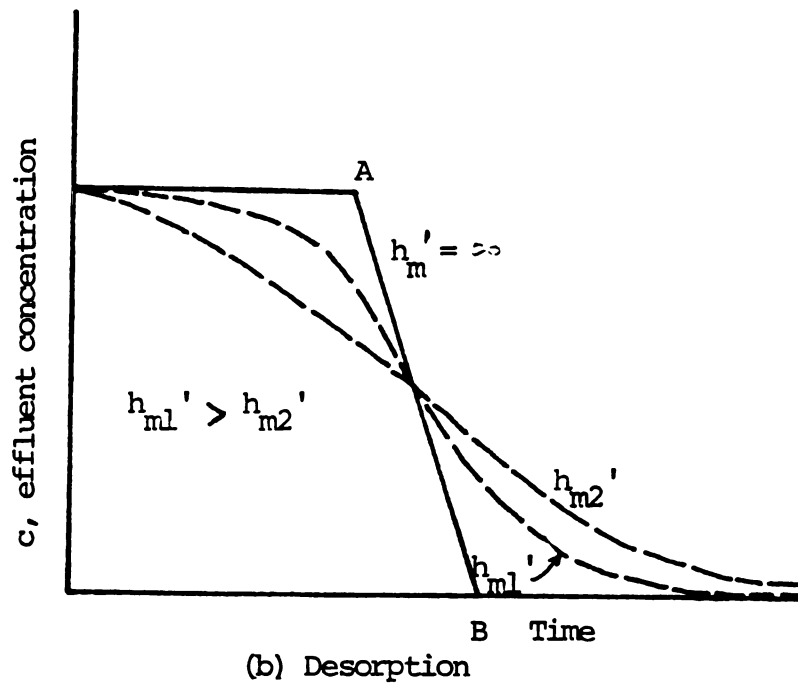
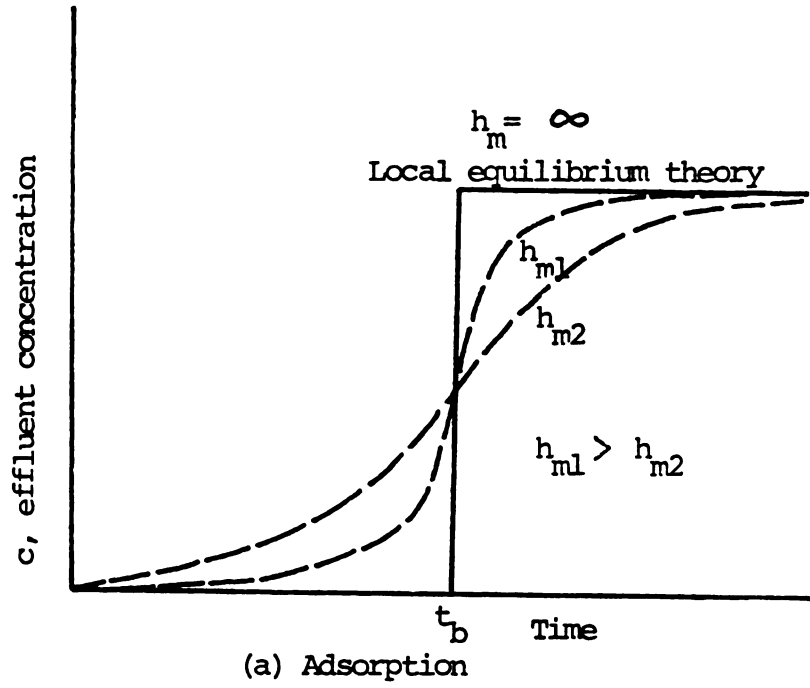


Figure 4.2. Influence of mass transfer coefficient on the adsorption and desorption concentration waves.

Equating the two and solving for the break-through time, t_b , gives:

$$t_b = \frac{x}{v} \left(1 + \frac{\rho_B q_0^*}{\epsilon C_0} \right) \quad (4.24)$$

In the case of $k \rightarrow \infty$ which is implied in local equilibrium theory, the concentration of the effluent is a step output at a discontinuous point of t_b . For points between A and B in the desorption curve (Figure 4.2b), the concentration in the effluent can be obtained from the following equation by solving C contained in the function $f'(C)$:

$$\frac{x}{t} = \frac{v}{1 + (\rho_B / \epsilon) f'(C)}$$

Actual breakthrough curves are affected by mass transfer resistance and by the longitudinal dispersion effect. As a result, sharp corners are rounded off. Comparing two sorption systems under exactly the same conditions, e.g. fluid flow rate, interstitial velocity, feed concentration, isotherm curves, temperature, etc., except the mass transfer coefficient, one of the round-off curves (dotted lines) closer to the local-equilibrium theory line has a larger mass transfer coefficient. A sharper breakthrough curve is acknowledged as a result of a larger mass transfer coefficient during adsorption. Consider the same bed (adsorption) capacity for these different sorption systems, the area below each adsorption curve ought to be the same. In other words, the integral $\int C dt$ is constant if integrated over the entire adsorption process. Similar cases can be expected for desorption processes with different mass transfer coefficients.

The effect of the mass transfer resistance between the fluid and solid phases on the breakthrough curve was demonstrated by Sherwood (1975). The slope of the breakthrough curve at the midpoint (where

$C = C_0/2$) is:

$$\left. \frac{d(C/C_0)}{dt} \right|_{C=C_0/2} = \frac{h_m a x}{\epsilon v} \cdot \frac{\epsilon v C_0}{\rho_B q_0 x} \cdot \frac{K_A p_0/4}{1+K_A p_0/2} \quad (4.25)$$

using a linear function $(C-C^*)$ as the driving force and C^* computed from the Langmuir isotherm. The factor $(h_m a x / \epsilon v)$ is defined as the number of transfer units (NTU) in the bed and $(\rho_B q_0 x / \epsilon v C_0)$ is the time required for the input flow to supply the bed with an amount of adsorbate equal to the bed capacity (TBC). A larger value of NTU and a smaller TBC value will contribute to a steeper slope of the breakthrough curve.

Weyde and Wicke (1940) observed a bed of carbon particles in adsorbing carbon dioxide from nitrogen. The effect of depth of packing on adsorption and desorption is shown in Figure 4.3 using a superficial fluid velocity (ϵv) of 4.26 cm/sec. The breakthrough adsorption curves showed a virtually constant pattern after a bed depth of about 18 cm. However, the slope of these curves at the midpoint $C = C_0/2$ is decreasing as the bed depth increases which is consistent with the results from Equation 4.25. Similar arguments can be stated for desorption.

4. The Thomas Solution of Break-Through Curves

Thomas (1944) derived the driving force function from the stoichiometry of the monovalent ion-exchange reaction and defined the so-called "kinetic driving force":

$$F'(C, q) = C(1 - q/q_m) - \frac{1}{K} (C_0 - C) q/q_m \quad (4.26)$$

where K is the equilibrium reaction constant which can be calculated when the driving force is zero, or

$$K = \frac{q(C_0 - C)}{C(q_m - q)} \quad (4.27)$$

The transport equation becomes

$$\rho_B \frac{\partial q}{\partial t} = \kappa a F'(C, q) \quad (4.28)$$

The mass transfer coefficient h_m in Equation 4.6 becomes κ (kappa), the kinetic coefficient which can also be shown to be related to the mass transfer coefficient which represents the diffusional resistance in the fluid and solid phases (Sherwood, 1975). Thomas (1944) also recognized that the rate $\partial q/\partial t$ includes the specific area since the actual rate is almost always diffusion-controlled and depends on the surface area available for interphase transfer.

Redefining the time scale as "the elapsed time" at a point after the fluid has arrived at the point: $\hat{t} = t - x/v$, the transport equations (Equations 4.5, 4.28) are then simplified to:

$$\frac{\rho_B}{\epsilon} \frac{\partial q}{\partial \hat{t}} + v \frac{\partial C}{\partial \hat{t}} = 0 \quad (4.29)$$

$$\rho_B \frac{\partial q}{\partial \hat{t}} = \kappa a F'(C, q) \quad (4.30)$$

Introducing a transformation of the dependent variables, Thomas (1944) solved these equations by reduction to a linear equation. With the boundary conditions $C(0, t) = C_0 = \text{constant}$ and $q(x, 0) = 0$, the concentrations are solved as:

$$C/C_0 = J(n/K, n T_r) / H' \quad (4.31a)$$

$$q/q_m = [1 - J(n T_r, n/K)] / H' \quad (4.31b)$$

where

$$H' = J(n/K, n T_r) + [1 - J(n, n T_r/K)] \exp[(1 - K^{-1})(n - n T_r)] \quad (4.32)$$

$$n = \frac{\kappa a x}{\epsilon v} = \text{dimensionless distance or NTU} \quad (4.33)$$

$$T_r = \frac{\epsilon v C_0 \hat{t}}{q_m \rho_B x} = \frac{\hat{t}}{TBC} \quad (4.34)$$

$$n T_r = \frac{\kappa a C_o \hat{t}}{q_m \rho_B} = \text{dimensionless time} \quad (4.35)$$

$$J(\alpha, \beta) = 1 - e^{-\beta} \int_0^\alpha e^{-\xi} I_0(2\sqrt{\beta\xi}) d\xi \quad (4.36)$$

$I_0(2\sqrt{\beta\xi})$ is the modified Bessel function of order zero of the first kind (Ozisik, 1968). The values of the J function are shown graphically in Figure 4.4 (Vermeulen et al., 1973). Approximation equations have been developed by Thomas (1944) for large $\alpha\beta$ values:

$$J(\alpha, \beta) \approx \frac{1}{2} [1 - \operatorname{erf}^*(\sqrt{\alpha} - \sqrt{\beta})] + \frac{\exp[-(\sqrt{\alpha} - \sqrt{\beta})^2]}{2\sqrt{\pi} [(\alpha\beta)^{1/4} + \sqrt{\beta}]} \quad (4.37)$$

The error is less than one percent when $\alpha\beta > 36$. Ledoux's (1948) approximation further neglects the second term on the right hand side of Equation 4.37 when $\alpha\beta > 3600$:

$$J(\alpha, \beta) \approx \begin{cases} 0.5 \operatorname{erfc}(\sqrt{\alpha} - \sqrt{\beta}) & , \text{ if } \beta < \alpha \\ 0.5 [1 + \operatorname{erf}(\sqrt{\alpha} - \sqrt{\beta})] & , \text{ if } \beta > \alpha \end{cases} \quad (4.38)$$

In the case that both concentrations in the fluid and solid or the change in concentration of fluid, are small enough, the equilibrium between the gas and solid phases behaves according to Henry's law:

$$C = (C_o/q_m) q = (\text{const.}) q \quad (4.39)$$

The above relationship makes the equilibrium reaction constant, K, equal to unity. The driving force becomes a linear expression:

$$F'(C, q) = C - (C_o/q_m) q \quad (4.40)$$

The solution of Equations 4.29 and 4.30 is thus simplified to:

* The error function is defined as: $\operatorname{erf} x = \frac{2}{\sqrt{\pi}} \int_0^x e^{-t^2} dt$ and can be approximated by an infinite series: $\operatorname{erf} x = \frac{2}{\sqrt{\pi}} (x - \frac{x^3}{1!3} + \frac{x^5}{2!5} - \frac{x^7}{3!7} + \dots)$

The complementary error function is defined as: $\operatorname{erfc} x = 1 - \operatorname{erf} x$.

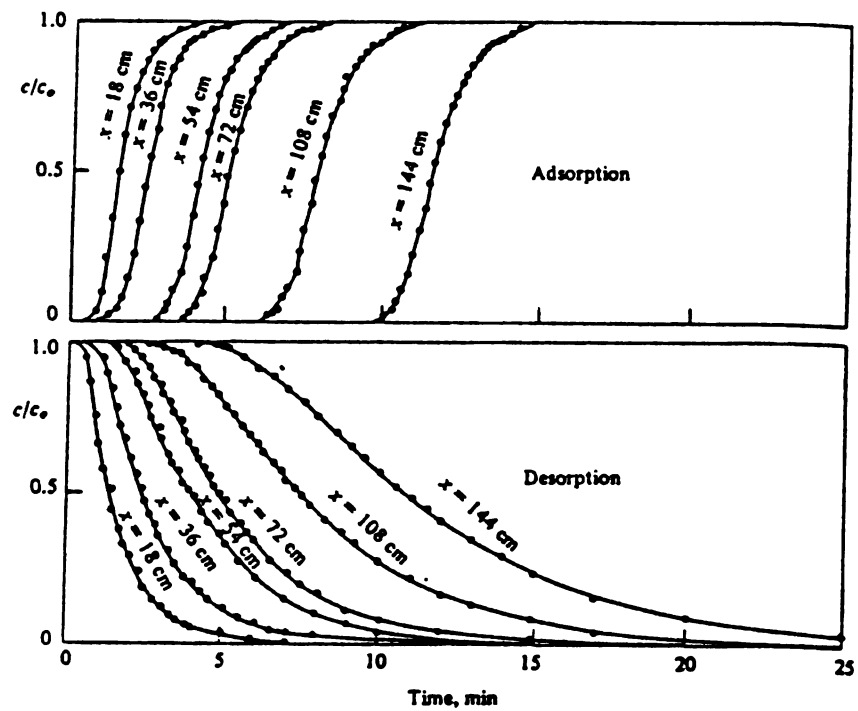


Figure 4.3. Breakthrough curves for carbon dioxide on solid carbon using bulk flow rate of 4.26 cm/s (Weyde and Wicke, 1940).

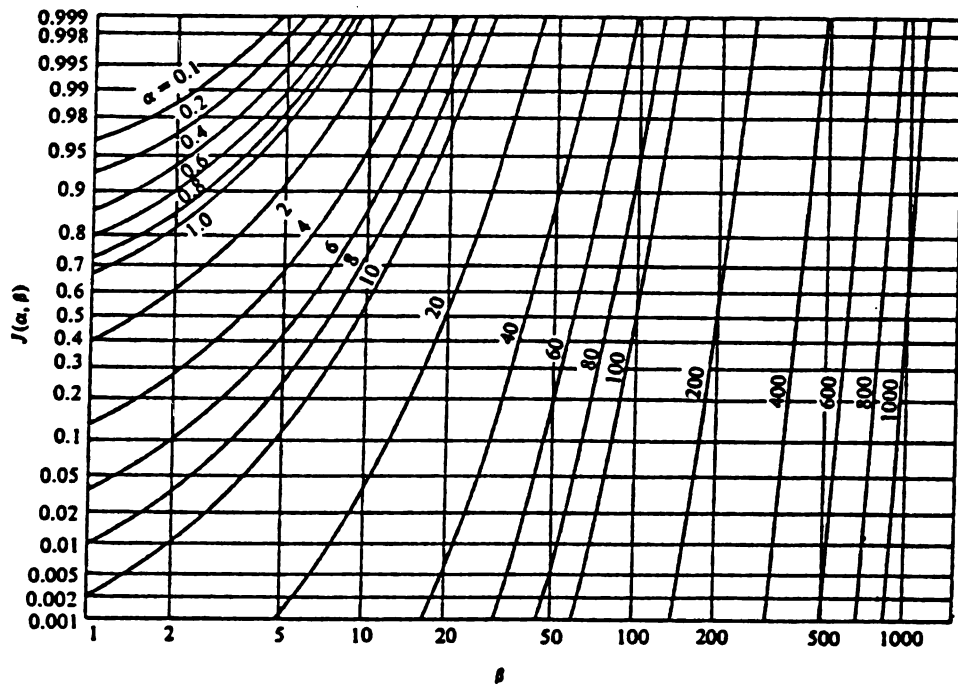


Figure 4.4. Function used in the Thomas' (1944) solution.

$$C/C_0 = J(n, nT_r) \quad (4.41a)$$

$$q/q_m = 1 - J(T_r, n) \quad (4.41b)$$

If the number of transfer units (n) is large enough and the Ledoux's (1948) approximation (Equation 4.38) is used, it is found that:

$$C/C_0 \approx 0.5 \operatorname{erfc}(\sqrt{n} - \sqrt{nT_r}) \quad (4.42)$$

The slope of the breakthrough curve at any position on the curve is found by differentiating Equation 4.42:

$$\frac{\partial(C/C_0)}{\partial t} = \frac{n T_r}{\hat{t}} e^{-n(T_r+1)} \frac{I_1(2n\sqrt{T_r})}{\sqrt{T_r}} \quad (4.43)$$

The above equation can be approximated using the asymptotic series for the Bessel function when n is sufficiently large*:

$$I_1(2n\sqrt{T_r}) = \frac{1}{2\sqrt{\pi}} \frac{e^{2n\sqrt{T_r}}}{(n^2 T_r)^{1/4}} \quad (4.44)$$

and Equation 4.43 becomes,

$$\frac{\partial(C/C_0)}{\partial t} = \frac{1}{2\sqrt{\pi}} \frac{n T_r}{\hat{t}} \frac{e^{-(\sqrt{n} - \sqrt{nT_r})^2}}{(n^2 T_r^3)^{1/4}} \quad (4.45)$$

or simply,

$$\frac{\partial(C/C_0)}{\partial t} = \frac{1}{2\sqrt{\pi}} \frac{\sqrt{n} T_r^{1/4}}{\hat{t}} e^{-(\sqrt{n} - \sqrt{nT_r})^2} \quad (4.46)$$

The slope at the midpoint $C = C_0/2$ on the break-through curve is when $T_r = 1$ (or $\hat{t} = q_m \rho_B x / \epsilon v C_0$) and can be expressed as:

$$\left. \frac{\partial(C/C_0)}{\partial t} \right|_{T_r=1} = \frac{1}{2\sqrt{\pi}} \frac{\sqrt{n}}{\hat{t}} \quad (4.47)$$

* $I_1(z) \approx \frac{e^z}{\sqrt{2\pi}} \frac{1}{\sqrt{z}} \left[1 - \frac{3}{8z} - \frac{15}{128z^2} - \frac{105}{1024z^3} \right]$ for $z \geq 10$.

If z is large enough, $I_1(z) \approx \frac{e^z}{\sqrt{2\pi}} \frac{1}{\sqrt{z}}$ (from Özisik, 1968).

Upon substitution of n and \hat{t} , Equation 4.47 becomes,

$$\frac{\partial(C/C_0)}{\partial t} \Big|_{T_r=1} = \frac{1}{2\sqrt{\pi}} \frac{C_0}{\alpha_m \rho_B} \sqrt{\epsilon\nu\kappa a/x} \quad (4.48)$$

CHAPTER 5

DESIGN OF AN AMMONIA ADSORPTION AND DRYING EXPERIMENT

1. The Grain -- Yellow Corn

The grain for the experimental phase was chosen to be yellow dent corn since Michigan is one of the corn-producing states. One hundred and twenty bushels of sample of the variety XL-12 was used. The corn was grown at a farm at Bellaire (25 miles NE of Traverse City), Michigan, and harvested on November 20, 1978.

The initial moisture content of the corn was 25.6 percent w.b. with a test weight of 53.0 lb/bu. The percentage of BCFM was 0.2 percent and the 100-kernel weight was 31.8 grams. A sample of 100 gram (dried in ambient air to 15.7 percent w.b.) was tested with the Stein breakage tester for 2 minutes, 2.7 gram of the sample passed through the 12/64 sieve. The initial grain depth in the bin was 183 cm (6 ft). The mold counts for freshly-harvested samples were very low and were assumed to be negligible. The sample in the bin was assumed to be homogeneous and isotropic with respect to the heat and mass transfer processes.

The initial viability of the sample was found to be 90 percent by the tetrazolium (TZ) solution test. The tetrazolium test is widely recognized as an accurate means of estimating seed viability (Copeland, 1976). The TZ test distinguishes between viable and dead tissues of

the embryo on the basis of respiration rate in the hydrated state. The test utilizes the activity of dehydrogenase enzymes as an index to the respiration rate and seed viability. The colorless tetrazolium salt solution in the soaked corn is oxidized into red formazan which is examined visually.

2. Experimental System

In order to investigate the ammonia adsorption behavior in a fixed bed of corn, an experimental system (Figure 5.1) was constructed which includes the following subsystems:

2-A. The Bin Structure

A 174 cm (5.7 ft) diameter bin with a capacity of 4.23 m^3 (120 bu) was used. A special bin roof was constructed to confine the airflow of the exhaust stream. A regular 4-inch house dryer hose was employed as the exhaust pipe. The bin height is 183 cm (6.0 ft) and the cross sectional area of the bin is 2.38 m^2 (25.6 ft^2).

The interior of the bin was painted with "oleum" paint to prevent possible corrosion of the galvanized steel by ammonia. Nofsinger et al. (1976) found that ammonia at concentrations under 0.1 percent in the air was not corrosive to unprotected galvanized bin surfaces. The entire structure was caulked to prevent leakage of ammonia from the bin. The bin is located inside a metal-structure shelter in which the auxiliary equipment is located.

2-B. The Fan

A 37.3 w (1/20 hp) tubaxial fan (blower) was employed. The static pressures throughout the bin were determined using a manometer. The pressure drop was 22.07 N/m^2 per meter (0.027 inches of water per foot)

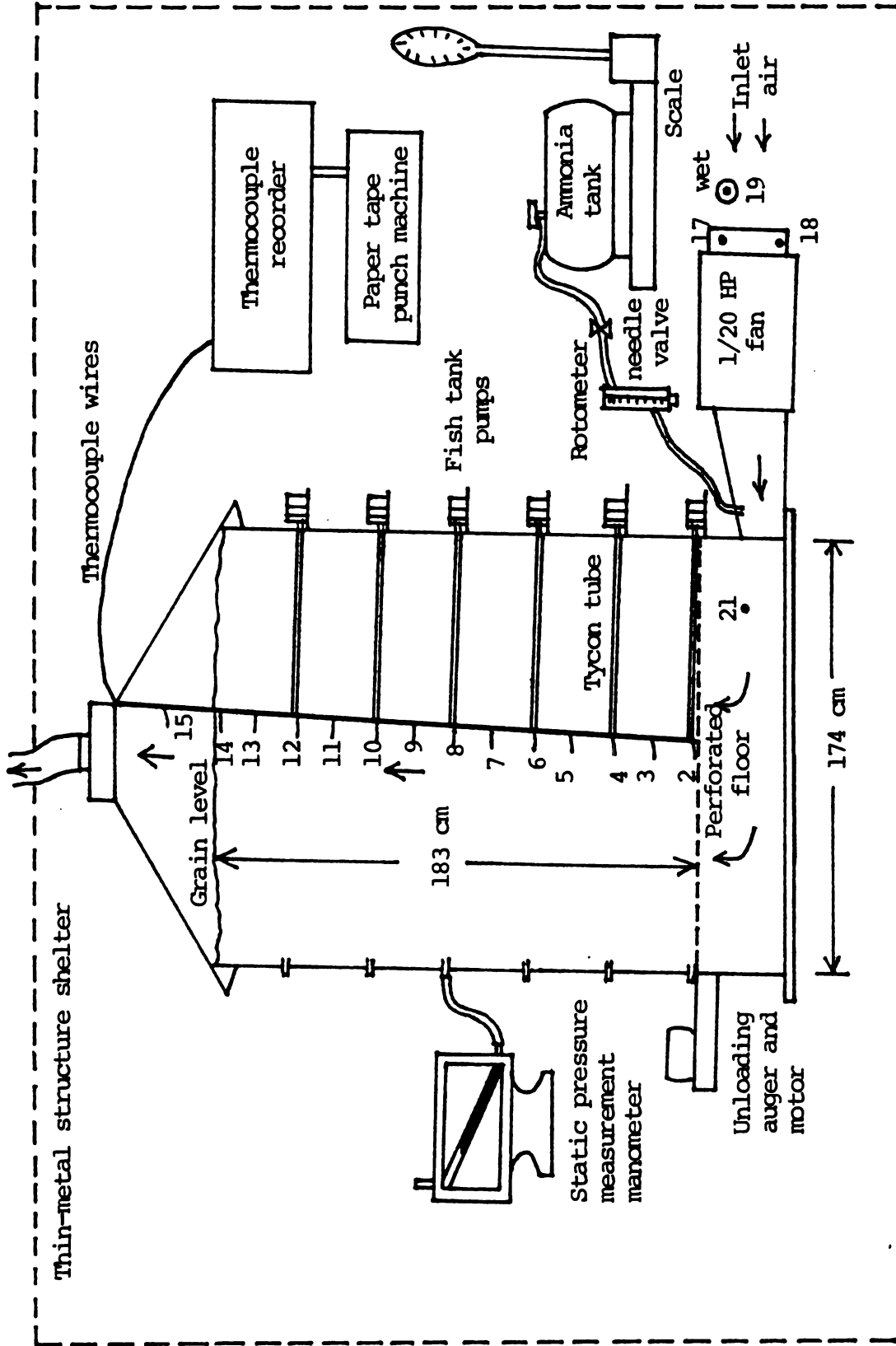


Figure 5.1. The experimental ammonia sorption and drying system. The entire system is located inside a metal structure shelter. The numbers represent thermocouple positions.

of grain which converted to $1.43 \text{ cm}^3/\text{m}^2$ ($4.70 \text{ cfm}/\text{ft}^2$) from Shedd's curve (Shedd, 1953) for 12.4 percent w.b. moisture shelled corn. Thus, the total airflow rate was about $3.4 \text{ m}^3/\text{min}$ (120 cfm) or close to $1.13 \text{ cm}^3/\text{ton}$ ($1.0 \text{ cfm}/\text{bu}$). The temperature rise due to the motor heat of the running fan was less than 1°C .

2-C. The Ammonia Application System

2-C.1. Ammonia Tank

A 15-gallon anhydrous ammonia tank was used. The ammonia tank was placed on a scale with 4-ounce divisions which allowed a weight estimation to an accuracy of ± 1 ounce. The ammonia tank is a regular farm-type anhydrous ammonia tank.

2-C.2. Ammonia Flow Controlling System

The most important component in controlling ammonia flow is a stainless steel needle valve. The desired ammonia flow rate in the experiment of $0.23 \text{ kg}/\text{hr}$ is too low to be regulated by the crude evaporation valve normally attached to an ammonia tank. At a flow rate of 0.23 kg of ammonia per hour, the flow rate must be measured in gaseous form. Therefore, a miniature needle valve was used to control the gaseous ammonia flow rate.

The flow was indicated by a rotometer attached to the needle valve. The needle valve is made of stainless steel to prevent ammonia corrosion. The valve has a teflon packing, is operable between -54°C and 232°C and can withstand a pressure up to 5000 psig (Linde, Specialty Gaseous and Equipment, Vol. IV, Union Carbide, 1977). The liquid anhydrous ammonia in the tank vaporizes and escapes through the pressure valve at the top of the tank. The rotometer also has a needle valve,

but it proved to be too crude and not sufficiently stable to control the ammonia flow. The stainless steel needle valve constitutes the main controlling valve to limit the flow.

During operation, the openings of both the pressure valve on the ammonia tank and the needle valve on the rotometer were kept as small as possible to prevent excess leakage of ammonia. The rotometer was calibrated at constant flow rates to indicate the true ammonia flow rate. There are ten divisions on the rotometer scale. It was found that at scale 8, the ammonia flow rate is 0.23 kg/hr. The ammonia flow rate was found to be proportional to the scale number.

2-C.3. Temperature Recording System

The temperature recording system consists of a Esterline Angus (An Esterline Company) digital thermocouple recorder (Model PD2064, Key programmable data system) and a paper tape puncher. The recorder can register up to 60 thermocouples with special attachments. Normally, 24 points are registered and programmed.

The recorder can be used with different kinds of thermocouple wires by changing the correction factors. The results for each individual channel can be programmed to display in degrees Centigrade, Fahrenheit or in millivolts. The recording time interval and channel scanning interval can be programmed and an ID number can be assigned to any special alteration in operation during the experiment. If the channel scanning interval is set to zero, the temperatures at all the thermocouples are recorded at the same moment and printed accordingly on the printer. The conventional thermocouple recorder equipped with a mechanical moving pen is unable to do this.

The paper tape punching machine punches the results in black paper tape in computer coding which can be transferred and stored directly in any computer system.

3. Sampling Systems

3-A. Grain Sampling

A grain sampling probe with ten compartments was used to collect samples from one to five feet levels at one foot interval as shown in Figure 5.2. Each grain sample was assigned to two compartments. Besides these five samples, the top level sample was gathered by hand and the bottom level sample was probed from side holes. This was found to be the most efficient way of collecting samples for each foot level and also minimize the disturbance and mixing of the grain in bin. The major disadvantage is the closing of the 10 holes manually while the probe is in the bin not only breaks corn but also needs strength to handle it. The grain samples were transported as soon as possible to the laboratory for immediate treatments.

3-B. Air Sampling

To gather air samples is always a problem since it is difficult to contain the air in a container for further treatments without inducing experimental errors. The most direct way of analyzing air samples is gas chromatography (GC) (Lancaster et al., 1975).

In the GC method, the air samples are collected using an air-tight syringe and injected into a GC machine equipped with a specified column (Porapak Q, N, or S, suggested by USDA Laboratory, Peoria). Helium is suggested as the carrier gas. This method is one of the most accurate methods. However, there are disadvantages: (1) the GC method requires

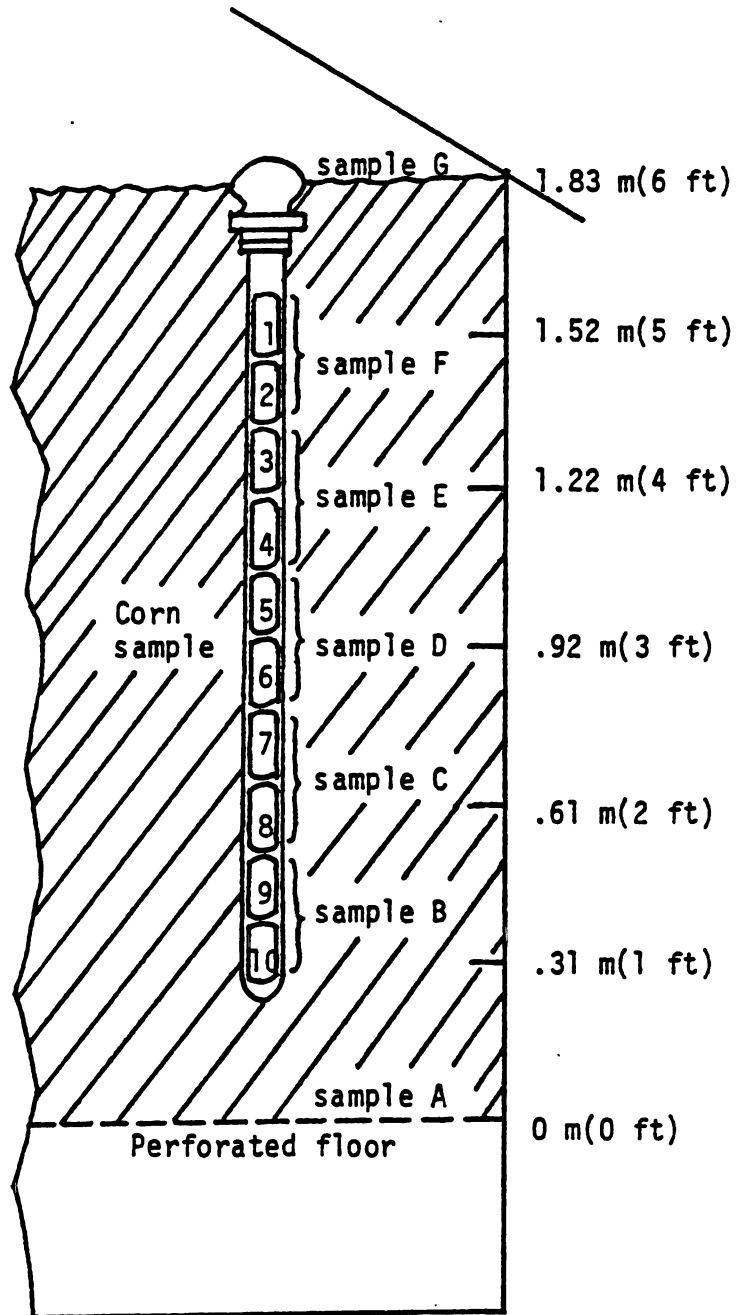


Figure 5.2. The position of a 10-compartment grain sampler in the grain bin during sampling. Samples from 1 to 5-ft levels are collected in the grain sampling probe while the 6-ft level sample is collected from the top of the grain mass manually and the bottom level sample is collected by side-probing.

a reliable, accurate, and precisely calibrated GC instrument equipped with a thermoconductivity detector (most of the commonly used GC instruments in biological laboratories are equipped with flame ionization detectors), (2) the column needs special packing instructions with respect to packing material, packing density, length and size of column, in order to effectively separate the components in air samples, (3) the operation requires constant attention, and (4) the method can only analyze one sample at a time, since the next sample has to wait until the previous one has run through the entire GC column. The throughput time ranges from several minutes to one hour depending on the sample type and the helium flow rate. Due to the unavailability of a reliable and properly equipped GC instrument, an alternative way of collecting air samples was developed.

The problem to be solved was how to collect a known air sample at six different depths in the bin at the same time. A miniature pump was used to pump the air out of the bin for a fixed period of time. Each air outlet of the pump was submerged in a bottle with a measured amount of distilled water. Since ammonia is the only component in which the concentration is concerned and ammonia dissolves readily in water, the ammonia concentration can be determined by direct titration using a standard acidic solution and a pH meter. The major advantages of this method are: (1) only inexpensive, easy to install, unsophisticated instruments are needed, (2) all six samples from the different levels can be collected at the same time, (3) it is relatively easy to collect samples, (4) the method is reasonably accurate if carefully calibrated, and (5) the final titration determination method is straightforward.

The miniature pumps used in this experiment were commercial fish-tank pumps. The pumps had to be modified since a regular fish-tank pump does not have a fixed inlet air source. The pumps were sealed externally except for the outlet air opening. An inlet hole for air was drilled on the opposite side of the plastic wall of the pump. The air inlet to the pump was connected with a piece of tycon tube placed in the bin horizontally and tied to the cable support for thermocouple wires to hold the tubes in position. The portion of tycon tubes in the bin was drilled with holes to minimize the pressure gradient during the air intake. The fish-tank pumps were tested in the laboratory and found by the water displacement method to pump an average of 1.4 liters of air per minute.

A standard procedure employed throughout the experiment consisted of using 100 ml distilled water for ammonia collection and aerate for 10 minutes. Thus 14 liters of air passed through water. This procedure was calibrated with a known concentration of air samples. The correction factor is assumed to be the same for all stations.

4. Weather Conditions During the Experiment

The tests are split into two parts because the severe 1979 winter weather in Michigan interrupted the experiment. The first part was extended from November 13, 1978, to January 10, 1979. The average air temperatures, relative humidities, and the measured average grain temperatures are shown in Figure 5.3. The measurement of relative humidity was interrupted when the air temperature dropped below freezing. An average relative humidity was assumed to be 70 percent for this period in the simulation. On January 10, the ambient air temperature decreased to below -12°C as did the average grain temperature. The fan was

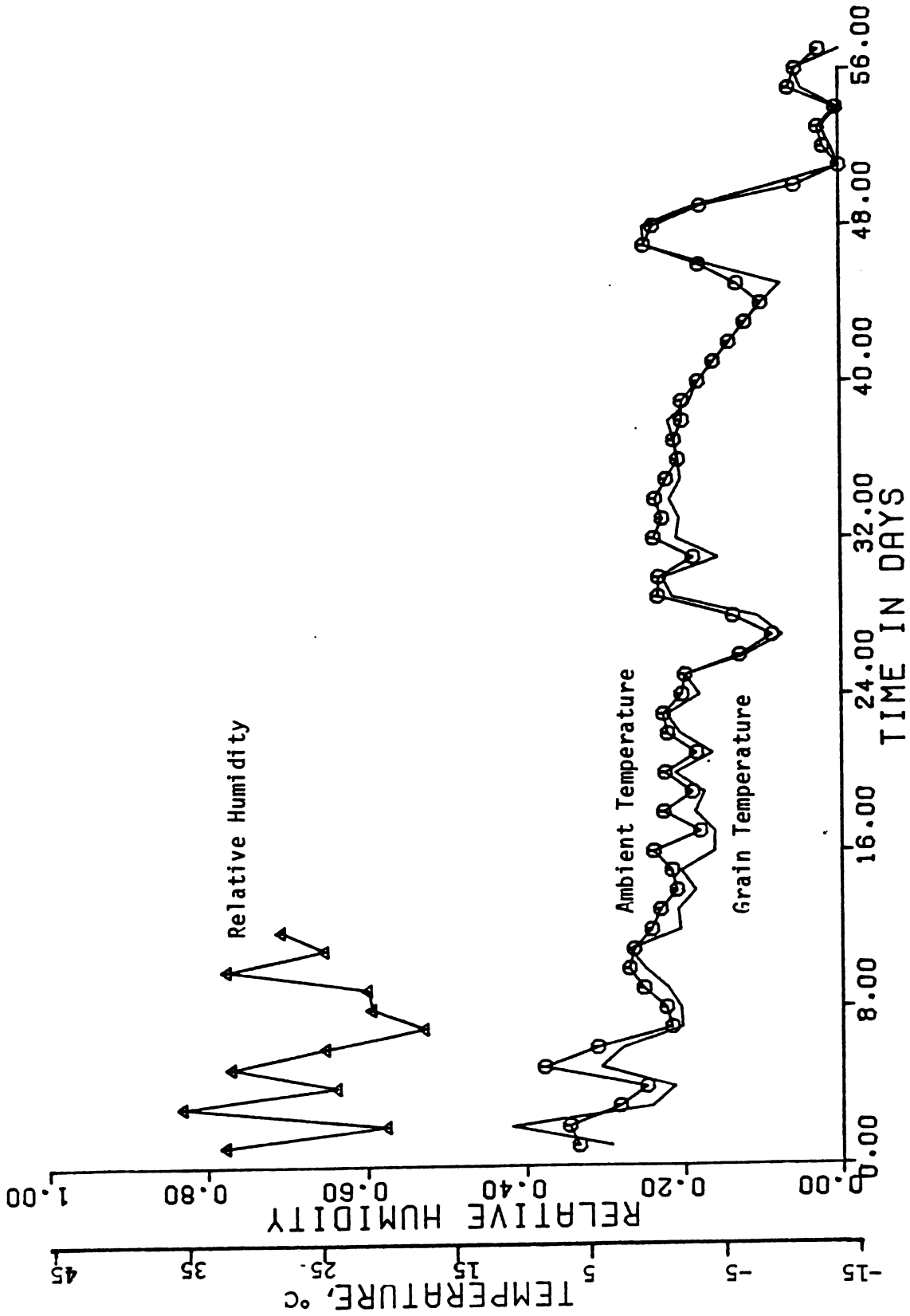


Figure 5.3. The average ambient air temperature, relative humidity and the measured average grain temperatures for the first part of experiment. The measurement of relative humidity was interrupted when the air temperatures dropped below freezing.

turned off and was not turned back on until April 4, 1979, when the ambient temperature had reached 4.5°C. The second part of the test was conducted between April 4 and April 24, 1979. The average ambient air temperatures, relative humidities, and the measured average grain temperatures during the experiment are shown in Figure 5.4. The average grain temperatures follow the ambient air temperatures very closely throughout the test periods. The local amplitudes of the variation of grain temperatures are less significant than those of the ambient air temperatures as indicated in Figure 5.4.

5. Timetable of Fan Operation and Ammonia Application

5-A. Part I. Trial Period (11/13/78-1/10/79)

The fan was started at 8:30 a.m., November 13, 1978, immediately after the bin had been loaded. The anhydrous ammonia was applied at the rate of 0.23 kg/hr (0.5 lb/hr) (a rate suggested by the researchers in North Regional Research Laboratory at Peoria, Illinois, Eckhoff and Bothast, 1978). Although 0.05 percent* ammonia is sufficient to kill microorganisms in 27 percent moisture (w.b.) corn, it takes about 0.5 percent ammonia to control molding during long-time preservation and in-bin natural air drying (Bothast et al., 1975). Thus, for 4.23 m³ (120 bu) of corn, 12.9 kg (28.4 lb) (4.23 m³ x 609.3 kg-dry corn/m³ x 0.5% = 12.9 kg-NH₃) of anhydrous ammonia should be adsorbed by corn during the entire treatment.

The amount of ammonia actually adsorbed by the corn permanently and the amount of ammonia applied through inlet air duct can be very different. The difference depends on the following factors:

* All the ammonia concentrations referred to in this thesis are based on the dry weight of corn unless otherwise mentioned.

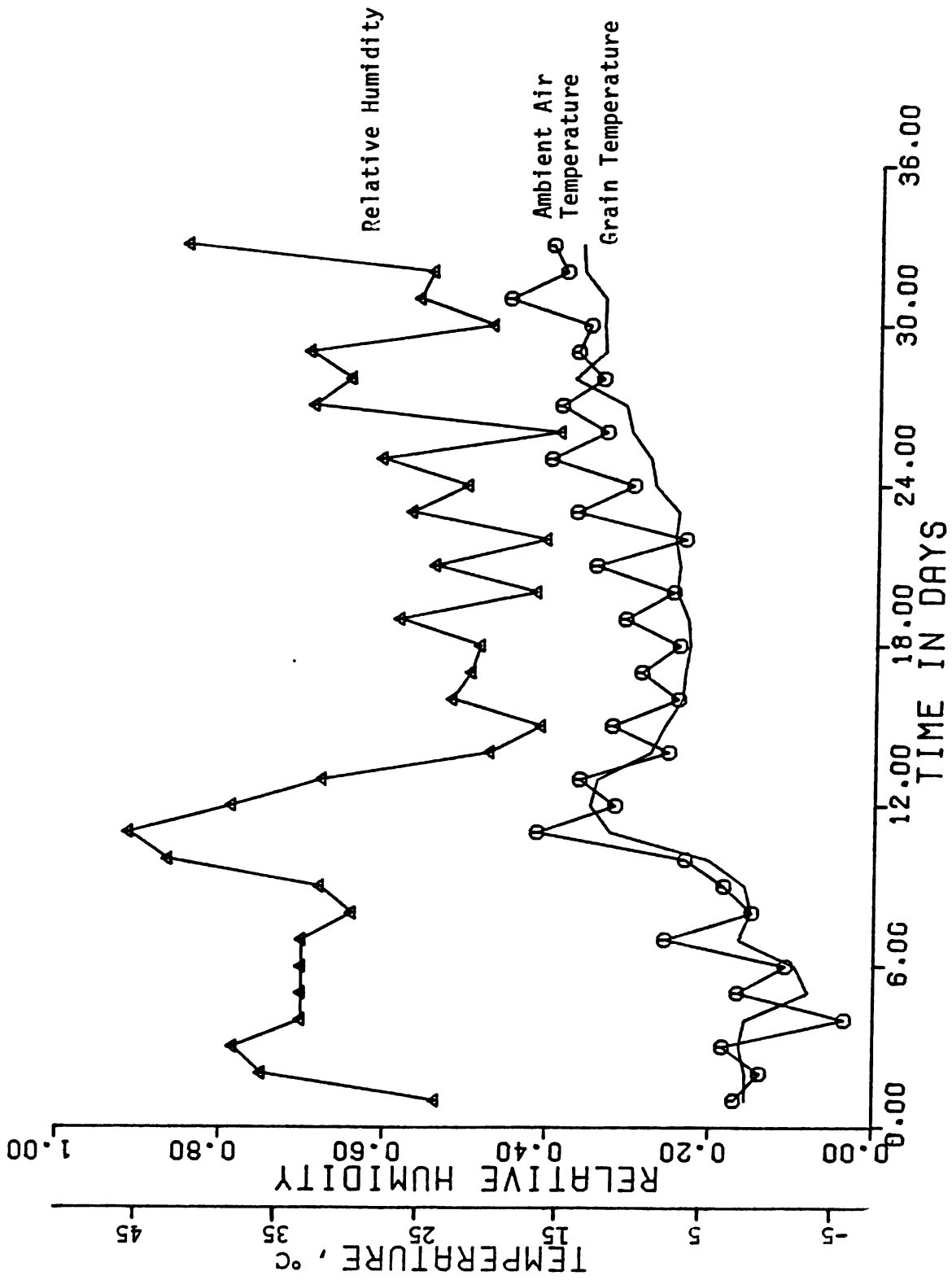


Figure 5.4 . The average air temperatures, relative humidities and the measured average grain temperatures for the second part of experiment.

(1) the rate of ammonia application, (2) the rate of ammonia diffusion into the micropores on the surface of the corn kernels, (3) the rate of adsorption of ammonia in the pores and surface area of the corn kernels, (4) the amount of ammonia loss in the exhaust air and, (5) the rate of ammonia leakage of the tank and the hook-up junctions.

The above factors are not totally independent. The rate of ammonia supply in the inlet air determines the ammonia concentration for diffusion into the micropores and the rate of adsorption. The losses of ammonia in the exhaust air increase with the increase of rate of ammonia application. Although the decrease of the ammonia application rate reduces the losses of ammonia, the effectiveness of ammonia in preventing molds depends on the adsorption of a sufficient amount of ammonia within a limited period of time. The deterioration of biological products is a continuous process. Thus, there is a trade-off between increasing molding risks and increasing ammonia losses.

The timetable for ammonia application and the ambient air temperatures in the first part of the experiment is shown in Figure 5.5. The ammonia was applied at a rate of 0.23 kg/hr for 8 hours after which the rate was changed to 0.057 kg/hr (1/8 lb/hr). A strong ammonia odor could be smelled at the top of the bin after about six hours of ammonia treatment at 0.23 kg/hr. The reason for the rate change was to reduce the rate of ammonia sorption and the losses to the environment. This high-rate initial injection of anhydrous ammonia to a batch of freshly harvested corn is important in reducing or eliminating the initial population of contaminants, e.g. bacteria, fungi, and other microorganisms, and in preventing further development of contaminants. This "dying" process for the entire grain mass, especially the top

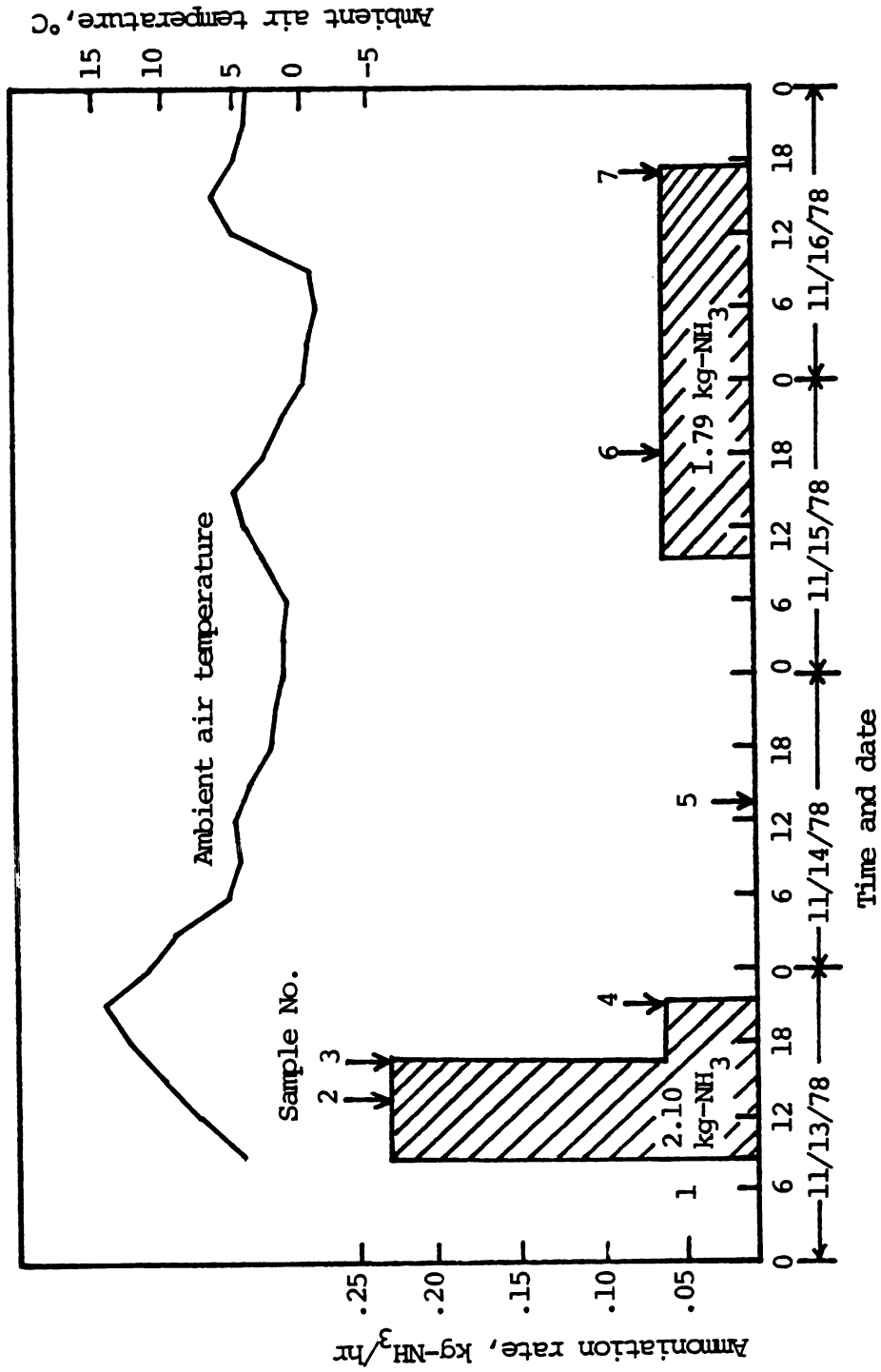


Figure 5.5. The timetable for ammonia application and the ambient air temperature in the first part of the experiment.

portion of the grain, is very effective if it can be done before significant deterioration occurs. The rate of 0.057 kg/hr is to maintain up the ammonia concentration while ammonia is being adsorbed by the corn. The ammonia flow was stopped after five hours at the rate of 0.057 kg/hr because some mistakes were identified in the procedure of determining total ammonia. It was not until 36 hours later that the ammonia flow was resumed at the rate of 0.057 kg/hr. This ammonia flow was continued for 31.5 hours. When the ambient temperatures at night in mid-November dropped to around -6.7°C (20°F), the ammonia application was stopped since the adsorption behavior of ammonia in corn at temperatures below the freezing point of corn is unknown. However, the fan kept on running to dry the corn while the corn was "protected" by a ammonia coating and low temperature. At the end of this part of the experiment, 3.89 kg of ammonia had been applied and the fan had been blowing for 56 days and 16 hours.

5-B. Part II. Constant Rate Periods (4/4/79-4/24/79)

Throughout the entire period of this part of the experiment, the ammonia flow rate was fixed at .113 kg/hr as shown in Figure 5.6 in order to study the constant ammonia flow sorption processes.

The fan was started at 11:30 a.m., April 4, 1979, when the ambient temperature had climbed to 4.5°C . The ammonia was applied four hours later. Visible mold was seen on the surface of the corn kernels at 15-30 cm depth below the top bin surface. The molding was not serious since the grain temperatures seldom had exceeded 4.5°C throughout the "cold storage" period when the fan was off. However, the molding is expected since the top layers received the least amount of ammonia and remained at the highest moisture content (about 25% w.b.) all the time.

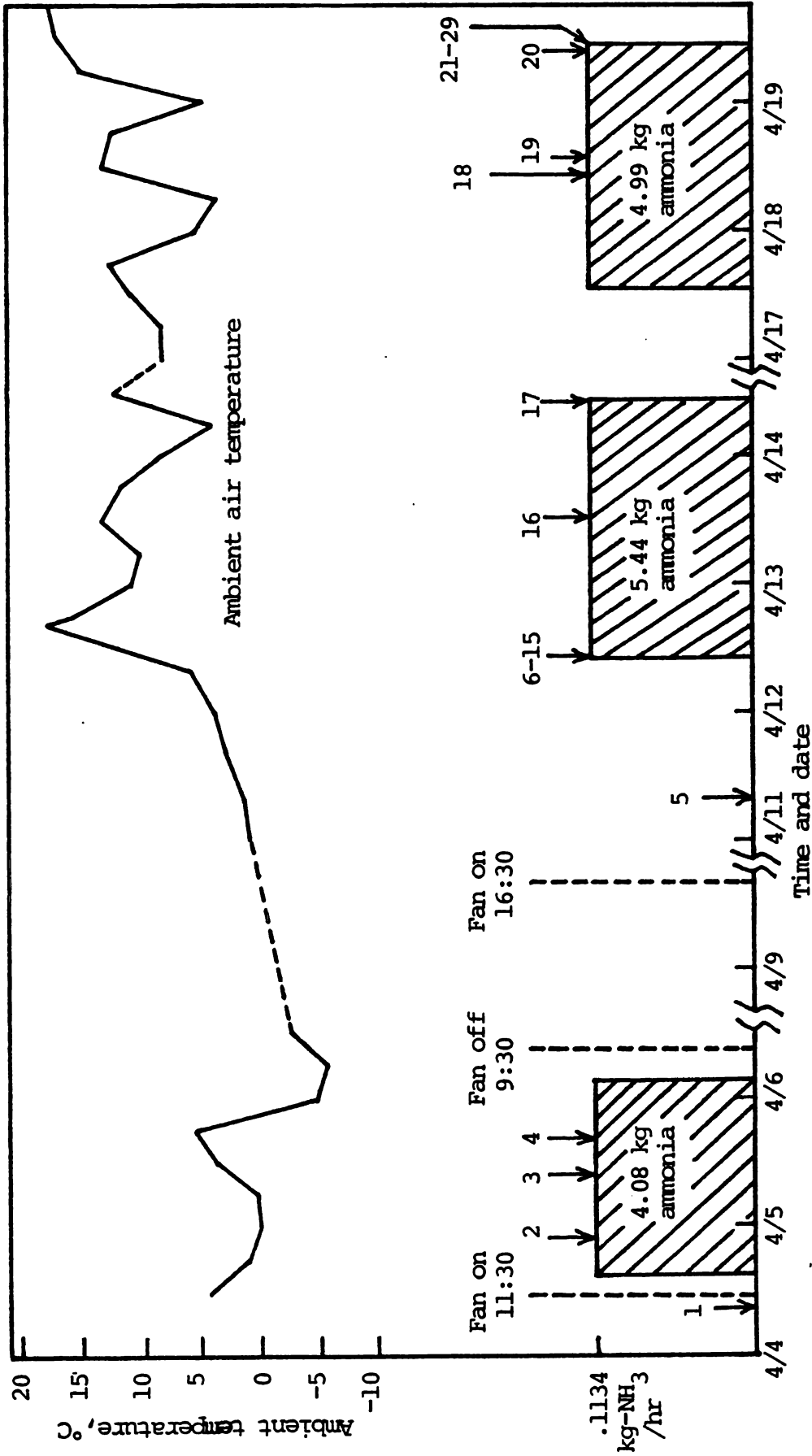


Figure 5.6. The timetable for ammonia application and the ambient air temperature in the second part of the experiment.

After 36 hours of ammonia flow, the application of ammonia was interrupted because of renewed cold weather. Five hours later, it was determined to shut off the fan because the ambient temperature had dropped to about -6.7°C .

It is assumed that no moisture migration and ammonia transfer in the bin occurred while the fan was turned off. The fan was not turned on until 4:30 p.m., April 9, when the ambient temperature had reached around 0°C . The ammonia flow was resumed at 10:00 a.m., April 12. A series of adsorption tests were performed to determine the ammonia profiles in the air at different levels of the bin. The tests were performed by taking air samples continuously from six different levels in the bin.

Each sampling process took 10 minutes; ten sets of samples (six samples per set) were collected. The ammonia was applied at the rate of 0.113 kg/hr (0.25 lb/hr) for another 46 hours immediately after these tests. The ammonia treatment was then discontinued for about three days because of illness of the technician in charge of the chemical analysis.

The ammonia test was completed at 11:00 a.m., April 19, 1979, after an additional 44 hours of ammonia application. A series of desorption tests similar to the adsorption tests were performed immediately after the ammonia flow was shut off. The fan was turned off at 12:00 noon, April 24, after the final samples were taken. The purpose of these desorption tests was to study the rate of ammonia removal in the air from the bin.

In this second part of the experiment 14.51 kg of ammonia was applied at the rate of 0.113 kg/hr; the fan was operated for 384 hours.

6. Procedures of Sample Analyses

6-A. Determination of Free Ammonia (Black, 1978)

- 1) Place approximately 20 g of whole kernel corn in a 500-ml glass bottle containing 300 ml of distilled water.
- 2) Cover the bottle, let it stand overnight.
- 3) Titrate a portion (known amount) of the solution with standard sulfuric acid ($0.02N H_2SO_4$) to a pH of 5.6 using a pH meter.
- 4) Method of Calculation:

$$(\% \text{ free } NH_3) = \frac{(\Delta ml) (N) (MW) (100\%) 300 \text{ ml}}{(1000) (g) (1-MC) b \text{ ml}}$$

where, $\Delta ml = (\text{ml } 0.02N H_2SO_4 \text{ needed for sample}) - (\text{ml } 0.02N H_2SO_4 \text{ needed for blank corn sample})$

N = concentration in normality of standard acid

g = sample weight, grams

MC = moisture content of sample, decimal, dry basis

b = portion of the solution using in titration.

6-B. Determination of Total Ammonia (Black, 1978)

- 1) Put the whole kernel corn sample in a 65 ml bottle, fill to the top to reduce headspace (about 25-30 g), add 1-2 ml of concentrated hydrochloric acid. Shake the bottle, allow to stand for an hour and then spread the sample on a paper towel for air drying overnight.
- 2) The dried sample is ground; around 5 g is ground (or chopped) for Kjeldahl distillation.
- 3) Place the ground sample in a Kjeldahl distillation flask, add 200-250 ml distilled water, more than 2 g carbonate free magnesium oxide and 2 or 3 drops of defoamer (Titon X-100).

Distill about 150 ml water into the distillate receiving bottle with 100 ml of 2 percent boric acid (mixed with indicator, as described in Step 5).

- 4) Titrate with 0.1 N HCl until the solution turns from blue to red.*
- 5) Preparation of Boric Acid Mixed with Indicator

Dissolve 2 g of Bromocresol green and 0.4 g of methyl red indicators in one liter 95% ethanol. Mix 4 ml of the above indicator for every one liter of 2% boric acid solution. The mixed solution is red colored.

- 6) Method of Calculation

$$\text{Total \% NH}_3 = \frac{(0.1N)[(\text{ml } 0.1 \text{ N HCl in sample}) - (\text{ml HCl Blank})] \times 17 \times 100\%}{(1000) (\text{sample wt. in g}) (1 - \text{MC}_{\text{d.b.}})}$$

6-C. Determination of Mold Count (Speck, 1976)

- 1) Weigh 25 g (± 0.1 g) of a representative portion of the corn kernels aseptically into a tared sterile blender cup.
- 2) Add 225 ml of sterile dilutant (phosphate buffered) and blend 2 minutes at low speed or until well blended.
- 3) Plate 0.1 ml of this solution (or 10^{-2} g sample) on acidified potato dextrose agar (PH=3.5 \pm 0.1).
- 4) Dilute 1 ml of the blended solution to 100 ml and plate 0.1 ml of the diluted solution (or 10^{-4} g sample) on acidified potato dextrose agar.
- 5) Repeat Step 4 and further dilute the solution to 1/100 sample concentration, or 10^{-6} g sample per plate.

* It takes 0.1 to 0.2 ml of 0.1 N HCl to titrate from blue to red for a blank corn sample.

- 6) Incubate for 5 days at 20°C and count colonies.

CHAPTER 6

DEVELOPMENT OF A SIMULATION MODEL FOR AMMONIA ADSORPTION IN FIXED-BED DRYING SYSTEMS

1. Introduction

The treatment of grain using anhydrous ammonia in a fixed-bed drying system is a unique problem in the area of sorption processes. According to the previous discussions, the ammonia sorption process in a packed bed of grain is not the same as any of the existing sorption systems encountered in chemical engineering. The ammonia-corn system cannot be explained by a single engineering process such as ion exchange, binary separation, chromatography, heterogeneous catalysis, or chemisorption.

Biological products are usually complex in composition and are "alive" since respiration and other biological, biochemical processes are still taking place. The composition of a biological product is thus changing continuously as a result of physical and chemical reactions occurring within the product. These unavoidable deteriorations of biological products are usually lumped into several macroscopic phenomena by assuming a black box model for the system and just considering the inputs and outputs. The input elements for the deterioration of corn are wet corn, oxygen, and environmental conditions such as temperature, humidity, and microbiological contamination, while the output elements involve carbon dioxide, water, and energy production which favors microbial growth.

The fixed-bed grain drying model developed by Bakker-Arkema et al. (1974, 1977) at Michigan State University (MSU) is a dynamic and iterative model that allows calculation of grain temperature, air temperature, absolute humidity, and grain moisture content for every specified bed location and time step employing the finite differences method for solving the simultaneous partial differential equations. The MSU numerical model can be applied to any fixed-bed grain drying system: high-temperature, natural air, low-temperature, and solar energy drying. Any type of inlet, initial, and boundary conditions can be modeled.

The four-equation fixed-bed grain drying model (Bakker-Arkema et al., 1974) as described in Chapter 4 predicts both air and grain temperatures along with the air absolute humidity and grain moisture content. Very small computing time steps have to be used in order to avoid instability in the numerical solution. The four-equation model was found to be very inefficient in computing slow drying processes such as natural air and low-temperature drying; it would have been advantageous if a larger computing time step could have been used. In order to overcome the stability problem encountered in a four-equation model using larger time steps, Bakker-Arkema et al. (1977) reduced the system to a three-equation model by assuming no difference in temperature for air and grain throughout the entire drying processes. This assumption is justified for slow grain drying processes. The major advantage of the three-equation model is the very stable characteristics of the model with respect to numerical integration. Larger computing time steps can thus be used in the three-equation than in the four-equation model. The three-equation model has also been proved to be reasonably

accurate in the simulation of fixed-bed drying processes. The three-equation model described by Bakker-Arkema et al. (1977) is expressed as follows:

$$\rho_p (c_p + Mc_w) \frac{\partial T}{\partial t} + G_a (c_a + Hc_v) \frac{\partial T}{\partial z} + G_a [(c_w - c_v)(100 - T) + h_{fg}] \frac{\partial H}{\partial z} = 0 \quad (6.1)$$

$$\rho_p \frac{\partial M}{\partial t} + G_a \frac{\partial H}{\partial z} = 0 \quad (6.2)$$

$$\rho_p \frac{\partial M}{\partial t} = r_m(T, H, M, t) \quad (6.3)$$

where r_m is the proper thin-layer drying or absorption function. Nevertheless, the author believes that the first term in the bracket of Equation 6.1 should be $C_v(T - \theta)$ instead of $(C_w - C_v)(100 - T)$. No significant difference is anticipated since both terms are very small compared to the latent heat of evaporation, h_{fg} .

2. Assumptions

One of the characteristics in developing a numerical simulation model for a complicated dynamic system is that the model must be based on some assumptions which idealize the system to a more "solvable" problem. The roles of assumptions cannot be overlooked in the derivation of model equations since they link the real and complicated world to the simplified interpretations of the numerical equations model.

For the ammonia sorption and drying model in a fixed bed of grain, the following groups of assumptions are made for the different components of the system:

Group A -- The Bin Structure

1. The grain bin is part of a perfect infinite hollow cylinder with a constant diameter.

2. The bin walls are adiabatic with negligible heat capacities and have negligible effect on the airflow.

Group B — The Grain

3. The corn kernels can be represented by uniform spheres.
4. The grain sample in the bin is homogeneous and isotropic.
5. The volume shrinkage due to loss of moisture and settling are negligible.
6. The dry matter change during the drying process is negligible.
7. Accurate thin-layer drying-absorption equations and equilibrium moisture isotherms are available within the temperature and humidity ranges under investigation.
8. The density, specific heat, and thermal conductivity do not vary significantly with temperature over the range of interest.

Group C — Heat and Mass Transfer

9. Heat conduction due to particle-to-particle contact is negligible.
10. Heat transfer in the radial direction is negligible.
11. Heat conduction within the bulk stream is negligible, i.e. heat transfer by convection only in the bulk stream.
12. The $\partial T/\partial t$ and $\partial H/\partial t$ terms are negligible compared to the $\partial T/\partial z$ and $\partial H/\partial z$ terms.
13. No significant temperature and moisture gradients exist within an individual corn kernel.
14. The surface heat and mass transfer coefficients are constant over the corn kernel surface.
15. No surface condensation of liquid water or ammonia solution; any condensed liquid is restored as part of the average moisture content of the grain.

Group D — Airflow

16. The bulk air stream behaves as an incompressible fluid.
17. Dry air, water vapor, and ammonia are assumed to be ideal gases and behave independently, in other words, the air bulk stream is an ideal mixture.
18. Dry air is considered inert, i.e. dry air is not involved in any mass transfer processes except acting as a carrier.
19. The generation and transport of gases other than water vapor and ammonia are negligible, e.g. CO_2 generation from dry matter loss is neglected.

Group E — Ammonia

20. The ammonia and water vapor are in constant thermal and concentration equilibrium with the dry air, i.e. no gradients exist in the bulk stream except in the z-direction.
21. The heat of adsorption of ammonia is constant within the temperature and concentration ranges considered.
22. The driving force of ammonia adsorption is linear and can be expressed as the concentration difference between the equilibrium value and the current value in the grain.
23. The ammonia sorption isotherm is known.
24. Part of the adsorbed ammonia remains in the grain as a residual during desorption and the amount of residuals is a fixed ratio (δ) of the free ammonia content.

The ammonia adsorption model in a fixed-bed drying system is composed of two major parts: the drying model and the ammonia sorption model. The two models are not independent since ammonia coexists with water vapor as a major transport species. Because of the assumptions,

the ammonia sorption model and the drying model can be simplified to a one-dimensional, spherical-particle packed-bed problem.

The transport phenomena of water vapor and ammonia are similar in the following aspects: (1) both processes involved the same solid particles (corn), (2) both processes are diffusion-controlled, and (3) water (H_2O) and ammonia (NH_3) molecules have the same molecular weight and approximately the same molecular size. The chemical properties of H_2O and NH_3 are not very different either.

Unlike water, ammonia reacts chemically with the corn components to form residuals. The diffusion rate of ammonia and water in corn can be very different. The affinity of ammonia for water is much higher than of water to itself. Hence, the ammonia isotherms do not relate to and cannot be derived from water moisture isotherms and thus must be developed separately as shown in Chapter 3.

3. Derivation of Model Equations

The derivation of model equations generally involves the following sequence:

- 1) Identify the components and subsystems according to the structure and nature of the system. There is no unique way of doing this, all the unrelated inert components in the same phase can be lumped in a component, such as dry air and dry matter of corn.
- 2) Identify the state variables based upon the characteristics of the problem involved. Very frequently, an unknown variable is also a state variable. Temperature and concentration are identified as state variables in the heat and mass transfer problems. The complexity of the problem, roughly speaking, depends on the number of independent state variables and their relationships to each

other and to other dependent and independent variables.

- 3) Identify the independent variables. Independent variables of a system refer to the variables which do not vary with the performance of the system. For most engineering problems, time and position are the most commonly identified independent variables.
- 4) Formulate the equations of conservation. For each independent state variable (i.e. unknown) one independent equation must be obtained. The equations describe the conservation of independent state variables for the bulk system or individual components. The conservation of heat and mass transfer is usually expressed by the differential change with respect to time and/or position. The formulation of model equations must be based on a series of assumptions as described in the previous section.

The following components can be identified in the ammonia sorption and drying model: (1) dry air, (2) dry corn, (3) liquid water in corn, (4) water vapor in the air, (5) ammonia in corn, and (6) ammonia gas in the air. The model to be presented results from mass balances on ammonia both in the air and in the corn and on moisture in the corn and in the air. Also included are energy balances on the solid and fluid phases. The state variables in the ammonia sorption model and the drying model are: (1) ammonia concentration in the air, x_1 , (2) absolute humidity in the air, H , (3) ammonia concentration in corn, x_2 , (4) average moisture content of the product, M , (5) air temperature, T , and (6) product temperature, θ .

The model equations can be derived from a control-volume analysis by considering the heat and mass balances within a differential volume representative of the entire system. The control volume in the case

of a grain bin can be described by a differential height (dz) of the grain bin with constant cross sectional area (S) perpendicular to the direction of airflow as shown in Figure 6.1. The balance usually takes the following form:

$$(\text{flow in}) + (\text{generation}) = (\text{flow out}) + (\text{accumulation})$$

In the case of depletion instead of generation, such as the consumption of free ammonia in corn as a result of the formation of residuals, the generation term becomes negative. The accumulation term expresses the internal energy change or concentration change in the solid or fluid phase. The heat and mass transfer between the solid and bulk stream is considered the accumulation change.

3-A. Mass Balance of Ammonia in Bulk Stream

According to assumptions 17 and 20, ammonia in the bulk stream is perfectly mixed with dry air and water vapor. The mass balance on the control volume is made for a very short period of time, dt . It should be noted that the definition of all the terms related to concentration, density, flow rate are expressed on a dry basis, i.e. the amount of dry matter of corn or the amount of dry air. The formulation of equations is thus simplified. The ammonia flow is expressed as the product of the dry air flow rate per unit area (G_a), the ammonia concentration (x_1), the cross sectional area of the bin (S), and time, dt . Thus, the amount of ammonia flowing into the control volume during time dt is:

$$G_a x_1 S dt$$

The amount of ammonia flowing out of the element in the same time period dt is:

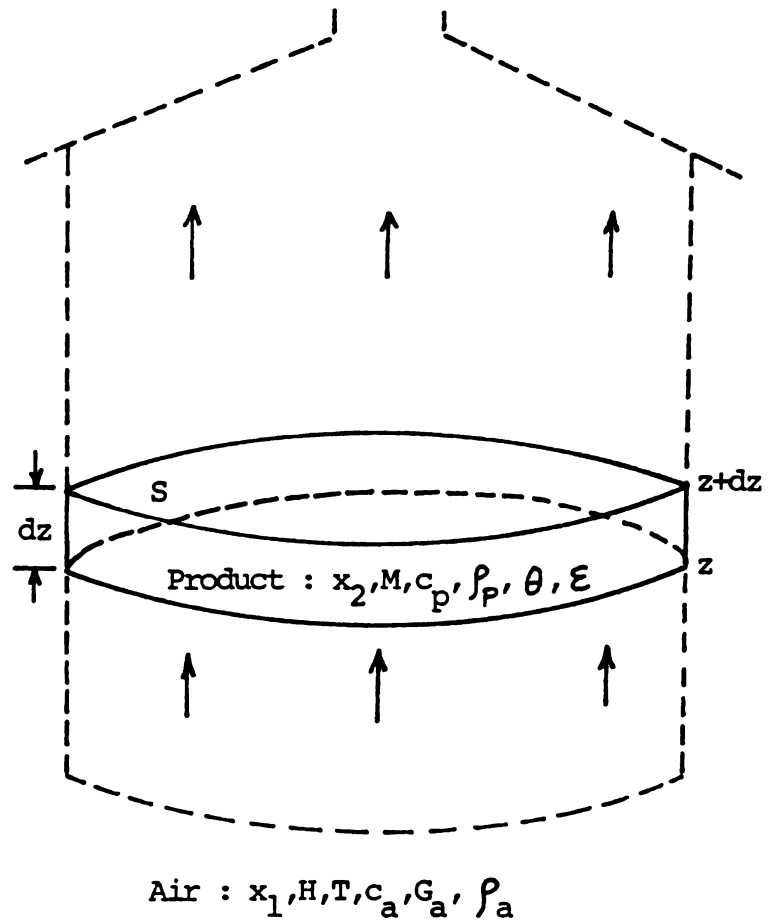


Figure 6.1. The graphical presentation of the control volume in a grain drying bin in the simulation model. Related parameters are shown for the air and the product.

$$G_a \left(x_1 + \frac{\partial x_1}{\partial z} dz \right) S dt$$

since G_a is assumed to remain constant. The amount of ammonia accumulated in the air within the control volume during time dt is:

$$\epsilon \rho_a \frac{\partial x_1}{\partial t} dt S dz$$

where ϵ is the void fraction and $\epsilon S dz$ is the void volume of the control element.

Besides the accumulation of ammonia in the air, accumulation of ammonia also occurs in the corn through interphase mass transfer. The accumulation in corn is expressed by the rate of the ammonia concentration change in the corn:

$$\rho_p (1+\delta) \frac{\partial x_2}{\partial t} dt S dz$$

where ρ_p is the dry matter density (solid, no void) of the corn, x_2 is the free ammonia concentration in the corn, and δx_2 is the amount of residuals. The amount of residuals is assumed to be a fixed ratio of the free ammonia content.

The mass balance of ammonia in the bulk stream can then be expressed as:

$$\left(\begin{array}{c} \text{ammonia} \\ \text{outflow} \end{array} \right) - \left(\begin{array}{c} \text{ammonia} \\ \text{inflow} \end{array} \right) = \left(\begin{array}{c} \text{ammonia} \\ \text{accumulation} \\ \text{in air} \end{array} \right) + \left(\begin{array}{c} \text{ammonia} \\ \text{accumulation} \\ \text{in corn} \end{array} \right)$$

Or simply,

$$\frac{\partial x_1}{\partial z} = - \frac{\epsilon \rho_a}{G_a} \frac{\partial x_1}{\partial t} - \frac{\rho_p}{G_a} \frac{\partial x_2}{\partial t} (1+\delta) \quad (6.4)$$

Equation 6.4 implies that the concentration gradient of the ammonia in the bulk stream decreases as the rates of ammonia accumulation in the air and in the corn increase. Comparing the absolute value of the two terms on the right hand side of Equation 6.4, it is obvious that the coefficient of the second term is much larger than that of the first term since the density of dry corn is much bigger than the bulk density of air in the void fraction. The influence of ammonia accumulation in the ammonia concentration gradient is thus more significant than that in the air.

However, the values of coefficient do not illustrate the entire picture; the rate of concentration changes also plays an important role. In practical ammonia adsorption system it is predictable that the rate of concentration change in the air ($\partial x_1/\partial t$) is faster than that in corn ($\partial x_2/\partial t$) during the early stages of adsorption since air has very limited capacity to hold ammonia and gets saturated sooner than the product. Although the rate of ammonia accumulation in corn decreases as time progresses under constant feed conditions, the higher rate of accumulation will maintain much longer than that in air due to the tremendously larger holding capacity for ammonia in the corn compared to that in air.

In short, the ammonia concentration gradient in the bin depends mostly on the rate of ammonia accumulation in the corn most of the time. Nevertheless, the rate of ammonia accumulation in the bulk stream does play a significant role in the early stages of adsorption. Thus, the $\partial x_1/\partial t$ term is remained in the equation.

3-B. Mass Balance of Water Vapor in Bulk Stream

The behaviors of water vapor are analogous to those of ammonia in the air. Similar analyses on mass balance can be made using the following

analogies: H (absolute humidity) $\leftrightarrow x_1$; M (average grain moisture content) $\leftrightarrow x_2$. The mass balance of water vapor in bulk stream is thus written as:

$$\frac{\partial H}{\partial z} = -\frac{\rho_p}{G_a} \frac{\partial M}{\partial t} - \frac{\epsilon \rho_a}{G_a} \frac{\partial H}{\partial t} \quad (6.5)$$

Despite the similarities of Equation 6.5 to Equation 6.4, the grain drying process is basically a water desorption process which is corresponding to the ammonia desorption process. Even though both Equations 6.4 and 6.5 can represent adsorption as well as desorption processes, the significance of the $\partial H/\partial t$ term in Equation 6.5 is much less than the $\partial x_1/\partial t$ term in Equation 6.4 for ammonia adsorption. Hence, $\partial H/\partial t$ term is ignored and Equation 6.5 becomes

$$\frac{\partial H}{\partial z} = -\frac{\rho_p}{G_a} \frac{\partial M}{\partial t} \quad (6.6)$$

3-C. Ammonia Sorption Rate in Corn

The amount of ammonia accumulated in corn within the control volume during time dt is expressed as the product of the rate of ammonia concentration change (rate of sorption) in corn and the mass of dry matter of corn ($\rho_p S dz$) in the differential element:

$$\rho_p \frac{\partial x_2}{\partial t} S dz dt = N S dz dt \quad (6.7)$$

The interphase transport phenomena of ammonia from the gas phase to the solid phase or vice versa were discussed in detail in Chapters 3 and 4. The rate of ammonia accumulation (N) is a function of the specific surface area and the driving force (F) which is a function

of both ammonia concentrations in the air and in the corn.

$$N = h_m a F(x_1, x_2) \quad (6.8)$$

where h_m is the mass transfer coefficient. The evaluation of h_m will be presented in Section 6. The driving force function is often approximated by the linear-driving-force function which is nondimensionalized as:

$$F(x_1, x_2) = \frac{x_2^* - x_2}{x_2^* - x_2^0} \quad (6.9)$$

where x_2^0 is the initial ammonia concentration in corn; x_2^* , the equilibrium concentration, is a function of x_1 and can be calculated by the ammonia sorption isotherm equation (Equation 3.16).

In Chapter 3, the ammonia concentration in the air was expressed as the partial pressure which is based on the total bulk air stream consisting of dry air, water vapor, and ammonia. Thus, the ammonia isotherm equation can be rewritten in terms of x_1 which is the concentration based on dry air:

$$x_2^* = A(T) M_{db} \left(\frac{x_1}{1 + H + x_1} \right)^{B(T)} \quad (6.10)$$

Combining Equations 6.7, 6.8, and 6.9, the rate of ammonia adsorption is obtained:

$$\frac{\partial x_2}{\partial t} = \frac{h_m a}{\rho_p} \frac{x_2^* - x_2}{x_2^* - x_2^0} \quad (6.11)$$

Equations 6.10 and 6.11 describe the ammonia concentration changes in corn kernels, in other words, the rate of ammonia adsorption depends on both x_1 and x_2 .

3-D. Changes of Moisture Content in Corn Kernel -- Thin-layer Drying Equations

The moisture removal rate in a deep-bed system is usually investigated using a thin layer of grain which is dried under specified air temperature and humidity for a certain period of time. The drying rate is then determined and the results are formulated as a thin-layer drying equation. Results of thin-layer experiment are applied to a deep-bed system based on the assumption that a deep bed is composed of layers of homogeneous grain and the airflow is a plug-type without concentration, temperature, and flow rate gradients in the radial direction.

Several thin-layer equations, both theoretical and empirical, were proposed for various grain products at different temperature ranges (Bakker-Arkema et al., 1978). Due to the difficulties in obtaining the diffusion coefficients for different products under some conditions, empirical or semiempirical thin-layer grain drying equations are frequently used in modeling.

Sabbah (1968) proposed an empirical thin-layer (one kernel deep) drying equation for corn at temperatures ranging from 2.2 to 21.1°C an 22 to 80 percent relative humidity:

$$\frac{M - M^*}{M_0 - M^*} = \exp (-k' t^{0.664}) \quad (6.12)$$

where

$$k' = \exp (-U t^V) \quad (6.12a)$$

$$U = [6.0142 + 1.453 \times 10^{-4} (\text{rh})^2]^{0.5} - (1.8 \theta + 32) \cdot [3.353 \times 10^{-4} + 3.0 \times 10^{-8} (\text{rh})^2]^{0.5} \quad (6.12b)$$

$$V = 0.1245 - 2.197 \times 10^{-3} (\text{rh}) + 2.3 \times 10^{-5} (\text{rh}) (1.8 \theta + 32) - 5.8 \times 10^{-5} (1.8 \theta + 32) \quad (6.12c)$$

A uniform airflow of approximately 15.24 cm/m^2 (50 cfm/ft^2) was used. The diffusion coefficient k' is a complicated function of relative humidity (decimal), grain temperature ($^{\circ}\text{C}$), and drying time. Constants are derived from experimental thin-layer drying results. The left term in Equation 6.12 is called the moisture ratio (MR); M^* is the equilibrium moisture content (EMC), and M_0 is the initial moisture content. In the case of average grain moisture content (dry basis) is higher than M^* , drying is taking place. Drying is essentially a moisture desorption process. Reabsorption of water in grain would occur if M is less than M^* . This rewetting process was described by a "thin-layer rewetting equation" (del Giudice, 1959) as follows:

$$\text{MR} = \exp[- 0.625 (p_s)^{0.466} \text{rh} (\text{rh})^{3.0} t] \quad (6.13)$$

Tests were run over a dry bulb temperature range of 15.6 to 40.6°C and a relative humidity range of 60 to 100 percent. Air velocities were 3.05 m/min . The saturation vapor pressure at the dry bulb temperature of product is expressed as p_s . The water sorption processes possess hysteresis and reabsorption curves are similar to those shown in Figure 3.7b.

3-E. Enthalpy Balance of the Bulk Air Stream

To analyze the energy balance in the bulk stream, the three components in the bulk stream, dry air, water vapor, and ammonia, are assumed to behave independently (assumption 17). The total amount of bulk stream flowing through the control volume is expressed as:

$$G_a (1 + H + x_1) S dt$$

and the enthalpy of the inflowing air is:

$$G_a (c_a + H c_v + x_1 c_g) T S dt$$

where c_g is the specific heat of gaseous ammonia. The enthalpy of the outflowing air is obtained by assuming the heat capacities of all components and their composition remain the same with respect to z in the control element and is expressed as:

$$G_a (c_a + H c_v + x_1 c_g) (T + \frac{\partial T}{\partial z} dz) S dt$$

Thus, the enthalpy change with respect to bed depth z is:

$$G_a (c_a + H c_v + x_1 c_g) \frac{\partial T}{\partial z} dz S dt$$

The change in the amount of sensible heat stored in the fluid phase during time dt is:

$$\rho_p (c_a + H c_v + x_1 c_g) \epsilon \frac{\partial T}{\partial t} dz S dt$$

and the total change in sensible heat is obtained by summing up the above two terms:

$$(c_a + H c_v + x_1 c_g) (G_a \frac{\partial T}{\partial z} + \epsilon \rho_a \frac{\partial T}{\partial t}) S dz dt$$

On the other hand, the convective heat transfer is taking place between the bulk stream and solid. The amount of energy transferred from the air to the product is:

$$h_a (T - \theta) S dz dt$$

where h is the convective heat transfer coefficient which will be discussed later in Section 5. Since the sensible heat change is resulted from the convective heat transfer due to temperature difference, the last two terms must add up to zero according to the conservation of energy. The enthalpy balance equation in the air is then written as:

$$G_a \frac{\partial T}{\partial z} + \epsilon \rho_a \frac{\partial T}{\partial t} = \frac{-h a}{c_a + H c_v + x_1 c_g} (T - \theta) \quad (6.14)$$

3-F. Enthalpy Balance in Corn

Corn is assumed to be composed of dry matter, water, and ammonia. Ammonia is dissolved in water as a solution. The aqueous solution can be considered as ideal binary solution in the case of low ammonia concentration which is held by the practical application of ammonia grain drying.

The total mass of corn within the control volume is expressed as the summation of individual components:

$$\rho_p (1 + M + x_2) S dz$$

and the change of enthalpy during time dt is:

$$\rho_p (c_p + c_w M + c_1 x_2) S dz \frac{\partial \theta}{\partial t} dt$$

where c_1 is the specific heat of liquid ammonia. This change of enthalpy is resulted from two sources: moisture loss and ammonia adsorption. The amount of moisture evaporated during time dt is indicated by the change of absolute humidity in the air, or

$$G_a \frac{\partial H}{\partial z} S dz dt$$

The latent heat required to evaporate this amount of water is expressed as:

$$h_{fg} G_a \frac{\partial H}{\partial z} S dz dt$$

The evaporation involves phase change as well as sensible heat change which is expressed as:

$$c_v (T-\theta) G_a \frac{\partial H}{\partial z} S dz dt$$

The total energy change (decrease) due to drying is:

$$[h_{fg} + c_v (T-\theta)] G_a \frac{\partial H}{\partial z} S dz dt$$

The heat of evaporation of water from the corn differs from free water evaporation and was found to be a function of grain temperature and moisture content (Rodriguez-Arias, 1956):

$$h_{fg} = (2502.10 - 2.386 \theta) [1.0 + 4.349 \exp(-28.25 M)] \quad (6.15)$$

for moisture content in the range of 0.0870–0.3514 d.b. and temperatures in the range of 5–40°C; $h_{fg} = 2326$ KJ/kg (1000 BTU/lb) otherwise.

The amount of ammonia adsorbed during time dt is equivalent to the change of ammonia concentration in the air and is written as:

$$G_a \frac{\partial x_1}{\partial z} S dz dt$$

Similar to the drying process, the total enthalpy change (increase) due to exothermic ammonia adsorption process is:

$$[H_{ad} + c_g (T-\theta)] G_a \frac{\partial x_1}{\partial z} S dz dt$$

where H_{ad} is the heat of adsorption* and $c_g(T-\theta)$ is the sensible heat term.

The heat*of adsorption differs from heat of vaporization for ammonia (1370 J/g at b.p. from Table 3.1 or 518.1 BTU/lb at 60°F) since ammonia is dissolved in water solution rather than condensing into liquid ammonia. Heat of solution for ammonia in water is given as 35.4 KJ/mole-NH₃ (or, 897 BTU/lb-NH₃) in very dilute (0.005 M[†] solution (Lancaster et al., 1975). Heat of ammonia adsorption, although it is not directly measured, is suggested to be approximated by the heat of solution of ammonia in water.

The latent heat expression for water (Equation 6.15) indicates that the heat of evaporation increases with lower temperature and lower moisture content. It is also comprehensible to state that heat of ammonia adsorption increases with lower temperatures. However, experimental results for H_{ad} in the corn similar to Equation 6.15 are not available, it is assumed that the heat of adsorption remains constant throughout the adsorption process. Since the solution of ammonia in water is a reversible physical process, ammonia desorption is expected to absorb the same amount of heat as in the adsorption process. Heat of desorption is thus of the same magnitude as H_{ad} but different sign.

Besides the enthalpy changes due to mass transfer, convective heat transfer between the product and air stream is taking place at the same time. The amount of heat transfer is

$$h a (T-\theta) S dz dt$$

* Note that all the heat expressions are taken as absolute values, appropriate signs are attached based on physical interpretation.

† M, a commonly used concentration unit for solution, stands for moles of solute per liter of solution.

The enthalpy balance in corn can be summarized as:

$$\left(\begin{array}{c} \text{change in} \\ \text{internal} \\ \text{product energy} \end{array} \right) = \left(\begin{array}{c} \text{energy} \\ \text{transferred} \\ \text{by convection} \end{array} \right) - \left(\begin{array}{c} \text{evaporation} \\ \text{energy} \end{array} \right) + \left(\begin{array}{c} \text{ammonia} \\ \text{adsorption} \\ \text{energy} \end{array} \right)$$

and is formulated as:

$$\begin{aligned} \rho_p (c_p + c_w M + c_1 x_2) \frac{\partial \theta}{\partial t} = h_a (T - \theta) - [h_{fg} + c_v (T - \theta)] G_a \frac{\partial H}{\partial z} \\ + [H_{ad} + c_g (T - \theta)] \left(-G_a \frac{\partial x_1}{\partial z} \right) \end{aligned} \quad (6.16)$$

where h_{fg} and H_{ad} are positive numbers. During drying, $\partial H / \partial z$ is positive (since $\partial M / \partial t < 0$) which tends to reduce the internal product energy ($\partial \theta / \partial t$ term); while $\partial x_1 / \partial z$ is negative (since $\partial x_2 / \partial t > 0$) during ammonia adsorption which tends to add heat to the product.

It is interesting to know that the effects of drying and adsorption on the heat content of the corn are counteractive and tend to dampen the temperature change of grain in the bin. The sensible heat changes for water and ammonia during interphase mass transfer is very small compared to the latent heat terms if the air and product temperatures are not far apart.

3-G. The Model Equations

In summary, six independent model equations were developed in order to solve six unknown variables. Model equations are listed below in terms of their differential changes with respect to the independent variables:

$$\frac{\partial x_1}{\partial z} = - \frac{\epsilon \rho_a}{G_a} \frac{\partial x_1}{\partial t} - \frac{\rho_p}{G_a} \frac{\partial x_2}{\partial t} (1 + \delta) \quad (6.4)$$

$$\frac{\partial H}{\partial z} = - \frac{\rho_p}{G_a} \frac{\partial M}{\partial t} \quad (6.6)$$

$$\frac{\partial x_2}{\partial t} = \frac{h_m a}{\rho_p} \frac{x_2^* - x_2}{x_2^* - x_2^o} \quad (6.11)$$

$$\frac{M - M^*}{M_o - M^*} = \exp (- k' t^{0.664}) \quad (6.12)$$

$$\begin{aligned} \rho_p (c_p + c_w M + c_l x_2) \frac{\partial \theta}{\partial t} = h a (T-\theta) - [h_{fg} + c_v (T-\theta)] G_a \frac{\partial H}{\partial z} \\ + [H_{ad} + c_g (T-\theta)] (- G_a \frac{\partial x_1}{\partial z}) \end{aligned} \quad (6.16)$$

together with the following auxiliary equations: Equations 6.10, 6.12a, b, c, and 6.15 to evaluate parameters used in model equations and Equation 6.13 replaces Equation 6.12 during rewetting process.

4. The Combined-Temperature Equation

The six-equation model described in the previous section is similar to the four-equation fixed-bed drying model (Bakker-Arkema et al., 1974). It was mentioned in the beginning of this chapter that in a slow drying process, such as ambient air drying, air and product temperatures could be considered equal without significant error. This assumption not only simplifies the computation but also helps to stabilize the numerical solution. The following method is expected to impose an insignificant error while combining the two temperature equations.

Equations 6.14 and 6.16 can be written as:

$$G_a c_{pa} \left(\frac{\partial T}{\partial z} + \frac{\epsilon \rho_a}{G_a} \frac{\partial T}{\partial t} \right) = - h a (T-\theta) \quad (6.17)$$

$$\rho_p c_{pp} \frac{\partial \theta}{\partial t} = h a (T-\theta) - G_a L \quad (6.18)$$

with,

$$c_{pa} = c_a + H C_v + x_1 c_g = \text{apparent specific heat of bulk air stream}$$

$$c_{pp} = c_p + M C_w + x_2 c_l = \text{apparent specific heat for ammonia-treated corn}$$

$$L = h_{fg} \frac{\partial H}{\partial z} + H_{ad} \frac{\partial x_1}{\partial z}$$

by assuming negligible sensible heat changes compared to the latent heat terms, i.e. $c_v(T-\theta) = c_g(T-\theta) = 0$. On the other hand, the error due to neglecting the convective heat transfer term, $h a(T-\theta)$, could be significant. However, Equations 6.17 and 6.18 are combined in such a way to cancel the convective heat transfer term. The combined equation is thus obtained by further assuming $\partial \theta / \partial t = \partial T / \partial t$:

$$\frac{\partial T}{\partial z} + \left(\frac{\epsilon \rho_a}{G_a} + \frac{\rho_p c_{pp}}{G_a c_{pa}} \right) \frac{\partial T}{\partial t} = - \frac{L}{c_{pa}} \quad (6.19)$$

Equation 6.19 is therefore replacing Equations 6.14 and 6.16 and constituting the five-equation model for ammonia adsorption and drying in a fixed-bed of grain.

5. Heat and Mass Transfer Coefficient for Forced Convection through Packed Beds

5-A. Forced Convection for a Single Sphere

The forced-convection heat transfer for a single sphere in an infinite fluid was described by Ranz and Marshall (1952) by plotting

the average Nusselt number versus $Re^{1/2} \cdot Pr^{1/3}$. The relation was then determined as:

$$Nu = 2.0 + 0.60 Re^{1/2} Pr^{1/3} \quad (6.20)$$

where the Nusselt number (Nu), Reynolds number (Re), and Prandtl number (Pr) are dimensionless numbers frequently used in heat transfer problems, they are defined as follows:

$$Nu = h D / k \quad (6.21)$$

$$Re = D G_a / \mu \quad (6.22)$$

$$Pr = c_p \mu / k \quad (6.23)$$

where h represents the average surface heat transfer coefficient over the entire spherical surface and Nu signifies a dimensionless temperature gradient in the fluid adjacent to the wall; D is the diameter or characteristic length; ρ , μ , k, c_p are fluid properties and stand for density, viscosity, thermal conductivity, and specific heat respectively.

Strictly speaking, all the thermal properties of fluid should be evaluated at the film temperature: $T_f = \frac{1}{2} (T_w + T_\infty)$, which is the average value of the solid surface and bulk stream temperatures. In a slow heat transfer process (i.e. small temperature difference) T_f may be estimated by T_∞ .

Equation 6.20 indicates a minimum value for convective heat transfer coefficient when $Nu = 2.0$ for motionless fluid due to heat conduction. This limiting value of Nu for heat transfer from spheres at low Re or Gr (Grashof number, used in free convection) can be theoretically derived by solving the following spherical steady state heat conduction equation:

$$\frac{1}{r^2} \frac{d}{dr} \left(r^2 \frac{dT}{dr} \right) = 0$$

with the boundary conditions that $T = T_w$ on the spherical boundary $r = R$ and $T = T_\infty$ as r approaches infinity. The temperature of fluid is then solved as inversely proportionally to r when $r \geq R$:

$$\frac{T - T_\infty}{T_w - T_\infty} = \frac{R}{r}$$

The surface heat transfer rate is equal to the heat conducted from inside the sphere to the surface, or

$$h (T_w - T_\infty) = - k \left(\frac{\partial T}{\partial r} \right)_{r=R}$$

Solving for h and substituting in Equation 6.21 gives $Nu = 2$. The minimum value of convective heat transfer coefficient for a single corn kernel in air is thus estimated as $1.82 \times 10^{-4} \text{ J}/(\text{hr}\cdot\text{m}^2\cdot^\circ\text{C})$ or $0.89 \text{ BTU}/\text{hrft}^2\cdot^\circ\text{F}$ with $D = 0.0098 \text{ m}$ (0.0322 ft) for corn kernel and $k = 89.1 \text{ J}/(\text{hr}\cdot\text{m}\cdot^\circ\text{C})$ or $0.0143 \text{ BTU}/\text{hrft}\cdot^\circ\text{F}$ for air at 10°C .

5-B. Evaluation of Heat Transfer Coefficients in Packed Beds

Unfortunately, heat transfer relationships for flow through a packed bed cannot be derived by extending those for a single sphere since the bed porosity is more important than the individual particle diameter in a packed-bed system. The following equation was derived experimentally by Yoshida et al. (1962), Hougen et al. (1960), and Bird et al. (1960) for a packed bed of spherical particles:

$$j_H = \begin{cases} 0.91 \text{ Re}^{-0.51} & , \text{ when } \text{Re} < 50 \\ 0.61 \text{ Re}^{-0.41} & , \text{ when } \text{Re} > 50 \end{cases} \quad (6.24)$$

where the Colburn factor, j_H , is defined by:

$$j_H = (St) (Pr)^{2/3} \quad , \text{ and} \quad (6.25)$$

$$St = \text{Stanton number} = \frac{Nu}{(Re) (Pr)} = \frac{h}{c_{pa} G_a} \quad (6.26)$$

In the case of a packed-bed system, the characteristic length is represented by the inverse of specific surface area (a) and Re becomes:

$$Re = \frac{G_a}{a \mu_a} \quad (6.27)$$

Solving for the convective heat transfer coefficient by substituting Equations 6.25, 6.26, and 6.27 into Equation 6.24 yields:

$$h = \begin{cases} 0.91 c_{pa} Pr^{-2/3} (a \mu_a)^{0.51} G_a^{0.49} & , \text{ when } Re < 50 \\ 0.61 c_{pa} Pr^{-2/3} (a \mu_a)^{0.41} G_a^{0.59} & ; \text{ when } Re > 50 \end{cases} \quad (6.28)$$

By substituting the properties of air at 10°C: $c_{pa} = 1005 \text{ J/kg}^\circ\text{C}$, $k_a = 0.0248 \text{ W/m K}$, $\mu_a = 0.06354 \text{ kg/m hr}$, $Pr = 0.7167$ and $a = 784 \text{ m}^2/\text{m}^3$ ($239 \text{ ft}^2/\text{ft}^3$) the above expressions are simplified to:

$$h = \begin{cases} 2.3278 G_a^{0.49} & , \text{ when } G_a < 2400 \text{ kg/hr/m}^2 \\ 1.0556 G_a^{0.59} & , \text{ when } G_a > 2400 \text{ kg/hr/m}^2 \end{cases} \quad (6.29)$$

where h has the units of $\text{W/m}^2 \text{ K}$ and air properties are assumed to remain constant and are approximated by the values at 10°C. Equation 6.29 indicates that the convective heat transfer coefficient is only a function of the flow rate.

5-C. Estimation of Mass-Transfer Coefficients at Low Mass-Transfer Rates

5-C.1. Ratio of Mass and Heat Transfer Coefficients

The determination of mass transfer or diffusion coefficients are usually more difficult than the heat transfer coefficients since solute concentrations are not like temperatures which can be easily recorded continuously for a number of measuring points at any specified scanning periods. Nevertheless, the solutions of many mass-transfer problems at low mass-transfer rates may be obtained by analogy with corresponding problems in heat transfer. The sorption processes in most biological products are relatively slow compared to other chemical-based sorption processes. A process with slower rate of mass transfer is expected to be solved with less error using this analogy.

One of the Chilton-Colburn (1934) analogies states that Colburn factors for heat and mass transfer are identical and are a function of Reynolds number, or

$$j_D = j_H = \text{a function of Re} \quad (6.30)$$

and the Colburn factor for mass transfer, j_D , is expressed by,

$$j_D = (St_D) (Sc)^{2/3} \quad (6.31)$$

where

$$St_D = \frac{Sh}{(Re) (Sc)} \quad (6.32)$$

$$Sc = \text{Schmidt number} = \frac{\mu}{\rho \alpha_D} \quad (6.33)$$

$$Sh = \text{Sherwood number} = \frac{h_D D}{\alpha_D} \quad (6.34)$$

$$\alpha_D = \text{mass diffusivity (m}^2/\text{hr)}$$

$$h_D = \text{mass transfer coefficient (m/hr)}$$

and Sc corresponds to Pr in heat transfer; Sh is in analogy with Nu and represents a dimensionless concentration gradient at the wall.

Equation 6.30 implies that,

$$\frac{Sh}{(Re)(Sc)^{1/3}} = \frac{Nu}{(Re)(Pr)^{1/3}} \quad (6.35)$$

or by substituting the original form for dimensionless numbers,

Equation 6.35 becomes:

$$\frac{h_D}{h} = \frac{\alpha_D}{k} \left(\frac{\alpha}{\alpha_D} \right)^{1/3}, \text{ or} \quad (6.36)$$

$$\frac{h_D}{h} = \frac{1}{\rho c_p} \left(\frac{\alpha_D}{\alpha} \right)^{2/3} \quad (6.37)$$

The mass transfer coefficient, h_m , used in the model equation (Equation 6.11) is related to h_D by:

$$h_m = \rho h_D \quad (6.38)$$

where h_m has the units of $kg/(hr \cdot m^2)$ while it is m/hr for h_D . Replacing h_D by h_m in Equation 6.37 gives:

$$\frac{h_m}{h} = \frac{1}{c_p} \left(\frac{\alpha_D}{\alpha} \right)^{2/3} \quad (6.39)$$

5-C.2. Estimation of the Mass Diffusivity

The only unknown parameter in computing the mass transfer coefficient from Equation 6.39 for ammonia diffusion problem is the mass diffusivity, α_D . The experimental values of α_D for ammonia sorption processes in corn or other grain products have not been acknowledged in the literature. Unlike the determination of moisture diffusion constants in which moisture contents are easily determined by standard air oven method

(103°C for 72 hours), chemical procedures in quantizing the ammonia concentrations in the corn (as described in Chapter 5) are rather complicated and time consuming.

Chu and Hustrulid (1968) developed the following empirical equation for moisture diffusion coefficient of the corn kernel:

$$\alpha_D = 1.513 \times 10^{-4} \exp[(0.045 \theta + 6.806) M - \frac{2513.00}{\theta + 273.15}] \quad (6.40)$$

where θ is the grain temperature in °C and M is the average corn moisture content in decimal d.b. The above equation was derived from the experimental results of the following test conditions — grain temperature 49–71°C, relative humidity 12–70 percent, and corn moisture content 25–35 percent d.b.

Equation 6.37 indicates that the values of water diffusion coefficient range from 5.89×10^{-7} (for 25 percent m.c. at 49°C) to $3.38 \times 10^{-6} \text{ m}^2/\text{hr}$ (for 35 percent m.c. at 71°C) under the above-specified conditions. A product with higher moisture contents at higher temperatures has a higher diffusion coefficient.

On the other hand, the experimental value of self-diffusion coefficient for water is $8.78 \times 10^{-6} \text{ m}^2/\text{hr}$ at 25°C (Robinson and Stokes, 1959). One would assume moisture in the corn as "free water", α_D should be equal to the self-diffusion coefficient of water. Comparing these two quantities, it is found that they are in the same order of magnitude and the self-diffusion coefficient is higher. This is an indication of extra diffusion resistances exerted by the solid portion of the product which hinders water from diffusing freely.

The experimental value of diffusion coefficient for ammonia gas at very low concentrations in liquid water was measured as 5.90×10^{-6}

m^2/hr at 12°C (Sherwood, 1975). This value may be considered as the maximum possible diffusion coefficient for ammonia diffusion in the corn at 12°C since in most cases the moisture content of shelled corn seldom exceeds 35 percent w.b. The value of α_D also varies with grain temperature besides the moisture content. As a matter of convenience, the diffusion coefficient (mass diffusivity) of ammonia in corn is assumed to be a constant of $5.90 \times 10^{-6} \text{ m}^2/\text{hr}$ throughout this investigation.

The ratio of mass transfer to heat transfer coefficient can thus be approximated by substituting $\alpha = k/\rho c_p = 0.0473 \text{ m}^2/\text{hr}$ and $c_p = 2161 \text{ J/kg}^\circ\text{C}$ at 10°C (Table 3.1) in Equation 6.39 as follows:

$$K_h = \frac{h_m}{h} = \frac{1}{c_p} \left(\frac{\alpha_D}{\alpha} \right)^{2/3} = 1.156 \times 10^{-6} \text{ kg } ^\circ\text{C}/\text{J} \quad (6.41)$$

Thus, the mass transfer coefficient for ammonia is estimated as:

$$h_m = K_h h = 1.156 \times 10^{-6} h \quad (6.42)$$

6. Dry Matter Decomposition

The deterioration of grain was indexed by the measurement of carbon dioxide production generated from both grain respiration and fungi growth (Steele and Saul, 1962). The measured amount of carbon dioxide is then translated into dry matter loss of grain. Saul and Steele (1966) suggested an allowable dry matter loss of 0.5 percent for field-shelled corn without a reduction in grade.

The percent dry matter decomposition was given by Thompson (1972) as follows:

$$\text{DM} = 0.0884 [\exp(0.006 t_e) - 1] + 0.00102 t_e \quad (6.43)$$

where t_e = equivalent storage time at the reference conditions of 15.6°C, 25 percent m.c. (w.b.), and 30 percent mechanical damage. The relationship between the equivalent storage time and the actual storage time under specified conditions was described by Steele et al. (1969) as:

$$t_e = \frac{t}{M_M M_T M_D} \quad (6.44)$$

where M_M , M_T , and M_D stand for moisture, temperature, and mechanical damage multipliers respectively. These multipliers were determined experimentally by Steele (1967) and Saul (1970) as follows:

(a) Moisture Multiplier (M_M)

$$M_M = 0.103 \left[\exp(455/M_{db}^{1.53}) - 0.00845 M_{db} + 1.558 \right] \\ \text{for } 15 < M_{db} < 54 \quad (6.45)$$

(b) Temperature Multiplier (M_T)

$$M_T = 128.76 \exp(-2.592 - 0.146 T) \quad , \quad T \leq 15.6^\circ\text{C} \quad (6.46a)$$

$$M_T = 32.3 \exp(-1.856 - 0.1044 T) \quad , \quad T > 15.6^\circ\text{C} \text{ and } M_{wb} < 19 \quad (6.46b)$$

$$M_T = 32.3 \exp(-1.856 - 0.1044 T) + [(M_{wb} - 19)/100] \\ \exp(-0.2847 + 0.0183 T) \quad , \quad T > 15.6^\circ\text{C} \text{ and } 19 < M_{wb} < 28 \quad (6.46c)$$

$$M_T = 32.3 \exp(-1.856 - 0.1044 T) + 0.09 \exp(-0.2847 + \\ 0.0183 T) \quad , \quad T > 15.6 \text{ and } M_{wb} > 28 \quad (6.46d)$$

(c) Mechanical Damage Multiplier (M_D)

Values for M_D at various levels of mechanical damage were given by Steele et al. (1969) as shown in Table 6.1.

Ammonia has been known as a very effective mold and bacteria inhibitor for stored grain. The dry matter loss is partly due to the microorganism growth which might overwhelm the effects of grain respiration under storage conditions favorable for molds and bacteria growth. The primary function of ammonia in ammonia-treated corn is to wipe out the initial or field contamination of microorganisms and further slow down or inhibit the growth of storage fungi and other microorganisms; the dry matter loss is thus reduced. The evidence of this "killing effect" on storage microorganisms (Bothast et al., 1973) due to proper ammonia treatment leads to the definition of an Ammonia Multiplier, or M_A .

Equation 6.44 can therefore be expanded to:

$$t_e = \frac{t}{M_M M_T M_D M_A} \quad (6.47)$$

The values for M_A is not presently available and it is only known that $M_A > 1$ with ammonia treatment and equals unity when no ammonia is applied. Experimental correlations must be established in order to determine the values of M_A in Equation 6.47. The experimental determination of M_A will not be performed in this investigation, however, it is suggested to take the following precautions:

- 1) The primary inhibitory function is due to free ammonia concentration both surrounding corn kernels and dissolved in corn (Lancaster et al., 1975).
- 2) The value of M_A is a function of the total amount of ammonia applied as well as the rate of ammonia application. The diffusion of ammonia

Table 6.1 . The mechanical damage multipliers.

Percent Mechanical Damage	M_D
2	3.22
5	2.90
10	2.41
15	1.98
20	1.60
25	1.29
30	1.00
35	0.76
40	0.55

From: Steele et al. (1969).

into the pores and dissolved in corn is a slow process. The faster the application rate is, the more ammonia is lost in the air.

7. Equilibrium Moisture Content

The experimental values and model equations of equilibrium moisture content (EMC) for various cereal grains were reviewed and summarized by a number of researchers: Brooker et al. (1974), Pfoest et al. (1976), and Bakker-Arkema et al. (1978). Bakker-Arkema et al. (1974) analyzed the EMC data of Rodriguez-Arias (1956) for shelled corn and developed the following empirical equations:

$$M_e = \frac{S_1 rh^3}{1.02} + \left(\frac{F_1}{0.17} - 0.028333 S_1 \right) rh, \quad 0.0 \leq rh < 0.17 \quad (6.48a)$$

$$M_e = \frac{S_1 (0.34-rh)^3}{1.02} + \frac{S_2 (rh - 0.17)^3}{1.02} + \left(\frac{F_2}{0.17} - 0.028333 S_2 \right) (rh-0.17) + \left(\frac{F_1}{0.17} - 0.028333 S_1 \right) (0.34-rh), \quad 0.17 \leq rh < 0.34 \quad (6.48b)$$

$$M_e = \frac{S_2 (0.51-rh)^3}{1.02} + \frac{F_3}{0.17} (rh-0.34) + \left(\frac{F_2}{0.17} - 0.028333 S_2 \right) (0.51-rh), \quad 0.34 \leq rh \leq 0.50 \quad (6.48c)$$

$$M_e = \frac{S_3 (rh-0.49)^3}{1.02} + \left(\frac{F_5}{0.17} - 0.028333 S_3 \right) (rh-0.49) + \frac{F_4}{0.17} (0.66-rh), \quad 0.50 < rh < 0.66 \quad (6.48d)$$

$$M_e = \frac{S_3 (0.83-rh)^3}{1.02} + \frac{S_4 (rh-0.66)^3}{1.02} + \left(\frac{F_6}{0.17} - 0.028333 S_4 \right) (rh-0.66) + \left(\frac{F_5}{0.17} - 0.028333 S_3 \right), \quad 0.66 \leq rh < 0.83 \quad (6.48e)$$

$$M_e = \frac{S_4 (1.00-rh)^3}{1.02} + \frac{F_7}{0.17} (rh-0.83) + \left(\frac{F_6}{0.17} - 0.028333 S_4 \right) (1.00-rh), \quad 0.83 \leq rh \leq 1.00 \quad (6.48f)$$

where:

$$F_1 = -0.0007060 T + 0.0874$$

$$F_2 = -0.0007835 T + 0.1189$$

$$F_3 = -0.0009646 T + 0.1475$$

$$F_4 = -0.0009675 T + 0.1452$$

$$F_5 = -0.0012735 T + 0.1849$$

$$F_6 = -0.0013408 T + 0.2294$$

$$F_7 = -0.0019278 T + 0.3588$$

$$S_1 = 13.83(-9F_1 + 6F_2 - F_3)$$

$$S_2 = 13.83(4F_3 - 9F_2 + 6F_1)$$

$$S_3 = 13.83(4F_4 - 9F_5 + 6F_6 - F_7)$$

$$S_4 = 13.83(4F_7 - 9F_6 + 6F_5 - F_4)$$

$$T = ^\circ\text{C}$$

$$M_e = \text{decimal, d.b.}$$

Pfost et al. (1976) gathered EMC data for various grain from several sources and developed the well-known equilibrium relative humidity-moisture content equations. They concluded that Henderson-Thompson and Chung-Pfost equations give results nearly as good as the other more complex equations. The Henderson-Thompson equation of desorption EMC for yellow dent corn is:

$$M_e = \left[\frac{\ln(1 - rh)}{-8.6541 \times 10^{-3}(T + 49.81)} \right] \frac{1}{1.8634} \quad (6.49)$$

and the corresponding Chung-Pfost equation is:

$$M_e = 0.379212 - 0.058970 \ln[-R'(T + 30.205) \ln(rh)] \quad (6.50)$$

where R' is the gas constant, T is in $^\circ\text{C}$, and M_e in dry basis decimal.

As it was indicated by all the EMC equations that EMC depends only on temperature and humidity for a particular kind of grain. The air humidity in equilibrium with a certain moisture content of grain is referred to as equilibrium relative humidity (ERH) which can be solved explicitly only by simplified EMC equations such as Equations 6.49 and 6.50.

8. The Finite Difference Method

8-A. Finite Difference Formulation

The finite difference approximation method is a powerful technique in solving partial differential equations. The formulation of finite difference equations is based on the Taylor's Series expansion which approximates the value of a function by its neighboring point and an infinite series of derivatives of such function. Basically, there are three ways of expressing the derivative functions: forward difference (implicit), backward difference (explicit), and central difference. For example, the first derivative of $T(z,t)$ can be expressed by:

$$T_z = \frac{T^{i+1,j} - T^{i,j}}{\Delta z} \quad (\text{implicit}) \quad (6.51a)$$

$$T_z = \frac{T^{i,j} - T^{i-1,j}}{\Delta z} \quad (\text{explicit}) \quad (6.51b)$$

$$T_z = \frac{T^{i+1,j} - T^{i-1,j}}{2\Delta z} \quad (\text{central difference}) \quad (6.51c)$$

where superscripts i and j stand for position and time indices respectively. The indices $(i\pm 1)$, $(j\pm 1)$ represent forward and backward positions and times relative to (i,j) . Similar equations for $\partial T/\partial t$ can be formulated.

The finite difference equations for state variables $x_1(z,t)$, $H(z,t)$, $x_2(z,t)$, $M(z,t)$, and $T(z,t)$ (Equations 6.4, 6.6, 6.11, 6.12, and 6.19) are formulated by explicit differences as follows by assuming $x_2^0 = 0$ in Equation 6.11:

$$x_1^{i,j} = \frac{G_a \Delta t x_1^{i-1,j} + \epsilon \rho_a \Delta z x_1^{i,j-1} - (x_2^{i,j} - x_2^{i,j-1}) \rho_p \Delta z (1+\delta)}{G_a \Delta t + \epsilon \rho_a \Delta z} \quad (6.52)$$

$$H^{i,j} = H^{i-1,j} - \frac{\rho_p \Delta z}{G_a \Delta t} (M^{i,j} - M^{i,j-1}) \quad (6.53)$$

$$x_2^{i,j} = \frac{x_2^{i,j-1} + \frac{h_m a \Delta t}{\rho_p}}{1 + \frac{h_m a \Delta t}{\rho_p x_2^{*i,j}}} \quad (6.54)$$

$$M^{i,j} = f_M (T^{i,j}, H^{i,j}, M_e^{i,j}, t) \quad (6.55)$$

$$T^{i,j} = \frac{1}{\Delta t + P \Delta z} [\Delta t T^{i-1,j} + P \Delta z T^{i,j-1} -$$

$$\frac{h_{fg} \Delta t}{c_{pa}} (H^{i,j} - H^{i-1,j}) - \frac{H_{ad} \Delta t}{c_{pa}} (x_1^{i,j} - x_1^{i-1,j})] \quad (6.56)$$

$$\text{where } P = \frac{\epsilon \rho_a}{G_a} + \frac{\rho_p c_{pp}}{G_a c_{pa}}$$

8-B. Solution of Finite Difference Equations

The solution of the above finite difference equations are not straightforward since the values of these state variables at (i,j) are interrelated. Their relationships are shown as follows in functions which contains state variables only:

$$x_1^{i,j} = f_1(x_2^{i,j}) \quad (6.57)$$

$$H^{i,j} = f_2(M^{i,j}) \quad (6.58)$$

$$x_2^{i,j} = f_3(x_2^{*i,j}) \quad (6.59)$$

$$x_2^{*i,j} = f_4(x_1^{i,j}) \quad (6.60)$$

$$M^{i,j} = f_5(H^{i,j}, T^{i,j}) \quad (6.61)$$

$$T^{i,j} = f_6(H^{i,j}, x_1^{i,j}) \quad (6.62)$$

where the specific heats of both bulk stream (c_{pa}) and product (c_{pp}) are assumed to be constant in Equation 6.61 within the finite difference grid. It is apparent that x_1 and x_2 must be solved simultaneously. Equations 6.57, 6.59, and 6.60 may be written as follows in accordance with Equations 6.52, 6.54, and 6.10:

$$x_1^{i,j} = A_1 + A_2 x_2^{i,j} \quad (6.63)$$

$$x_2^{i,j} = \frac{A_4 x_2^{*i,j}}{A_3 + x_2^{*i,j}} \quad (6.64)$$

$$x_2^{*i,j} = A_5 \left(\frac{x_1^{i,j}}{A_6 + x_1^{i,j}} \right)^{A_7} \quad (6.65)$$

where, assuming $H^{i,j}$ can be approximated by $H^{i-1,j}$, the absolute humidity at the previous node, and the following coefficients are known:

$$A_1 = \frac{G_a \Delta t x_1^{i-1,j} + \epsilon \rho_a \Delta z x_1^{i,j-1} + \rho_p \Delta z x_2^{i,j-1} (1+\delta)}{G_a \Delta t + \epsilon \rho_a \Delta z}$$

$$A_2 = - \frac{\rho_p \Delta z (1+\delta)}{G_a \Delta t + \epsilon \rho_a \Delta z}$$

$$A_3 = 100 h_m a \Delta t / \rho_p$$

$$A_4 = A_3 + x_2^{i,j-1}, \quad A_6 = 1 + H^{i-1,j}$$

$$A_5 = A(T) M_{db}, \quad A_7 = B(T)$$

Equations 6.63, 6.64, and 6.65 can be solved by iteration or they may be combined into a single equation with one unknown variable; e.g. substituting Equation 6.65 in Equation 6.64 which is then substituted in Equation 6.63 yields:

$$g(x_1^{i,j}) = A_1 + \frac{A_2 A_4 A_5 (x_{1H}^{i,j})^{A_7}}{A_3 + A_5 (x_{1H}^{i,j})^{A_7}} = 0 \quad (6.66)$$

where $x_{1H}^{i,j} = x_1^{i,j} / (A_6 + x_1^{i,j})$. The value of $x_1^{i,j}$ is solved by trial and error using the subroutine ZEROIN. Once $x_1^{i,j}$ is known, $x_2^{*i,j}$ can be calculated from Equation 6.65 and $x_2^{i,j}$ from Equation 6.64. The model equations are left with three equations, 6.58, 6.61, 6.62, for H, M, and T which must be solved by a search algorithm. The general order of the computation in the search algorithm is outlined below:

- 1) Guess $H^{i,j} = H^{i-1,j}$, i.e. take the humidity of the previous position as a guess.
- 2) Calculate $T^{i,j}$ from Equation 6.56.
- 3) If $RH^{i,j} < 100$ percent, go to 5.
- 4) Simulate condensation and find $T^{i,j}$, $H^{i,j}$. Set flag.
- 5) Calculate $M^{i,j}$ from Equation 6.55.
- 6) If condensation flag is set, exit.
- 7) Calculate $(EMC)^{i,j}$ from Equation 6.48.
- 8) Estimate new $H^{i,j}$ from $(EMC)^{i,j} - M^{i,j}$.
- 9) If $\Delta H < 0.0001$, go to the next node.

Subroutine ZEROIN is utilized to perform the search for an acceptable H value. Condensation occurs whenever the temperature is below the dew point. The condensed water is assumed to be added to the grain moisture according to Equation 6.6 and the estimation of EMC is skipped

because it is not applicable.

8-C. Temperature Condensation Simulator

During the solution of temperature and absolute humidity, the corresponding relative humidity is also checked for condensation. If the relative humidity exceeds 100 percent in which the psychrometric chart does not apply, H must be readjusted. The new value for H is computed along the constant enthalpy line. The intersection point with the saturation line gives the desired temperature and absolute humidity. The grain moisture content must be reevaluated because of the assumption that any condensed water be restored to the grain moisture content.

The search for a new T and H in this temperature condensation simulator is illustrated in Figure 6.2. The temperature at the intersection can be solved from the simultaneous equations for the constant enthalpy line and for the saturation curve which is approximated by a straight line. The temperature equation (Equation 6.56) can be written as follows:

$$T^{i,j} = \frac{1}{\Delta t + P \Delta z} (\Delta t T^{i-1,j} + P \Delta z T^{i,j-1} - Q_1 - Q_2) \quad (6.67)$$

where

$$Q_1 = \frac{h_{fg} \Delta t}{c_{pa}} (H^{i,j} - H^{i-1,j})$$

$$Q_2 = \frac{H_{ad} \Delta t}{c_{pa}} (x_1^{i,j} - x_1^{i-1,j})$$

A saturation point (T_s, H_s) can be located by assuming $H^{i,j} = H^{i-1,j}$ and T_s lies between T and T':

$$T_s = \frac{1}{\Delta t + P \Delta z} (\Delta t T^{i-1,j} + P \Delta z T^{i,j-1} - Q_2) \quad (6.68)$$

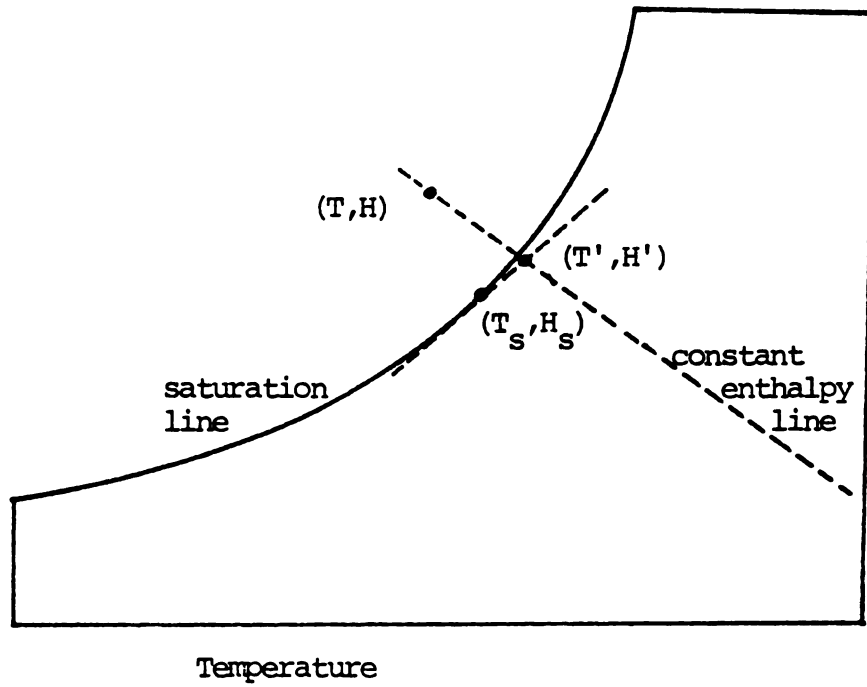


Figure 6.2. Graphical presentation of the condensation simulator.

and H_s is known once T_s is solved on saturation line. The slope of the line which approximates the local saturation line is then,

$$\frac{\Delta H}{\Delta T} = H_s - H_s' \quad (6.69)$$

where H_s' is evaluated at temperature $(T_s - 1)$ on saturation line.

The equation for the constant enthalpy line with respect to (T, H) and (T', H') is:

$$(\Delta t + P \Delta z)(T' - T) + Q_3(H' - H) = 0 \quad (6.70)$$

where $Q_3 = h_{fg} \Delta t / c_{pa}$ and the superscripts on T and H are omitted.

The equation for the saturation line with respect to (T_s, H_s) and (T', H') can be expressed as:

$$H' = (T' - T_s) \frac{\Delta H}{\Delta T} + H_s \quad (6.71)$$

Substituting Equation 6.71 into Equation 6.70, the readjusted temperature T and humidity H are:

$$T' = \frac{(\Delta t + P \Delta z)T + Q_3(\Delta H / \Delta T)T_s - Q_3(H_s - H)}{\Delta t + P \Delta z + Q_3(\Delta H / \Delta T)} \quad (6.72)$$

$$H' = H_s + (T - T_s) \frac{\Delta H}{\Delta T} \quad (6.73)$$

9. The Flowcharts

The flowchart analysis is a very important and powerful step in solving the complicated differential equations and numerical logic by digital computers. The most important matter in using a digital computer to solve numerical problems is the solution sequence which can be easily followed by a flowchart. The flowchart is essentially a detailed algorithm.

The computer program for ammonia adsorption and drying in a fixed-bed system consists of a main program (ADSFIX) which serves as a skeleton for the entire computation (Figure 6.3). The main program is composed of a depth loop enclosed by a time loop. The depth loop computes the results of state variables in each node at the same instant while the time loop performs the calculations in the depth loop at each specified computing time increment throughout the entire process.

The computing and print time scheme in the main program is flexible and has the capability of handling irregular input and output time intervals (Figure 6.4). The input conditions can be from any irregular time interval but computes at a constant and specified computing time interval. The printed outputs are controlled by either a fixed value of print time increment (TBTPR) or at each time the new input conditions are read.

The major subroutines used in the main program are as follows:

- 1) LAYEQ: finds the grain moisture content by a thin-layer drying equation (6.12) and a rewetting equation (6.13).
- 2) SOLVE: computes temperature, moisture content, and relative humidity by given absolute humidity, also performs the condensation simulation described in Section 8-C.
- 3) ZEROIN: solves an equation by guessing a high and low limit for the unknown variable and narrowing the range for the solution within an acceptable error.
- 4) ADSPT (Figure 6.5): computes the ammonia concentrations in the air as well as in the corn by solving Equation 6.66 using ZEROIN. The solution for $x_1^{i,j}$ must lie between the guessed high and low values. If multiple solutions occur, the solution range should be narrowed.

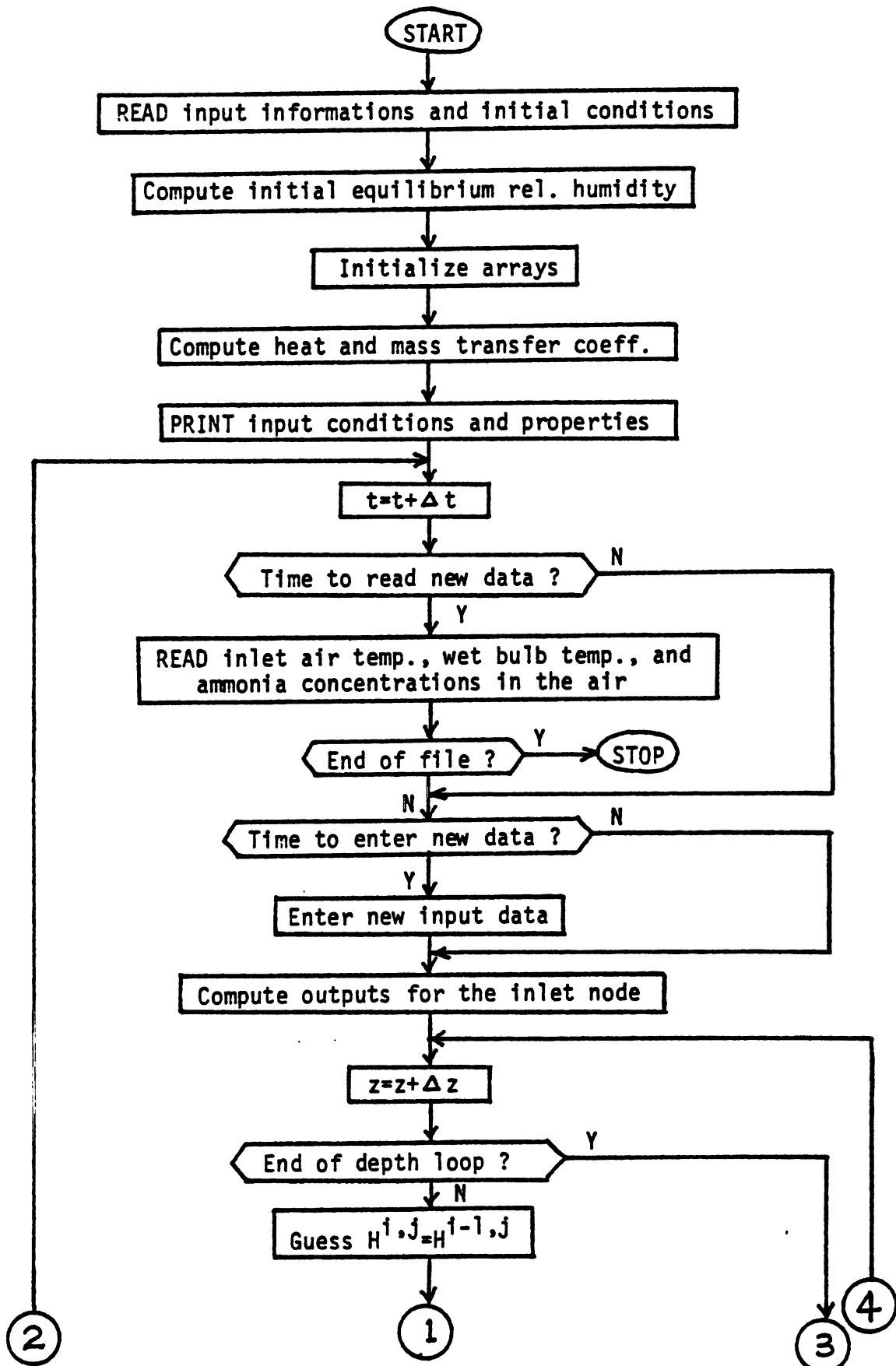


Figure 6.3 . The flowchart presentation of the main program ADSFIX.

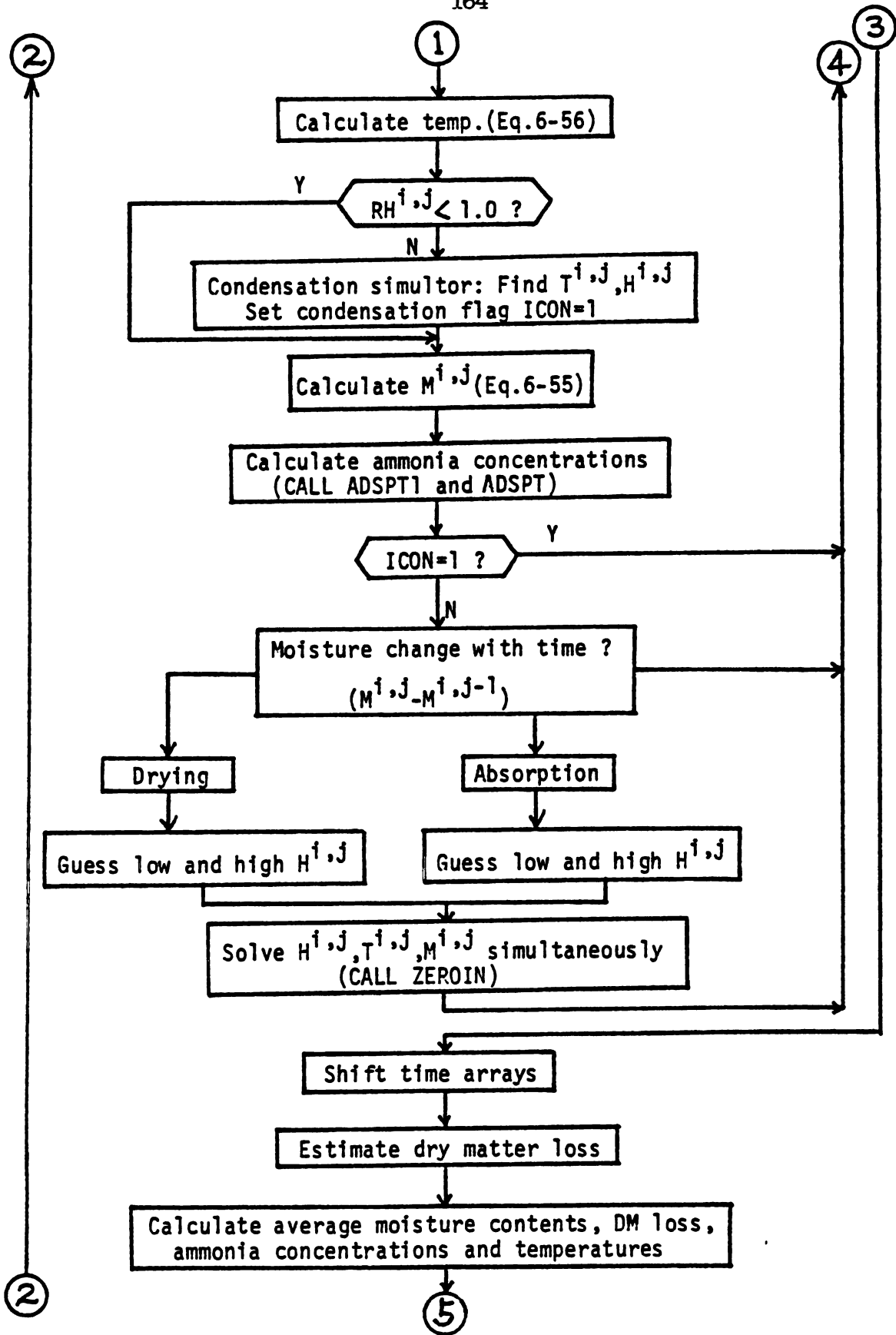


Figure 6.3 . continued

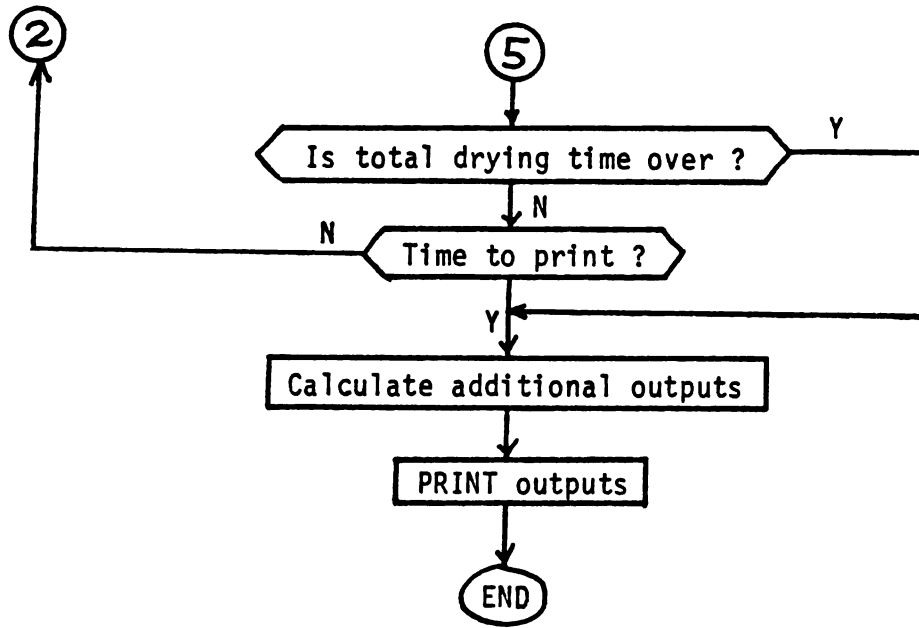


Figure 6.3. continued

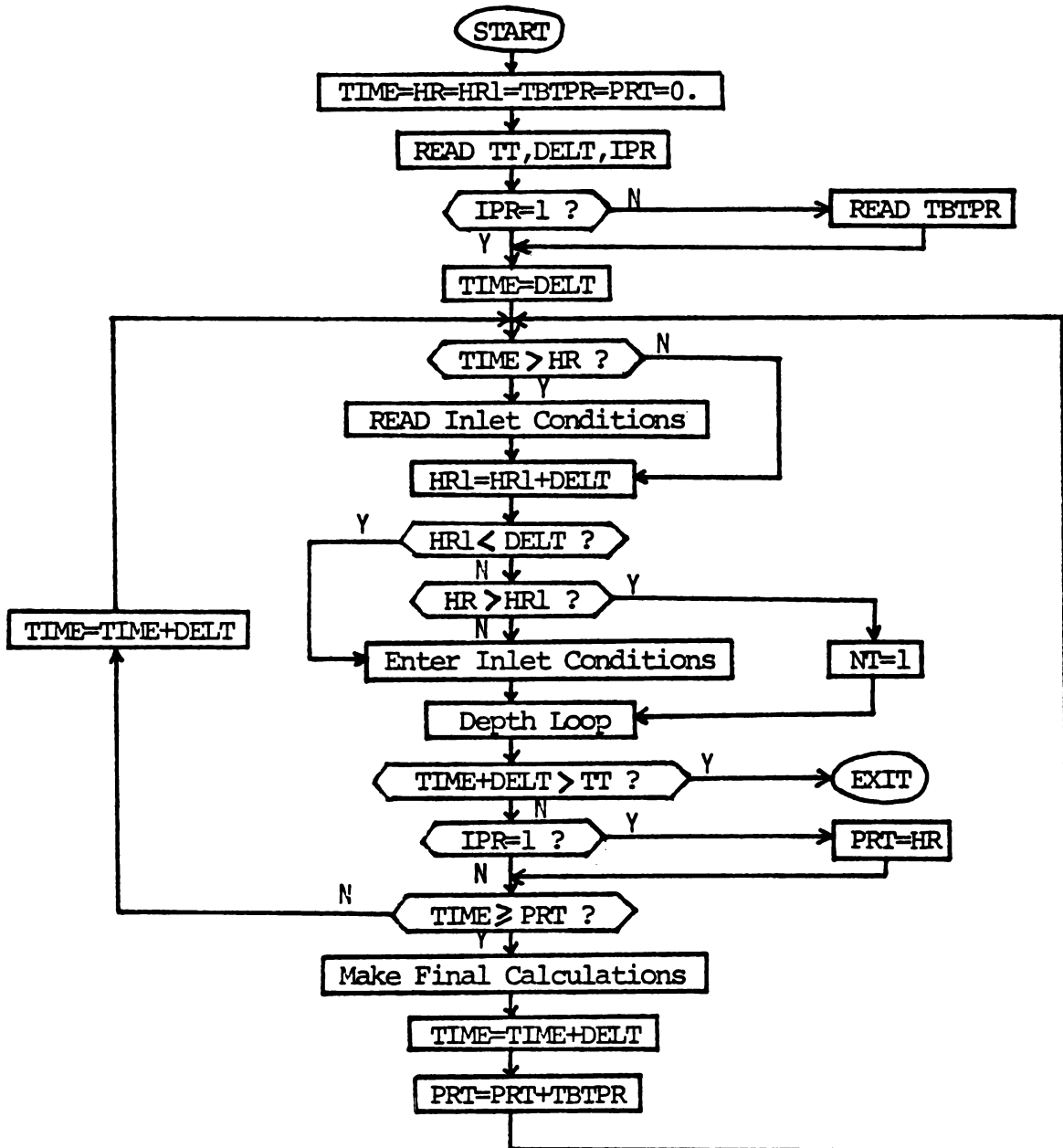


Figure 6.4. The computing and print time scheme in the main program ADSFIX.

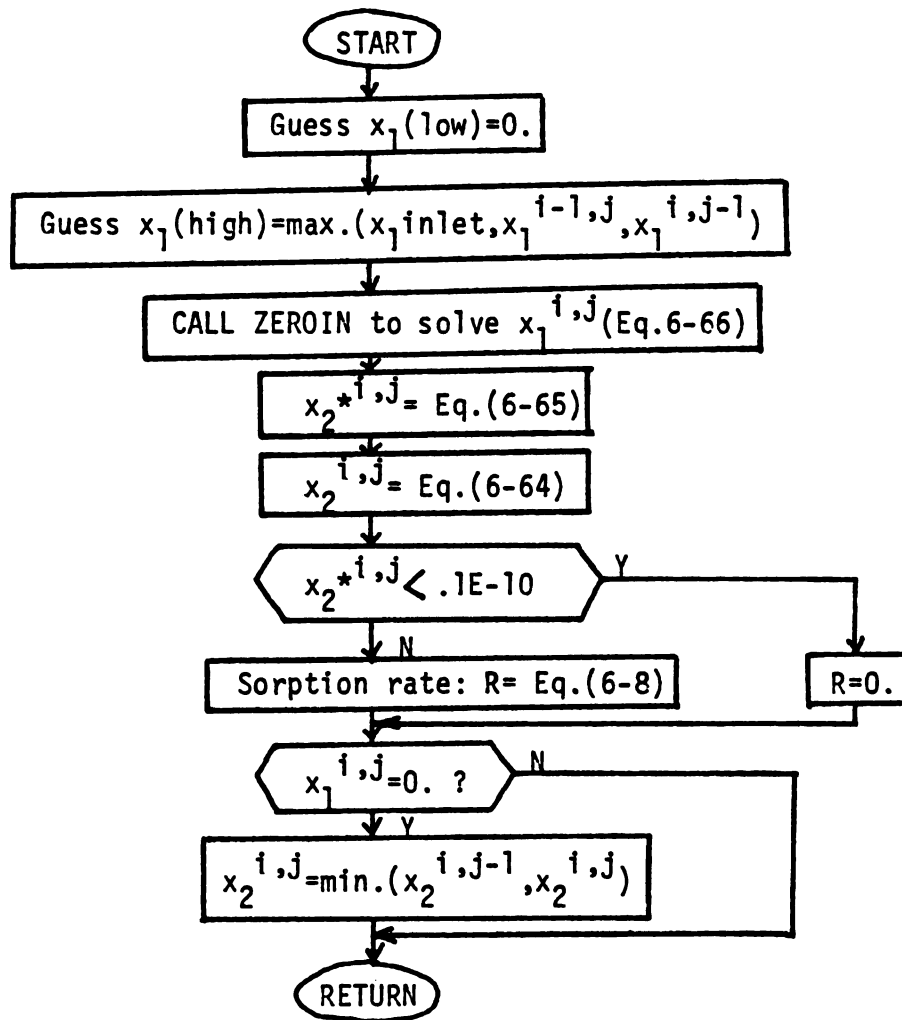


Figure 6.5. The flowchart presentation of the subroutine ADSPT.

The maximum possible value for $x_1^{i,j}$ will not exceed the maximum values of: (1) inlet x_1 concentration, (2) x_1 concentration of the previous position at the same time, and (3) x_1 concentration in the previous computing time interval.

During the ammonia desorption processes, the total ammonia concentration in the corn, $x_2^{i,j}$, cannot be lower than the residual concentration (x_{2R}) which is not removable by aeration. Another precaution in subroutine ADSPT is made that the ammonia concentration in corn does not increase with time if there is no ammonia in the air.

- 5) ADSPT1 (Figure 6.6): calculates the ammonia concentrations for the first inner node by further dividing the computing time interval into NT intervals. By doing so, the errors due to discontinuities of boundary and initial conditions are reduced and the numerical solution stability is improved. In other words, the effects of a step input on the evaluation of x_1 at the first time step will be damped. The rate of sorption is taken at the first subdivided computing time increment ($\Delta t/NT$) for the first computing time interval.
- 6) EMC: calculates the equilibrium moisture content of the corn according to Equation 6.48.
- 7) Psychrometric package: includes several subroutines to estimate all of the air properties related to psychrometrics. It serves as a psychrometric chart for digital computers.

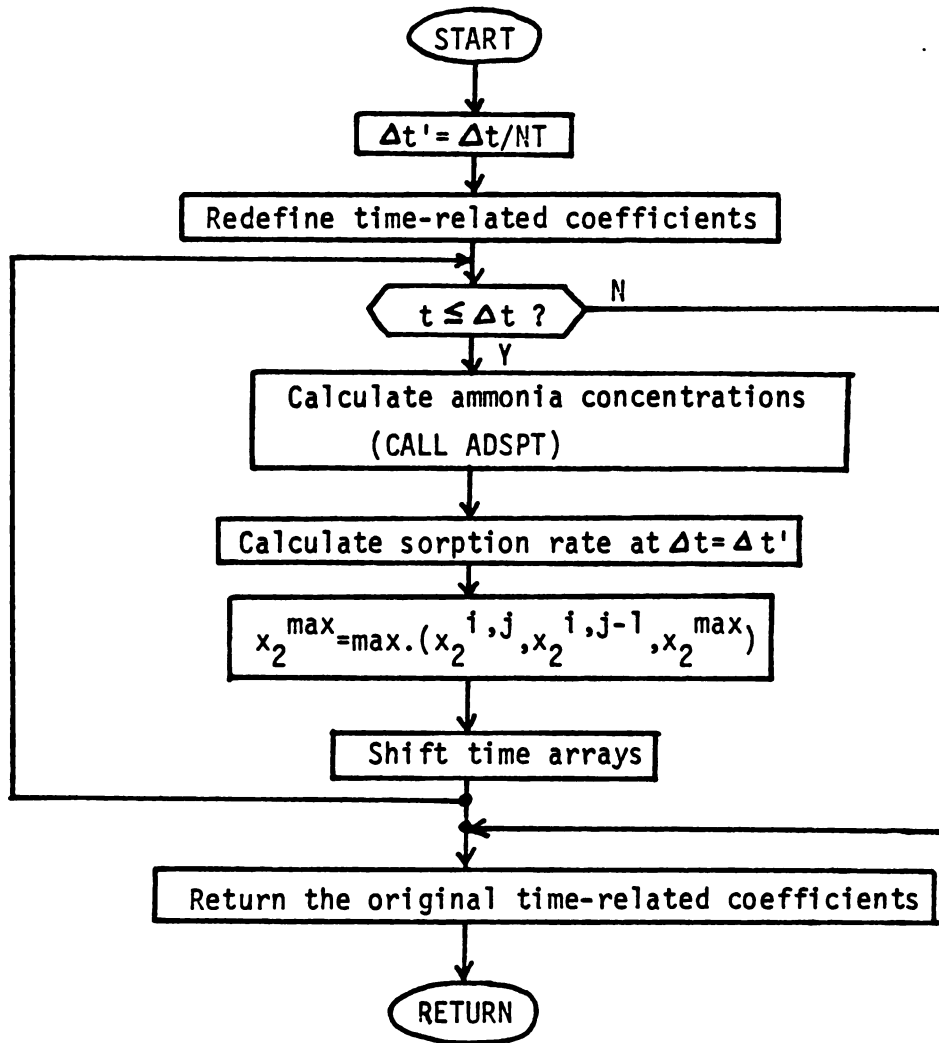


Figure 6.6. The flowchart presentation for the subroutine ADSPT1-- ammonia sorption at the first inner node in the first computing time interval.

CHAPTER 7

RESULTS AND DISCUSSION

1. Introduction

The results presented in this chapter consist of three major parts:

- 1) The accuracy tests of the ammonia sorption and drying model. These tests concentrate on the analysis of the accuracy of the predicted ammonia concentrations both in the air and in the grain. The finite difference method is imbedded with errors in the computation due to the nature of nodal definition and computational grid sizes.

Only the grid sizes of the independent variables (time and position) are investigated. The computing time and depth intervals will be varied to observe the changes in the predicted results of the ammonia concentrations. The numerical calculations should be performed at the computing time and computing depth intervals approaching zero; this can be obtained by extrapolation since it is impossible to perform computation at the zero computing interval. After the acceptable values for the computing time (Δt) and depth intervals (Δz) have been determined with reasonable accuracy (± 10 percent) by the accuracy tests, the values of Δt and Δz can be fixed in the tests thereafter.

- 2) The sensitivity tests of important parameters. The sensitivity tests are designed to determine the influence of each individual parameter on the ammonia sorption characteristics of the ammonia drying process.
- 3) Comparison of the predicted results with the experimental results. The predicted results generated by the computer simulation of the ammonia sorption and drying model are compared with the experimental results obtained in the model bin test performed at Michigan State University.

2. Definition of the Standard Conditions

The standard conditions referred to in this chapter are defined as a set of selected parameters under which the accuracy and sensitivity tests are performed.

The parameters in the standard conditions were chosen as close as possible to those to be expected in practical ammonia drying installations. All the results in the accuracy and sensitivity tests are obtained under standard conditions unless otherwise mentioned in the text.

The standard conditions are listed below (the notations in the parenthesis are the variable names used in the simulation program):

- 1) Grain depth (DEPTH) = 183 cm (6.0 ft)
- 2) Airflow rate (CFM) = $1.43 \text{ cm}^3/\text{m}^2$ ($4.7 \text{ cfm}/\text{ft}^2$)
- 3) Initial grain moisture (XMOWB) = 0.25 w.b.
- 4) Initial grain temperature (THIN) = 10°C (50°F)
- 5) Inlet air temperatures = 10°C (50°F) for the dry bulb temperature (TIN) and 8.3°C (47°F) for the wet bulb temperature (WTIN). The corresponding relative humidity is 80 percent.
- 6) Inlet ammonia concentration in the air (X1IN) = 0.05 percent d.b.

for ammoniation, zero for aeration.

- 7) Ratio of mass/heat transfer coefficients (KH) = 1.156×10^{-6} Kg°C/J (0.00484 lb°F/BTU).
- 8) Fraction of residuals (RC) = 0.3
- 9) The division factor, or the number of intervals the first computing increment is sub-divided into for the first inside node (NT) = 1. The first inside node is located at the position of one computing depth interval from the bottom (inlet) node.

3. The Accuracy Tests of the Ammonia Sorption and Drying Model

The accuracy tests are designed to determine the true numerical solutions of the state variables. The tests concentrated on the accuracy of the predicted ammonia concentrations in the air and grain (both of the average ammonia concentrations and of the concentration profiles in the grain bed).

The following values of the independent variables were tested:

- (1) computing time increment (Δt): 0.05, 0.1, 0.25, 0.5, 0.1, and 2.0 hours, and
- (2) computing depth interval (Δz): 3.05 cm (0.1 ft), 7.62 cm (0.25 ft), 15.24 cm (0.5 ft), 30.48 cm (1 ft), 60.96 cm (2 ft), and 91.44 cm (3 ft).

3-A. The Accuracy of the Average Ammonia Concentrations

A set of results was generated for different Δt values at each specified Δz for the test of the average ammonia concentration in the air after two hours of ammoniation. Six sets of results were obtained for six Δz values as shown in Figure 7.1. It is surprising to find that different computing schemes give such different results (from 1.28×10^{-4} to 2.52×10^{-4} kg-ammonia/kg-dry air) under standard

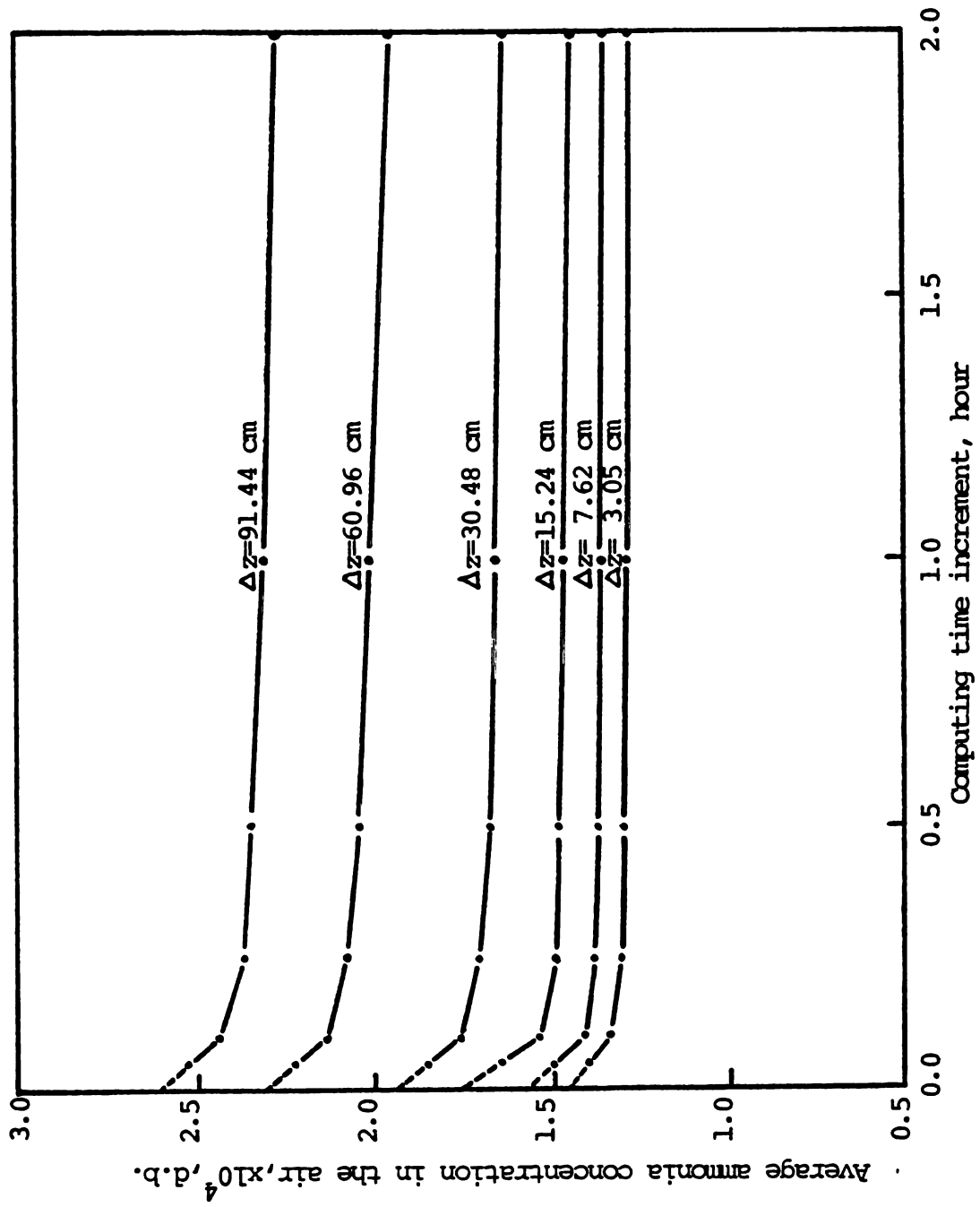


Figure 7.1. Influence of computing time increment on the average ammonia concentration in the air.

conditions. Generally speaking, a larger Δz and a smaller Δt predict larger ammonia concentrations. The smallest Δt used in the test was 0.05 hr which is the best estimate without using too much computing time. The CP (central processor) time was 59.6 seconds for $\Delta t = 0.05$ hr, $\Delta z = 3.05$ cm, and two hours of ammoniation.

The average ammonia concentrations in the air as the computing time increment approaches zero were obtained by a straight-line extrapolation of the two smallest Δt values (0.05 and 0.1 hr). A similar analysis was performed for the average ammonia content in corn under the same conditions (Figure 7.2). Similar shapes of curves were obtained for the free ammonia content. The variation of free ammonia concentrations ranged from 0.44×10^{-4} to 0.82×10^{-4} kg-ammonia/kg-dry corn. The values of the extrapolated results of the free ammonia and the ammonia in the air for different Δz are plotted in Figure 7.3. The true numerical results for the average ammonia concentrations were obtained by the straight-line approximation of the two smallest Δz values (3.05 and 7.62 cm). The intercepts at $\Delta t = \Delta z = 0$ are 1.38×10^{-4} kg-ammonia/kg-dry air for the average ammonia concentration in the air and 0.49×10^{-4} kg-ammonia/kg-dry corn for the average free ammonia content in the corn after two hours of ammoniation under standard conditions.

The relative percentage error in the computation of the average ammonia concentrations using various time and depth intervals was estimated by comparing them with the true numerical solutions (Table 7.1). The results in Table 7.1 demonstrate an important phenomenon: the zero-error line is expected to pass through the point where $\Delta t = \Delta z = 0$ and run diagonally. The zero error is expected to occur at a larger Δt when a larger Δz is used. In other words, to accurately

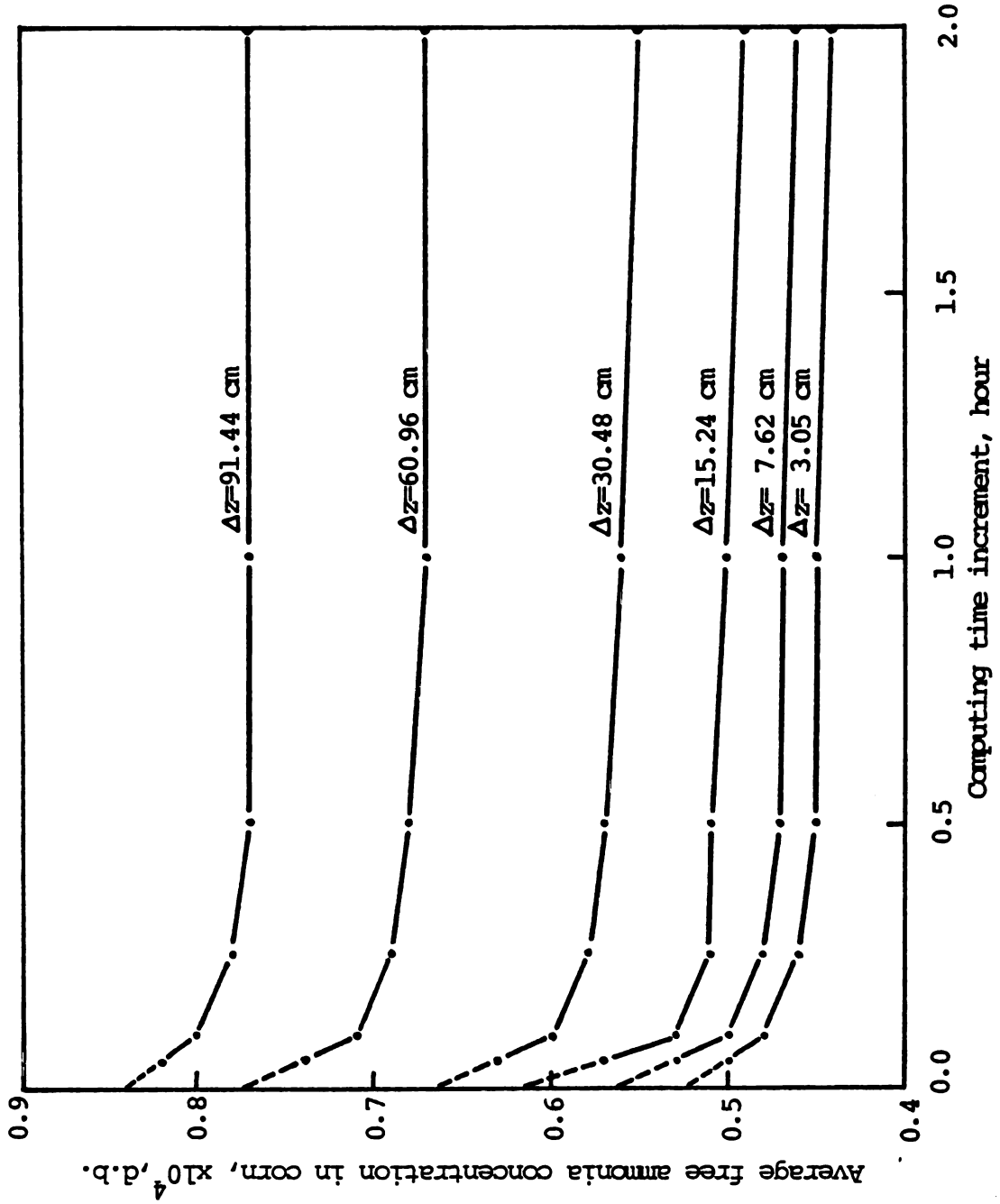


Figure 7.2. Influence of computing time increment on the average free ammonia content in corn.

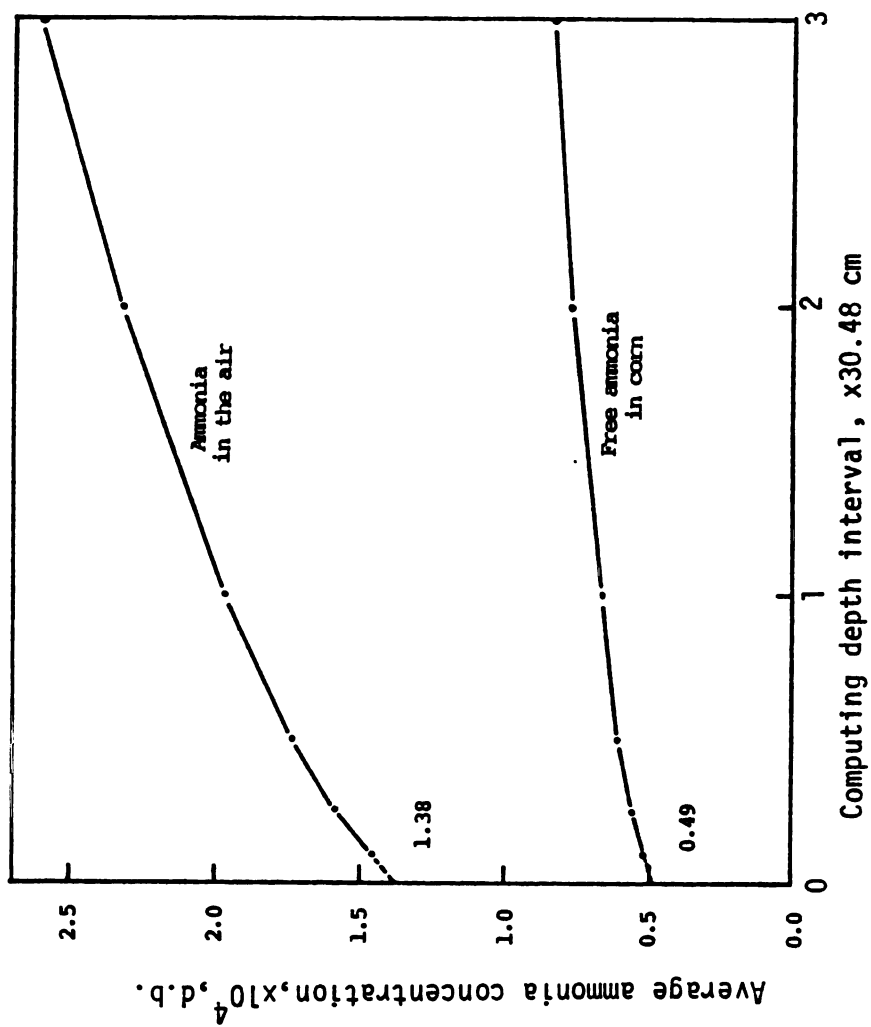


Figure 7.3. Influence of the computing depth interval on the estimation of average ammonia concentrations which are obtained by extrapolating at zero computing time increment.

Table 7.1. Relative percentage errors in the computation of average ammonia concentrations in the air and in corn after 2 hours of ammoniation using various computing time and depth intervals compared to the true numerical results* extrapolated at $\Delta t=0$ and $\Delta z=0$.

Δt (hr)	Relative percentage errors of average ammonia conc. in the air (x_1)				Relative percentage errors of average free ammonia content in corn (x_2)							
	Δz (cm)				Δz (cm)							
	3.1	7.6	15.2	30.5	61.0	91.4	3.1	7.6	15.2	30.5	61.0	91.4
0.05	1.5	8.7	18.8	34.8	61.6	82.6	2.0	6.1	16.3	28.6	51.0	67.4
0.10	-2.9	2.9	11.6	27.5	55.1	76.8	-2.0	2.0	6.1	22.5	44.9	63.3
0.25	-5.8	0.0	8.0	23.9	50.7	72.5	-6.1	-2.0	4.1	18.4	40.8	59.2
0.50	-5.8	-0.7	7.3	21.7	48.6	70.3	-8.2	-4.1	4.1	16.3	38.8	57.1
1.00	-6.5	-1.5	6.5	20.3	45.7	67.4	-8.2	-4.1	2.0	14.3	36.7	57.1
2.00	-7.3	-2.9	4.4	17.4	41.3	63.8	-10.2	-6.1	0.0	12.2	36.7	57.1

* The true numerical results are $x_1=1.38 \times 10^{-4}$ kg-NH₃/kg-dry air, and $x_2=0.49 \times 10^{-4}$ kg-NH₃/kg-dry corn.

predict the average ammonia concentrations in a long-time simulation, a larger computing time increment has to be accompanied by a larger computing depth interval. Nevertheless, the average ammonia concentrations alone do not describe the entire nature of the accuracy in the prediction model. Other important results which may indicate the accuracy of the prediction model are the ammonia concentration profiles in the grain bed which will be discussed in the next section.

In general, larger Δz and smaller Δt values create larger prediction errors on the right-hand side of the zero-error line in Table 7.1. However, on the left-hand side of the zero-error line, a smaller Δz and a larger Δt impose a larger error. This phenomenon is evidenced by the sharp upward turn of the curves close to the zero computing time increment in Figures 7.1 and 7.2.

The error in the prediction of the ammonia concentrations in the air and in the corn decreases as the ammoniation time increases up to about five hours as shown in Figures 7.4 and 7.5. After five hours of ammoniation, the variation in errors are not as significant as at smaller times. The reason for choosing two hours of ammoniation time in the analysis of relative errors in Table 7.1 is that the error at two hours ammoniation seems to be at the position which imposes an average amount of error.

The rate of ammonia adsorption also affects the prediction error. Generally speaking, as the adsorption rate decreases a smaller error is found in the computation of the average ammonia concentrations.

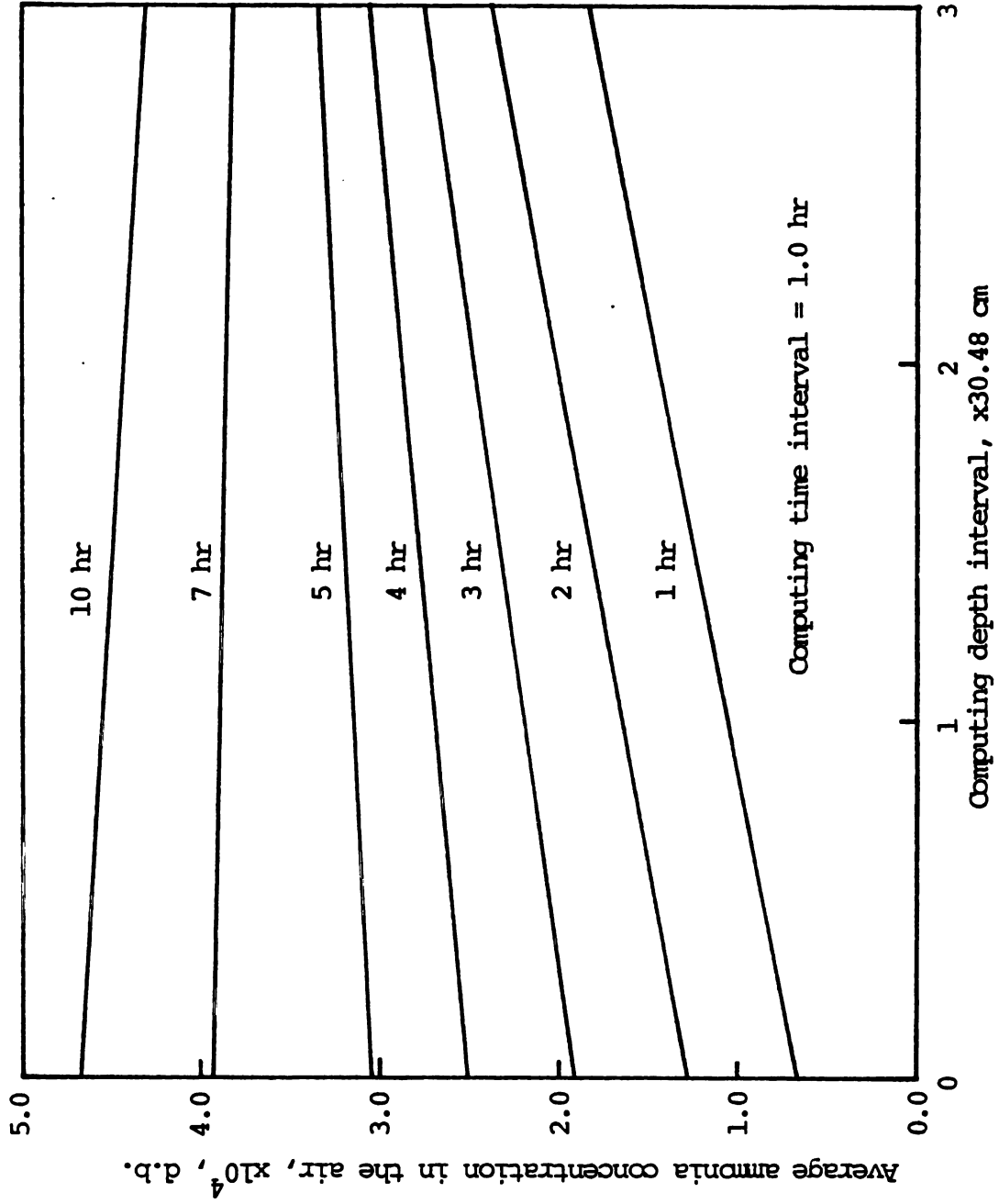


Figure 7.4. Influence of computing depth interval on the average ammonia concentration in the air.

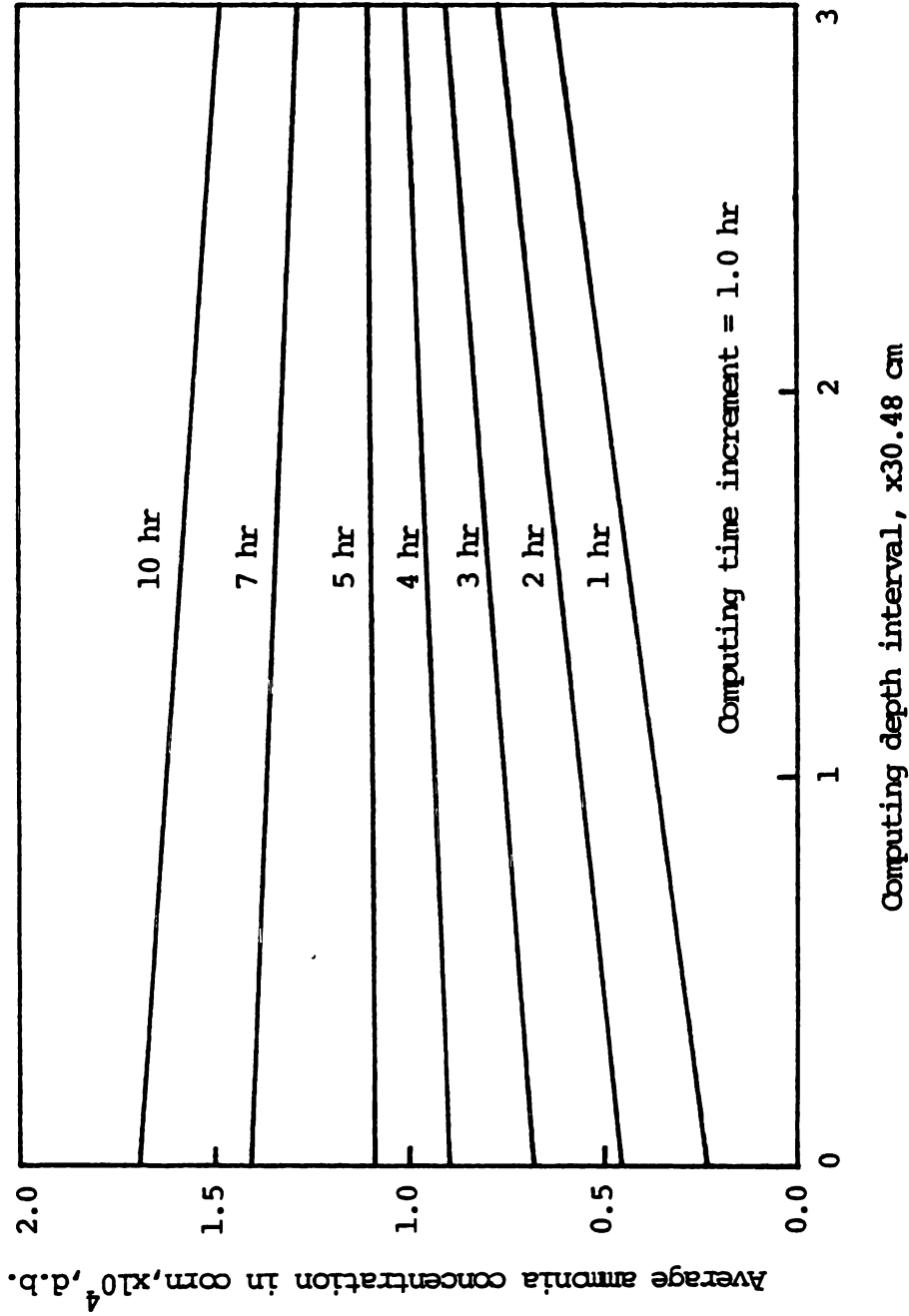


Figure 7:5. Influence of computing depth interval on the average free ammonia content in corn.

3-B. The Ammonia Concentration Profiles in the Air as Influenced by the Computing Scheme

The ammonia concentration profiles can give another view of the accuracy of the prediction model as influenced by a different computing time and/or depth interval. Comparison of the concentration profiles using various computing schemes are shown in Figures 7.6, 7.7, and 7.8 for $\Delta z = 3.05, 15.24, \text{ and } 30.48$ cm, respectively.

In general, the model predicts higher concentrations at the lower portion of the bed as a smaller Δz is used. The variations in the prediction of the concentration profiles are less significant for the results using different computing time increments when a larger computing depth interval is employed. Thus, even though a larger Δt accompanied by a larger Δz predicts the average concentrations more accurately than using a smaller Δz , the deviations in the prediction of ammonia concentration profiles are larger.

3-C. The Selection of a Proper Combination of the Operating Time and Depth Increments

The influence of computing intervals on the estimation of the prediction error is mixed according to the above discussion. In summary, a smaller Δz predicts more accurately both the average concentrations and the concentration profiles when the computing time increment is fixed. On the other hand, a smaller Δt predicts the concentration profiles more accurately but the results of the average ammonia concentrations deviate further from the true numerical results for the same computing depth interval.

The selection of the proper computing time and depth interval depends on the following factors: (1) the time of ammoniation, (2) the

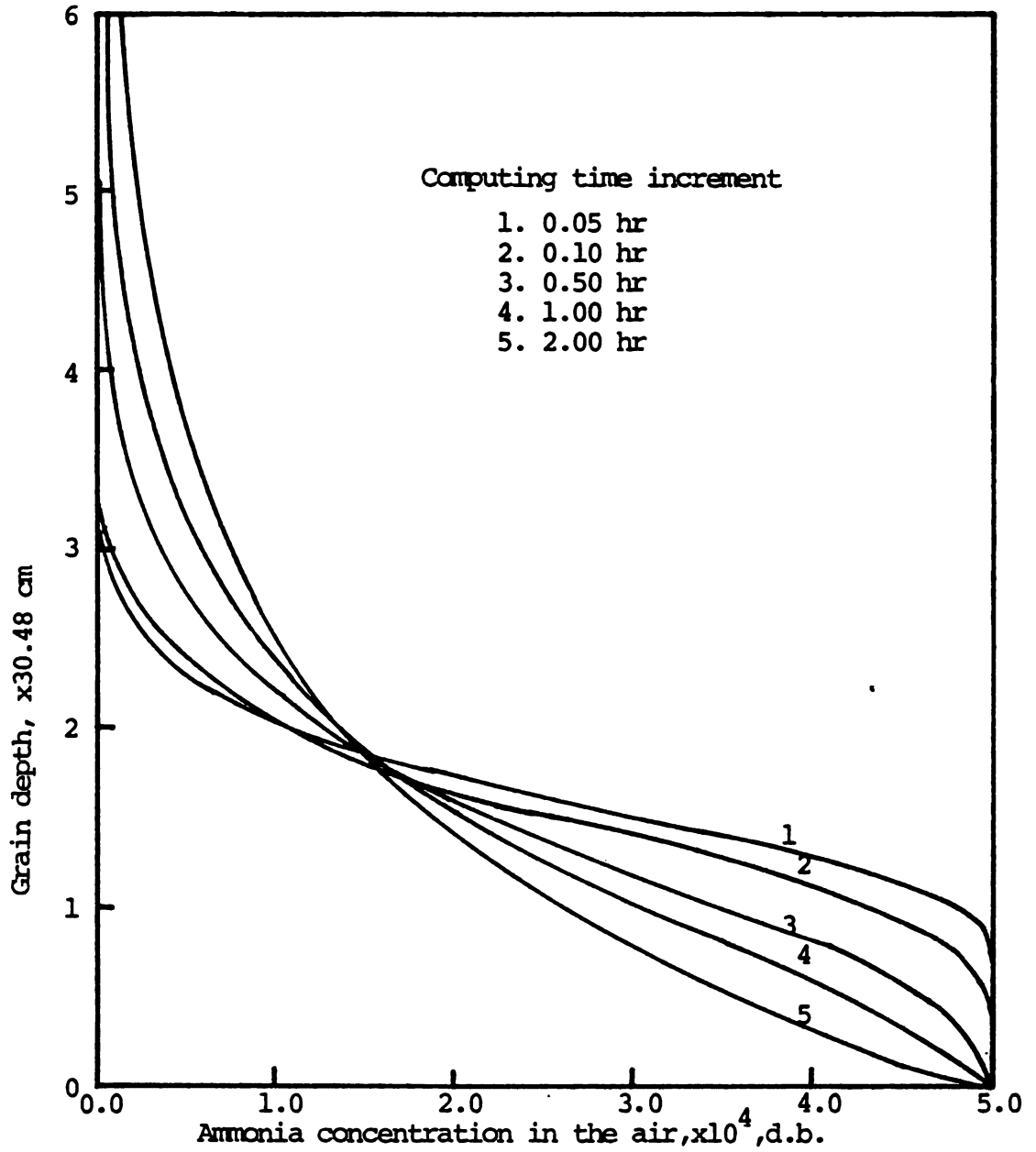


Figure 7.6. Influence of computing time increment on the ammonia concentration profile in the air using $\Delta z=3.05$ cm after 2 hours of ammoniation.

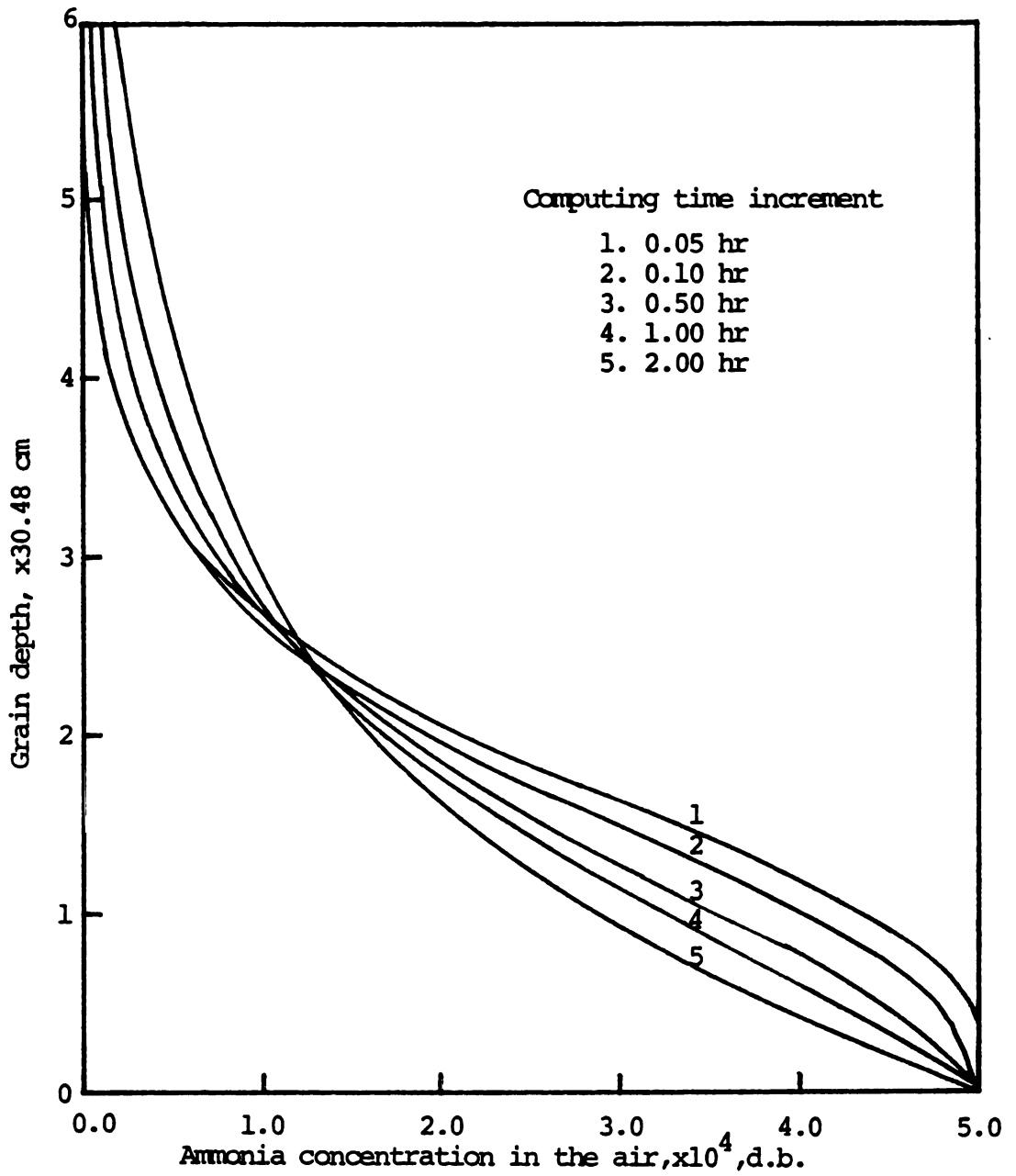


Figure 7.7. Influence of computing time increment on the ammonia concentration profile in the air using $\Delta z=15.24$ cm after 2 hours of ammoniation.

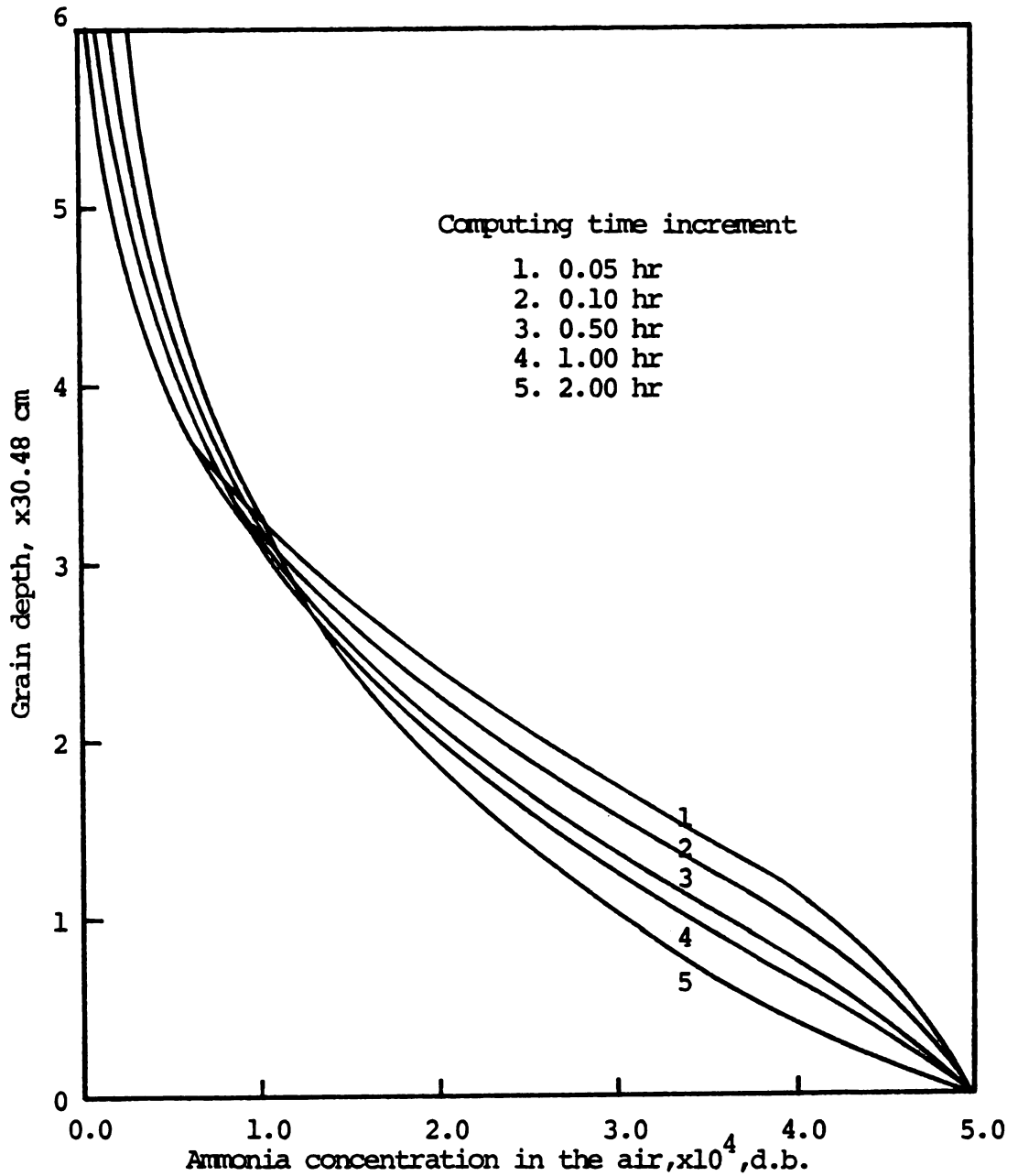


Figure 7.8. Influence of computing time increment on the ammonia concentration profile in the air using $\Delta z=30.48$ cm after 2 hours of ammoniation.

total simulation time, (3) if accuracy is required in either the concentration profile or the average concentration, (4) the tolerable errors, (5) the inlet ammonia concentration, and (6) the initial grain moisture content.

As the time of ammoniation increases, the error in the concentration profile and the average concentration decreases. In the practical application of the ammonia sorption and drying model, a long-time simulation process is usually encountered. To avoid using an excess amount of computing time it is advisable to employ the largest Δt and Δz values possible within the acceptable range of error. A larger computing time increment can be applied if the average ammonia concentrations are more important than the concentration profiles in the analysis. The computing depth interval is chosen depending on the physical dimensions of the system and the sensitivity of grain depth interval in the analysis.

Values of $\Delta z = 15.24$ cm and $\Delta t = 1$ hr were chosen in the simulation of the ammonia grain drying process. The ammonia-supplemented ambient air drying requires several months before the grain has dried to 15.5 percent w.b. The total time to be simulated for the experimental test was 1744 hours. With such a long-time test and the main concern being the average ammonia concentrations, it seems appropriate to use one hour as the computing time increment.

The total grain depth of the experimental test bin was 183 cm (6 ft). Thirteen nodes within the grain bed were assigned by using 15.24 cm (0.5 ft) as the computing depth interval. The prediction errors due to using $\Delta t = 1$ hr and $\Delta z = 15.24$ cm are 6.5 percent in the average ammonia concentration in the air and 2.0 percent in the average ammonia content in the corn (Table 7.1). These errors are considered tolerable

in this investigation.

Even though the inlet ammonia concentration and the grain moisture content influence the selection of Δt and Δz , their variations in practical application are usually very small and do not significantly alter the selection criteria for Δt and Δz .

4. The Ammonia Breakthrough Characteristics

4-A. The Adsorption Concentration Profiles

The analysis of the ammonia concentration profiles is one of the methods of investigating the breakthrough characteristics. The concentration profiles of ammonia in the air in the experimental bin are shown in Figure 7.9. The applied ammonia is completely adsorbed before one hour of ammoniation and no ammonia is found in the exhaust air. As time progresses, the adsorption of ammonia in the corn cannot keep up with the amount of ammonia applied, and thus more ammonia is exhausted in the air. After about 15 hours of ammoniation under the standard conditions, the corn in the bin is almost completely saturated with ammonia and thus the amount of ammonia applied equals the amount of ammonia lost in the exhaust air.

The ammonia adsorption profile of free ammonia at different times in the corn is shown in Figure 7.10. The shape of the curves is similar to the ammonia concentration profiles in the air except that the curves are shifted upwards beginning at a lower portion of the grain bed. The free ammonia content at positions very close to the air inlet decreases with time due to the drying of corn. As the grain loses moisture, the free ammonia content also decreases since the water moisture in corn is the only active component in the grain holding the free ammonia.

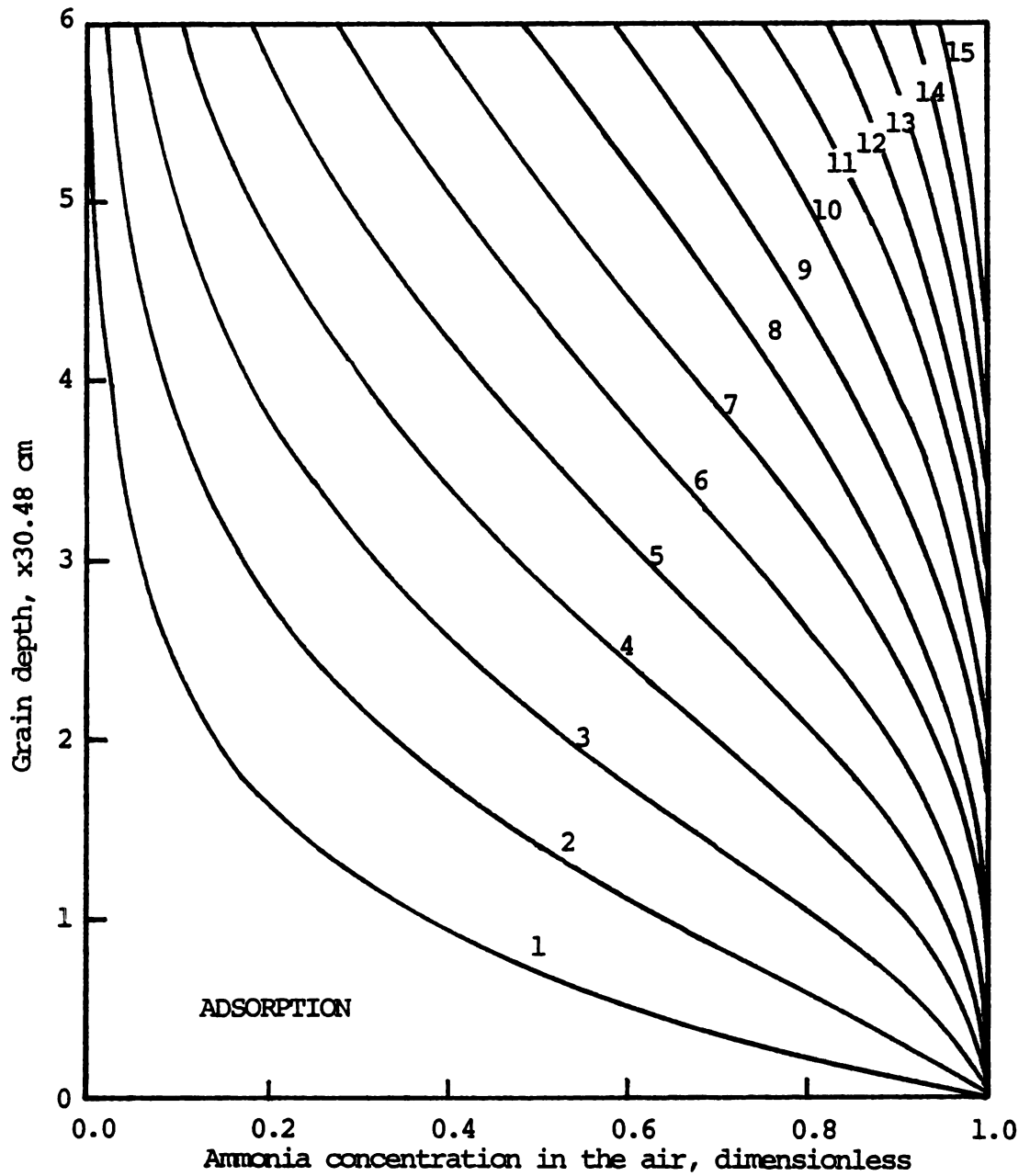


Figure 7.9. The concentration profile of ammonia in the air at different times (in hours).

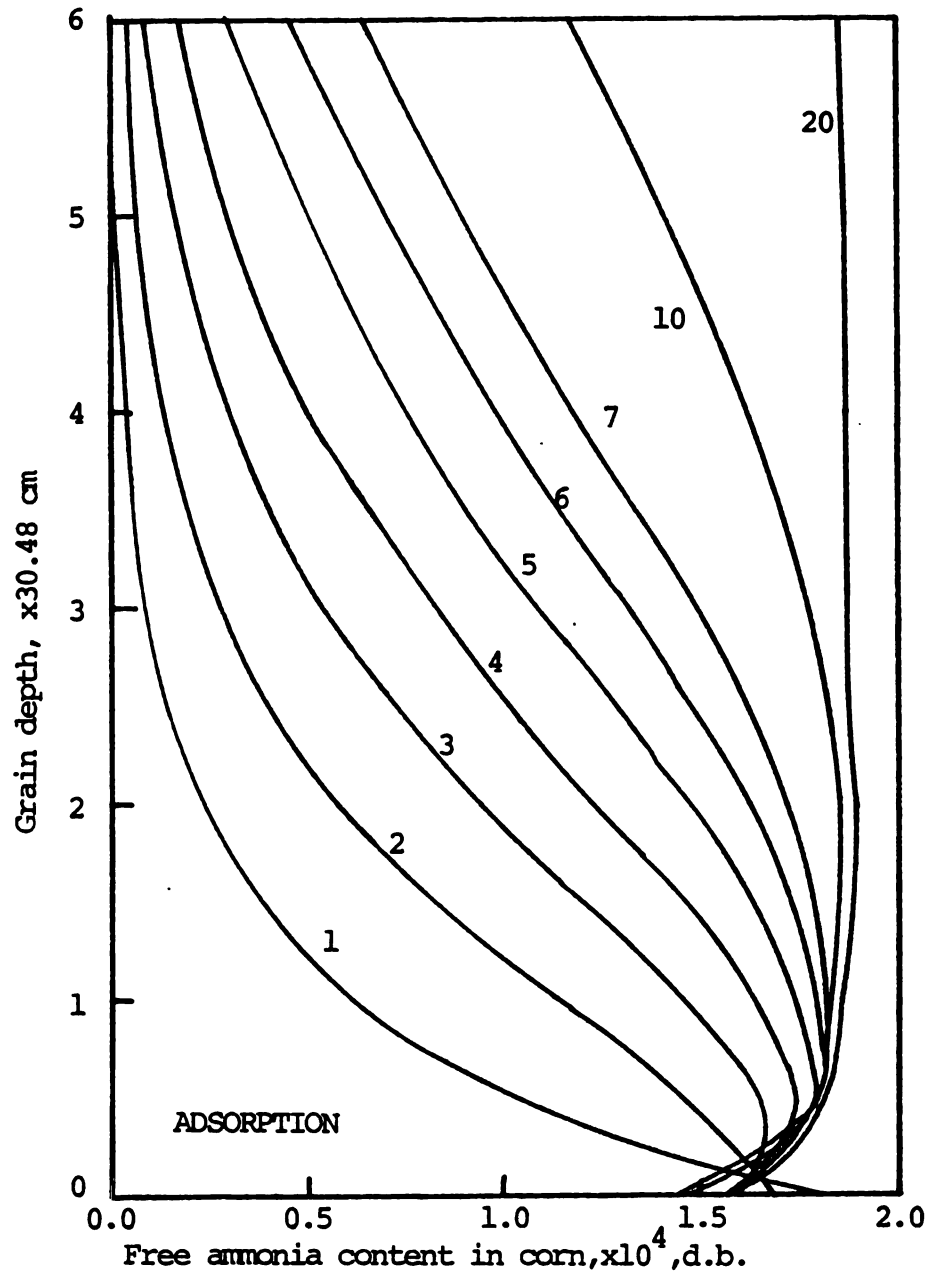


Figure 7.10. The concentration profile of free ammonia in corn at different times (in hours).

The free ammonia holding capacity of the corn becomes larger as time progresses. The free ammonia concentration profiles are shifted toward the right-hand side (higher concentration) in Figure 7.10 due to the combination of the following effects:

- 1) Changes in grain moisture content: Some drying is taking place near the bottom of the grain bed (the relative humidity of the inlet air is 80 percent). The inlet air soon becomes saturated with moisture as it travels through the grain bed. The grain moisture content is not significantly changed at bed positions higher than 61 cm (2 ft) at the end of the 20-hour treatment. Thus the drying effect only influences the portion of the grain below 61 cm.
- 2) Changes in grain temperature: The drying of grain tends to decrease the grain temperature due to evaporative cooling. On the other hand ammonia adsorption tends to increase the grain temperature due to the release of adsorption heat. The combined effects was found to decrease the grain temperature under the standard conditions. Thus, the heat of adsorption is not large enough to compensate for the evaporative cooling of the grain. The air temperature, and accordingly the grain temperature, is lowered as the air passes through the drying zone. It is this cooling effect which increases the free ammonia-holding capacity of the grain since cooler grain can adsorb a larger amount of free ammonia (see the ammonia adsorption isotherm in Figure 3.5).

At grain positions closer to the bottom more drying takes place and the free ammonia adsorbing capacities are reduced due to lower grain moisture content. However, the reduction is not large enough to compensate for the increase in the ammonia-holding capacity due to the

temperature decrease.

4-B. The Desorption Concentration Profiles

The desorption concentration profiles were also calculated for the standard conditions except for the initial and inlet ammonia conditions. The initial ammonia concentration in the air in the bin was 0.05 percent. The free ammonia concentration in the corn was calculated and defined as the equilibrium ammonia content at 10°C. The inlet air was ammonia-free.

The desorption profiles for the ammonia in the air (Figure 7.11) are similar, but not identical, to the mirror image of the adsorption profiles. This is due to the difference between the desorption profiles for the free ammonia in corn (Figure 7.12) and the desorption profiles (Figure 7.10). The lower portion of the curves in Figure 7.12 is different from that in Figure 7.10. Despite more significant drying in the portion of the grain closer to the bin bottom, the desorption process removes the ammonia from the air in the void spaces and the corn in those positions very rapidly. Therefore, the shifting of desorption curves is not apparent (Figure 7.12) due to changes in the grain moisture content, temperature, and accordingly, the holding capacities of free ammonia in corn close to the bin bottom. Nonetheless, the decrease in the grain temperature is more pronounced in the desorption than in the adsorption process. The combination of the evaporative cooling due to drying in parallel with desorption cooling of ammonia is expected to further decrease the grain temperatures. As a result, the process of free ammonia desorption in corn is slowed down.

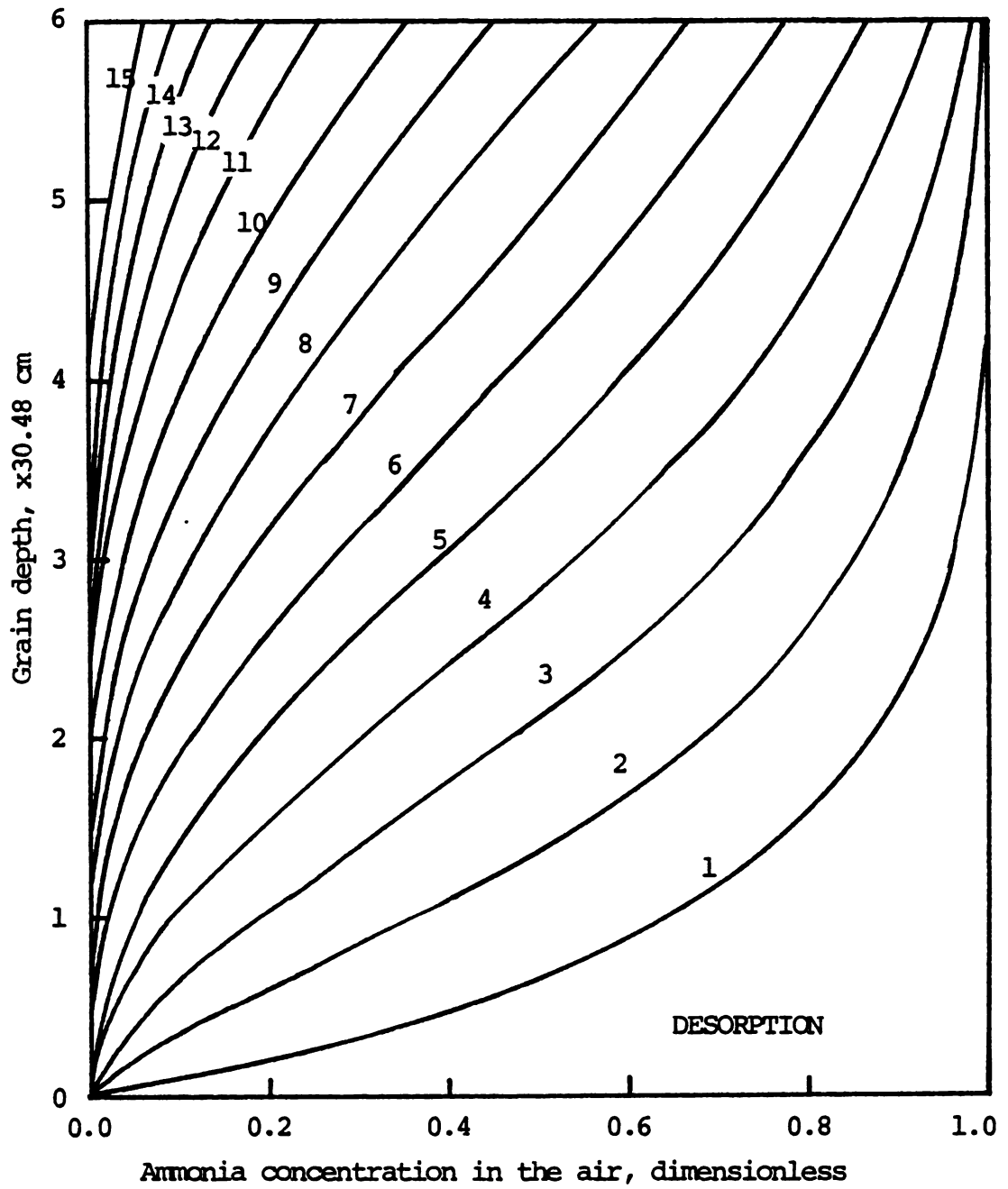


Figure 7.11. The desorption profile of ammonia in the air at different times (in hours).

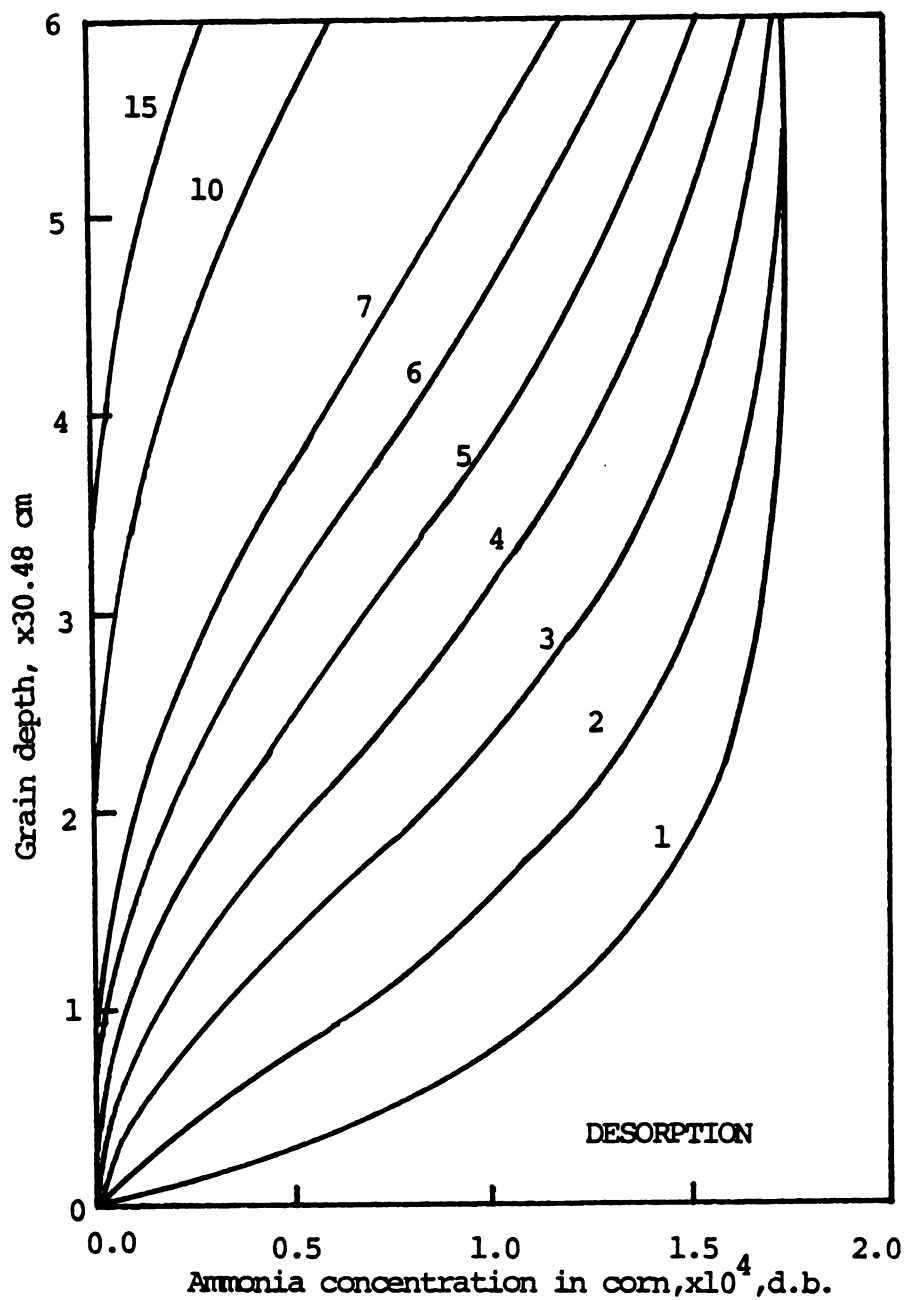


Figure 7.12. The desorption profile of free ammonia in corn at different times (in hours).

4-C. The Ammonia Adsorption and Desorption Rates

The rates of ammonia adsorption at different levels in the grain bin under standard ammoniation conditions are shown in Figure 7.13. The adsorption rate is the highest when the ammonia-free corn first encounters ammonia in the air. This is expected since there are more vacant "adsorption sites" available. The adsorption rate drops rapidly as fewer vacant adsorption sites become available and approaches zero asymptotically.

At higher bed levels in the bin, less ammonia is left in the air stream since most of the ammonia applied has already been adsorbed by the corn at the lower bed levels. The adsorption rate reaches a maximum value of $h_m a$ (from Equations 6.8 and 6.9), or $0.0937 \text{ kg-NH}_3/(\text{hr m}^2)$ under standard conditions, as soon as the ammonia-free corn ($x_2^0 = x_2 = 0$ in Equation 6.9) first encounters ammonia.

The ammonia desorption rates are shown in Figure 7.14. The shape of the curves resembles the rate of drying curves. The absolute values of the ammonia desorption rate increase as the aeration time increases. In the beginning of the desorption process, the desorption is not significant at the upper grain levels. The inlet ammonia-free air mixes with the ammonia "saturated" air and corn (saturated at 0.05 percent ammonia concentration in the air) and soon becomes saturated in the air; no more desorption occurs once the ammonia concentration reaches 0.05 percent in the air. As more and more ammonia is removed, the air in the bin becomes more unsaturated. The absolute value of the desorption rate increases as shown in Figure 7.14. The desorption rate at the lower bin level decreases rapidly and the corn at that level soon becomes practically ammonia-free; the desorption zone thus moves

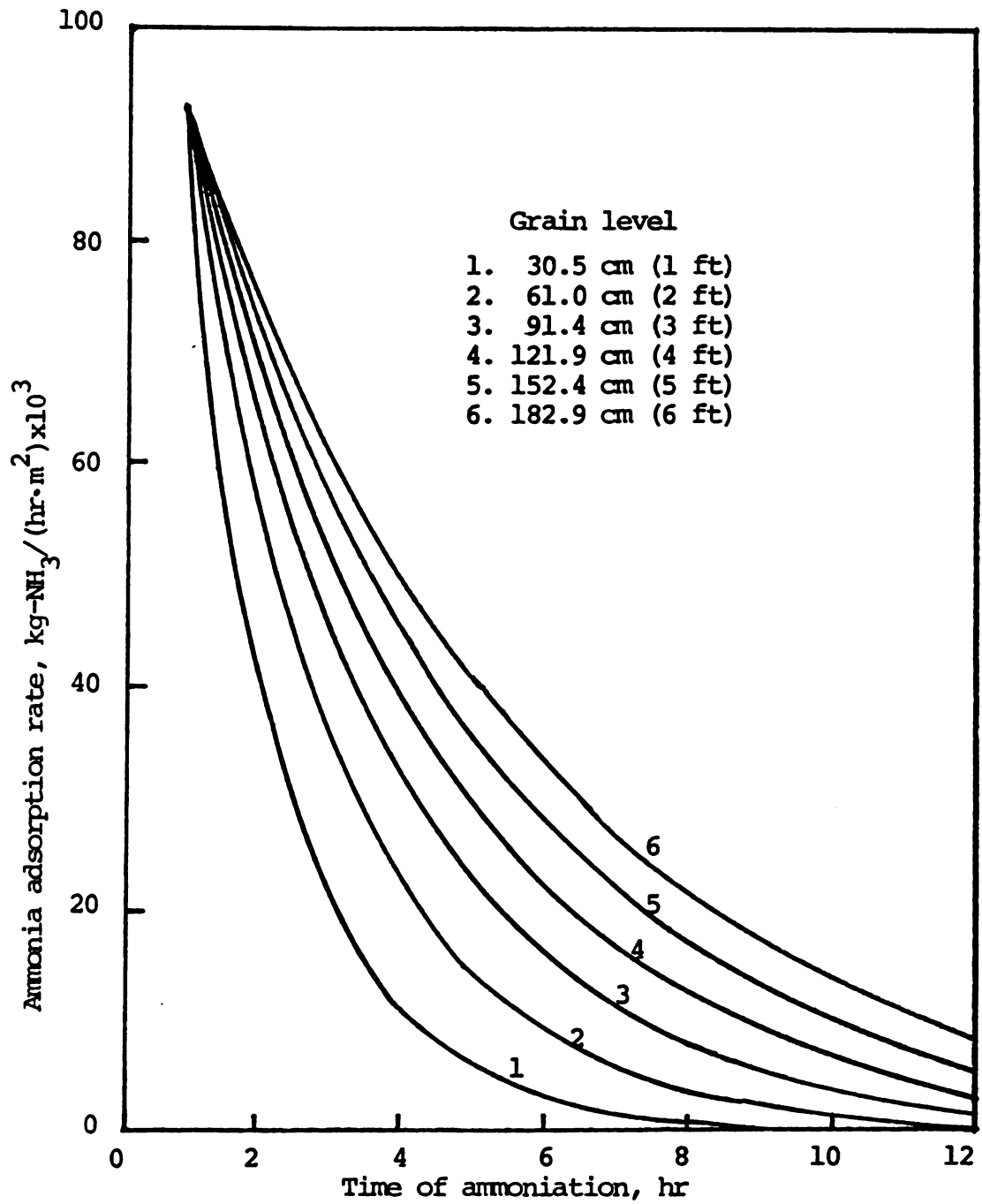


Figure 7.13. Ammonia adsorption rate at different grain levels.

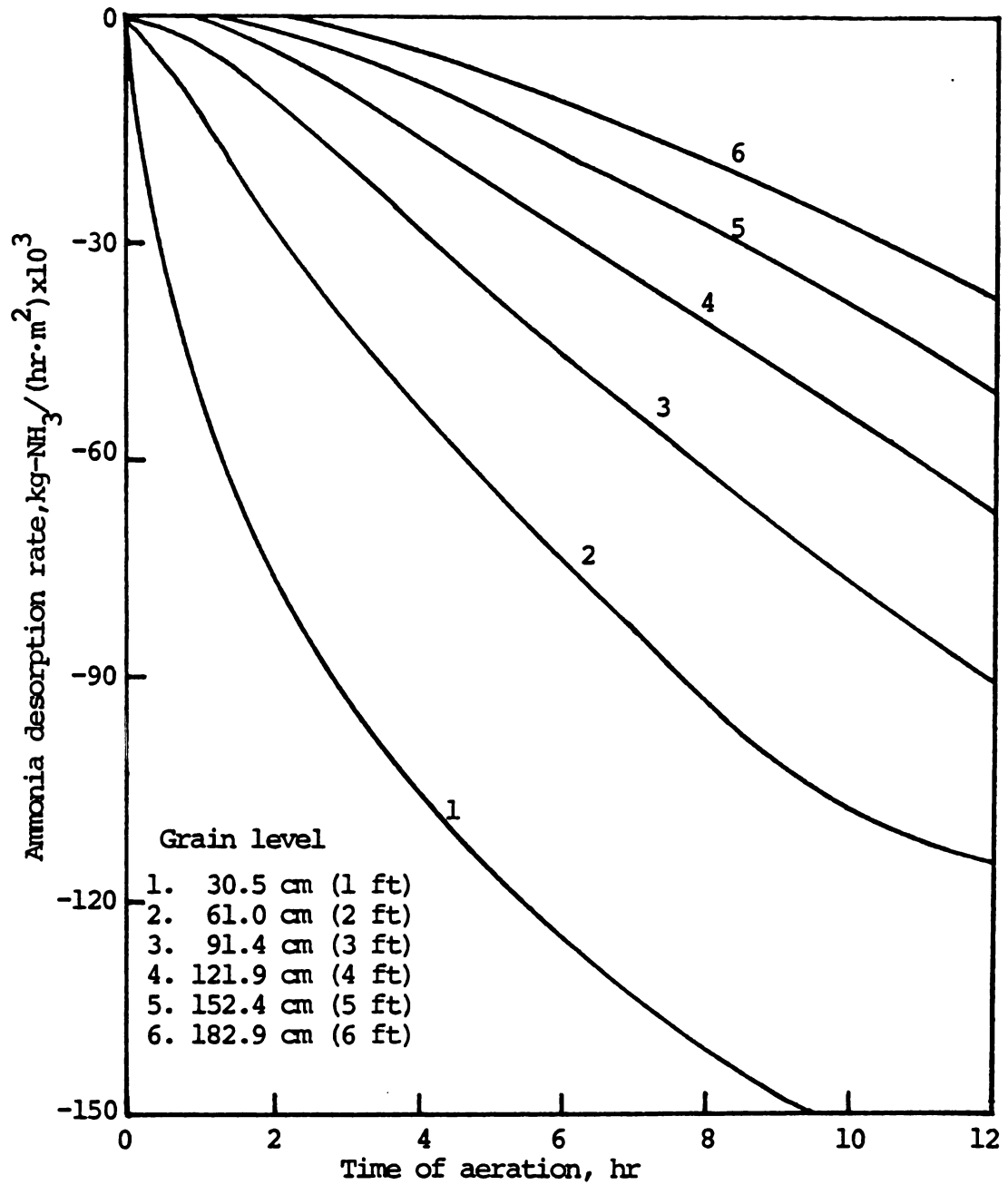


Figure 7.14. Ammonia desorption rate at different grain levels.

forward.

4-D. The Breakthrough Curves

The breakthrough curves under standard conditions are shown in Figure 7.15 for the adsorption and Figure 7.16 for the desorption. The smaller the grain depth the steeper is the breakthrough curve. It requires 34 hours to reach a 90 percent breakthrough for 6.1 m of grain. Thus, the ammonia concentration in the air will reach 90 percent of that of the inlet air after 34 hours of ammoniation. On the other hand, it takes about four hours for 0.31 m of grain to reach 90 percent breakthrough. The shape of the breakthrough curves is greatly influenced by the following factors: (1) the airflow rate (larger airflow will shorten the breakthrough times), (2) the mass transfer rate (larger mass transfer rates will generate steeper breakthrough curves), (3) the grain moisture content (larger grain moisture contents will adsorb more ammonia and thus prolong the breakthrough time), and (4) the grain temperature (grain at lower temperature tends to prolong the breakthrough time since the cooler grain has higher ammonia-holding capacities).

The desorption breakthrough curves (Figure 7.16) are also influenced by the above factors in parallel to the adsorption process. The 90 percent desorption breakthrough time is about 38 hours for 6.1 m of grain which is longer than that in the adsorption process. The desorption process lowers the grain temperatures and increases the breakthrough time.

5. The Sensitivity Tests of the Important Parameters

The purpose of the sensitivity tests was to investigate the influence of certain parameters in the simulation model on the predicted ammonia

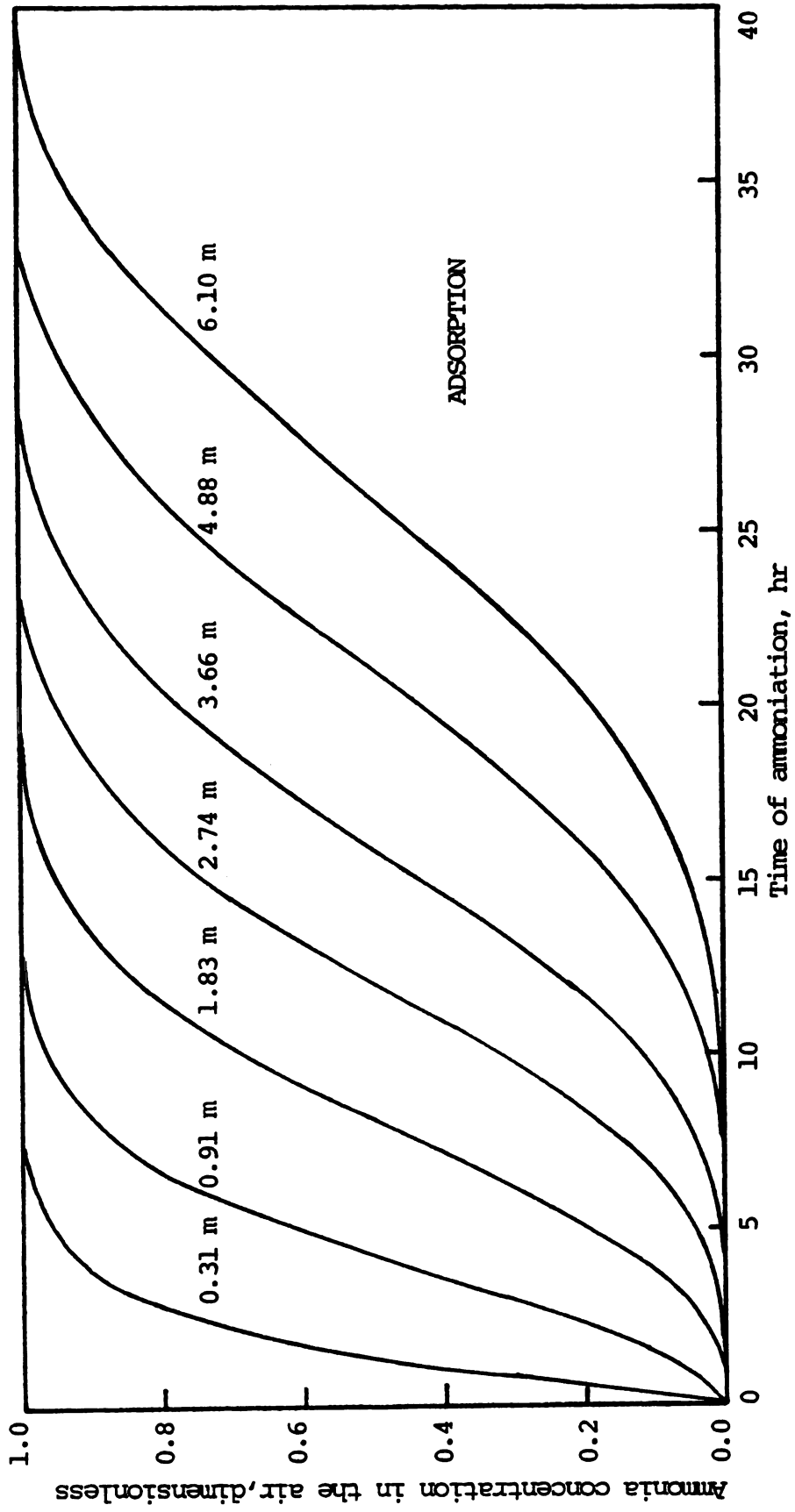


Figure 7.15. Influence of grain depth on the breakthrough curve under standard conditions.

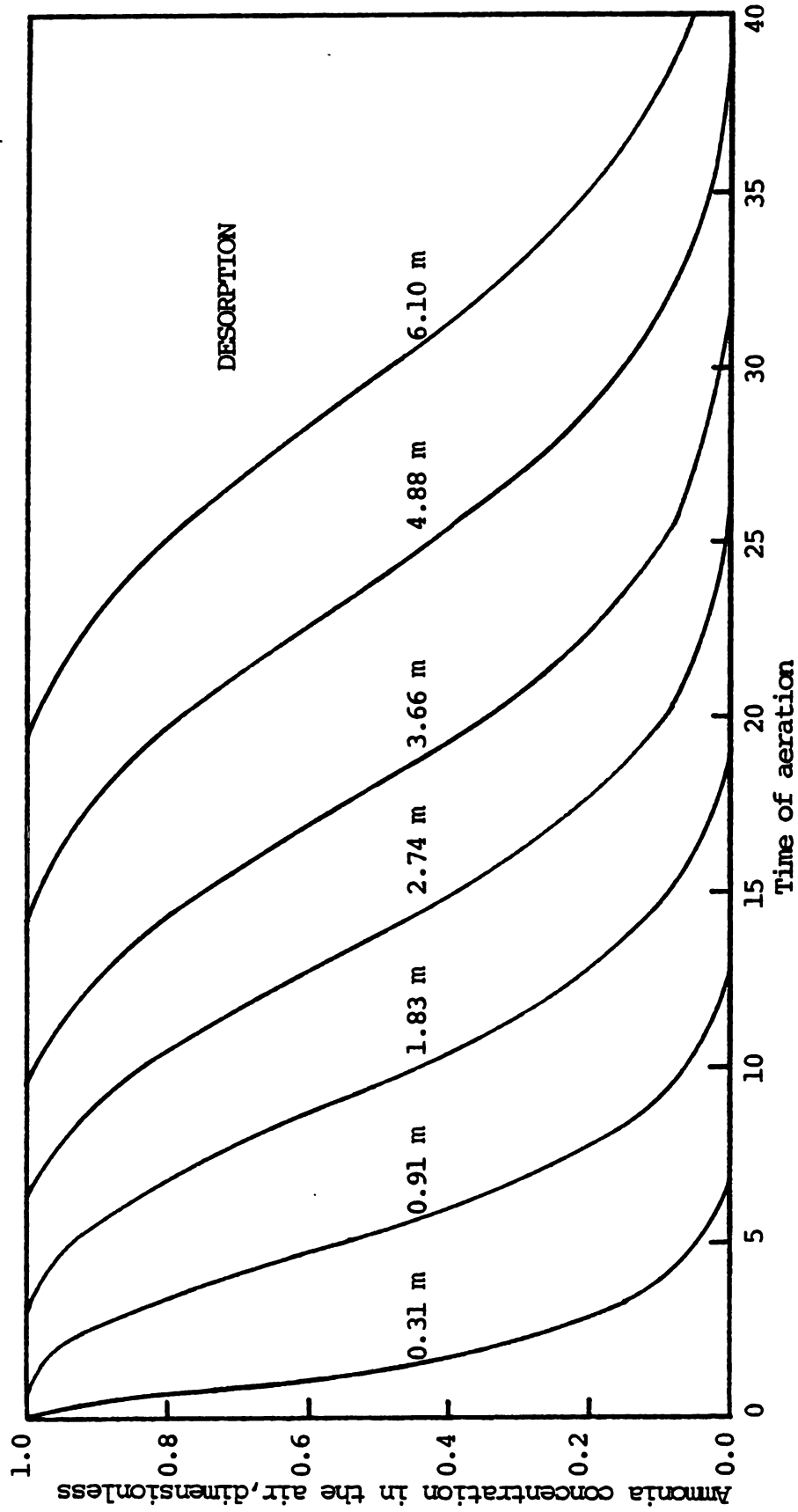


Figure 7.16. Influence of grain depth on the desorption breakthrough curve under standard conditions.

concentrations. The investigated parameters included are: (1) the initial grain moisture content, (2) the initial grain temperature, (3) the airflow rate, (4) the ratio of the mass/heat transfer coefficients (KH), and (5) the division factor (NT), i.e. the number of time intervals in which the first inside node is subdivided at the first computing time interval.

5-A. The Initial Grain Moisture Content

The influence of grain moisture content on the ammonia adsorption process is rather straightforward since water in the corn is assumed to be the only active component in holding the free ammonia. The more ammonia is adsorbed by the corn, the less ammonia is left in the air under the same inlet conditions.

The average ammonia concentration for different grain moisture content is shown in Figure 7.17. The range of grain moisture content tested is from 15 to 36 percent, w.b. It shows that the higher the grain moisture content, the longer time the ammonia takes to break through the bed. This is further evidenced by the difference in the ammonia concentration profiles in the air after three hours of ammonia-tion at different grain moisture contents (Figure 7.18). The corresponding concentration profiles for free ammonia in the corn (shown in Figure 7.19) demonstrate an interesting variation at the lower portion of the grain bed. At grain moisture contents higher than 20 percent (w.b.), the S-shaped curves are due to the evaporative cooling effect. However, the concentration profiles at 15 percent moisture are shifted to the left at the lower bed positions. This is the result of moisture re-adsorption instead of drying since the grain moisture content is lower than the corresponding equilibrium moisture content. The combined

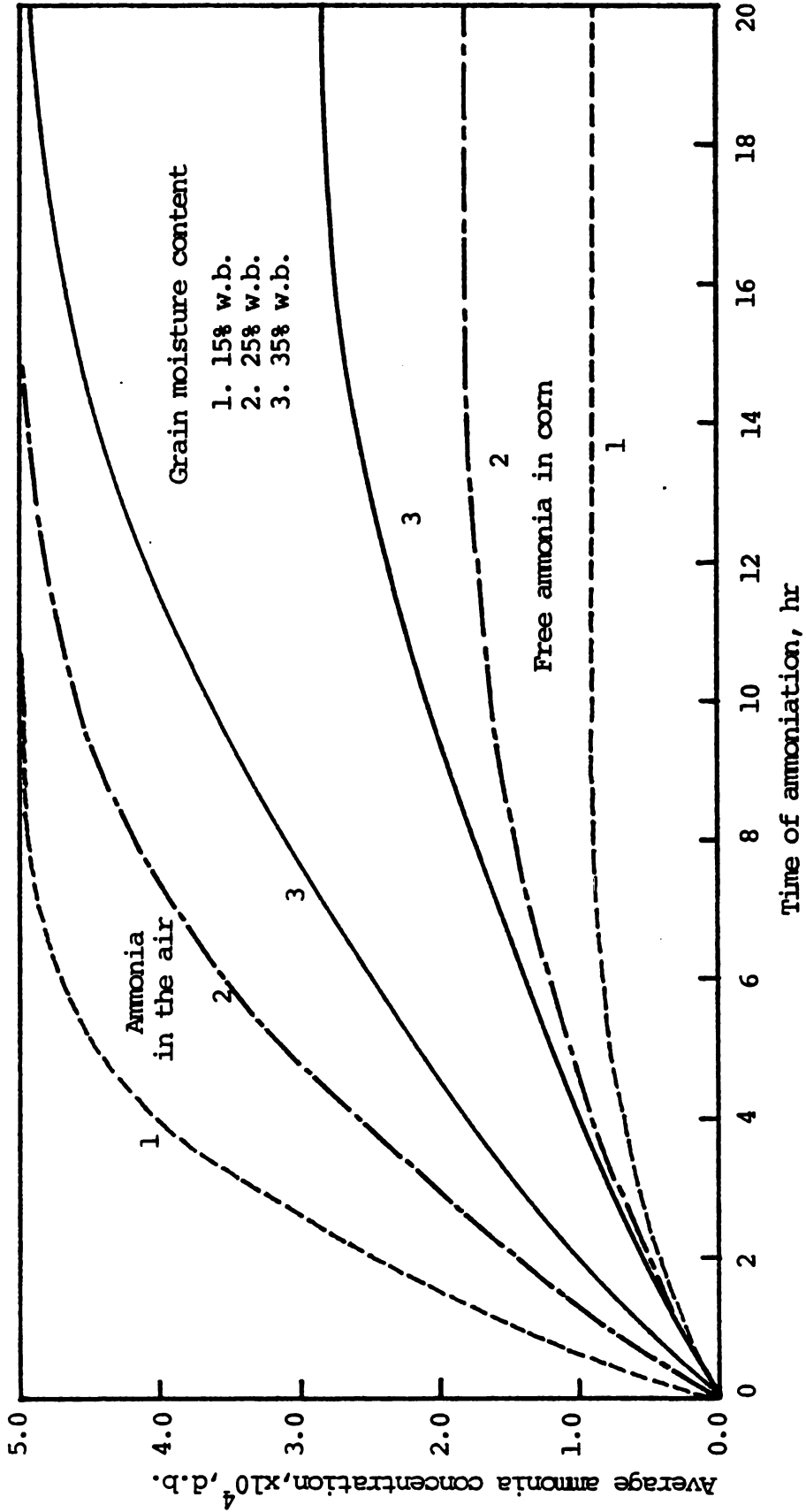


Figure 7.17. Influence of initial grain moisture content on the ammonia concentrations.

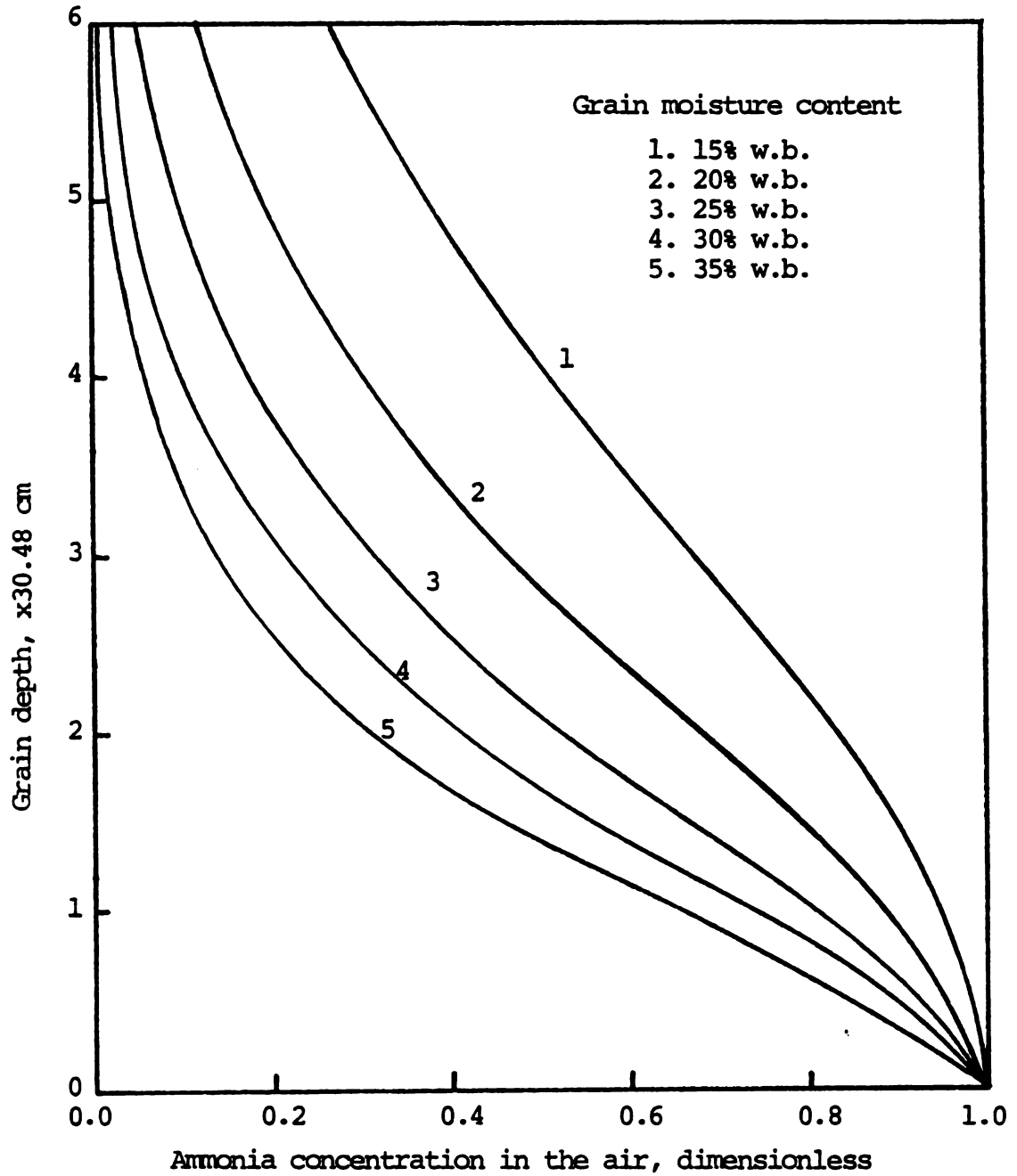


Figure 7.18. Influence of grain moisture content on the ammonia concentration profile in the air after 3 hours of ammoniation.

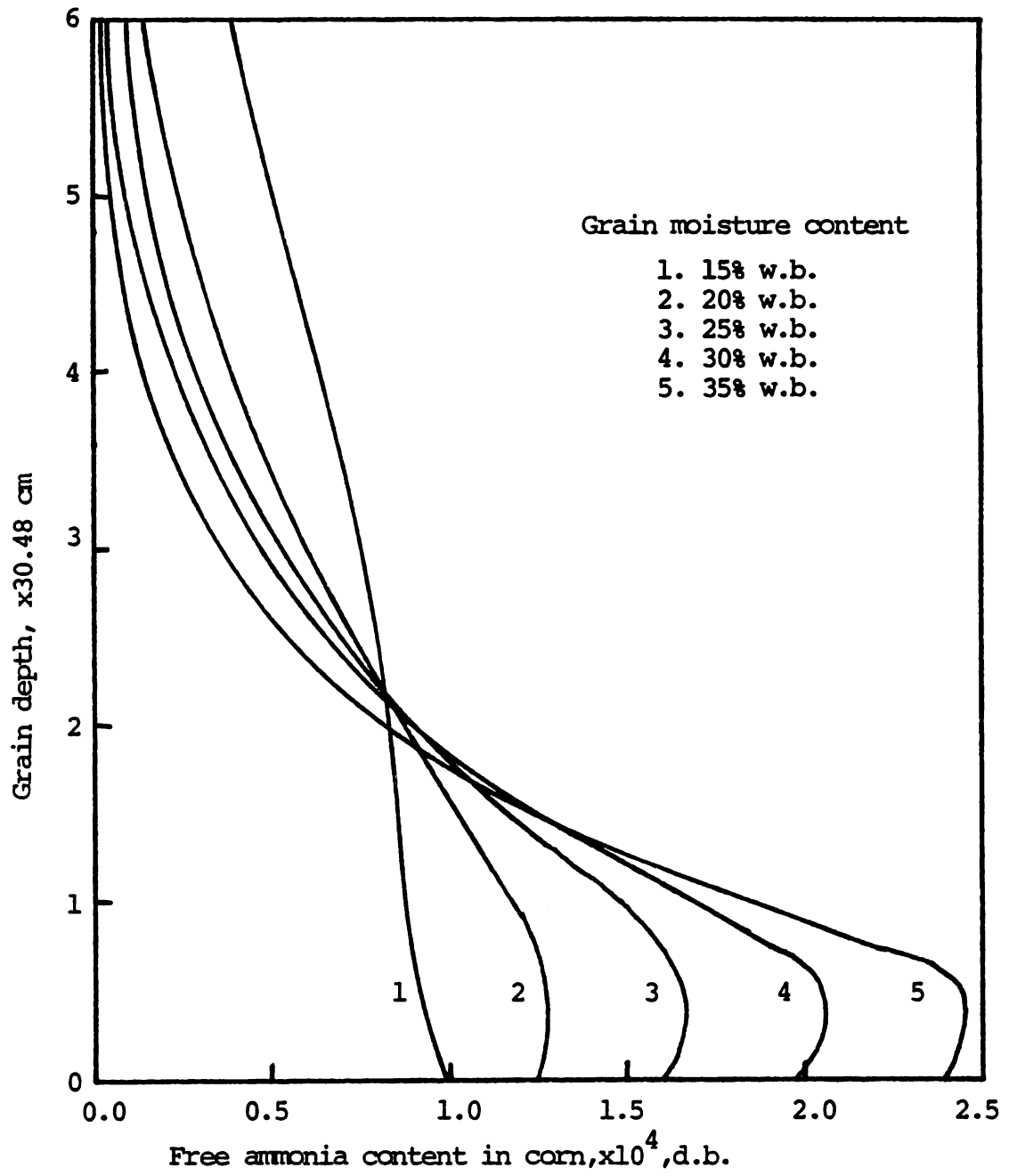


Figure 7.19. Influence of grain moisture content on the free ammonia concentration profile in corn after 3 hours of ammoniation.

effect of ammonia adsorption and grain rewetting increases the grain temperatures which subsequently results in a decrease of the free ammonia contents in the corn. As the moisture content is lowered, the free ammonia is more evenly distributed throughout the bed in the first few hours of the ammoniation process.

The lower the grain moisture content, the more ammonia is left in the grain void fraction and more ammonia is thus lost in the exhaust air (see Figure 7.18). Knowing that grain at a lower moisture content adsorbs ammonia at a slower rate, it is advisable to apply a smaller inlet ammonia concentration or use an air recycling system in the ammonia grain drying process. An air recycling system will not only reduce the ammonia loss but also reduce the possibility of grain rewetting.

5-B. The Initial Grain Temperature

The initial grain temperature was varied from -1.1 to 32.2°C . This range covers the temperature for most ambient air drying conditions in the U.S. The variation of ammonia concentration in the air with the initial grain temperature is not large as shown in Figure 7.20. The average ammonia concentration in the air is slightly higher for a higher initial grain temperature in the first few hours (about nine hours under standard conditions) of ammoniation. The buildup of free ammonia in the corn at a lower grain temperature is faster than at a higher grain temperature as a result of the changes of the equilibrium ammonia content with temperature (Figure 7.21).

The average ammonia adsorption rate is proportional to the slope of the average free ammonia concentration curve in Figure 7.21. The adsorption rate of the grain with a lower initial grain temperature is faster in the beginning but slower after about nine hours of ammoniation.

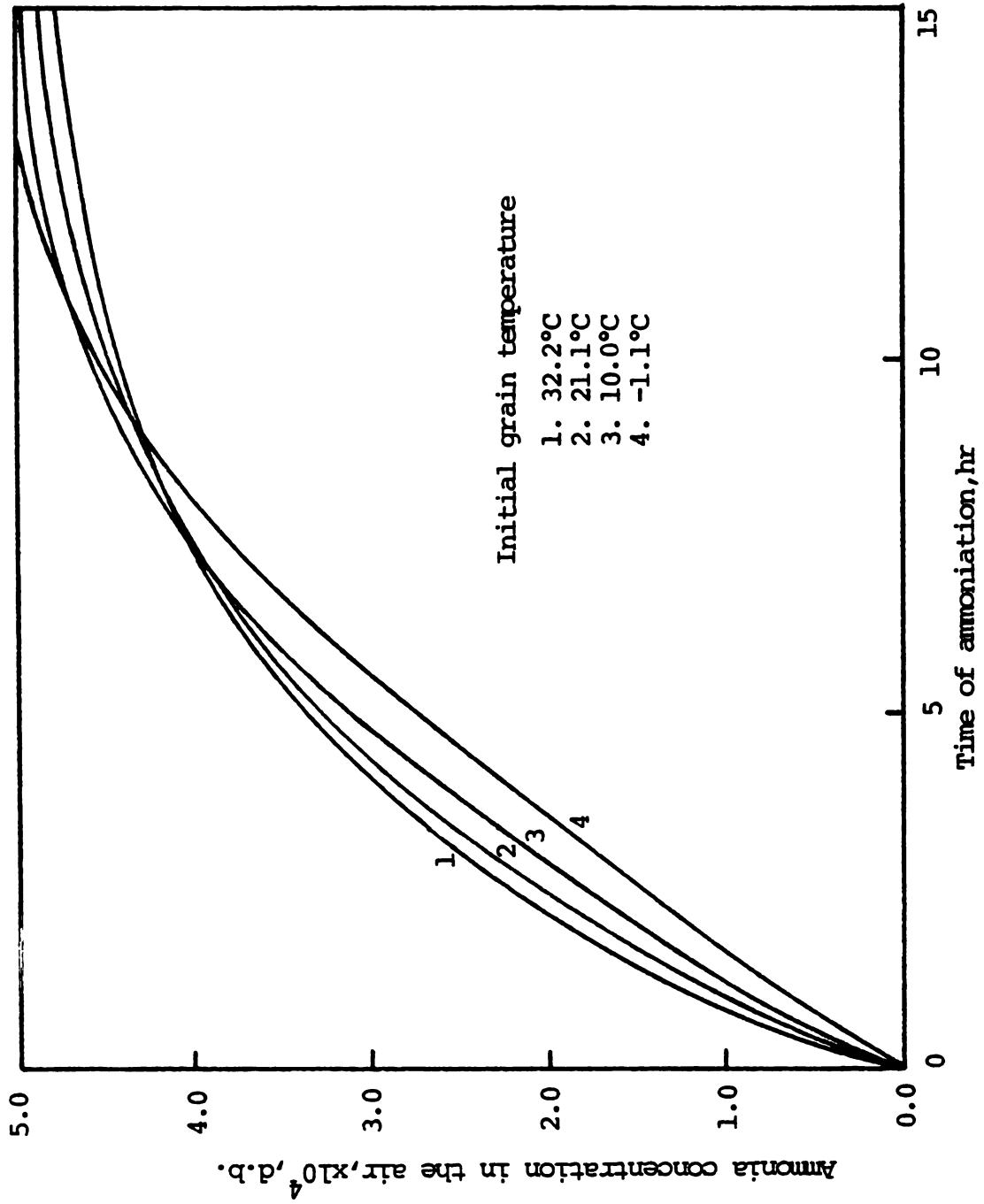


Figure 7.20. Influence of initial grain temperature on the ammonia concentration in the air.

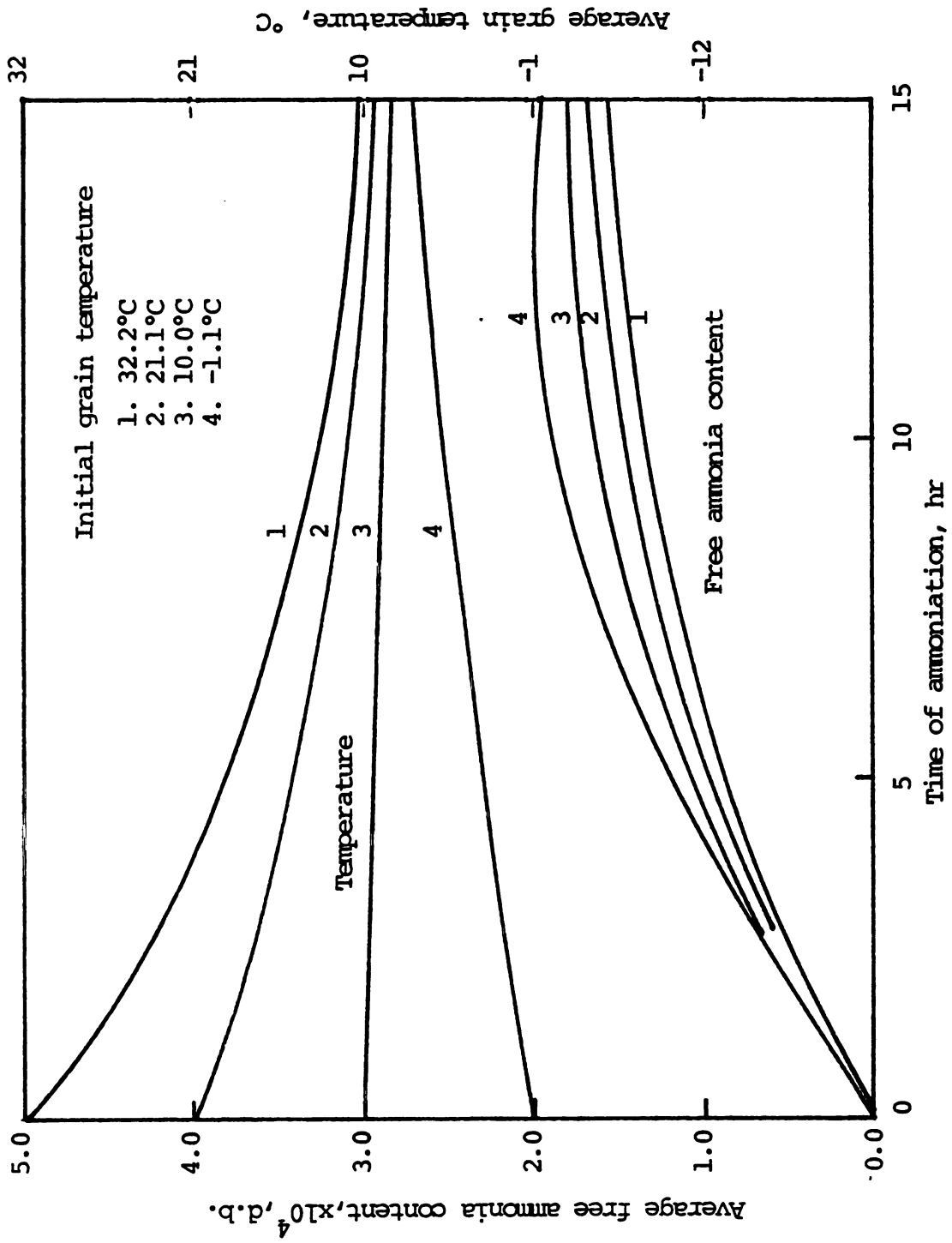


Figure 7.21. Influence of the initial grain temperature on the average free ammonia content in corn.

This result is consistent with that of the average ammonia concentrations in the air (Figure 7.20) as the curves cross and switch relative positions at about nine hours.

The upper group of curves in Figure 7.21 indicates convergence of the average grain temperatures as time increases. The inlet air temperature and humidity remain the same for different initial grain temperatures. The two groups of curves for the grain temperature and the free ammonia content in Figure 7.21 are expected to converge into two separate fixed values after a long-time treatment. The temperature curve at 10°C initial grain temperature drops slightly with time because the drying-cooling effect is larger than the ammonia adsorption heating effect.

5-C. The Airflow Rate

The airflow rate is one of the most important parameters in all types of grain drying problems. The unsaturated air humidity ($RH < 1.0$) is the driving force for the drying process in the case of ambient air grain drying. The drying rate of the total grain bed depends on the degree of unsaturation of the inlet air as well as the rate of the supply of the unsaturated air.

Analogously, the ammonia adsorption rate is determined by a driving force and the airflow rate. The range of airflows investigated falls between $0.305 \text{ cm}^3/\text{m}^2$ ($1.0 \text{ cfm}/\text{ft}^2$) to $6.096 \text{ cm}^3/\text{m}^2$ ($20 \text{ cfm}/\text{ft}^2$). It should be noted that as the airflow rate increases, the rate of ammonia input (kg/hr) increases proportionally if the inlet ammonia concentration (in percentage) remains the same. Thus, more ammonia is applied at larger airflow rates during the same period of ammoniation.

More ammonia is lost in the exhaust air after three hours of ammoniation when a higher airflow rate is used as shown in Figure 7.22. The buildup of ammonia in the air is faster at a higher airflow rate after the same period of ammoniation under standard conditions.

Unlike the influence of the initial grain temperature and moisture content on the ammonia concentrations, the rate of accumulation of both ammonia in the air and in the corn is increased by a larger airflow rate as shown in Figures 7.23 and 7.24. This is an indication of larger amounts of ammonia being supplied when larger airflow rates are used.

The sensitivity of ammonia accumulation to the airflow is more significant at smaller airflow rates. At an airflow rate larger than 2.29 cm/m^2 (7.5 cfm/ft^2), the increase in the speed of ammonia penetration is less sensitive than that of smaller airflow rates. Further increase in the airflow rate (larger than 6.10 cm/m^2) will not only increase the ammonia loss in the exhaust air but also do very little in improving the ammonia breakthrough time.

Similar shapes for the curves were found in the penetration curves for the free ammonia concentration in the corn (Figure 7.24) and the ammonia concentration in the air (Figure 7.23). This conclusion is based on the fact that a larger airflow rate will not only increase the ammonia concentration in the air but also will increase the mass transfer rate (Equations 6.29 and 6.42).

5-D. The Ratio of the Mass/Heat Transfer Coefficients

The estimation of the value of the heat transfer coefficient has been presented in Chapter 6. Assuming constant thermal properties for the air, the heat transfer coefficient is solely dependent on the airflow rate as shown in Equation 6.29. Thus, the mass transfer rate is determined

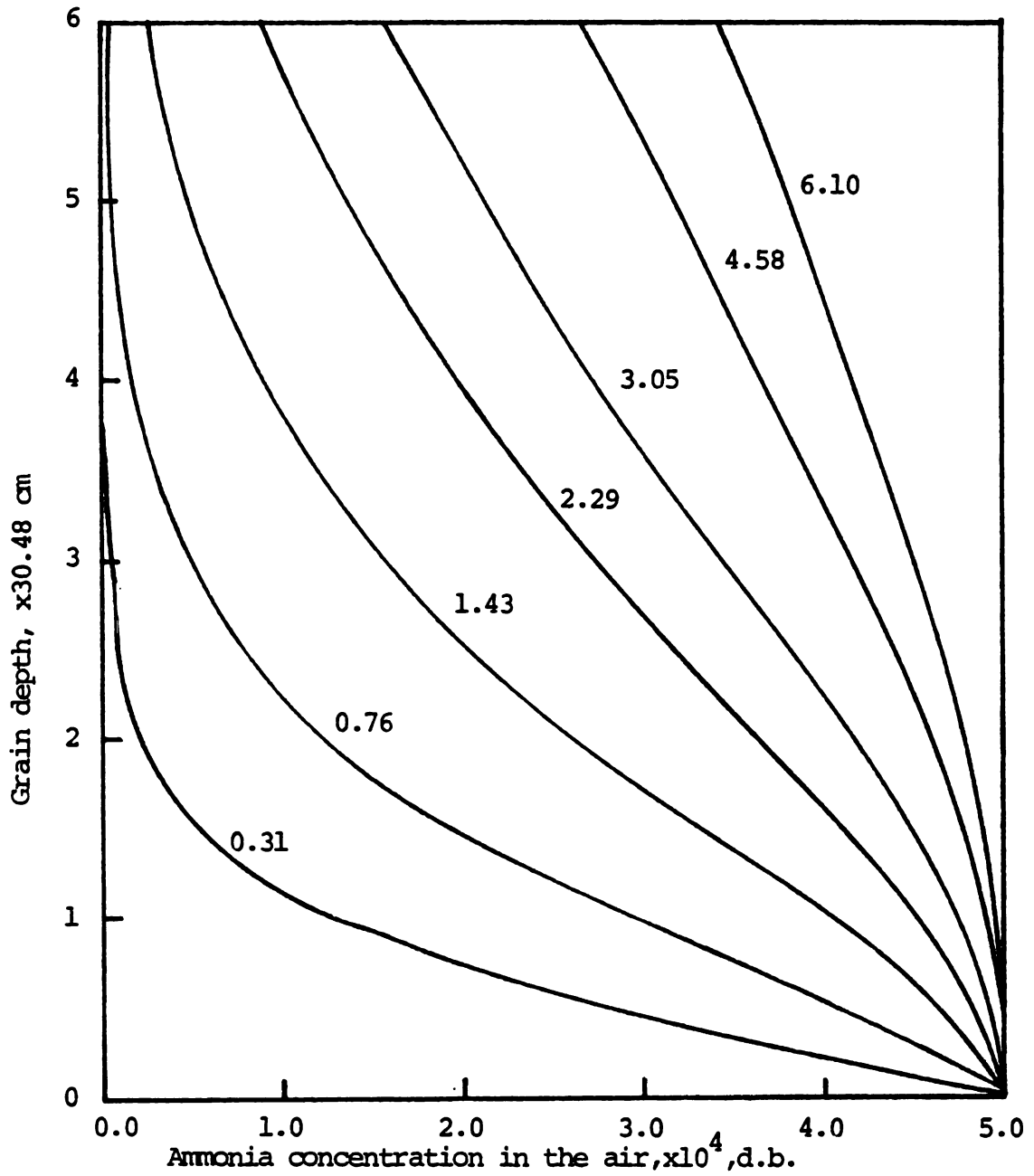


Figure 7.22. Influence of airflow rate (cm^3/m^2) on the ammonia concentration profile in the air after 3 hours of ammoniation.

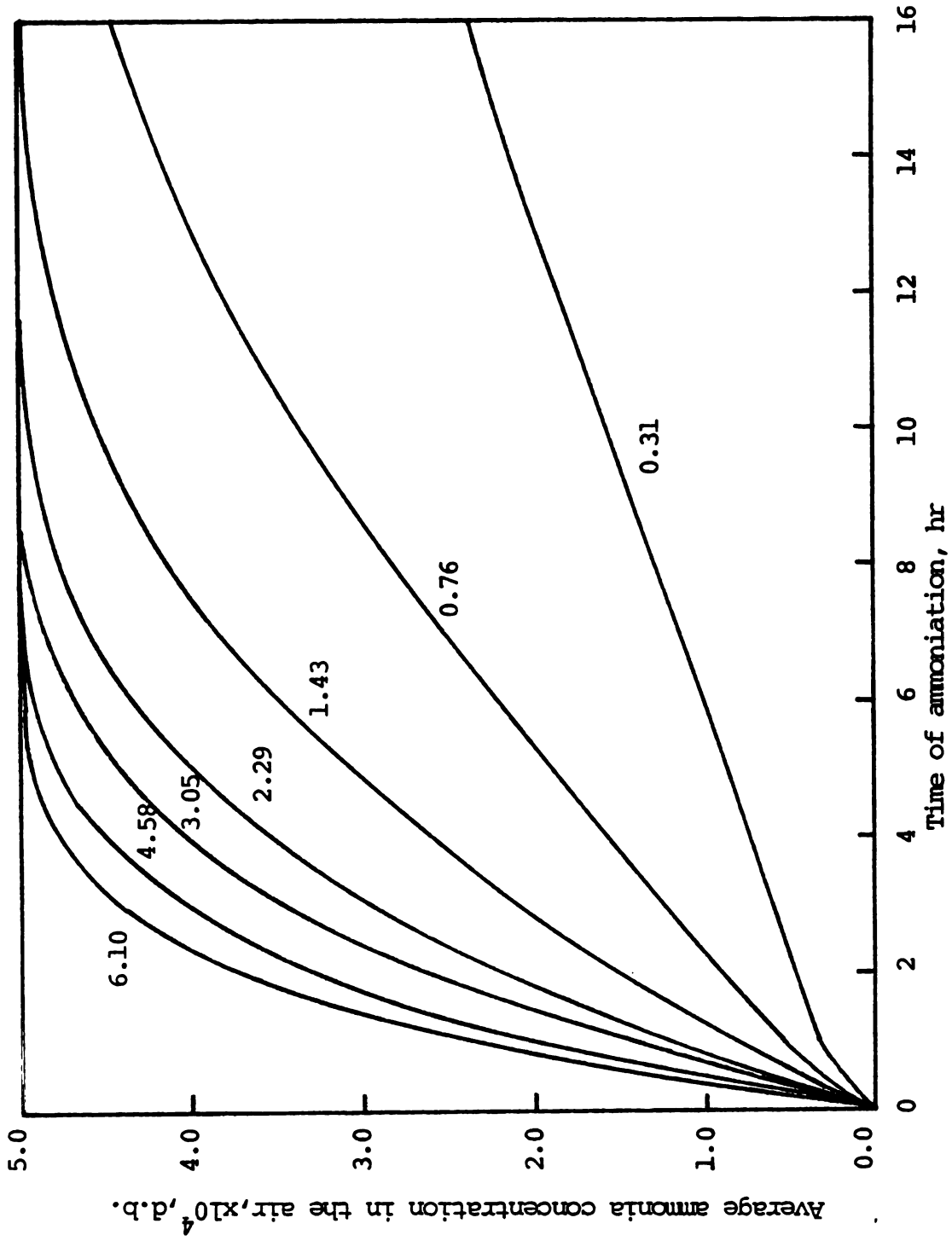


Figure 7.23. Influence of the airflow rate (cm^3/m^2) on the average ammonia concentration in the air.

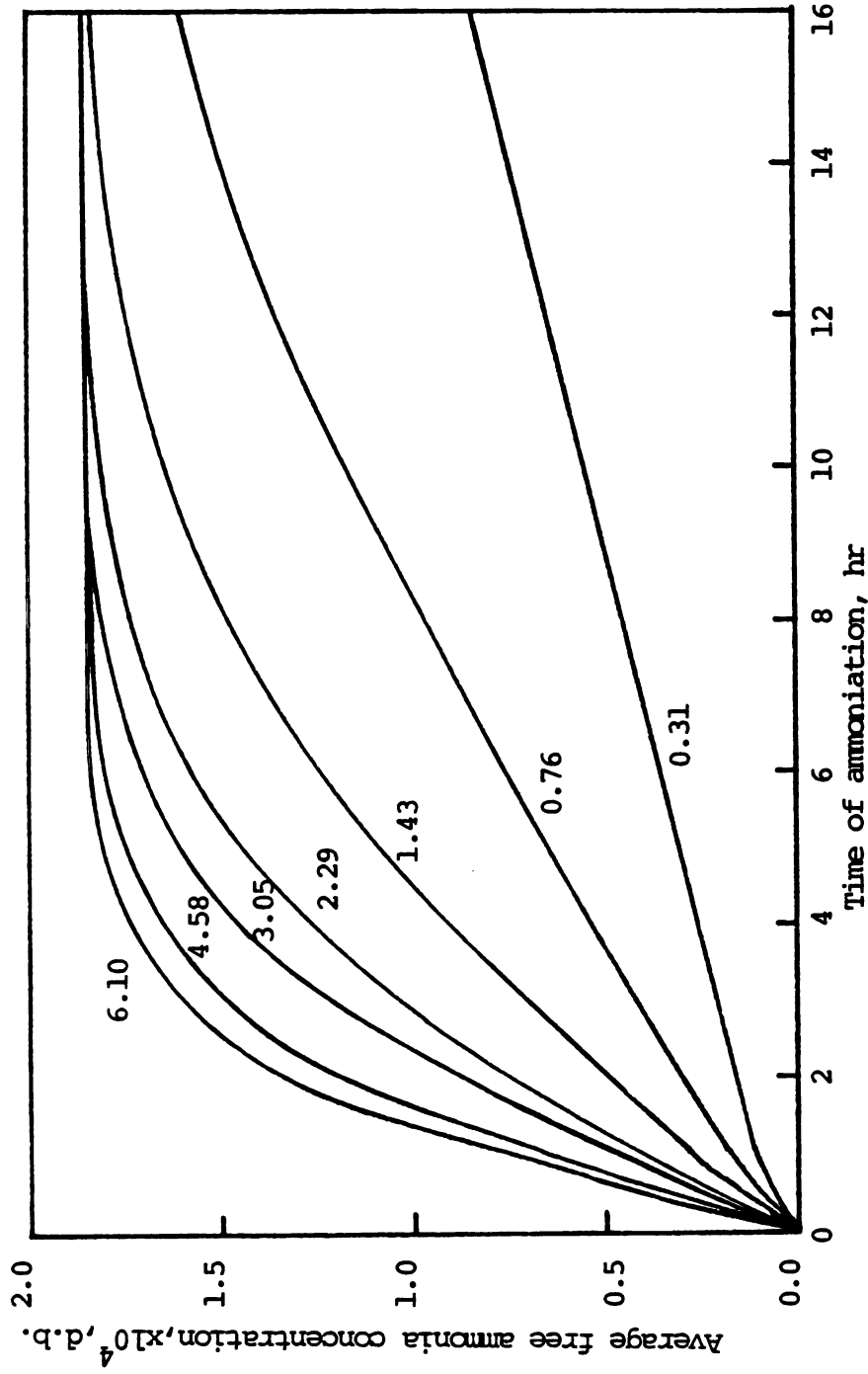


Figure 7.24. Influence of the airflow rate (cm^3/m^2) on the free ammonia content in corn.

by the airflow rate and the specified ratio for mass/heat coefficients (KH). This section focuses on the investigation of the influence of the KH ratio on the ammonia adsorption process. At constant airflow rate the mass transfer coefficient is proportional to the KH ratio which is assumed constant.

The influence of the KH ratio on the free ammonia concentration profile is shown in Figure 7.25. The test range of the KH ratio was between 1.0×10^{-3} and 1.0×10^{-6} . As the KH ratio is higher than 1.0×10^{-3} , the mass transfer coefficient is almost large enough to have instant equilibrium between the ammonia in the air and in the corn.

The crossover of the curves in Figure 7.25 is due to the higher ammonia concentration in the air at the upper portion of the bed when a smaller mass transfer coefficient is used. In other words, more ammonia is left in the air and carried to the upper levels when the mass transfer rate is lower.

An extremely slow adsorption process is found at the smallest KH ratio. The free ammonia content remains almost constant at bed levels higher than 15 cm after three hours of ammoniation as indicated in Figure 7.25. This is because the adsorption rate is so small that most of the ammonia in the inlet air is carried through the bed with only a small amount transferred to the corn. The entire grain bed encounters about the same ammonia concentration in the air and adsorbs ammonia at the same rate. The bottom level was assumed to reach equilibrium with the inlet ammonia instantaneously no matter how small the mass transfer rate is. The free ammonia concentration after the inlet node drops considerably and remains essentially constant throughout the bed for the smallest KH ratio.

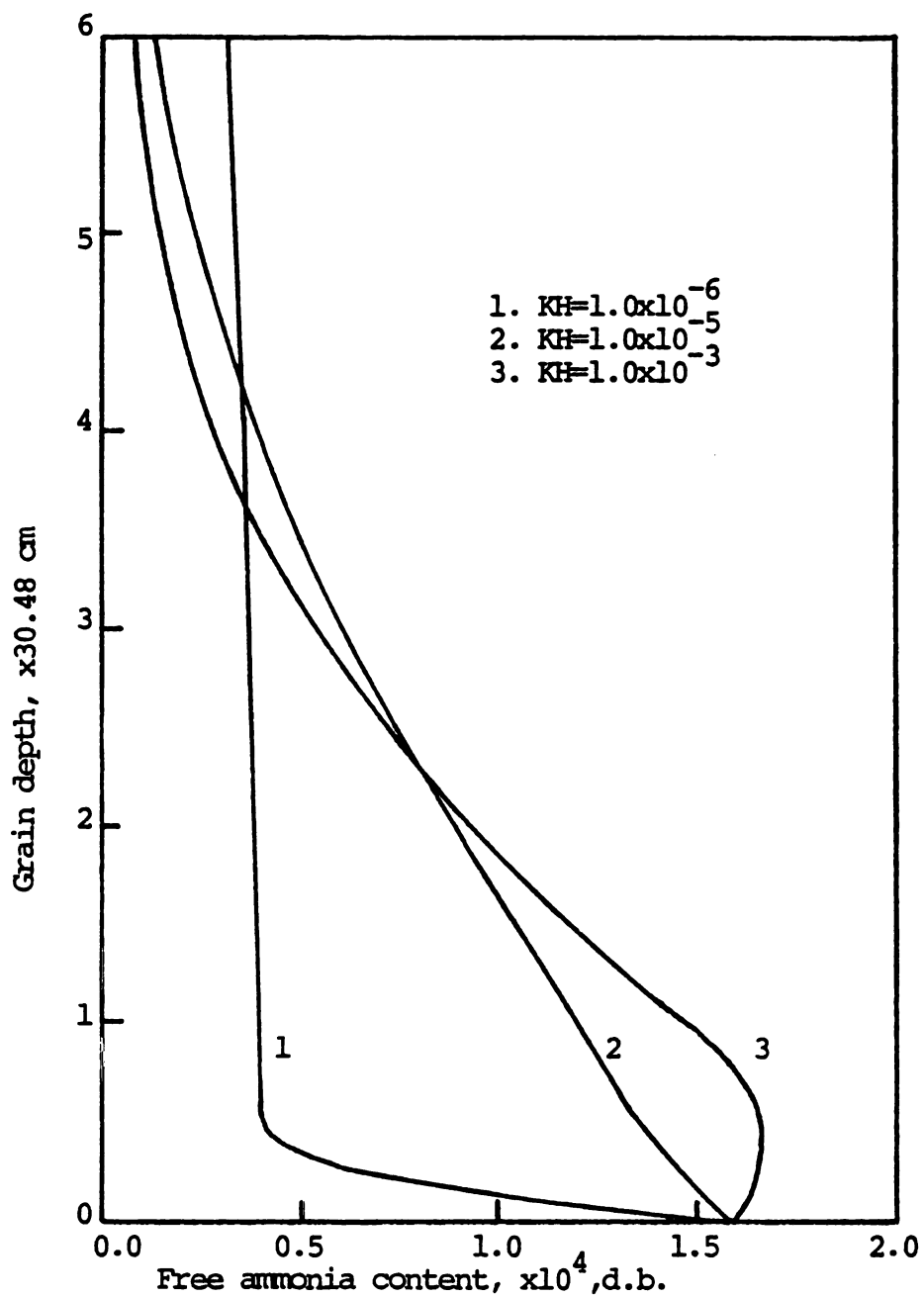


Figure 7.25. Influence of the ratio of mass/heat transfer coefficients on the free ammonia profile in corn after 3 hours of ammoniation.

The ammonia concentration profiles in the air are expected to be of similar shape to the mirror image of Figure 7.25.

The penetration curves of the average ammonia concentration are presented in Figure 7.26 for different KH ratios. The accumulation of ammonia is more sensitive to the mass transfer coefficient when a smaller ratio is used as indicated by the shape of curves using $KH = 1.0 \times 10^{-6}$ in Figure 7.26. The crossover phenomenon of the ammonia penetration curves in the air in Figure 7.26 can be explained by considering the value of the KH ratio. After about eight hours of ammonia treatment under the standard conditions, the concentration curves for $KH = 1.0 \times 10^{-5}$ or higher are getting closer to the saturation. The adsorption is thus reduced considerably. On the other hand, the free ammonia contents in corn are still far from saturation for values of $KH = 1.0 \times 10^{-6}$, and also the reduction in the adsorption rate is less significant. The "delayed" adsorption at small KH ratios explains a lower ammonia concentration in the air after the crossover region in Figure 7.26.

5-E. The Inlet Ammonia Concentrations

The sensitivity test of the inlet ammonia concentration was designed to investigate its effect on the change in the ammonia concentration profiles. One of the major problems in applying ammonia grain drying on a practical basis is the selection of a proper ammonia flow rate to utilize the ammonia efficiently by reducing the ammonia loss in the exhaust air to a minimum.

The ammonia concentration profile in the air is shown in Figure 7.27 for various levels of inlet ammonia concentration. At the end of a three-hour ammoniation, the ammonia concentration gradient across the bed is larger as a higher inlet ammonia concentration is applied. The amount

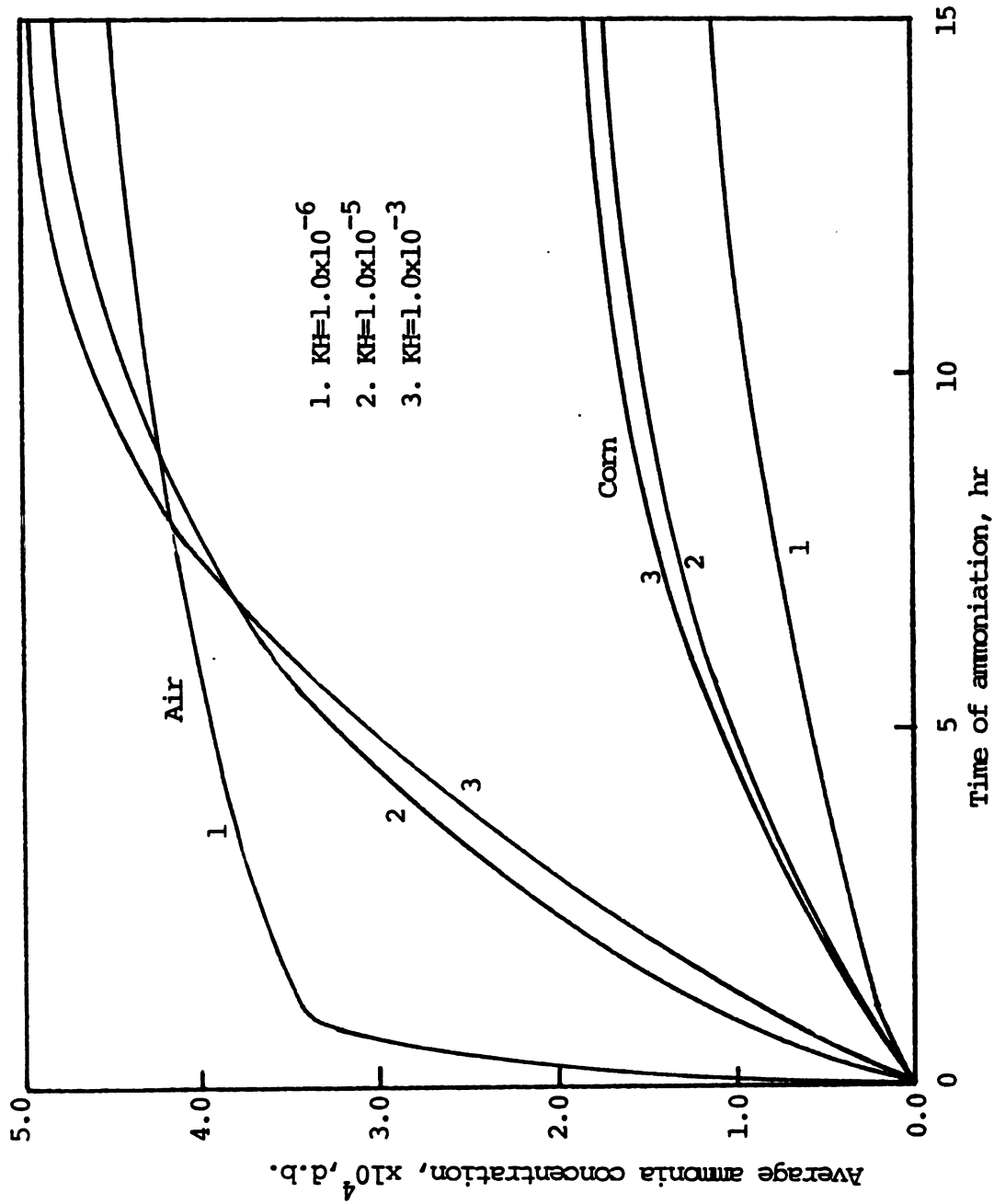


Figure 7.26. Influence of the ratio of mass/heat transfer coefficients on the average ammonia concentration in the air and in the corn.

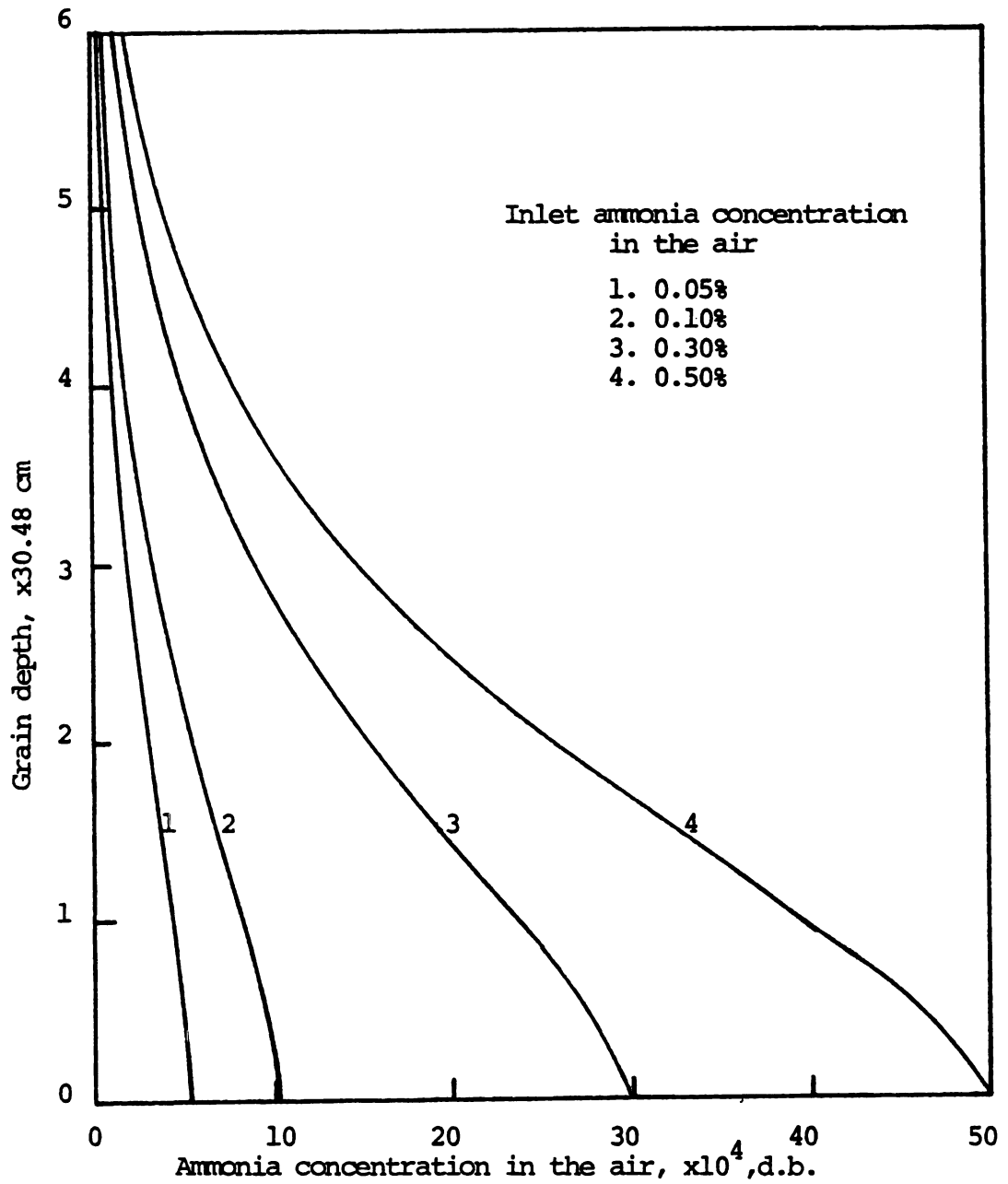


Figure 7.27. Ammonia concentration profile in the air at different inlet ammonia concentrations in the air after 3 hours of ammoniation.

of ammonia lost in the air is not significant after three hours of ammonia application even at an ammonia concentration in the inlet air of as high as 0.5 percent.

The comparison between the fraction of ammonia loss at different ammonia inlet levels in the exhaust air is presented in Figure 7.28 for different inlet ammonia levels. It is surprising to find that the relative concentrations (based on their corresponding inlet concentrations) of ammonia in the exhaust air are nearly independent of the applied ammonia concentrations. About half of the ammonia is lost in the air after eight hours of ammonia treatment at a constant inlet ammonia level. Despite the similarities of the relative amount of ammonia loss, the results in Figure 7.28 still imply that a larger (absolute) amount of ammonia is lost in the air at the higher inlet ammonia concentrations. The ammonia loss will increase as the ammonia-tion time increases. This is the reason why the inlet ammonia concentration should be maintained at a lower level in order to reduce the ammonia loss. Although a smaller inlet ammonia concentration has the advantages of reduced ammonia loss and an even distribution of ammonia during the early stages of ammoniation, the maximum level of free ammonia adsorption in the corn is limited by the ammonia concentration levels in the air. There exists a minimum inlet ammonia level in order to maintain a minimum level of free ammonia content in the corn to be able to effectively inhibit microbiological activities. The determination of a minimum level of inlet ammonia depends on the temperature, humidity, grain moisture content, and the physical condition of the grain.

The corresponding profiles of the free ammonia content for different ammonia inlet concentrations are compared in Figure 7.29 after

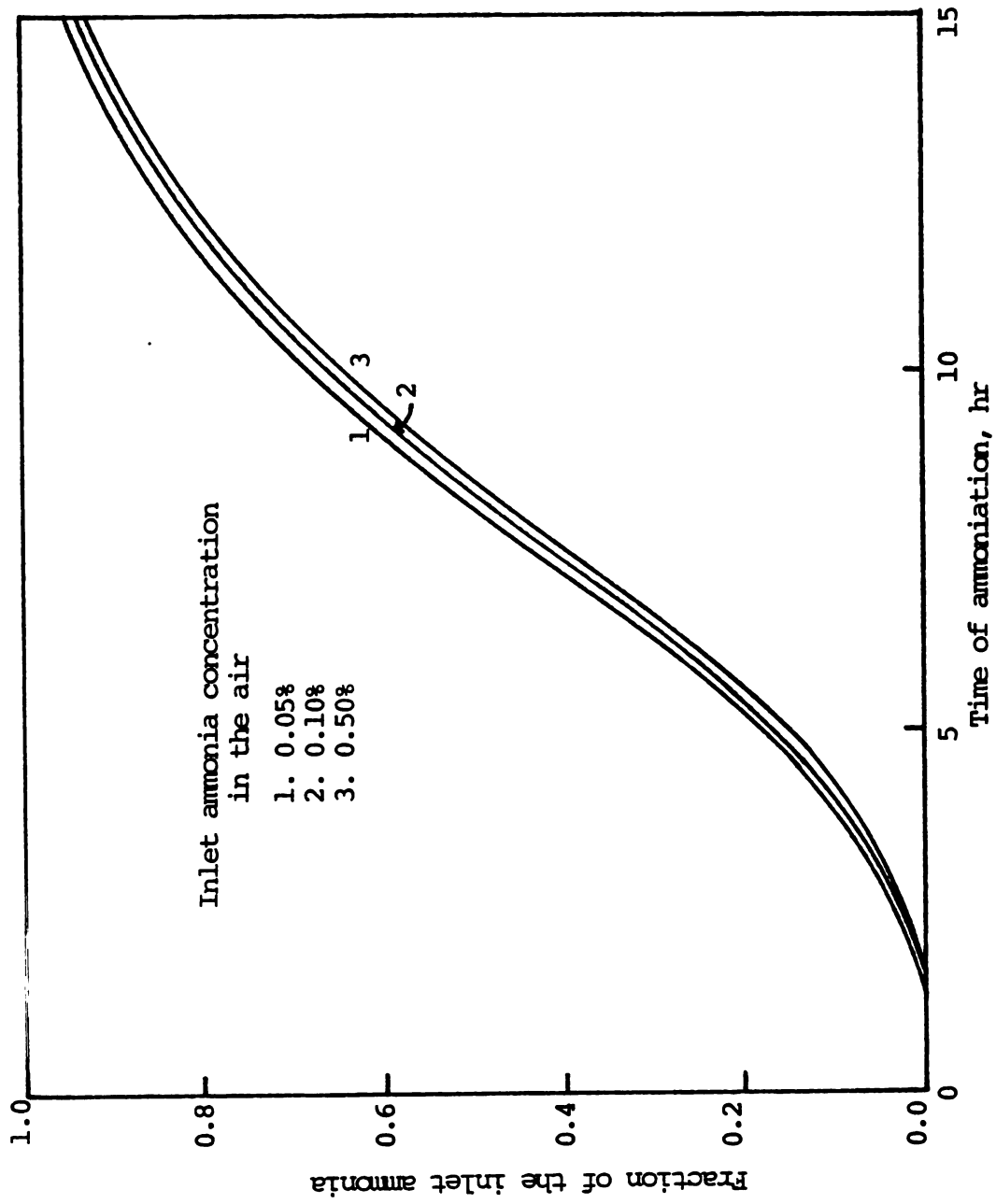


Figure 7.28. Fraction of ammonia lost in the exhaust air at different ammonia inlet levels.

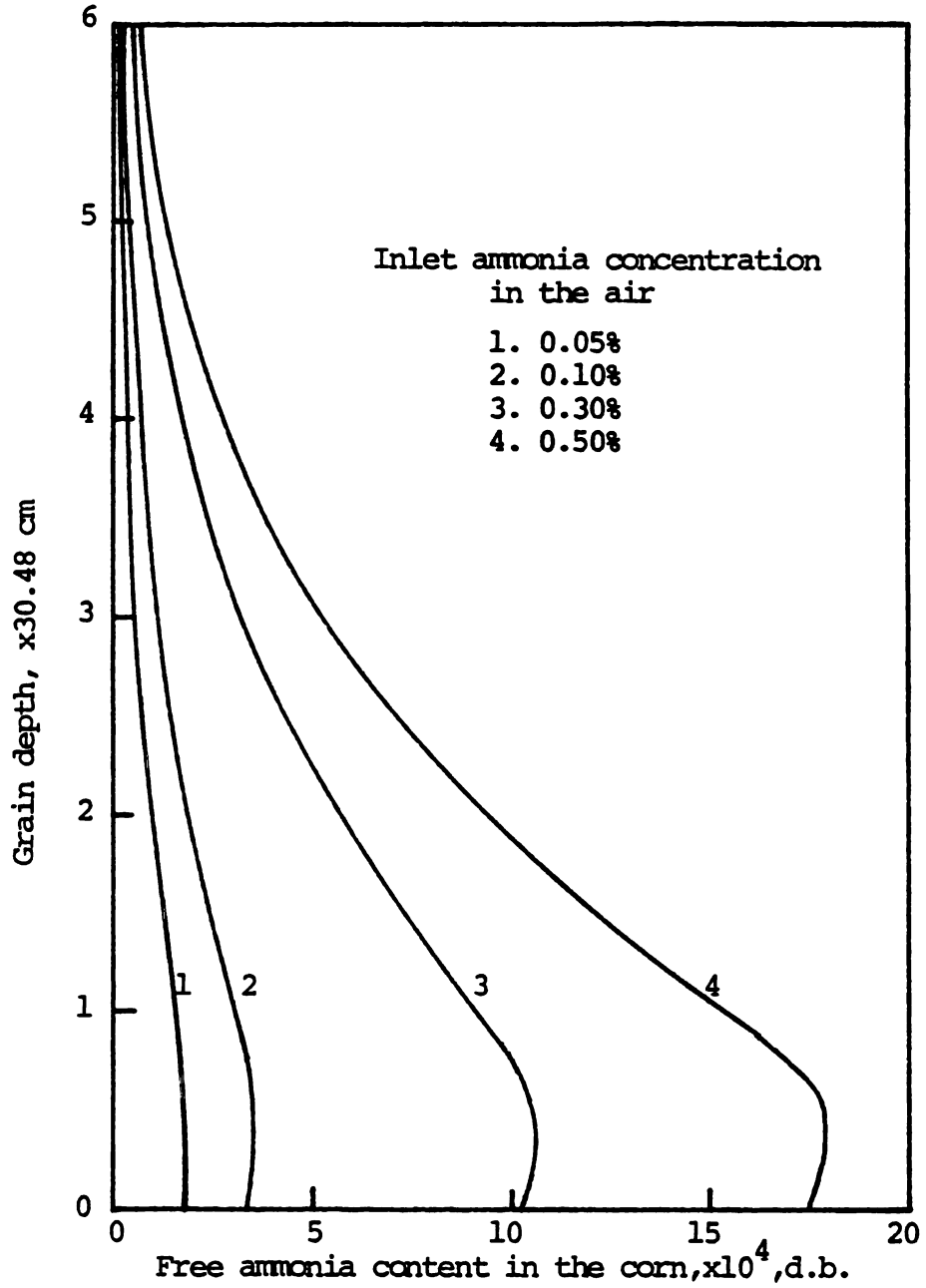


Figure 7.29. Free ammonia concentration profile in the corn at different inlet ammonia concentrations after 3 hours of ammoniation.

three hours of ammonia treatment. The shape of the curves resembles that of the ammonia concentration profiles in the air (Figure 7.27) except that the lower portion of the curves is slightly shifted in the direction of the higher concentration. The 0.5 percent concentration curves in Figure 7.29 indicate that even at 0.5 percent inlet ammonia concentration, the amount of adsorption heat released due to ammonia adsorption is still less than the latent heat loss due to the drying process and therefore the grain temperature decreases.

5-F. The Division Factor

The division factor in the simulation model was designed to overcome instability often encountered in numerical integration processes using finite difference methods. Unexpectedly, the instability did not occur throughout the entire tests.

The significance of using the division factor (NT) is shown in Figures 7.30 and 7.31. The following three computing schemes are compared: (1) $\Delta t = 0.1$ hour, $NT = 1$, (2) $\Delta t = 1.0$ hour, $NT = 10$, and (3) $\Delta t = 1.0$ hour, $NT = 1$.

The ammonia concentration profile in the air after two hours of ammoniation are compared in Figure 7.30 using the above NT values. Even though the division factor was only applied once in the computation at the first inside node and the first computing time increment, significantly different results are obtained. The computation using $\Delta t = 0.1$ hour gives a more accurate numerical result than a $\Delta t = 1.0$ hour.

The computing scheme using $\Delta t = 1.0$ hour and $NT = 10$ predicts a more accurate result at the lower portion of the bed (Figure 7.30) but not as good as using $\Delta t = 1.0$ hour and $NT = 1$ at the upper levels. The improvement in the computational accuracy closer to the bed bottom

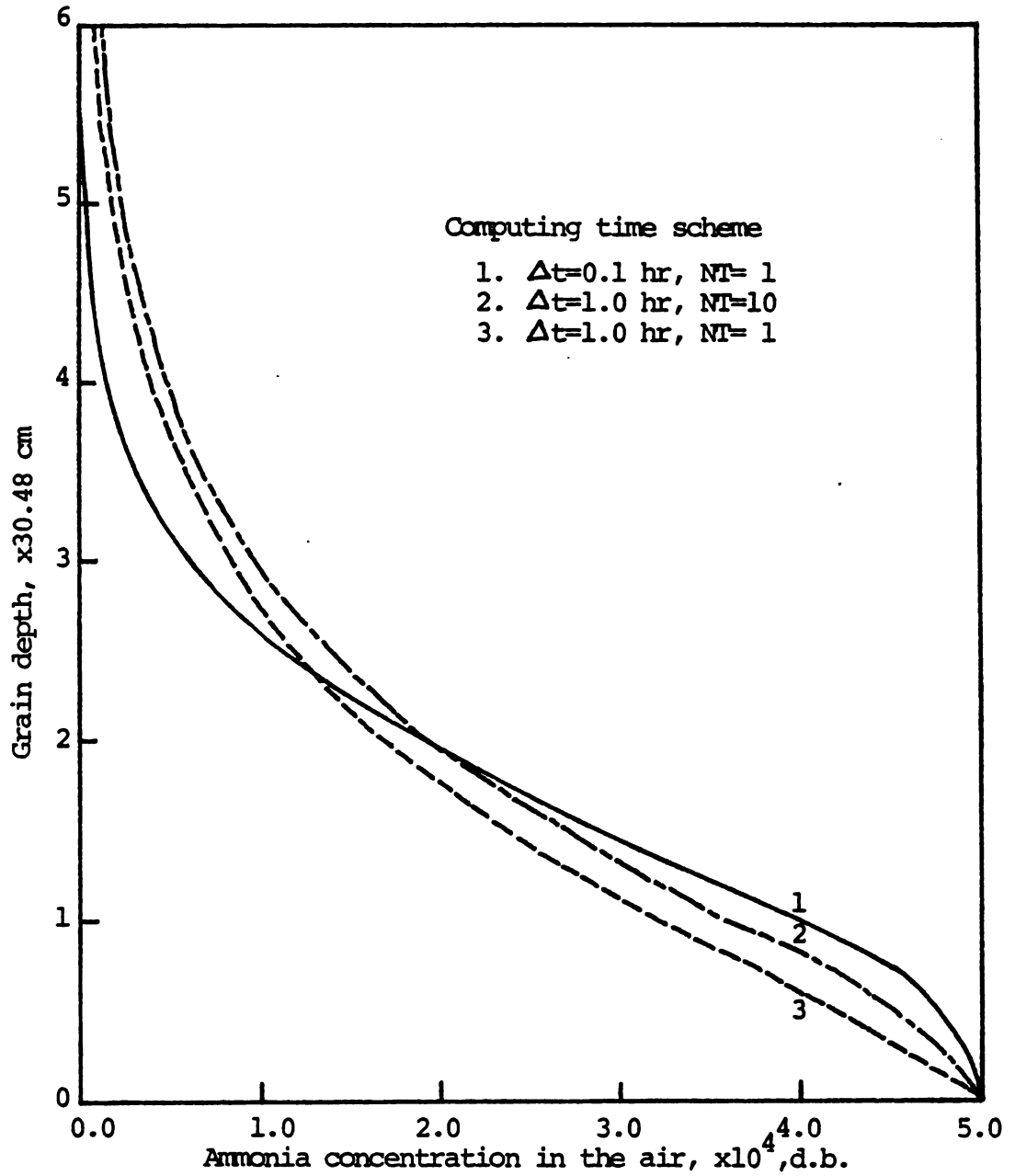


Figure 7.30. Ammonia concentration profile in the air using different computing schemes after 2 hours of ammoniation.

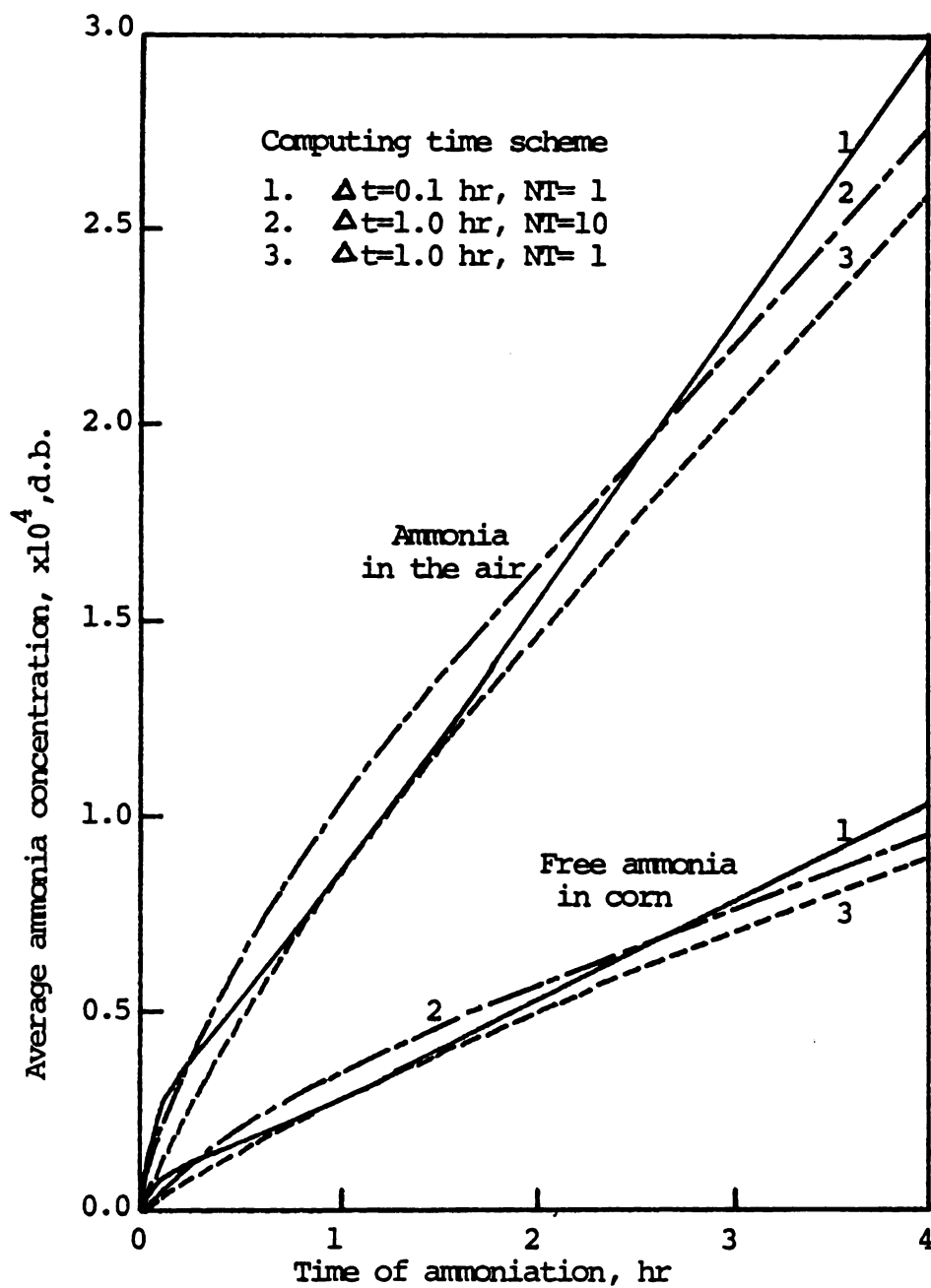


Figure 7.31. Average ammonia concentrations in the air and in the corn using different computing schemes.

is expected since that is where the division factor functions.

The results of the average ammonia concentration in the air and in the corn (Figure 7.31) show the same trend in improving the accuracy close to the bed bottom for the computation using $NT = 10$. After the first hour of computation, the division factor is no longer operative and the second and third computing schemes using $\Delta t = 1.0$ hr predict parallel results. Nevertheless, the residual effect of the division factor indicates a slightly better accuracy at a value of $NT = 10$ at prolonged treatment. Both results using the second and third computing schemes are farther apart from the results using $\Delta t = 0.1$ hour after four hours of ammoniation.

6. Experimental Verification of the Ammonia Sorption and Drying Model

The experimental results presented in this section were obtained from the bin tests performed at Michigan State University.

The tests were designed to verify the simulation model as well as to gain practical ammonia-assisted ambient air grain drying experience. The sampling frequency was limited due to the long-time nature of the test and the lack of sufficient manpower to perform the necessary chemical analyses regularly as would have been desired.

6-A. The Ammonia Concentration in the Air during Adsorption

Once the ammonia treatment has been started, the residuals built up in the corn. The residuals are assumed to be a permanent part of the ammonia-treated corn. Further aeration can only remove the free ammonia in the corn and the ammonia in the void spaces. The major concern in this part of the experiment was the change of the ammonia concentration in the air.

Before the adsorption test began, the corn was aerated with ammonia-free ambient air for about three days. The purpose of this process was to make sure that there was no free ammonia within the system. Each air sampling period lasted 10 minutes; a set of six samples from six levels in the bin was taken at the same time as described in Chapter 5. The samples were taken continuously for about two hours. The measured average ammonia concentration values in the air are shown in Figure 7.32 along with the simulation model results predicted by the simulation model.

The predicted curves were generated by defining the initial conditions as the experimentally measured conditions at the start of the ammonia treatment. The measured initial conditions include the grain moisture content and the temperature.

The predicted results in Figure 7.32 are found to have satisfactory correlation with the experiment results. The correlation coefficient between the experimental and the predicted results is 0.918. The model predicts lower values in the early stages of the test but higher values after about one hour of ammoniation. The reason for this deviation can be explained by either of the following factors or their combined effect: (1) an incorrect value of the mass transfer coefficient, (2) the error in the measurement of the airflow rate and the deviation of the airflow from ideal plug-type in the actual bin system, and (3) the error in the prediction of the grain and air temperatures. The results in Figure 7.26 imply that a curve with a smaller slope can be obtained by using a smaller mass transfer coefficient which would have reduced the prediction errors. The airflow deviates somewhat from the ideal plug-type. In addition, the uneven distribution of ammonia at the same depth level will create significant errors in the experimentally determined ammonia

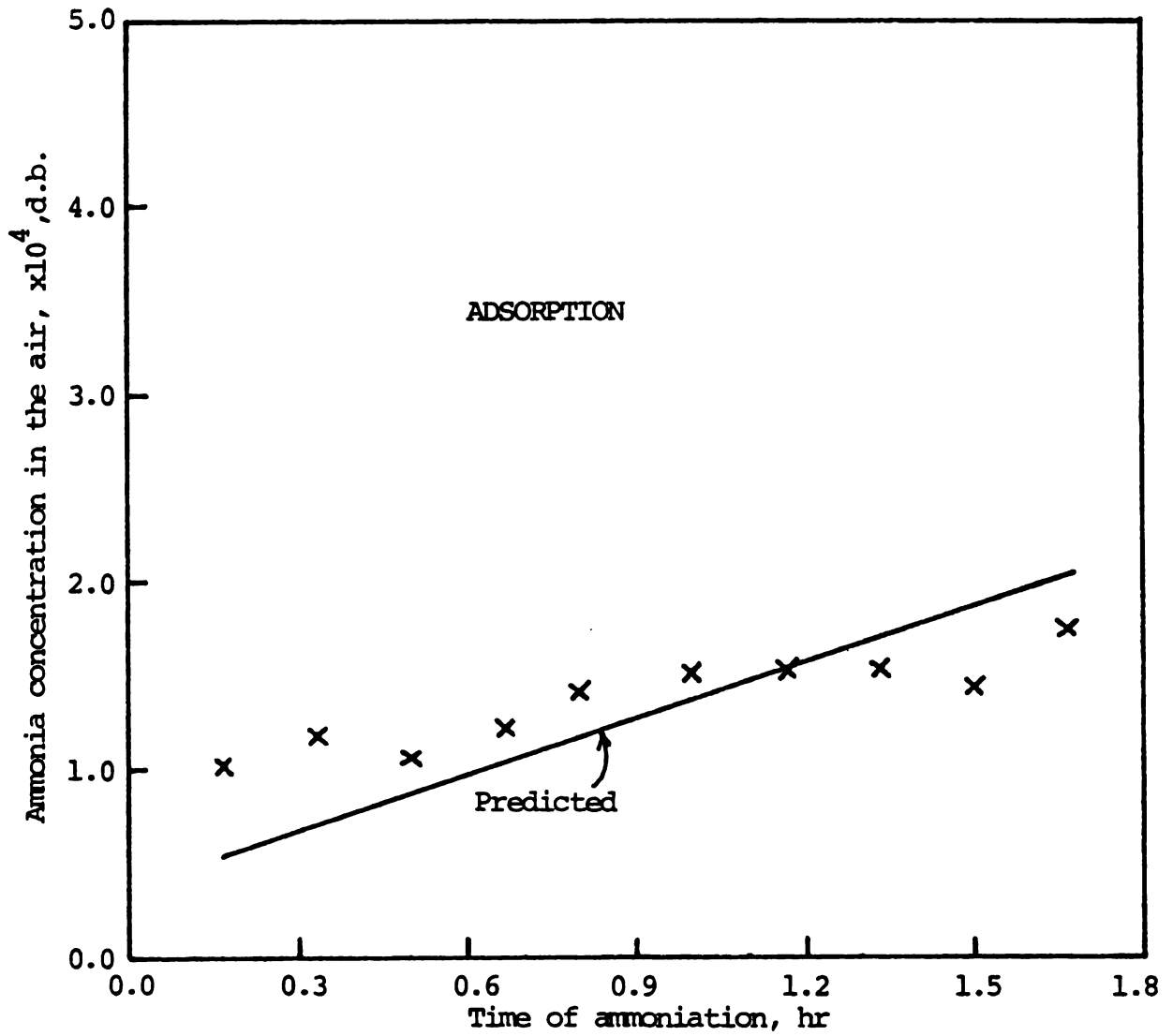


Figure 7.32. Comparison of the predicted and the experimental values of the ammonia concentration in the air in the ammonia adsorption test.

concentrations. The error in the prediction of the grain temperatures is less significant since the ammoniation tests lasted less than two hours during which the temperature fluctuations were small.

The comparison between the experimental concentration profiles in the air and the predicted profiles is presented in Figure 7.33. Even though the experimental results for the concentration profiles at a specific ammoniation time do not form a smooth curve, the relative positions of the measured results agree reasonably well with the predicted results throughout the entire bed. The measured ammonia concentrations in the air at a specific bed level, in general, increase with time within the prediction range.

6-B. The Ammonia Concentration in the Air during Desorption

The desorption tests are similar to the adsorption tests except for the initial and inlet conditions. The entire grain sample in the bin was treated with a constant ammonia flow for an extended period of time (about two days) to guarantee an ammonia-corn equilibrium condition before the desorption tests began. The profiles of grain temperature, moisture content, and free ammonia content at the start of the ammonia desorption tests are shown in Figure 7.34. The ammonia concentration in the air was 0.0475 percent throughout the bed before the tests started. The initial free ammonia concentration at the different bin levels is different even in equilibrium with a constant ammonia concentration in the air. The difference is attributed to the variations in the grain moisture content and temperature. The inlet air was the ambient air free of ammonia.

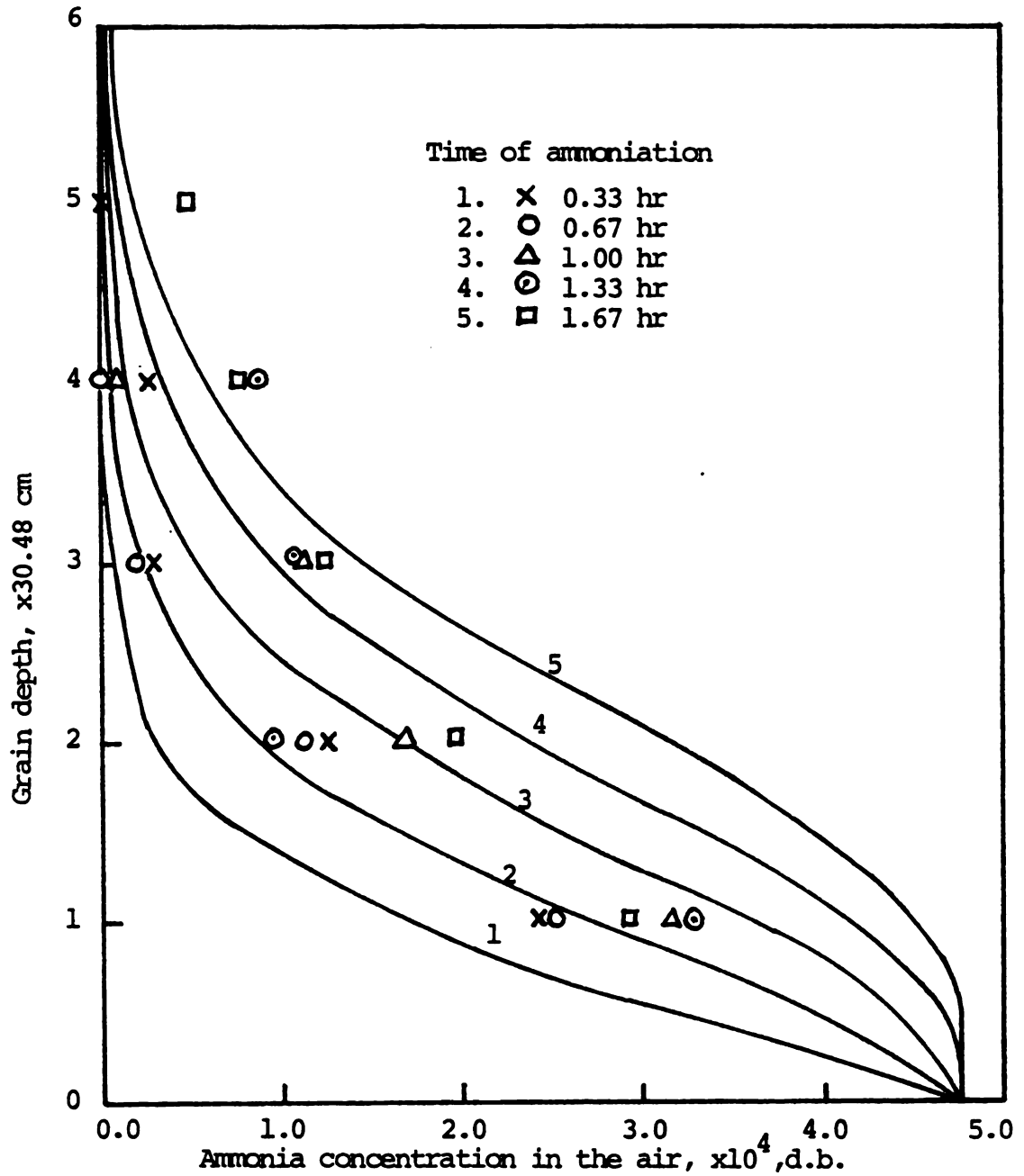


Figure 7.33. Comparison of the predicted and the experimental ammonia concentration profile in the air in the ammonia adsorption test.

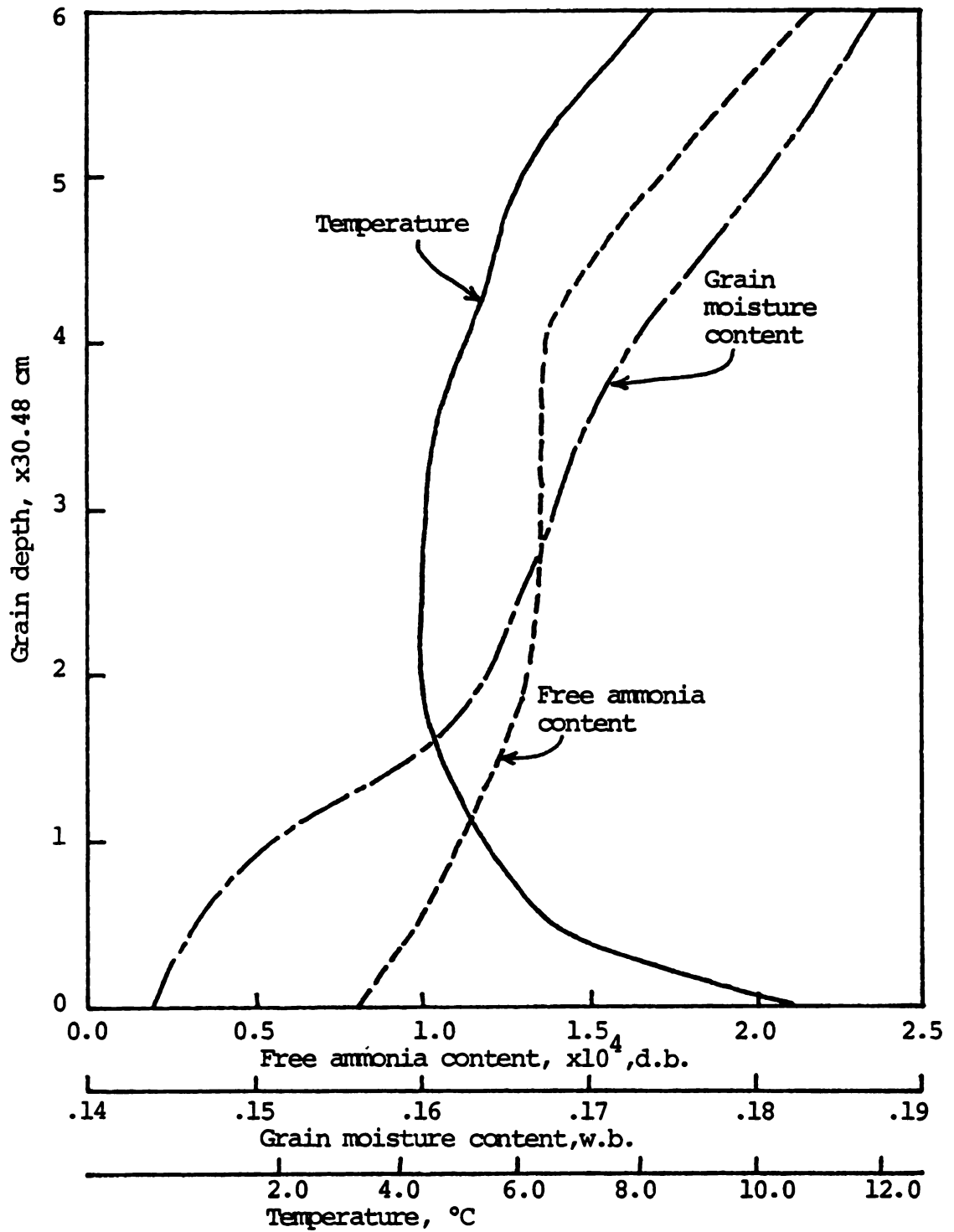


Figure 7.34. The measured grain temperature, moisture content and free ammonia content at the start of the ammonia desorption test.

The experimental results of the desorption test are compared with the predicted values in Figure 7.35. The model predicts the average ammonia concentrations with reasonable accuracy. The deviation between the predicted and experimental results can be explained by the same reasoning as for the adsorption process. The correlation coefficient is 0.782.

Most of the experimentally determined desorption concentration values fall within the neighborhood of the predicted values as shown in Figure 7.36. The experimental results after one hour of desorption are closer to the predicted results than those at earlier times.

Despite the deviation of experimental results from the predicted values, it is encouraging to have such a close comparison between the experimental results with the "ideal" model with so many assumptions and necessary guesses of some unknown parameters such as the mass transfer rate, heat of adsorption, ammonia sorption isotherm, and the amount of residuals.

6-C. Comparison of the Experimental and Predicted Ammonia Concentration Profiles

The experimental results which are compared with the predicted results were obtained from the second part of the experiment -- the constant ammonia application rate (0.0475 percent ammonia) period. The grain and air sample were obtained at most of the test period. The selected experimental results were taken at the following times: 10, 22, 140, 161, 242, and 262 hours. The total test period in the second part of the experiment was 384 hours; the ammonia application was ended at the 264th hour.

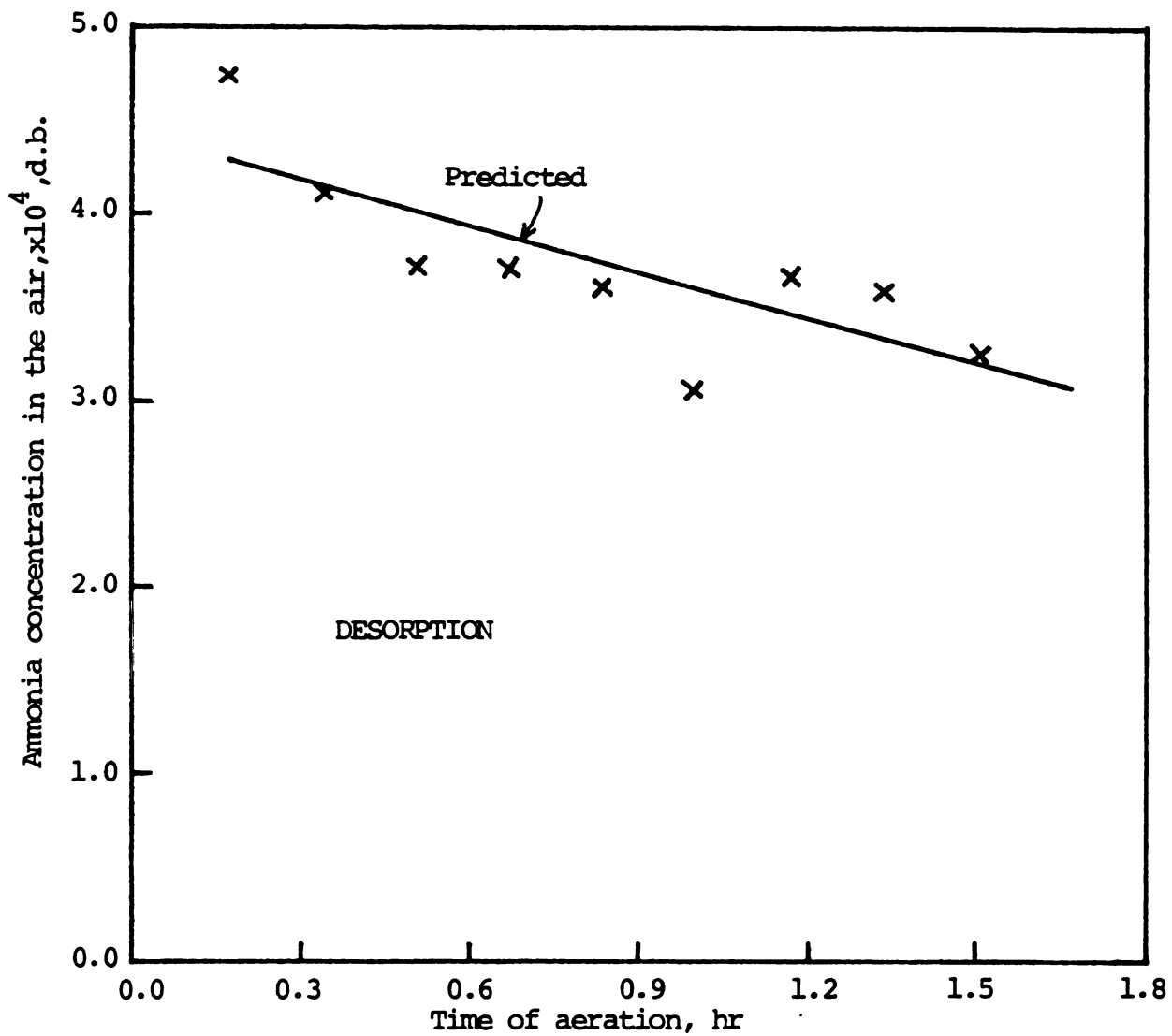


Figure 7.35. Comparison of the predicted and the experimental values of the ammonia concentration in the air in the ammonia desorption test.

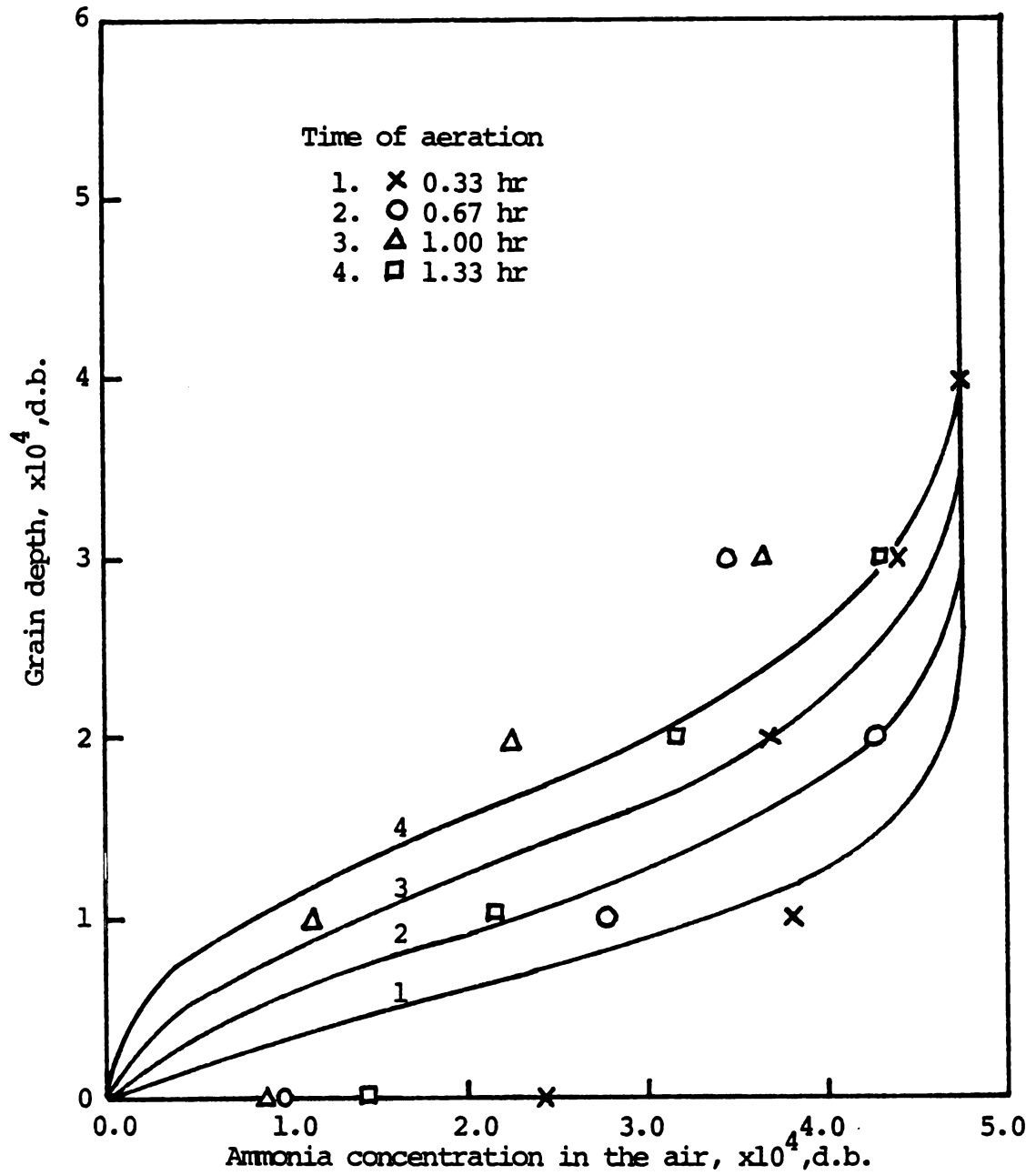


Figure 7.36. Comparison of the predicted and the experimental values of the ammonia concentration profile in the air in the ammonia desorption test.

The measured ammonia concentration in the air, the total ammonia content and the free ammonia content in corn were compared with the predicted results. The ammonia was applied four hours after the fan had started to stabilize the grain temperature with the ambient air. At the 10th hour (Figure 7.37), the corn had been treated with ammonia continuously for six hours. The predicted ammonia concentration profiles had not yet completely broken through as indicated by the unsaturation of ammonia in the air at grain levels higher than one meter. The experimental results of the ammonia concentration in the air are lower than the predicted values at the tenth hour. Although the prediction model accepts variations in the inlet conditions at any input time interval, the prediction of ammonia contents in the corn is complicated by the constant varying inlet ambient air temperatures and humidities as indicated in Figure 5.4.

The corn had been treated with a constant inlet ammonia concentration continuously for 18 hours in the samples taken at the 22nd hour (Figure 7.38). The air in the bin was predicted to be completely saturated with ammonia at the inlet concentration level. However, the experimental results are lower. Furthermore, the model predicts higher ammonia concentrations in the corn at higher levels in the grain bed due to higher moisture contents and lower grain temperatures. The experimental results showed a similar trend in that region. The changes of grain temperatures lag behind the inlet air temperature which was constantly changing. The density of the corn is much greater than that for the air. At higher levels of the grain bin, the time lag is even greater.

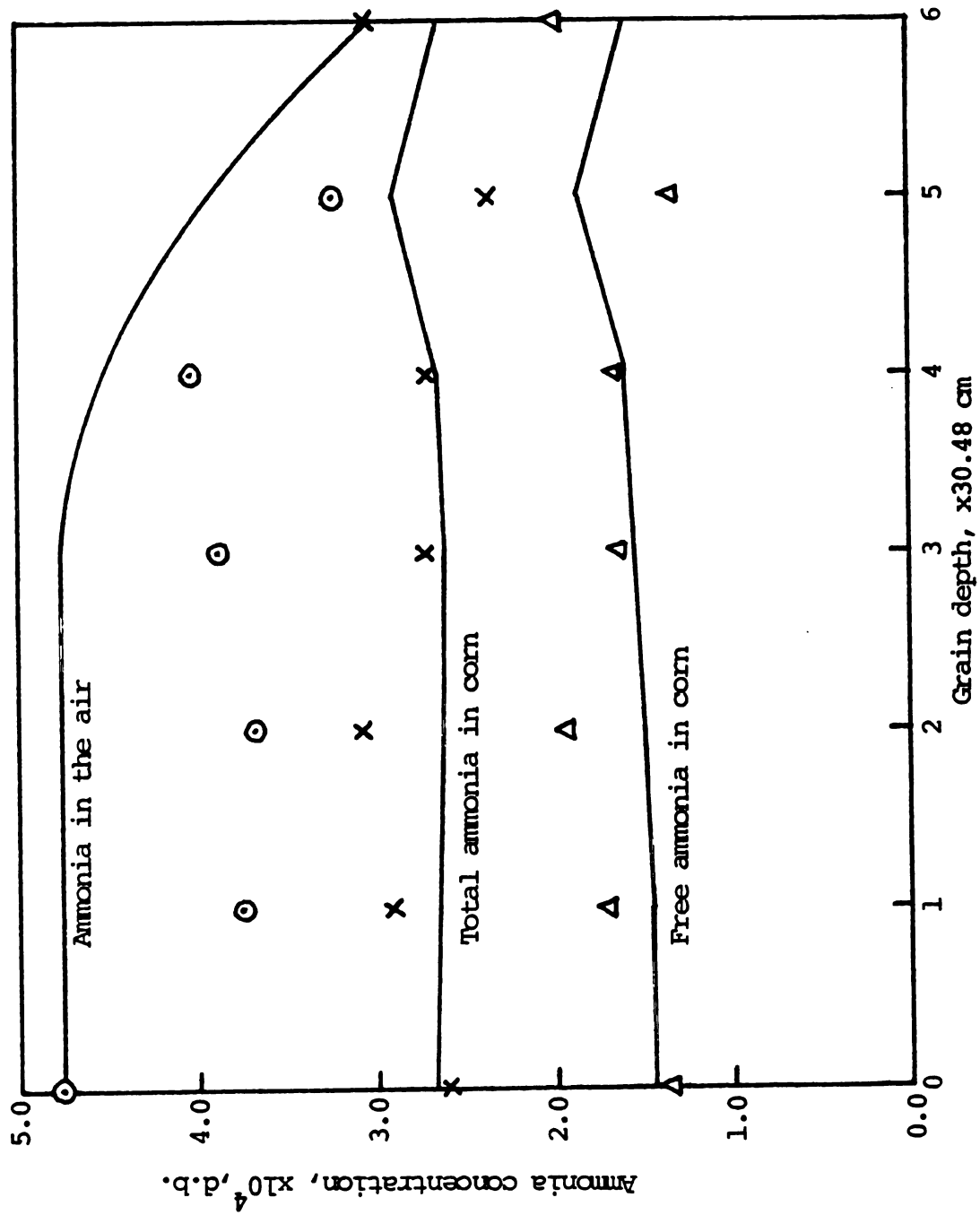


Figure 7.37. Comparison of the predicted and the experimental values of ammonia concentrations at the 10th hour in the second part of experiment.

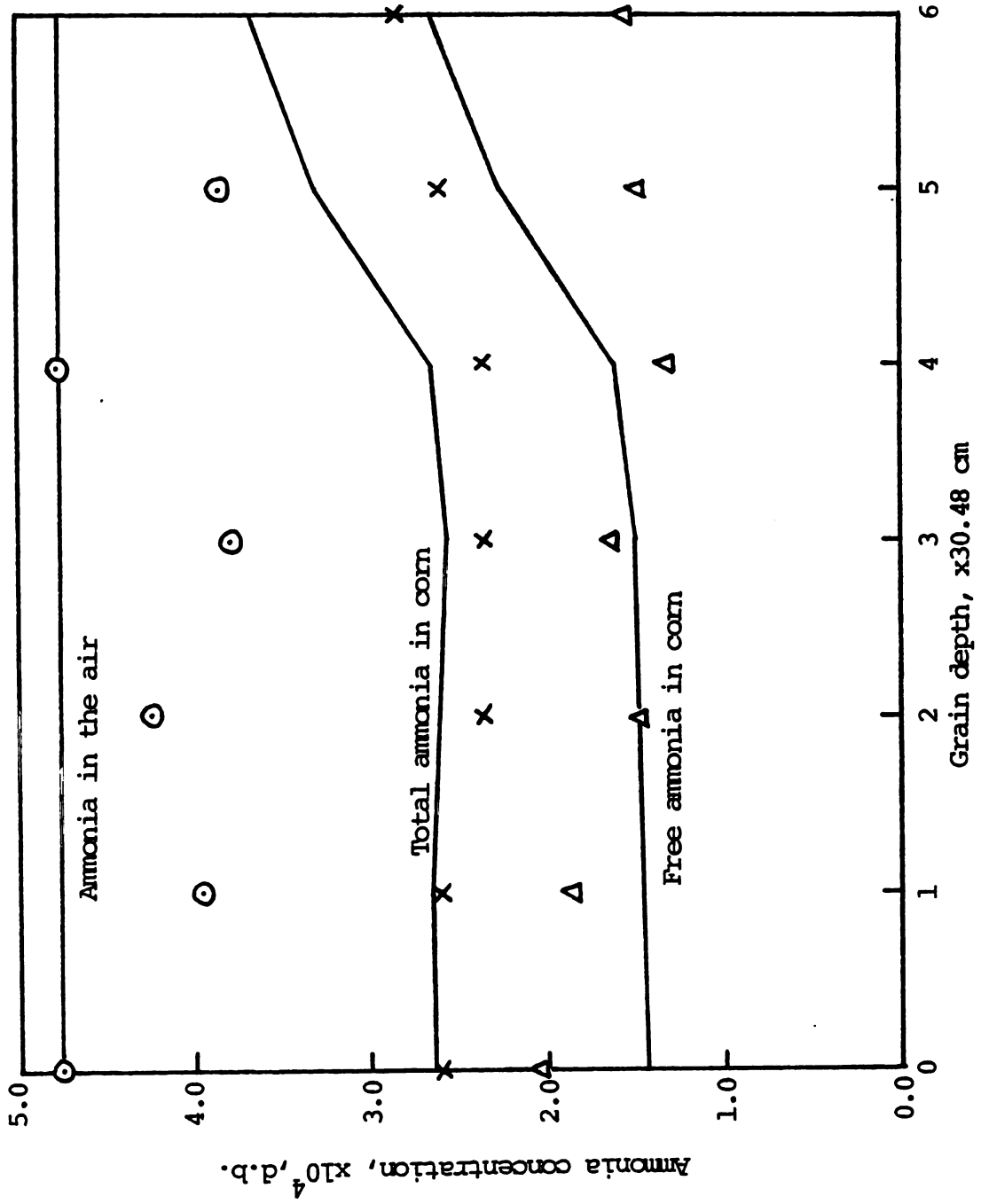


Figure 7.38. Comparison of the predicted and the experimental values of ammonia concentrations at the 22nd hour in the second part of experiment.

At the 140th hour, the grain had been treated with ammonia continuously for 27 hours (Figure 7.39) as shown in Figure 5.6. The ammonia concentrations in the corn were lower than those at the 22nd hour due to the higher ambient air temperatures and, consequently, the higher grain temperatures.

The ammonia concentrations were found to be consistently higher at higher levels in the grain than at the lower portions. This is due to the higher moisture contents at higher levels. Good agreement was observed between the experimental and predicted results at the 161st hour of treatment (Figure 7.40) which is at the end of the second ammonia injection period after 48 hours of ammonia treatment at a constant inlet ammonia concentration. Air samples were not taken at the 161st hour.

The results in Figure 7.41 show the same degree of agreement as the previous sample at the 242nd hour which is after 24 hours of ammoniation in the third ammonia injection period as indicated in Figure 5.6. The last ammonia samples were analyzed at the 262nd hour (Figure 7.42), 44 hours after the ammoniation at constant inlet ammonia level in the third ammonia injection period. Better agreement between the experimental and predicted results were found for the ammonia concentrations in the air at the 262nd hour than for the samples at the other times. However, the experimental results of ammonia concentrations in the corn failed to show higher concentrations at higher levels in the grain as did the predicted results.

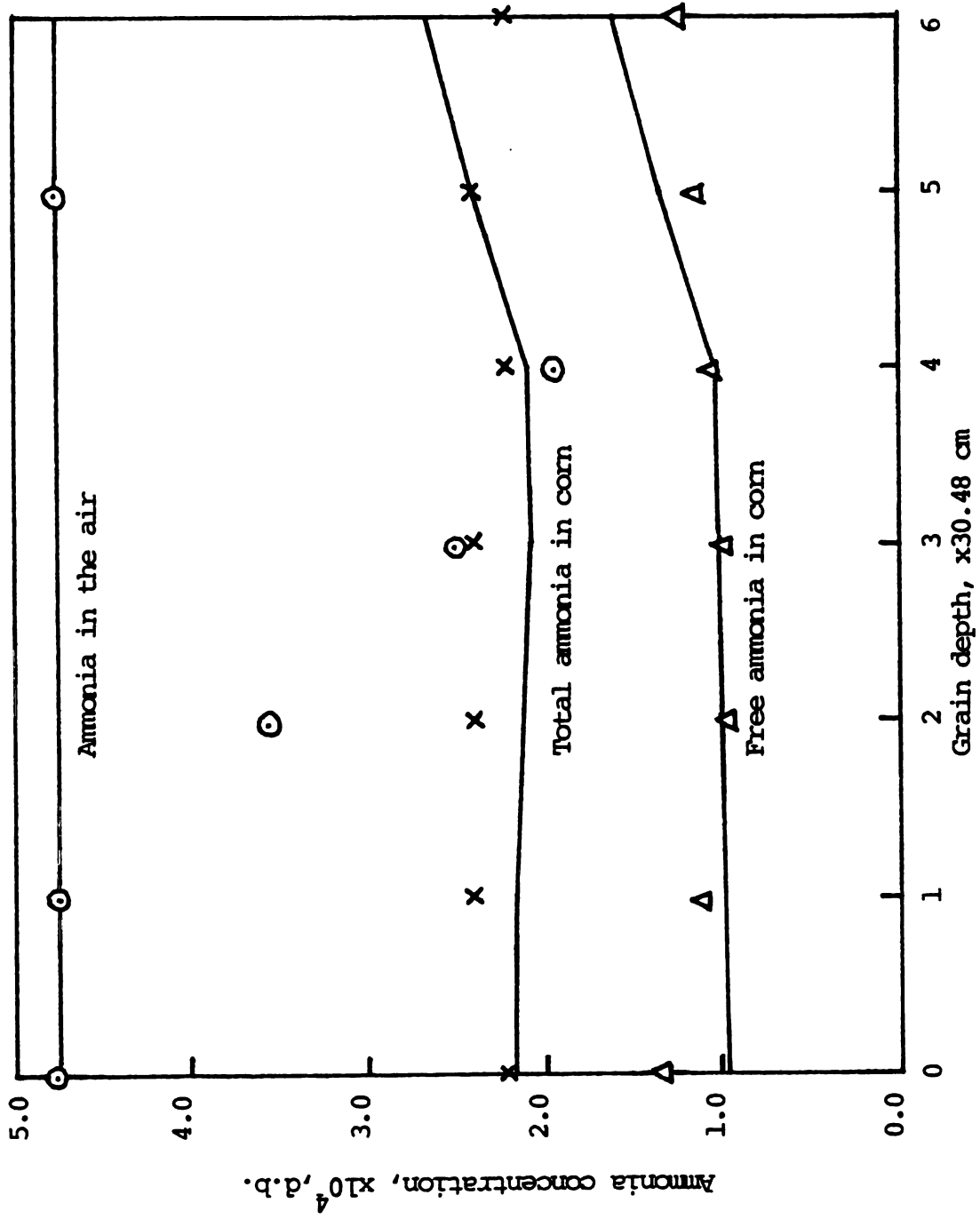


Figure 7.39. Comparison of the predicted and the experimental values of ammonia concentrations at the 140th hour in the second part of experiment.

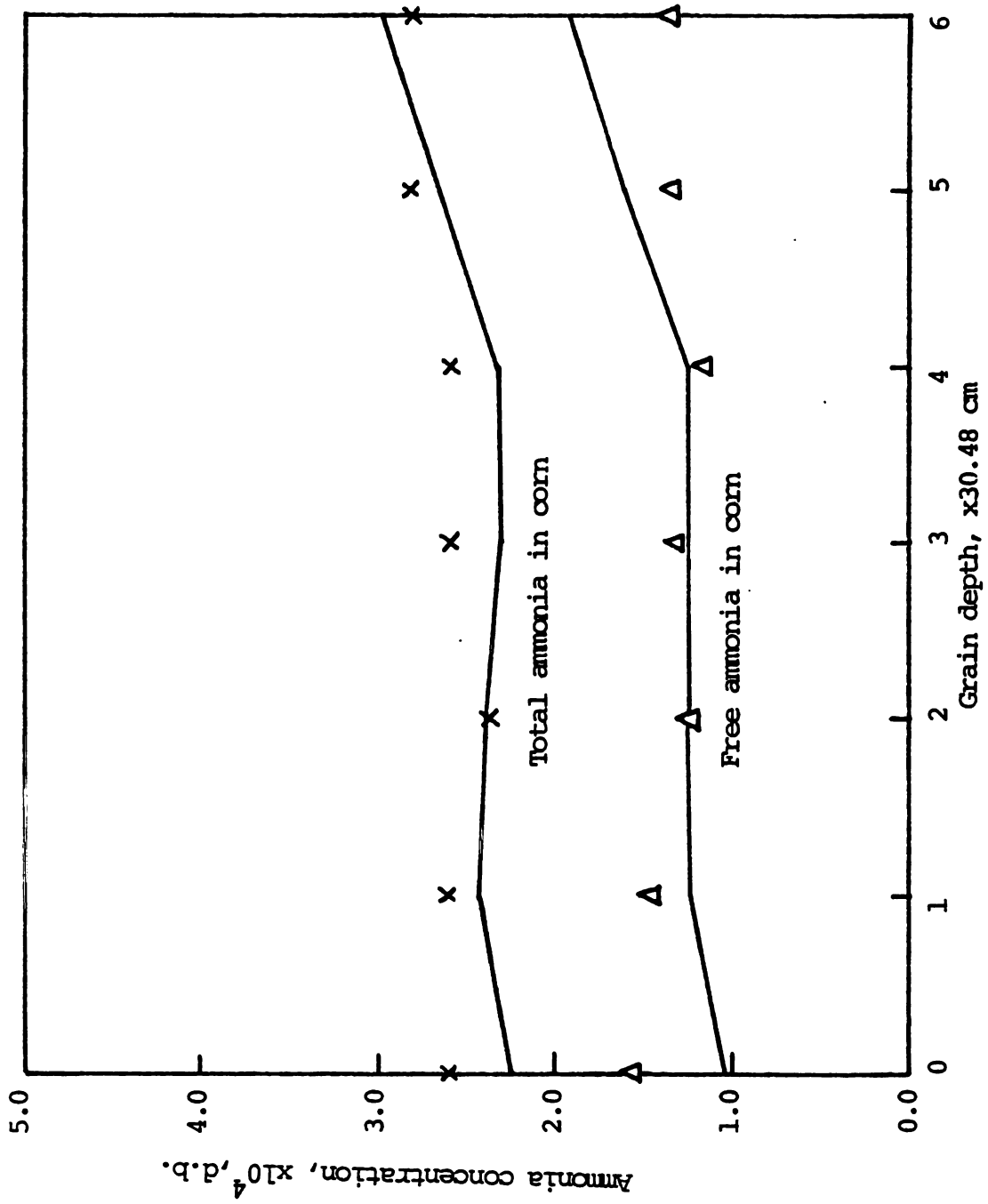


Figure 7.40. Comparison of the predicted and the experimental values of ammonia concentrations at the 16th hour in the second part of experiment.

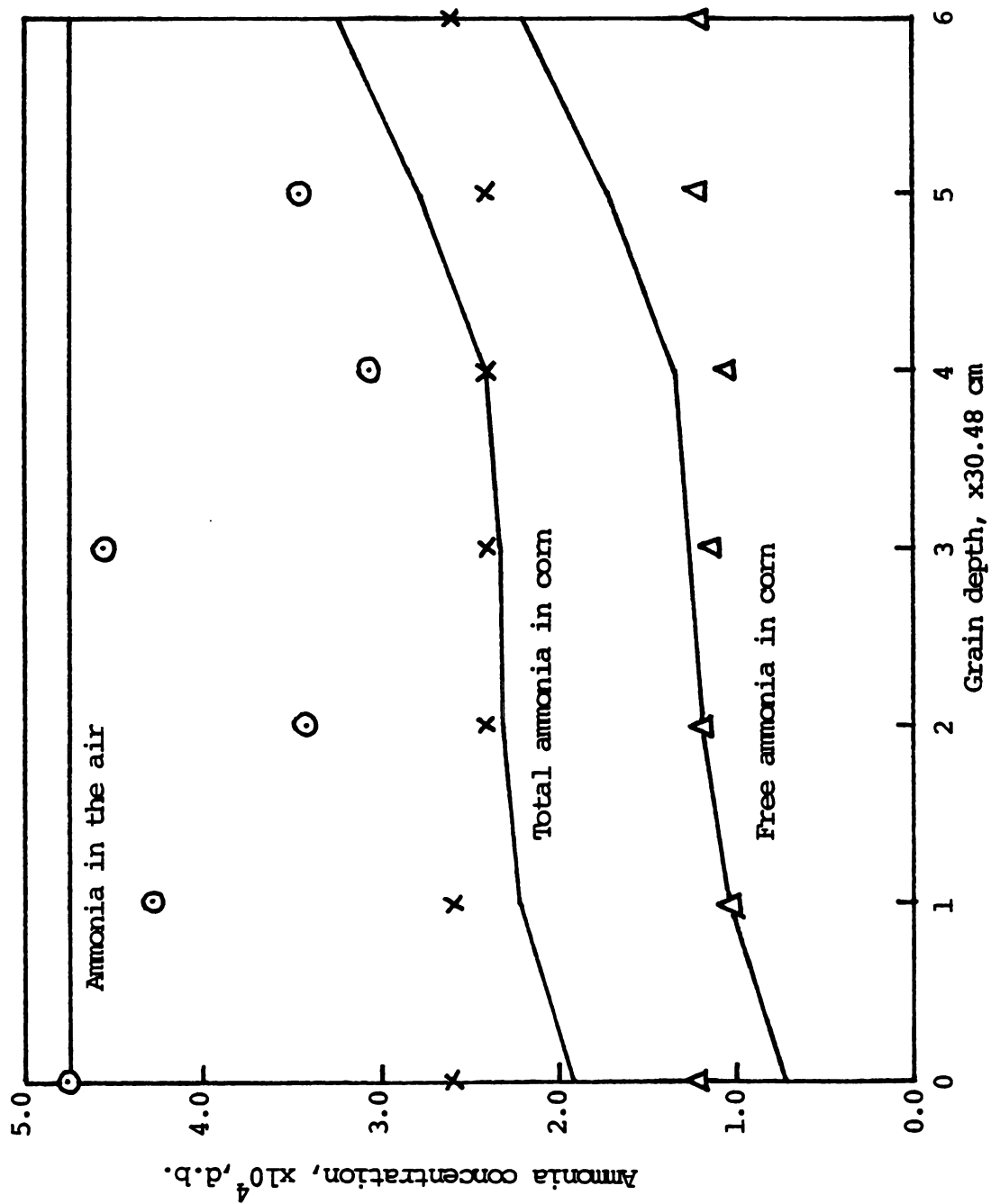


Figure 7.41. Comparison of the predicted and the experimental values of ammonia concentrations at the 242nd hour in the second part of experiment.

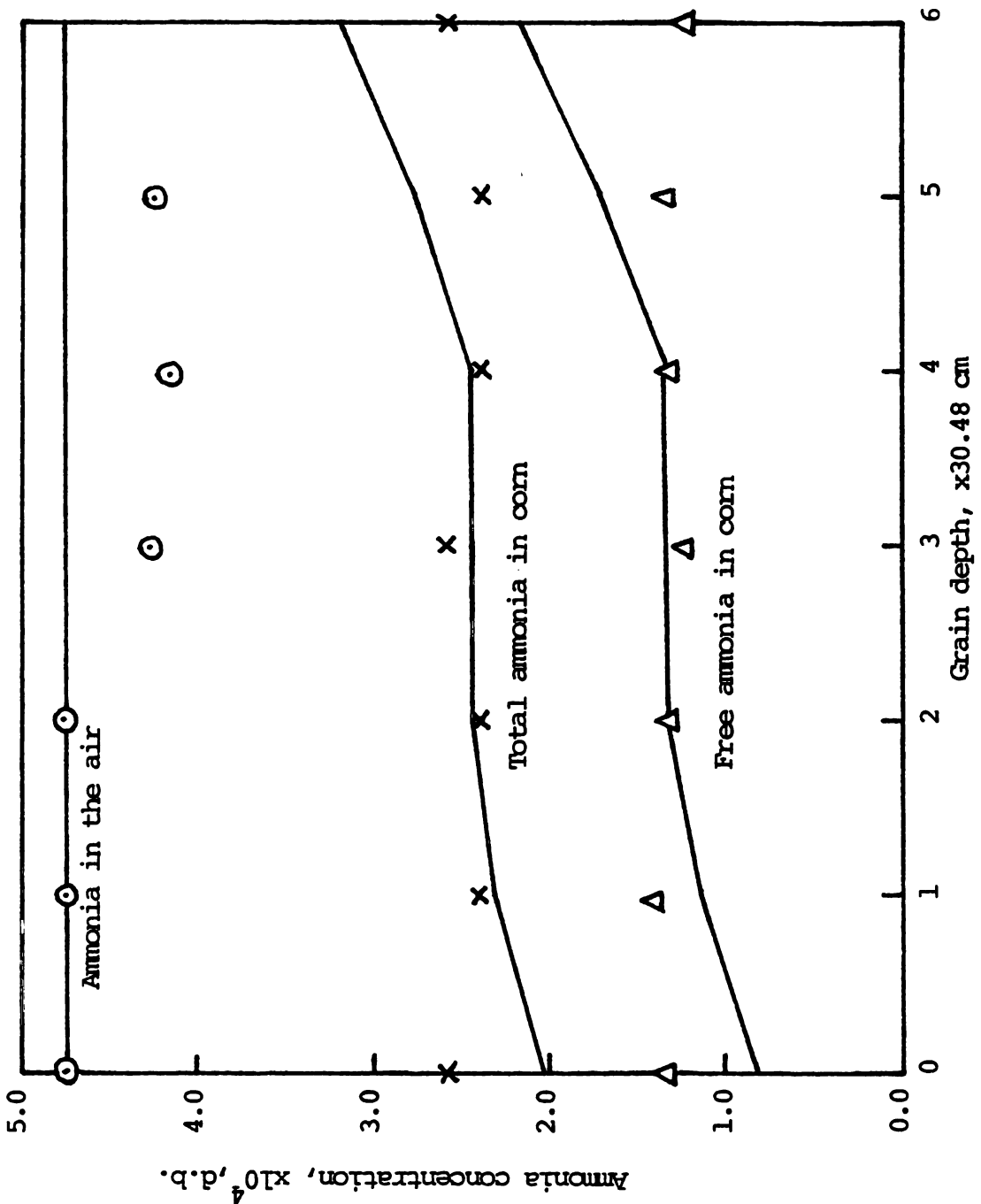


Figure 7.42. Comparison of the predicted and the experimental values of ammonia concentrations at the 262nd hour in the second part of experiment.

6-D. Comparison of the Experimental and Predicted Grain Moisture Contents and Temperatures

Even though the prediction of the ammonia concentrations is the major concern in the ammonia sorption and drying model, the simulation model also predicts the grain moisture content and the temperature. The reason for the emphasis on the prediction of ammonia concentrations in this investigation is that the simulation of the chemical preservation process in a fixed-bed grain drying system is a new research area. Fixed-bed grain drying models have been developed, tested, and modified by various researchers (Roth and Bakker-Arkema, 1977, and Rugumayo, 1979). The addition of the ammonia sorption process to the fixed-bed grain drying model necessitated major modifications in the fixed-bed grain drying model developed by Roth and Bakker-Arkema (1977).

The ammonia drying model not only describes the ammonia sorption behavior but also predicts the grain temperature and moisture content as influenced by the ammonia sorption process. The verification of the ammonia sorption characteristics has been presented in the previous sections. This section will cover the verification of the predicted grain moisture content and temperature.

The ammonia grain drying experiment lasted for 1744 hours. The experimental values of the grain temperature and moisture content of the ammonia preservation and drying test were compared at different bin levels with the predicted results at the following times: 13, 392, 1447, and 1744 hours after the start of the experiment.

The initial grain moisture content was 25.61 percent w.b. At the 13th hour of the experiment, there was little drying in the grain and only the portion of the grain near the bottom of the bin was predicted

to have lost some moisture as shown in Figure 7.43. The thermocouple readings of the temperature actually read the air temperatures in the void spaces. The grain temperature was assumed to be the same as the air temperature. With varying inlet air temperatures, this assumption might be partially responsible for the error in the prediction of grain temperatures as compared to the experimental results.

Only the latent heat and sensible heat changes are taken into account in the formulation of the temperature equations (Equations 6.14 and 6.16). In addition, the heat generation due to the dry matter degradation, and the respiration of grain and of the microorganisms may attribute the temperature increase. Still the maximum deviation of the predicted results from the experimental results was less than 3°C as shown in Figure 7.43.

After 392 hours of ambient air drying (Figure 7.44), the upper 2/3 of the grain still stayed at the initial moisture content. The grain was drier as it was closer to the bin bottom in the lower 1/3 portion of the grain. The predicted grain moisture contents are in good agreement with the experimental results. The simulation model predict higher temperatures in most of the grain bin. The shape of the temperature profile reflects the variations of the inlet air conditions. Theoretically, the inlet air reaches the top of the bin in less than 30 seconds at an airflow rate of 1.43 m/min in a 1.83 m-high bin of corn with 38 percent void spaces. The density of corn is approximately 580 times greater than that of the air while the specific heat of the air (0.242 cal/g°C) is about the same as that for the corn (0.268 cal/g°C). In the case of using an infinite heat transfer coefficient, the temperature variation in the corn at different levels

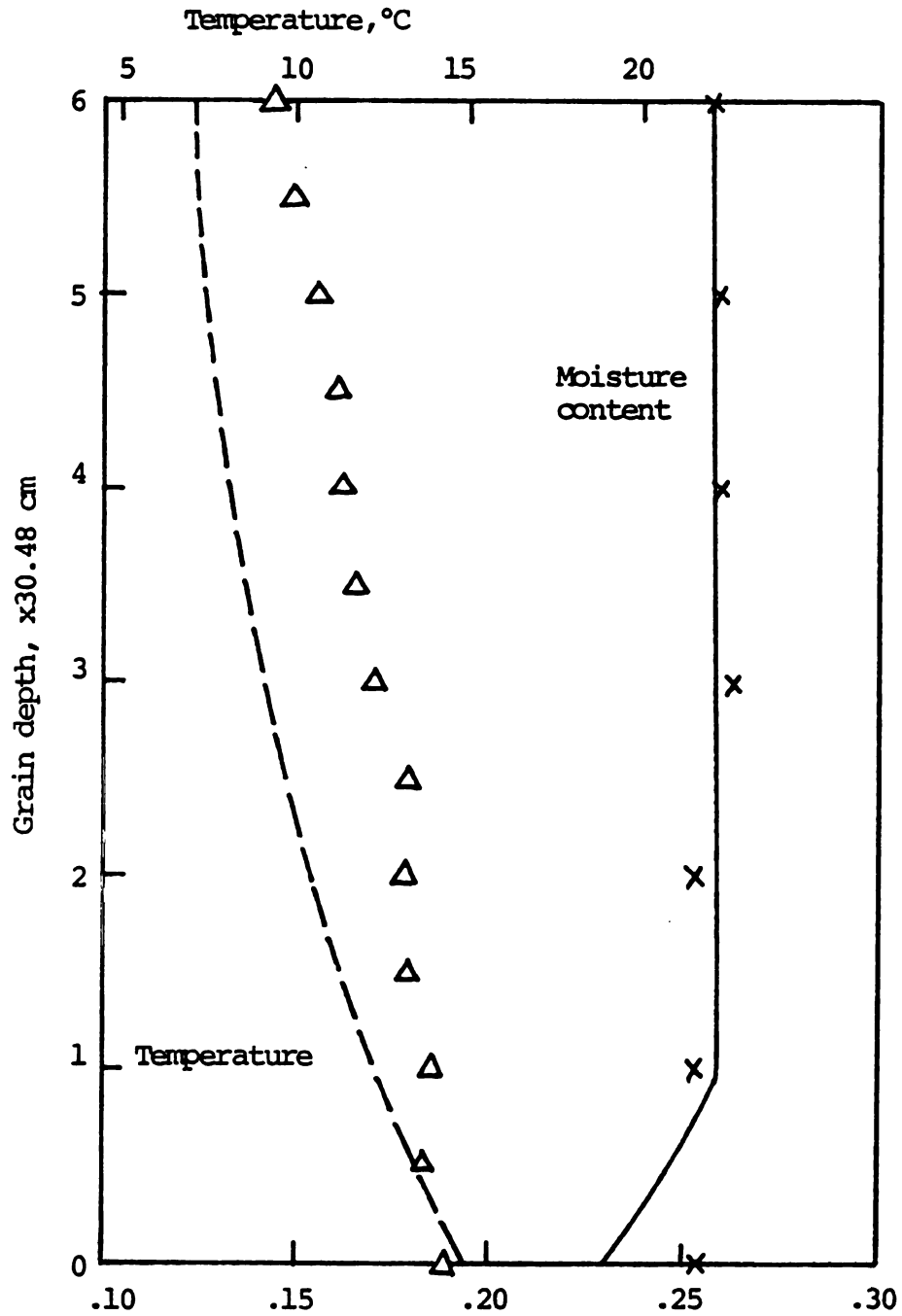


Figure 7.43. Comparison of the predicted and the experimental values of the grain moisture content and temperature at the 13th hour of experiment.

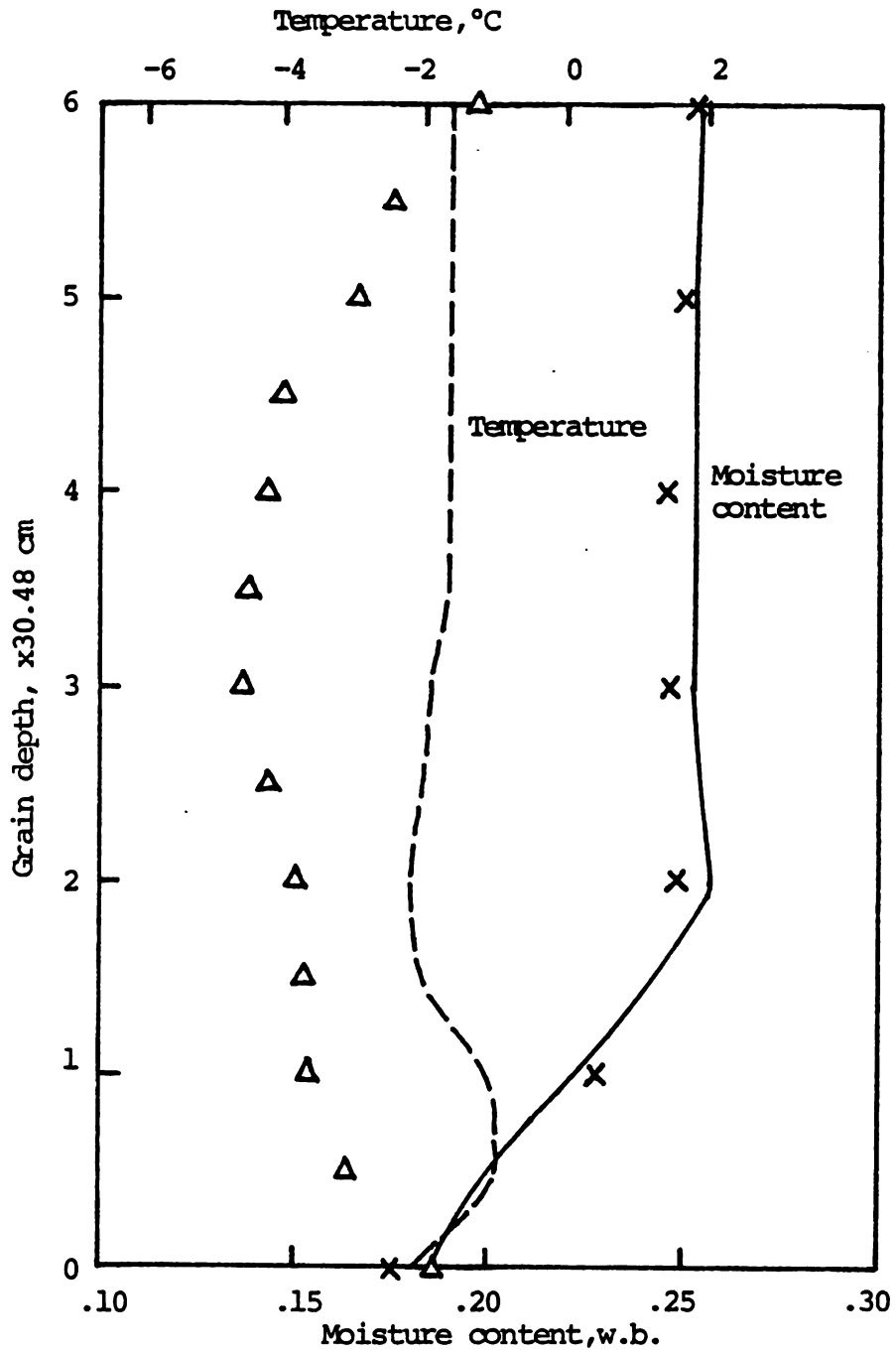


Figure 7.44. Comparison of the predicted and the experimental values of the grain moisture content and temperature at the 392nd hour of experiment.

will follow the air temperature change at a speed of $1/600$ of that in the air. In other words, it would take five hours for the grain to reach the same temperature as the inlet air of 1.43 m/min is used and the temperature change due to mass transfer is neglected.

The results of the above two samples were taken during the first part of the experiment which lasted 1360 hours. The wet grain was kept in the bin throughout the winter without aeration due to the severe cold which lasted about three months.

The drying front had traveled to about $1/3$ from the bin top at the 1447th hour of the experiment (Figure 7.45). The model predicts the grain moisture contents accurately except at the top level. The temperatures throughout the bin were nearly constant and good correlation was found between the experimental and predicted results in Figure 7.45.

The last set of samples for the grain moisture determination was taken at the end of the experiment after 1744 hours fan operation (Figure 7.46). The model predicts higher moisture contents and lower temperatures than the experimental results throughout the entire grain bed. The desirable final average grain moisture content was 15.5 percent w.b. Both the experimental and the predicted results showed some over-drying near the bottom of the bin. The model predicts higher moisture contents at positions close to the bin top than the experimental values.

A second drying front is predicted at an equilibrium moisture content of about 13.5 percent moving from the bottom of the bin as shown in Figure 7.46. The experimental results also indicate the existence of a second drying front. The formation of the new drying front is due to the warm and dry weather of the spring which is capable of drying the grain to a moisture content lower than the desired final grain moisture

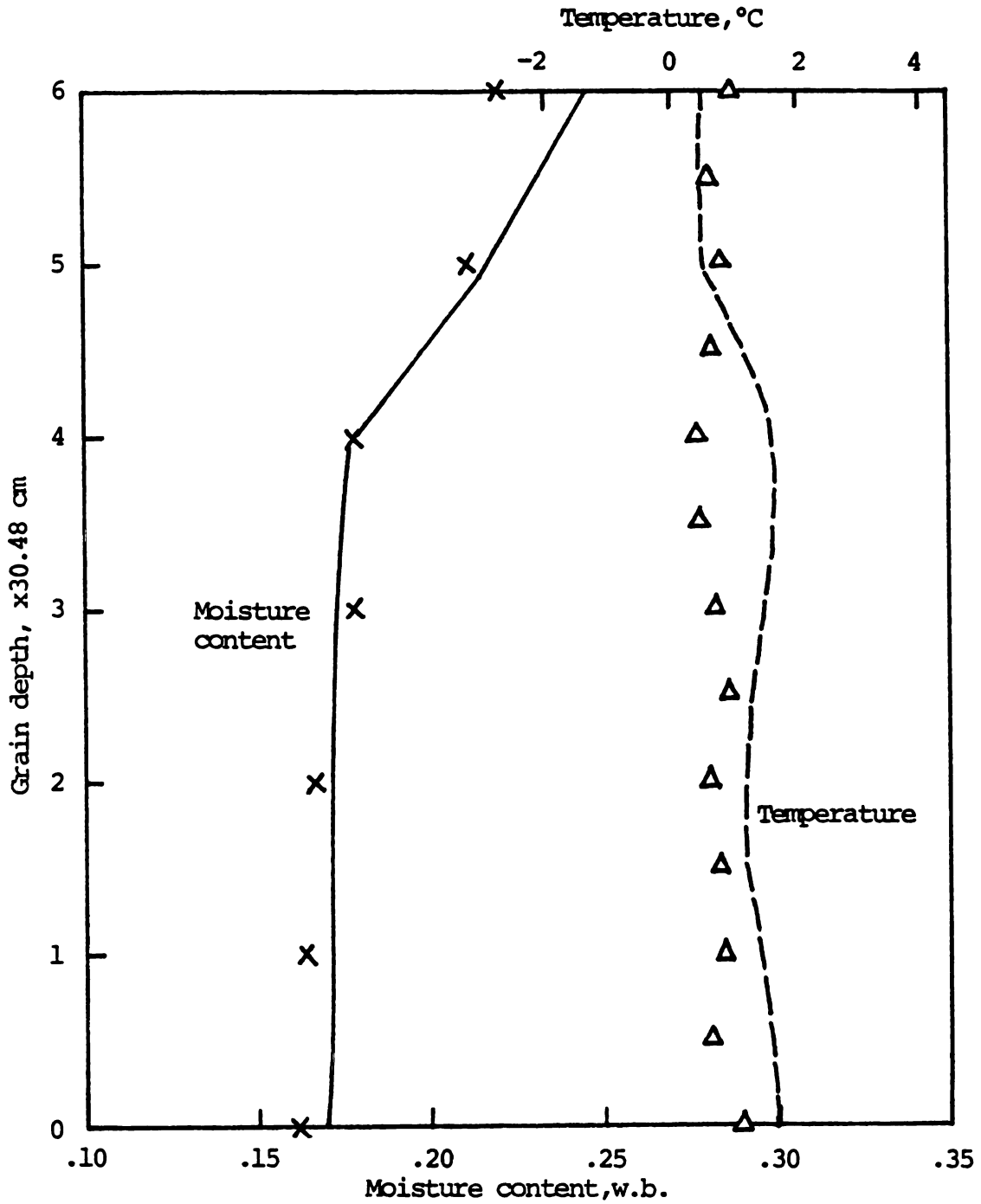


Figure 7.45. Comparison of the predicted and the experimental values of the grain moisture content and temperature at the 1447th hour of experiment.

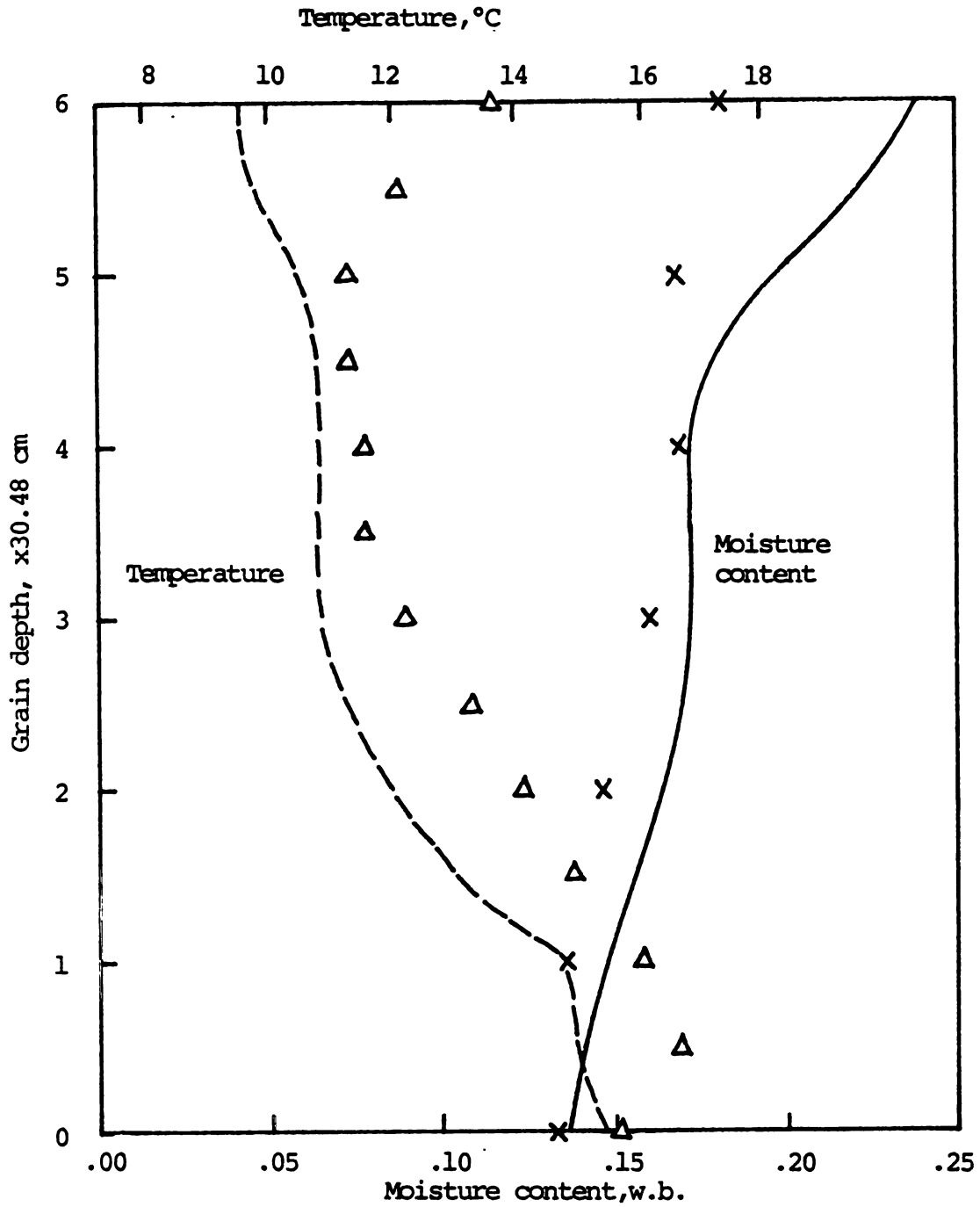


Figure 7.46. Comparison of the predicted and the experimental values of the grain moisture content and temperature at the 1744th hour of experiment.

content of 15.5 percent. As more moisture is evaporated near the bottom of the bin, not much drying takes place at the top of the bin since the air is saturated before it reached the top.

The final average moisture content was determined as 15.61 percent w.b. while the model predicted a final moisture content of 17.40 percent w.b. The grain drying rate depends on the ambient air temperatures and humidities as indicated in Equation 6.12. A higher grain temperature (θ) and a lower relative humidity (RH) in the inlet air will predict a smaller moisture ratio (MR) and, consequently, a lower moisture content. If the model predicts lower temperatures in the grain for an extended period of time, the predicted grain drying rate is decreased and thus higher grain moisture contents are predicted as shown in Figure 7.46.

6-E. The Experimental Results of Mold Contamination

The mold contamination was determined at various stages of the corn drying and preservation test. The grain sample taken immediately after harvest was free of mold contamination. The average mold number during the test is shown in Figure 7.47 together with the change in grain moisture content and the amount of ammonia added during the various test periods. During the first 360 hours of the drying test, the average mold number increased rapidly despite the addition of ammonia. The average mold count was less than 10,000/g which is still below the dangerous level. Still, this is an indication that the ammonia treatment was not sufficient for the wet grain to completely inhibit the mold growth. Had a higher dosage of ammonia been applied, the mold count would have been lower. After 360 hours, the mold growth leveled off because of the cold temperatures. Significant mold growth was found at the top after the 600th hour in spite of the cold ambient

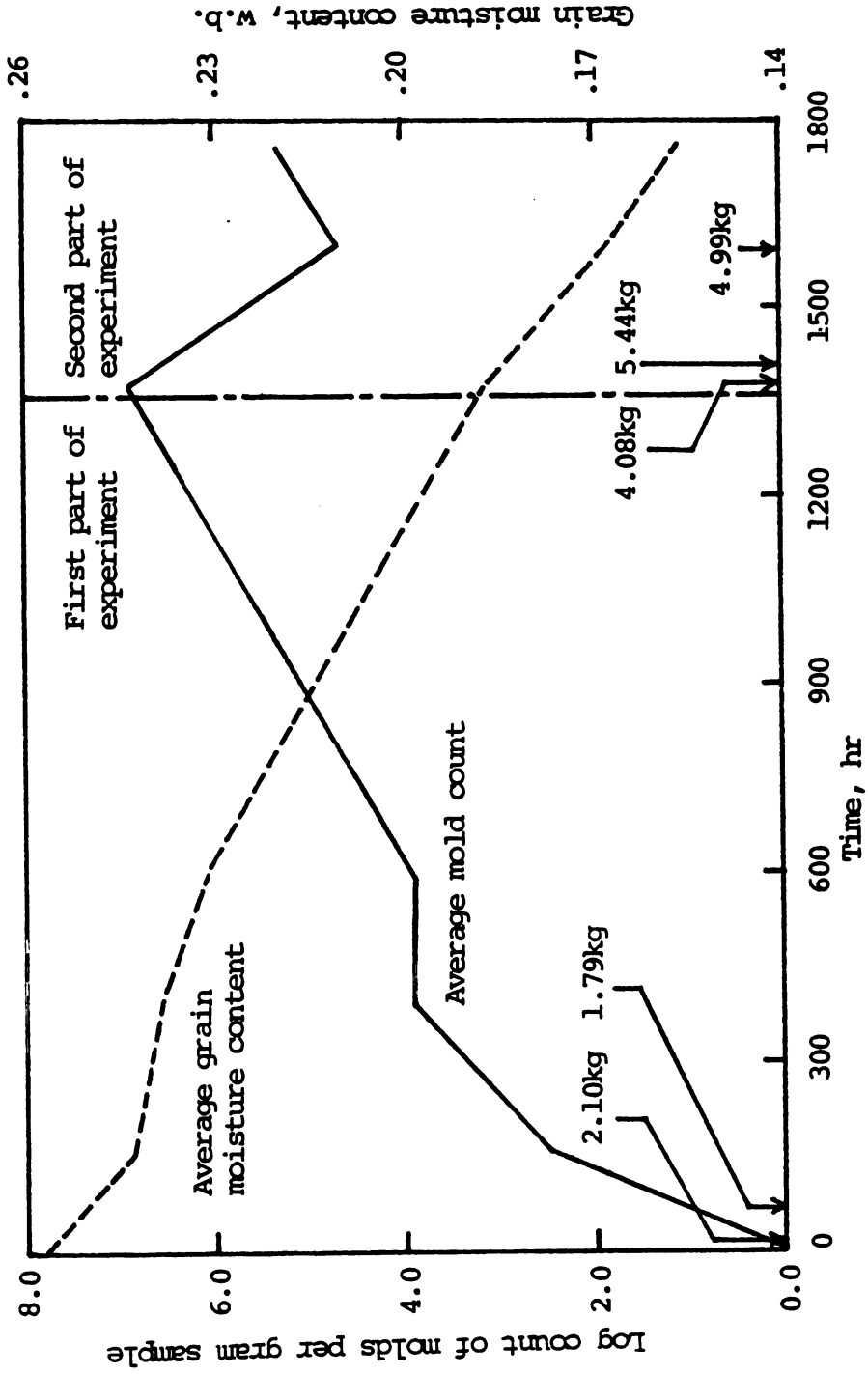


Figure 7.47. The relationship between the average mold count, average grain moisture content and the grain temperature throughout the entire ammonia corn drying process. The amount of ammonia applied is also indicated.

temperatures. The mold growth at this stage was mostly attributed to the significant growth at the upper portion of the grain bin as shown in Figure 7.48. The mold growth at the lower portion of the grain bed was not obvious during this period even without the ammonia.

The application of ammonia at around the 1400th hour reduced the mold count significantly at all levels (Figure 7.48). The mold growth then increases again after the ammoniation has been stopped at the 1623rd hour.

Visible molds were detected at the grain level just below the top surface at the 1360th hour. The infected portion of the grain was less than 20 cm deep. The visible mold growth was concentrated on the broken corn kernels and was contained significantly after the ammonia was applied. The inhibitory effects of ammonia on the grain molds could readily be observed by the naked eye.

A representative sample of ammonia-treated corn taken at the end of the experiment was sent to the U.S. Grain Marketing Research Laboratory (Miller, 1979) for determination of the mold count. One seed in 25 and one seed in 100 were found containing *Fusarium* in two separate tests. The ammonia-treated sample was found to be cleaner than the regular commercial samples. No *Aspergillus* and *Penicillium* were found. Thus no aflatoxin test was performed.

6-F. Energy Consumption in Ammonia Grain Drying

The ammonia grain drying is one of the alternative energy-saving grain drying techniques. In this particular bin experiment, 3048 kg (120 bu) of corn was dried from 25.6 percent (w.b.) moisture content to 15.6 percent. The test weight (density) for the wet corn is 682 kg/m^3 . Thus, a total amount of 342 kg water was removed throughout the entire

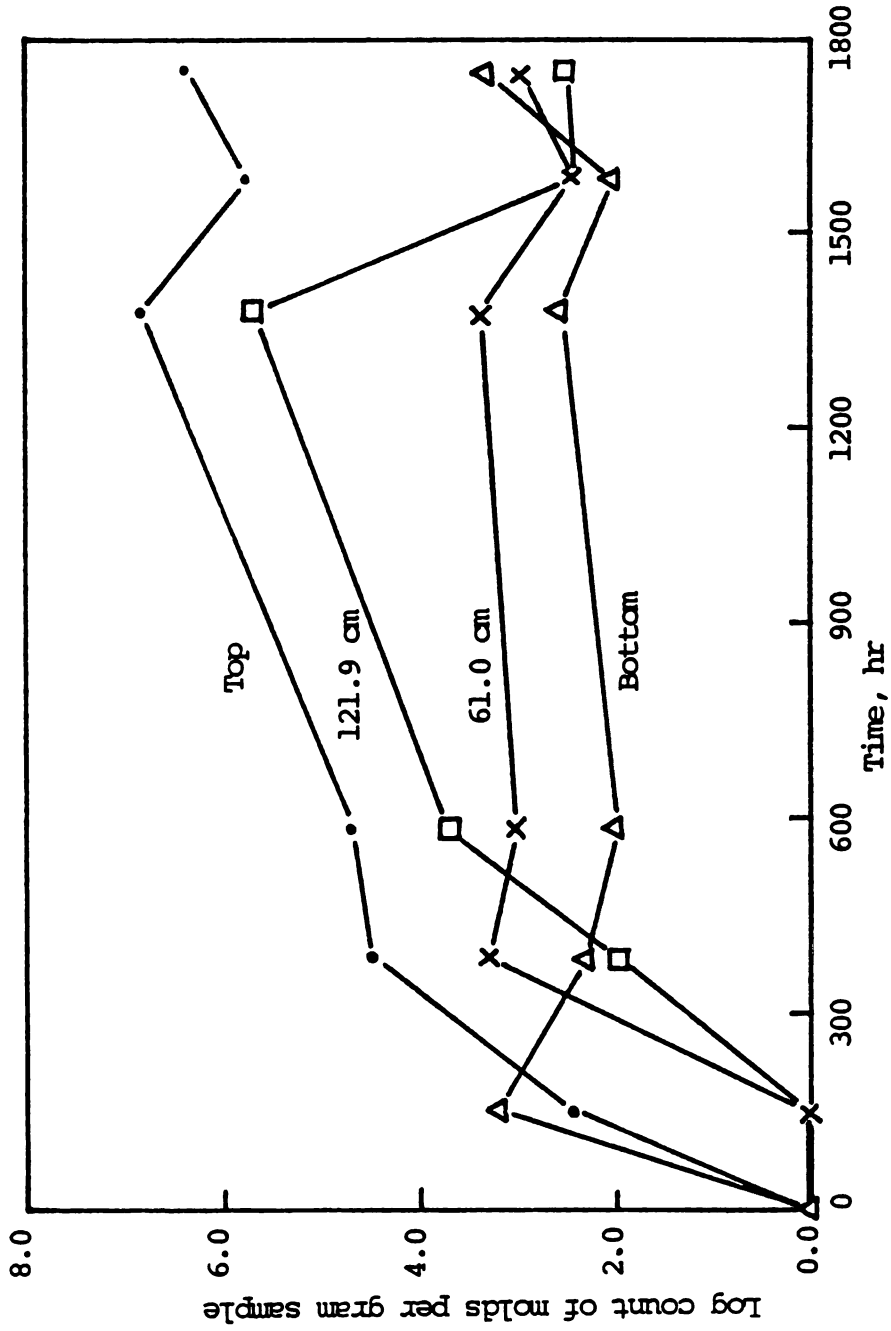


Figure 7.48. The variation of mold counts at different levels and times in the bin throughout the entire ammonia corn drying process.

drying process. The 1/20-hp fan operated for 1744 hours and the total amount of ammonia applied was 18.4 kg.

The energy requirement in the ammonia grain drying process consists of two major parts (excluding loading and unloading): the energy in producing ammonia and the fan operation energy. The energy required in the ammonia production is 5.598×10^4 KJ/kg and the total amount of energy in producing 18.4 kg of ammonia is 1.030×10^6 KJ. The 1/20-hp fan consumes energy at a rate of 37.3 watts (1.343×10^2 KJ/hr) and the total fan energy amounts to 2.342×10^5 KJ. The total amount of energy required in the ammonia grain drying was 1.264×10^6 KJ, among which 81.47 percent for the production of ammonia and only 18.53 percent for the fan operation.

The dryer efficiency is 3696 KJ/kg-water (1589 BTU/lb-water) removed which is a saving of over 50 percent compared to 7500 KJ/kg-water removed for high-temperature dryer and 33 percent saving compared to 5500 KJ/kg-water for bin drying systems.

CHAPTER 8

CONCLUSIONS

1. A theoretical analysis of the ammonia-assisted grain drying process has been made, a five-equation model was developed and solved numerically.
2. An experimental bin test of ammonia grain drying has been performed employing 4.35 m^3 (120 bu) of corn. The 1.83 m deep corn was dried from 25.6 to 15.6 percent (w.b.) moisture within 72 days and 16 hours of fan operation at $1.43 \text{ cm}^3/\text{m}^2$ (1 cfm/bu) without unacceptable grain spoilage. The total amount of anhydrous ammonia applied was 18.3 kg.
3. The five-equation model solves the dynamic changes of the ammonia concentration in the air and in the corn with respect to time, position, temperature, humidity and grain moisture content. A sensitivity model established the important parameters in the prediction model.
4. A newly-developed ammonia sorption isotherm, which is approximated from the ammonia-water solution isotherm, serves as an essential stepstone in solving the equilibrated condition between the grain and the ammonia.
5. The computer simulation program of the five-equation model was tested and compared with the experimental results. Good agreement

between the experimental and predicted results was obtained.

6. The prediction model is dynamic and is capable of handling varying ambient conditions, inlet ammonia concentrations, and other grain properties at any specified time interval which can be variable.
7. The ammonia sorption and drying model was tested for numerical accuracy. A set of values for the computing time and depth intervals was established at 1.0 hour and 15.3 cm (0.5 ft) which were shown to have reasonable prediction accuracy and do not consume an excess amount of computing time.
8. The sensitivity of the important parameters in the prediction model has been determined. It was found that the ammonia adsorption rate could be significantly increased with a higher grain moisture content and a lower grain temperature.
9. The prediction model can be used to simulate a practical-scale experiment with a set of predetermined initial and operating conditions without actually performing the time-consuming experiment. On the other hand, the prediction model enables the design of future experiments in a more efficient manner and is able to predict the results of a future experiment.
10. The general grain drying simulation model using fungicidal chemicals was established. The general model can easily be made specific to simulate the treatment of a certain type of grain with a specific fungicidal chemical by specifying relevant property parameters.

CHAPTER 9
SUGGESTIONS FOR FUTURE RESEARCH

1. Conduct experiments to determine the following important but unknown parameters:
 - (1) the mass transfer coefficient between the ammonia and the grain,
 - (2) the heat of adsorption and desorption of ammonia in the grain,
 - (3) the amount of fixed-ammonia (residual) in the grain as a function of ammonia concentration in the air, free ammonia content in the corn, airflow rate, grain moisture content, temperature and time, and
 - (4) the ammonia multiplier (M_A) in the determination of dry matter loss and/or mold growth in the grain.
2. Conduct an experiment to determine the ammonia adsorption and desorption isotherms and compare with the equations developed in Chapter 3.
3. Conduct an experiment to establish the dry matter loss or the mold growth as a function of the temperature and the free ammonia content in the grain.
4. Perform experiments with grain samples other than corn, such as wheat, sorghum, rice, soybeans, barley, peanuts, pea beans, etc., and compare the experimental results with the predicted ones of the ammonia sorption and drying model.
5. Perform experiments with fungicidal chemicals other than anhydrous ammonia, such as propionic acid, acetic acid, methylene bis-propionate

(MBP), formalin, sulfur dioxide, etc., and compare with the prediction model.

6. Compare the fungicidal effect of the same amount of ammonia in two identical bins at the same location by using a trickle (intermittent injection) process and a continuous (at a constant rate) process.

APPENDICES

APPENDIX A
UNIT CONVERSIONS

Quantity	Unit	Equivalent
Airflow	m^3/min (cmm)	3.532×10^1 cfm
	cmm/m^2	3.281 cfm/ft ²
	cmm/kg	8.971×10^2 cfm/bu
	cmm/ton	8.830×10^{-1} cfm/bu
Area	m^2	1.076×10^1 ft ²
Convective heat transfer coefficient	$\text{W}/\text{m}^2 \text{ K}$	1.762×10^{-1} BTU/hr ft ² °C
		3.600×10^3 J/hr m ² K
Convective mass transfer coefficient	m/hr	3.281 ft/hr
Density	kg/m^3	6.242×10^{-2} lb/ft ³
		7.768×10^{-2} lb/bu (corn)
Diffusivity	m^2/hr	1.076×10^1 ft ² /hr
Energy	J	9.479×10^{-4} BTU
		2.390×10^{-4} Kcal
Force	N	2.260×10^{-1} lb _f
Heat content	J/kg	4.299×10^{-4} BTU/lb
Heat transfer rate	W/m^3	9.662×10^{-2} BTU/hr ft ³
Length	m	3.281 ft
Mass	kg	2.205 lb
		1.000×10^{-3} tonne
		9.843×10^{-4} ton
Mass transfer rate*	$\text{kg}/\text{hr m}^2$	2.046×10^{-1} lb/hr ft ²
Power	W	1.341×10^{-3} hp
		3.414 BTU/hr
Pressure	N/m^2	9.872×10^{-6} atmosphere
		4.014×10^{-3} in. water
		1.450×10^{-4} psi
		7.500×10^{-3} mm Hg

* The mass transfer rate can also represent the mass transfer coefficient as defined in Equation 6.11.

APPENDIX A

Quantity	Unit	Equivalent
Specific heat	J/kg°C	2.388×10^{-4} BTU/lb°F
Specific surface area	m ² /m ³	3.048×10^{-1} ft ² /ft ³
Thermal conductivity	W/m K	5.778 BTU/hr ft°F 3.600×10^3 J/hr m K
Velocity	m/hr	3.281 ft/hr
Viscosity	kg/m hr	6.719 lb/ft hr
Volume	m ³	3.531×10^1 ft ³ 2.838×10^1 bu 2.642×10^2 U.S. gal

APPENDIX B

FORTRAN LISTING OF THE AMMONIA SORPTION AND DRYING MODEL

```

PROGRAM ADSFIX(INPUT,OUTPUT,TAPE60=INPUT,TAPE51=OUTPUT)
C*****
C***** M I C H I G A N   S T A T E   U N I V E R S I T Y
C***** A G R I C U L T U R A L   E N G I N E E R I N G   D E P A R T M E N T
C***** F I X E D   B E D   G R A I N   D R Y E R   M O D E L
C***** F.W. BAKKER-ARKEMA, PROJECT LEADER
C***** G. ROTH, FIXED BED PROGRAMMER
C***** RONG-CHING HSIEH, AMMONIA ADSORPTION PROGRAMMER
C*****
C***** DESCRIPTION
C***** MAIN PROGRAM FOR THE SIMULATION OF A FIXED BED DRYER
C***** AND THE AMMONIA ADSORPTION IN A FIXED BED
C*****
C***** SUBROUTINES USED
C***** BLOCKDATA
C***** LAYEQ
C***** READYTH
C***** ZERGIN
C***** ADSPT
C***** ADSPT1
C*****
C***** FUNCTION SUBPROGRAMS USED
C***** SOLVE
C***** SYCHART PACKAGE
C***** FUNC
C*****
COMMON /MAIN/ XMT,TMT,RHT,DELT,CFM,XMO,IAB
COMMON /PRPRIY/SA,CA,CF,CV,CW,RHCP,HFG
COMMON /PRESS/FATM
COMMON /NAME/INAME,IPRCD
COMMON /ARRAYS/ T(65,2),H(65,2),XM(65),RH(65)
COMMON /FLAGS/ J,JM,ICON
COMMON /X1/X1IN,X2IN,X2E,Y
COMMON /ADSMT/XMA,TA
COMMON /XN/XN,HN,RC
COMMON /CONS/C1,C2,C3,C4,C5,C6,C7,C8,C9,C21
COMMON /NT/NT
COMMON /C10/C10
DIMENSION X1(65,2),X2(65,2),R(65)
DIMENSION X2*AX(65),X2R(65),X2RR(65),Y2ER(65)
DIMENSION XMEPR(65),GM(65),TEQ(65),DEEP(21),LB(65)
DIMENSION X1PR(65),X2FR(65),X2RFR(65),X2EQPR(65),RFR(65)
REAL KH
EXTERNAL SOLVE
C***** DEFINE EQUILIBRIUM RH FUNCTION (THOMPSON, 1972)
F(T)=T+459.69
ERH(T,XX)=1.-EXP(-.392+(T+50.)*XX**2)
DATA RHC,D,TIME,IXIT,JK,KCON,KAB/.999999999,2+.0,4+0/
DATA IAB,HR,CG,CL,HAD,VCID,X1IN,X2IN,X2TZ/O,0.,.512,1.12,8.97
+.36,3+0./
C----- CL IS THE SPECIFIC HEAT FOR AMMONIA AT TEMPS. 5-86 F
C----- FROM ENVIRONMENTAL ENGINEERING BY JENNING, 1970
C----- HADP IS THE HEAT OF ADSORPTION OF AMMONIA IN WATER ADOPTED
C----- FROM HEAT OF SOLUTION OF AMMONIA IN WATER
HADP=HAD+100.
TETPR=PRT=0.
C***** INPUT CONDITIONS OF DRYER TO BE SIMULATED
C----- DEPTH=GRAIN DEPTH, DELX=COMPUTING DEPTH INTERVAL
C----- INDPR=PRINT DEPTH, INDICATOR, TT=TOTAL TIME OF DRYING
C----- DELT=COMPUTING TIME INCREMENT
C----- IPRINT=1 SHORT OUTPUT, 2 OTHER, INTEGER LONG OUTPUT
C----- INIT=1 FOR NONHOMOGENEOUS INITIAL CONDITIONS
C----- XMOW=INITIAL GRAIN MC WB
C----- THIN=INITIAL GRAIN TEMP
C----- CFM=AIRFLOW RATE, CFM/SQ FT OF BED AREA.
C----- TCFM=TOTAL AIRFLOW, CFM
C----- KH=RATIO OF MASS/HEAT TRANSFER COEFFICIENT
C----- RC=FRACTION OF THE FREE AMMONIA AS RESIDUALS
C----- IPR=1,PRINT OUTPUT AT EVERY INPUT
C----- TETPR=PRINT TIME INCREMENT,IF IPR.NE.1
READ 90,DEPTH,DELX,INDPR,TT,DELT,IPR,INIT
READ 91,XMOW,THIN,CFM,TCFM,KH,RC,IPR
IF(IPR.EQ.1) GO TO 55
READ 92,TETPR
55 CONTINUE
90 FORMAT(2F10.0,I5,5X,2F10.0,2I5)
91 FORMAT(6F10.0,I5)
92 FORMAT(F10.0)
C***** ENERGY REQUIREMENT FOR FORCING AIR FROM SHEED
HP=DEPTH*(CFM**1.944)*3.0792E-6
HPCUR=HP*TT
AKUPR=HPCUR*.7455
FTUAIR=HPCUR/3.62E-4
C***** COMPUTE STEP SIZE, NUMBER OF NODES AND DEPTH BETWEEN PRINTS
PRT=TETPR
IND=IFIX(DEPTH/DELX+.00001)
IND1=IND+1
C***** COMPUTE OUTPUT DEPTHS FOR PRINTING
OCTPR=IND*DELX

```



```

C3=RHO*DELTA
C***** PRINT HEADER PAGE OF CONDITIONS AND PROPERTIES
C----- IPRINT=1 SHORT OUTPUT, OTHERWISE LONG OUTPUT
IF (IPRINT.EQ.1) GO TO 99
PRINT 240
PRINT 240, INAKE, IPPOD
PRINT 230, THIN, XNO, WEO, SA, VOID, RHOP
PRINT 231, CFM, HC, KH, HM, GA
PRINT 232, CA, CF, CV, CW, CG, CL
PRINT 233, PATM, RADP
PRINT 234, DEPTH, DELT, DETPR, TT, ETUAIR, AKLHR
PRINT 235, DELT
C***** PRINT DEPTHS FOR WHICH LATER OUTPUT CORRESPONDS
PRINT 211, (DEEP(I), I=1, JK)
99
CONTINUE
C***** BEGIN TIME LOOP
HR1=0.
TIME=DELT
4
CONTINUE
C----- READ INPUTS ON FIRST DELT, ALWAYS
IF (TIME.GT. (HR+.1E-8)) 5 10
C***** CHECK IF TIME TO READ NEW DATA INPUT
C----- READ INLET AIR TEMP. AND RELATIVE HUMIDITY; INLET AMMONIA
C----- CONCENTRATION IN AIR AND THE NUMBER OF SUBDIVISION ON TIME
C----- OF THE SECOND NODE AT FIRST DELT OF CHANGE IN INLET AMMONIA
C----- CONCENTRATION IN AIR
5
CONTINUE
Y=X1IN
C----- READ DYNAMIC INPUT CONDITIONS
C----- HR=PROCESS HOUR COUNTER, MUST BE INCREASING BY AT LEAST DELT
C----- X1INZ=INLET AMMONIA CONC. IN THE AIR
C----- TINZ=INLET AIR TEMPERATURE, DRY BULB
C----- WTINZ=INLET AIR TEMPERATURE, WET BULB
C----- NTZ=NO. OF DIVISIONS FIRST NODE AT FIRST DELT BE DIVIDED
C----- NTZ IS DESIGNED TO PREVENT INSTABILITY PROBLEMS
80
READ 60, HR, X1INZ, TINZ, WTINZ, NTZ
FORMAT (2F5.0, 2F10.0, I5)
IF (EOF(60).NE.0) GO TO 14
C----- HP1=ACCUMULATIVE HOUR COUNTER IN LOOP
90
HR1=HR1+DELT
IF (HR1.LE. (DELT+.1E-8)) GO TO 7
C----- CHECK IF TIME TO ENTER NEW INPUTS
IF ( (HR-HR1).GT. (.1E-8) ) GO TO 9
7
TIN=TINZ
WTIN=WTINZ
X1IN=X1INZ
NT=NTZ
IF (NT.EQ.0) NT=1
IF (WTIN.LT.0.) 251, 252
251
RHIN=.7
GO TO 8
C----- CALCULATE RH FROM DB AND WB AIR TEMP.
252
CONTINUE
PVIN=FVDEWB(F(TIN), F(WTIN))
PSIN=PSDB(F(TIN))
RHIN=RHSPV(PSIN, PVIN)
GO TO 8
9
NT=1
8
CONTINUE
IF (X1IN.LE.0.) 50, 51
50
X1(1,2)=0.
X2(1,2)=0.
X2EQ(1)=0.
P(1)=0.
GO TO 52
C----- COMPLETE OUTPUTS FOR FIRST NODE IF X1IN>0.
C----- ASSUMING INSTANT EQUILIBRIUM FOR THE FIRST NODE
51
X1(1,2)=X1IN
X2(1,2)=108.*TIN**(-1.155)*X1(1)*X1IN**(.10971-1.1652E-3*TIN)
X2EQ(1)=X2(1,2)
X212=AMAX1(X212, X2(1,2))
X2R(1)=PC*X212
R(1)=100.*HM*(X2EQ(1)-X2(1,1))/X2EQ(1)
52
CONTINUE
T(1,2)=TIN
PH(1)=RHIN
H(1,2)=HABRH(F(T(1,2)), AH(1))
X2(1,1)=X2(1,2)
C***** EVALUATE THIN LAYER CRYING EQUATION AT AIR INLET
THT=T(1,1)
XMT=XM(1)
RHT=RHDEHA(F(THT), H(1,1))
CALL LAYEG
XM(1)=XMT
C***** BEGIN DEPTH LOOP
DO 102 J=2, INCI
JM=J-1
JNM=JM-1
C***** USE PREVIOUS VALUE OF H FOR INITIAL GUESS
HJ2=H(JM, 2)
HRA=1./VSDPHA(F(T(JM, 2)), HJ2)

```

```

11
12
13
14
15
16
17
18
19
20
21
22
23
24
25
26
27
28
29
30
31
32
33
34
35
36
37
38
39
40
41
42
43
44
45
46
47
48
49
50
51
52
53
54
55
56
57
58
59
60
61
62
63
64
65
66
67
68
69
70
71
72
73
74
75
76
77
78
79
80
81
82
83
84
85
86
87
88
89
90
91
92
93
94
95
96
97
98
99

```

```

C4=VOID*DELX*RHCA
C----- CFA IS THE OVERALL SPECIFIC HEAT OF AIR
CPA=CA+HJ2*CV+X1(JM,2)/100.*CG
C----- CPP IS THE OVERALL SPECIFIC HEAT OF AMMONIATED GRAIN
CPF=CP+XM(JM)*CW+X2(JM,2)/100.*CL
C5=VOID*RHOA/GA+RHOP*CFE/GA/CPA
C6=C5*DELX
C----- ASSUMING VARIABLE LATENT HEAT FOR WATER
HFG=(1094.-.57*T(JM,2))*(1.+4.349*EXP(-28.25*XM(JM)))
C7=HFG*DELX/CPA
C8=HAC*DELX/CPA
C----- C21 IS DEFINED FOR THE USE IN FUNCTION FUNC
C21=1.+H(JM,2)
IF(J.EQ.2)15,16
15 C10=0
GO TO 17
16 C10=C8*(X1(JM,2)-X1(JMM,2))
17 CONTINUE
C***** CALL SOLVE TO COMPUTE TRIAL T, XM, H, RH
DIFF=SOLVE(HJ2)
XPA=XM(J)=XMT
TA=T(J,2)
C----- X1 AND X2 AT J=2 HAVE BEEN EVALUATED
IF(J.EQ.2)73,74
C----- COMPUTE AMMONIA CONC. AT SECOND NODE
73 CALL ADSPT1(X1(2,1),X1(2,2),X2(2,1),X2(2,2),X2MAX(2))
GO TO 75
C----- EVALUATE AMMONIA CONC. IN AIR AND GRAIN
74 CALL ADSPT(X1(JM,2),X1(J,1),X1(J,2),X2(J,1),X2(J,2))
C----- X2MAX IS THE MAX. CONC. OF AMMONIA IN CORN AT ANY
C----- PARTICULAR NODE, X2RMIN IS THE MIN. AMOUNT OF RESIDUAL
75 CONTINUE
X2MAX(J)=AMAX1(X2(J,1),X2(J,2),X2MAX(J))
X2P(J)=RC*X2MAX(J)
X2R(J)=AMAX1(X2R(J),X2RR(J))
C----- SHIFT TIME ARRAYS FOR AMMONIA CONCENTRATIONS
X1(J,1)=X1(J,2)
X2(J,1)=X2(J,2)
X2EQ(J)=X2E
P(J)=XM
C***** CHECK CONDENSATION FLAG
IF(ICON)31,31,30
30 KCON=KCCN+1
GO TO 43
C***** SET LIMITS ON H
31 IF(DIFF)36,43,32
C***** SOLVING FOR ABSORPTION CONDITIONS
32 HLOW=.5*ERH(THT,XMT)
C***** CHECK FOR FEASIBLE HLOW
33 IF(XMT-EMC(HLOW,THT))34,35,35
C***** DECREASE HLOW UNTIL XM .GT. EMC
34 HLOW=.5*HLOW
GO TO 33
35 HLOW=HADERH(F(THT),HLOW)
HHI=H(J,2)
KAB=KAB+1
GO TO 42
C***** SOLVING FOR DRYING CONDITIONS
36 HLOW=H(J,2)
C***** CHECK FOR SUPERSATURATED GRAIN
IF(XMT-EMC(RHC,THT))38,37,37
37 HHI=HADERH(F(THT),RHC)
GO TO 42
38 HHI=.5*(1.+ERH(THT,XMT))
C***** CHECK FOR FEASIBLE HHI
39 IF(EMC(HHI,THT)-XMT)40,41,41
C***** INCREASE HHI UNTIL EMC .GT. XM
40 HHI=.5*(1.+HHI)
GO TO 39
41 HHI=HADERH(F(THT),HHI)
C***** INITIATE SEARCH FOR H, T, XM
C*****
42 CALL ZEROIN(HLOW,HHI,.0001,SOLVE)
43 XM(J)=XMT
C***** END DEPTH LOOP
*C2 CONTINUE
XMAVE=0. ; GMAVE=0. ; WAVE=0.
X1AVE=X2AVE=TAVE=0.
DO 103 J=1,IND1
C***** SHIFT ARRAYS
T(J,1)=T(J,2)
H(J,1)=H(J,2)
C***** COMPUTE EQUILIBRIUM MOISTURE CONTENT
X1EPR(J)=EMC(RH(J),T(J,2))
C***** SUM MOISTURE CONTENTS
XMAVE=XMAVE+XM(J)
C***** CALCULATE DRY MATTER DECOMPOSITION (THOMPSON, 1972)
X1DE=100.*X1(J) ; X1WB=X1DE/(1.+XM(J)) ; TJ=T(J,1)
WB(J)=.01*X1WB ; WAVE=WAVE+WB(J)
C***** COMPUTE TEMPERATURE MULTIPLIER FOR EQUIVALENT TIME

```

```

011
012
013
014
015
016
017
018
019
020
021
022
023
024
025
026
027
028
029
030
031
032
033
034
035
036
037
038
039
040
041
042
043
044
045
046
047
048
049
050
051
052
053
054
055
056
057
058
059
060
061
062
063
064
065
066
067
068
069
070
071
072
073
074
075
076
077
078
079
080
081
082
083
084
085
086
087
088
089
090
091
092
093
094
095
096
097
098
099
100

```

```

C----- IF(TJ=0.) 21,22,27
C----- T.LT.30DEG
21 AMT = 128.76*EXP(-4.68*(TJ/60.))
GO TO 26
C----- (T.GE.60DEG) AND (XM.LE.19WB)
22 AMT = 32.3*EXP(-3.48*(TJ/60.))
IF(XM.WB=19.) 26,26,23
23 IF(XM.WB=28.) 26,24,25
C----- (T.GE.60DEG) AND (XM.GT.19WB) AND (XM.LE.28WB)
24 AMT = AMT + (XM.WB-19.)/100.*EXP(.61*(TJ-60.)/60.)
GO TO 26
C----- (T.GE.60DEG) AND (XM.GT.28WB)
25 AMT = AMT + .09*EXP(.61*(TJ-60.)/60.)
26 CONTINUE
C----- COMPUTE MOISTURE CONTENT MULTIPLIER FOR EQUIVALENT TIME
C----- RESTRICT MOISTURE CONTENT VALUES TO 13 - 35 WB
IF(XM.WB.LT.13.) XMDB=13./1.87
IF(XM.WB.GT.35.) XMDB=35./1.87
AMM = 103*(EXP(455./XMDB*1.23) - .0084 + XMDB + 1.558)
C----- COMPUTE EQUIVALENT TIME INCREMENT AND SUM
TEQ(J) = TEQ(J) + DELT/(AMT*AMM)
C----- COMPUTE PERCENT DRY MATTER LOSS
DM(J) = .0883*(EXP(.006*TEQ(J))-1.) + .00102*TEQ(J)
C----- SUM DRY MATTER LOSSES
DMAVE = DMAVE + DM(J)
X1AVE = X1AVE + X1(J,2)
X2AVE = X2AVE + X2(J,2)
TAVE = TAVE + T(J,2)
103 CONTINUE
C----- THE FOLLOWING AVERAGE VALUES ARE TAKEN AS WEIGHTED AVG.
C----- AVERAGE MOISTURE CONTENT
XMAVE = (XMAVE*2. - XM(1) - XM(IND1))/IND/2.
WBAVE = (WBAVE*2. - WB(1) - WB(IND1))/IND/2.
C----- AVERAGE DRY MATTER LOSS
DMAVE = (DMAVE*2. - DM(1) - DM(IND1))/IND/2.
C----- AVERAGE AMMONIA CONCENTRATIONS IN THE UNITS OF
C----- 1/100 OF 1 PERCENT
X1AVE = 100.*(X1AVE*2. - X1(1,2) - X1(IND1,2))/IND/2.
X2AVE = 100.*(X2AVE*2. - X2(1,2) - X2(IND1,2))/IND/2.
TAVE = (TAVE*2. - T(1,2) - T(IND1,2))/IND/2.
C----- IF TIME IS UP, SET EXIT FLAG
IF(TIME + DELT - TT) 11,11,12
11 CONTINUE
C----- IF IPR=1 THE NEXT PRINT TIME IS THE INPUT HR
IF(IPR.EQ.1)PRT=HR
C----- TIME TO PRINT?
IF(TIME.GE.(PRT-.1E-8))13,18
18 TIME=TIME+DELT
GO TO 4
C----- SET FLAG IF EXIT CONDITION MET
12 IEXIT=1
13 CONTINUE
C----- MAKE FINAL CALCULATIONS AND PRINT
C----- COMPUTE TOTAL WATER REMOVED
WATER = (XMO - XMAVE)*RHCP*DEPTH
C----- COMPUTE PERCENTAGE CONDENSATION AND ABSORPTION
PKCON = KCON*100./IND1
PKAB = KAB*100./IND1
KAB = 0.5 KCON = 0
C----- COMPUTE EQUILIBRIUM MOISTURE CONTENT FOR PRINTING
DO 106 J=1,IND1,INDPR
106 XM(EPR(J)) = EMC(RH(J),T(J,2))
PRINT 223,TIME
223 FORMAT(/, 'XGHTIME =F8.2,3H HR,20X26H+NH3 ARE .01 CF 1 PERCENT*')
TIME=TIME+DELT
PRT=PRT+IBTPR
IF(IEXIT.EQ.1)GO TO 98
PRINT 212,XMAVE,X1AVE,PKCON,WBAVE,X2AVE,PKAB,DMAVE,TAVE,
+WATER
PRINT 215,(XM(I),I=1,IND1,INDPR)
PRINT 208,(WB(I),I=1,IND1,INDPR)
PRINT 219,(XM(EPR(I)),I=1,IND1,INDPR)
PRINT 214,(DM(I),I=1,IND1,INDPR)
PRINT 217,(H(I,2),I=1,IND1,INDPR)
PRINT 215,(RH(I),I=1,IND1,INDPR)
98 CONTINUE
DO 20 I=1,IND1
X1PR(I) = X1(I,2)*100.
X2PR(I) = X2(I,2)*100.
X2RPR(I) = X2R(I,2)*100.
Y2EGPR(I) = X2EG(I)*100.
RPR(I) = R(I)*100.
20 CONTINUE
PRINT 213,(T(I,2),I=1,IND1,INDPR)
PRINT 220,(X1PR(I),I=1,IND1,INDPR)
PRINT 221,(X2PR(I),I=1,IND1,INDPR)
PRINT 224,(X2RPR(I),I=1,IND1,INDPR)
PRINT 220,(X2EGPR(I),I=1,IND1,INDPR)
PRINT 222,(RPR(I),I=1,IND1,INDPR)
220 FORMAT('CHOLHS AIR 15F.2)
221 FORMAT('CHCFREE NH3 15F.2)

```

262
 263
 264
 265
 266
 267
 268
 269
 270
 271
 272
 273
 274
 275
 276
 277
 278
 279
 280
 281
 282
 283
 284
 285
 286
 287
 288
 289
 290
 291
 292
 293
 294
 295
 296
 297
 298
 299
 300
 301
 302
 303
 304
 305
 306
 307
 308
 309
 310
 311
 312
 313
 314
 315
 316
 317
 318
 319
 320
 321
 322
 323
 324
 325
 326
 327
 328
 329
 330
 331
 332
 333
 334
 335
 336
 337
 338
 339
 340
 341
 342
 343
 344
 345
 346
 347
 348
 349
 350
 351
 352
 353
 354
 355
 356
 357
 358
 359
 360
 361
 362
 363
 364
 365
 366
 367
 368
 369
 370
 371
 372
 373
 374
 375
 376
 377
 378
 379
 380
 381
 382
 383
 384
 385
 386
 387
 388
 389
 390
 391
 392
 393
 394
 395
 396
 397
 398
 399
 400
 401
 402
 403
 404
 405
 406
 407
 408
 409
 410
 411
 412
 413
 414
 415
 416
 417
 418
 419
 420
 421
 422
 423
 424
 425
 426
 427
 428
 429
 430
 431
 432
 433
 434
 435
 436
 437
 438
 439
 440
 441
 442
 443
 444
 445
 446
 447
 448
 449
 450
 451
 452
 453
 454
 455
 456
 457
 458
 459
 460
 461
 462
 463
 464
 465
 466
 467
 468
 469
 470
 471
 472
 473
 474
 475
 476
 477
 478
 479
 480
 481
 482
 483
 484
 485
 486
 487
 488
 489
 490
 491
 492
 493
 494
 495
 496
 497
 498
 499
 500


```

C***** CHECK IF DERIVATIVE IS VERY LARGE...IF IT IS ASSIGN T2=0.0
      IF(XMR.LT..999) GO TO 2
      T1=0.0
      GO TO 4
C***** CHECK FOR EQUILIBRIUM CONDITIONS
      IF(XMC - XME.LT..0001) GO TO 6
      U=ALOG(-ALOG(XMR))
C***** IF Y IS POSITIVE, SABBAN WILL NEVER REACH XME
C***** T1MAX IS THE CLOSEST APPROACH USED TO LIMIT SEARCH .
      T1MAX = 2000.
      IF(Y.LE.0.) GO TO 3
      IF(Y.LE.0.) GO TO 3
      T1MAX = (C.664/(X*Y))**(1.0/Y)
C***** NEWTON-RAPHSON TECHNIQUE TO FIND EQUIVALENT TIME
      Z1=X*T1**Y-.664*ALOG(T1)+U
      IF(ABS(Z1).LT..001) GO TO 4
      Z2=X*Y-T1**Y-.664/T1
      T2=T1-Z1/Z2
      K=K+1
      IF(T2.LE.C.0) T2 = T1/5.
      IF(T2.GE.T1MAX) GO TO 4
      T1=T2
      IF(K.LT.20) GO TO 3
      PRINT 210,K
      210 FORMAT(23H)THE METHOD HAS NOT CONVERGED IN I2,11H ITERATIONS)
      PRINT 211,XMC,TH,RH,XME
      211 FORMAT(11H)LAYER 6, XMC=*F8.5* TH=*F8.3* RH=*F8.5* XME=*F8.5)
C***** ADD DELT TO EQUIVALENT TIME, SOLVE FOR NEW M AND RETURN
      4 T1=T1+DELT
      XMC=DELM*EXP(-EXP(-X*T1**Y)+T1**.664)+XME
      RETURN
C***** ABSORPTION SIMULATION
C***** FIND NEW M AND INCREMENT COUNTER
      5 DIV=-.625*PSDB(TH+459.69)**(.466*RH)*RH*RH*RH
      XMC=(XMC-XME)*EXP(DIV*DELT)+XME
      KAB=KAB+1
      RETURN
      6 XMC = XME
      RETURN
      END

```

```

SUBROUTINE READYTH(TXMC,DELM,XME,ICOPS,XMR)
C*****
C***** L.E. LEREW, PROGRAMMER
C*****
C***** DESCRIPTION
C***** SUBROUTINE TO MAKE PRELIMINARY CHECKS AND CALCULATIONS
C***** FOR THINLAYER EQUATIONS
C***** USAGE
C***** USED WITH LAYEQ FOR FIXED BED AND CROSSFLOW DRYER MODELS
      COMMON /MAIN/XMC,TH,RH,DELT,CFM,XMO,KAB
      ICOPS=0
C***** COMPUTE EQUILIBRIUM MOISTURE CONTENT, COMPARE TO PRESENT
C***** MOISTURE CONTENT...IF GREATER SET ICOPS=1
      XME=EMC(RH,TH)
      IF(XME-XMC)2,1,1
      1 ICOPS=1
C***** COMPARE PRESENT MOISTURE CONTENT TO INITIAL MOISTURE CONTENT
C***** SET TXMC=THE LARGER VALUE
      2 IF(XMO-XMC)3,4,4
      3 TXMO=XMC
      GO TO 5
      4 TXMO=XMC
C***** COMPUTE MOISTURE RATIO
      5 DELM=(TXMO-XME)
      XMR=(XMC-XME)/DELM
      RETURN
      END

```

4139
4140
4141
4142
4143
4144
4145
4146
4147
4148
4149
4150
4151
4152
4153
4154
4155
4156
4157
4158
4159
4160
4161
4162
4163
4164
4165
4166
4167
4168
4169
4170
4171
4172
4173
4174
4175
4176
4177
4178
4179
4180
4181
4182
4183
4184
4185
4186
4187
4188
4189
4190
4191
4192
4193
4194
4195
4196
4197
4198
4199
4200
4201
4202
4203
4204
4205
4206
4207
4208
4209
4210
4211
4212
4213
4214
4215
4216
4217
4218
4219
4220
4221
4222
4223
4224
4225
4226
4227
4228
4229
4230
4231
4232
4233
4234
4235
4236
4237
4238
4239
4240
4241
4242
4243
4244
4245
4246
4247
4248
4249
4250
4251
4252
4253
4254
4255
4256
4257
4258
4259
4260
4261
4262
4263
4264
4265
4266
4267
4268
4269
4270
4271
4272
4273
4274
4275
4276
4277
4278
4279
4280
4281
4282
4283
4284
4285
4286
4287
4288
4289
4290
4291
4292
4293
4294
4295
4296
4297
4298
4299
4300

4139
4140
4141
4142
4143
4144
4145
4146
4147
4148
4149
4150
4151
4152
4153
4154
4155
4156
4157
4158
4159
4160
4161
4162
4163
4164
4165
4166
4167
4168
4169
4170
4171
4172
4173
4174
4175
4176
4177
4178
4179
4180
4181
4182
4183
4184
4185
4186
4187
4188
4189
4190
4191
4192
4193
4194
4195
4196
4197
4198
4199
4200
4201
4202
4203
4204
4205
4206
4207
4208
4209
4210
4211
4212
4213
4214
4215
4216
4217
4218
4219
4220
4221
4222
4223
4224
4225
4226
4227
4228
4229
4230
4231
4232
4233
4234
4235
4236
4237
4238
4239
4240
4241
4242
4243
4244
4245
4246
4247
4248
4249
4250
4251
4252
4253
4254
4255
4256
4257
4258
4259
4260
4261
4262
4263
4264
4265
4266
4267
4268
4269
4270
4271
4272
4273
4274
4275
4276
4277
4278
4279
4280
4281
4282
4283
4284
4285
4286
4287
4288
4289
4290
4291
4292
4293
4294
4295
4296
4297
4298
4299
4300

```

FUNCTION SOLVE(HJ2)
C***** COMPUTES T(J,2), XMT, RH(J) AND ICCN GIVEN H(J,2)
C***** SOLVE RETURNS THE DIFFERENCE BETWEEN THE COMPUTED M AND
C***** THE M PREDICTED BY THE DRYING EQUATION
C*****
COMMON /ARRAYS/ T(65,2),H(65,2),XM(65),RH(65)
COMMON /FLAGS/ J, JM, ICCN
COMMON /MAIN/ XMT, THT, RHT, DELT, CFM, XMG, KAB
COMMON /KFRTY/ S, L, CA, CP, CV, CW, RHC, HFG
COMMON /CONS/ C1, C2, C3, C4, C5, C6, C7, C8, C9
COMMON /C10/ C10
F(T)=T+459.69
DATA RHC / .095, .099999/
ICCN=0
C----- INITIAL GUESS FOR H(J,2)
H(J,2)=HJ2
JMM=J*-1
IF (J.EC.2) 10,11
11 C9=C7*(H(J,2)-H(JMM,2))
GO TO 14
10 C9=C7*(H(2,2)-H(1,2))
14 CONTINUE
C----- CALCULATE THE TEMPERATURE BASED ON GUESSED H VALUES
T(J,2)=(DELT*T(JM,2)+C6*T(J,1)-(C9-C10)/(DELT+C6))
IF (f(J,2).LT.0.) GO TO 7
TABS=F(T(J,2))
C***** COMPUTE RH AND CHECK FOR CONDENSATION
RH(J)=RHDPHA(TABS,H(J,2))
IF (RH(J)-RHC)111,7,7
C***** CONDENSATION SIMULATOR
C----- ESTIMATE TEMPERATURE AND ABS. HUMIDITY
7 TS=(DELT*T(JM,2)+C6*T(J,1)-C10)/(DELT+C6)
HS=HADBRRH(TABS,RHC)
C----- CALCULATE THE SLOPE TANGENT TO SATURATION LINE ON TS AND HS
DHDT=HS-HADBRRH(TABS-1.,RHC)
C11=DELT+C6
C12=C7*DHDT
C13=C7*(HS-H(J,2))
C----- ESTIMATE THE ADJUSTED TEMP. AND ABS. HUMIDITY
T(J,2)=(C11*T(J,2)+C12*TS-C13)/(C11+C12)
H(J,2)=HS+DHDT*(T(J,2)-TS)
RH(J)=RHDPHA(F(T(J,2)),H(J,2))
ICCN=1
C***** FIND M ACCORCING TO THIN LAYER DRYING EQUATION
111 XMT=XM(J) $ THT=T(J,2) $ RHT=RH(J)
CALL LAYER
CONS=C2/C3
C----- SOLVE SHOULD CONVERGE TO ZERO UPON ITERATION IN ZEROIN
SOLVE=XMT-XM(J)+CON6*(HJ2-H(JM,2))
C***** M EQUATION
XMT=XM(J)-CON6*(H(J,2)-H(JM,2))
RETURN
END

```

```

SUBROUTINE ADSFT(X112,X121,X122,X221,X222)
C----- THIS SUBROUTINE COMPUTES THE AMMONIA CONCENTRATIONS EGTH IN
C----- AIR AND IN GRAIN AS WELL AS RESIDUALS OF AMMONIA IN GRAIN
C----- THE DRIVING FORCE OF AMMONIA ADSORPTION IS DEFINED AS
C----- THE DIFFERENCE OF PRESENT AND EQUILIBRIUM AMMONIA CONC.
C----- IN GRAIN, AND THE EQUILIBRIUM AMMONIA CONC. IN GRAIN IS
C----- COMPUTED BASED ON THE ASSUMPTION THAT THE ONLY ACTIVE
C----- COMPONENT IN ADSORBING AMMONIA BE WATER ONLY IN GRAIN
C-----
COMMON /Y1/ X1IN, X2IN, X2E, Y
COMMON /ADSMT/ XMA, TA
COMMON /XN/ XN, HM, RC
COMMON /CONS/ C1, C2, C3, C4, C5, C6, C7, C8, C9
COMMON /COEFF/ CONA, CO4C, CON6, CONE, EB
EXTERNAL FUNC
C----- DEFINE PARAMETERS USED IN AMMONIA ADSORPTION ISOTHERM
A(T)=108.*T**(-1.155)
B(T)=1.0971-1.7e52E-3*T
R6=R(TA)
CONA=A(TA)*XMA
CONC=X221+C1
CON6=(C2*X112+C4*X121+C3*(1.+RC)*X221)/(C2+C4)
CONE=-C3*(1.+RC)/(C2+C4)
C----- HIGHEST VALUE FOR X1 CAN NOT EXCEED X1IN, X112 OR X121
X1HIGH=MAX(X1IN,X112,X121)
X1LOW=.1E-10
IF (X1HIGH.LE.X1LOW) GO TO 1
C----- SOLVE X1 BY ITERATION IN THE COMBINED EQUATION
CALL ZEROIN(X1LOW,X1HIGH,.00001,FUNC)
X122=(X1LOW+X1HIGH)/2.

```

```

      GO TO 2
      X122=0.
      CONTINUE
C----- IF INPUT CONC. INCREASES, X122 MUST NOT DECREASE
      IF ((X1IN.GE.Y).AND.(X1IN.NE.0.))X122=AMAX1(X122,X121)
      Y2E=C0NA*X122**BB
      IF (X2E.LT.0.)X2E=0.
      X222=CONC*X2E/(C1+X2E)
      IF (X2E.LT..1E-10) X2E=1E-10
      XN=100.-HM*(X2E-X221)/Y2E
      GO TO 5
      XN=0.
      CONTINUE
C----- IF CONC. IN AIR IS ZERO, CONC. IN GRAIN CAN NOT INCREASE
      IF (X122.EG.0.)X222=AMIN1(X221,X222)
      RETURN
      END

```

6
 7
 8
 9
 10
 11
 12
 13
 14
 15
 16
 17
 18
 19
 20
 21
 22
 23
 24
 25
 26
 27
 28
 29
 30
 31
 32
 33
 34
 35
 36
 37
 38
 39
 40
 41
 42
 43
 44
 45
 46
 47
 48
 49
 50
 51
 52
 53
 54
 55
 56
 57
 58
 59
 60
 61
 62
 63
 64
 65
 66
 67
 68
 69
 70
 71
 72
 73
 74
 75
 76
 77
 78
 79
 80
 81
 82
 83
 84
 85
 86
 87
 88
 89
 90
 91
 92
 93
 94
 95
 96
 97
 98
 99
 100

```

      SUBROUTINE ADSFT1(X121,X122,X221,X222,X2MAX)
C----- THIS SUBROUTINE COMPUTES AMMONIA CONCS. IN AIR AND GRAIN
C----- FOR THE SECOND NODE, I.E. THE FIRST INSIDE NODE
C-----
      COMMON/X1/X1IN,X2IN,X2E
      COMMON/CONS/C1,C2
      COMMON/XN/XN,HM,RC
      COMMON/NT/NT
C----- REDEFINING TIME RELATED CONSTANTS
      C1=C1/NT
      C2=C2/NT
      Y=X1IN
      INT=0
      1 IF (INT.GE.NT) GO TO 2
      CALL ACSPT(Y,X121,X122,X221,X222)
C----- DEFINE THE DESORPTION RATE AS THE RATE AT FIRST INSTANT
      IF (INT.EQ.0)R2=XN
C----- DEFINE X2MAX FOR THE CALCULATION OF RESIDUALS
      X2MAX=AMAX1(X222,X221,X2MAX)
      X121=X122
      X221=X222
      INT=INT+1
      GO TO 1
      2 CONTINUE
      XN=R2
C----- RETURN TIME RELATED CONSTANTS
      C1=C1*NT
      C2=C2*NT
      RETURN
      END

```

5970
 5971
 5972
 5973
 5974
 5975
 5976
 5977
 5978
 5979
 5980
 5981
 5982
 5983
 5984
 5985
 5986
 5987
 5988
 5989
 5990
 5991
 5992
 5993
 5994
 5995
 5996
 5997
 5998
 5999
 6000
 6001
 6002
 6003
 6004
 6005
 6006
 6007
 6008
 6009
 6010
 6011
 6012
 6013
 6014
 6015
 6016
 6017
 6018
 6019
 6020
 6021
 6022
 6023
 6024
 6025
 6026
 6027
 6028
 6029
 6030
 6031
 6032
 6033
 6034
 6035
 6036
 6037
 6038
 6039
 6040
 6041
 6042
 6043
 6044
 6045
 6046
 6047
 6048
 6049
 6050
 6051
 6052
 6053
 6054
 6055
 6056
 6057
 6058
 6059
 6060
 6061
 6062
 6063
 6064
 6065
 6066
 6067
 6068
 6069
 6070
 6071
 6072
 6073
 6074
 6075
 6076
 6077
 6078
 6079
 6080
 6081
 6082
 6083
 6084
 6085
 6086
 6087
 6088
 6089
 6090
 6091
 6092
 6093
 6094
 6095
 6096
 6097
 6098
 6099
 6100
 6101
 6102
 6103
 6104
 6105
 6106
 6107
 6108
 6109
 6110
 6111
 6112
 6113
 6114
 6115
 6116
 6117
 6118
 6119
 6120
 6121
 6122
 6123
 6124
 6125
 6126
 6127
 6128
 6129
 6130
 6131
 6132
 6133
 6134
 6135
 6136
 6137
 6138
 6139
 6140
 6141
 6142
 6143
 6144
 6145
 6146
 6147
 6148
 6149
 6150
 6151
 6152
 6153
 6154
 6155
 6156
 6157
 6158
 6159
 6160
 6161
 6162
 6163
 6164
 6165
 6166
 6167
 6168
 6169
 6170
 6171
 6172
 6173
 6174
 6175
 6176
 6177
 6178
 6179
 6180
 6181
 6182
 6183
 6184
 6185
 6186
 6187
 6188
 6189
 6190
 6191
 6192
 6193
 6194
 6195
 6196
 6197
 6198
 6199
 6200

```

      FUNCTION FUNC(X122)
C----- THIS SUBROUTINE DEFINES A FUNCTION OF X1 COMBINED FROM
C----- X1, X2 AND X2E EQUATIONS FOR THE SOLUTION OF X1 IN ZERGIN
      COMMON/CONS/C1,C2,C3,C4,C5,C6,C7,C8,C9,C21
      COMMON/COEFF/C0NA,CCNC,CONB,CONC,CONE,BB
      X122H=X122/(C21+X122/10.)
      IF (X122H.LT.0.)X122H=0.
      FUNC=CONB+(CONC*CONC+CONA*X122H**BB)/(C1+C0NA*X122H**BB)-X122
      RETURN
      END

```

6199
 6200
 6201
 6202
 6203
 6204
 6205
 6206
 6207
 6208
 6209
 6210
 6211
 6212
 6213
 6214
 6215
 6216
 6217
 6218
 6219
 6220
 6221
 6222
 6223
 6224
 6225
 6226
 6227
 6228
 6229
 6230
 6231
 6232
 6233
 6234
 6235
 6236
 6237
 6238
 6239
 6240
 6241
 6242
 6243
 6244
 6245
 6246
 6247
 6248
 6249
 6250
 6251
 6252
 6253
 6254
 6255
 6256
 6257
 6258
 6259
 6260
 6261
 6262
 6263
 6264
 6265
 6266
 6267
 6268
 6269
 6270
 6271
 6272
 6273
 6274
 6275
 6276
 6277
 6278
 6279
 6280
 6281
 6282
 6283
 6284
 6285
 6286
 6287
 6288
 6289
 6290
 6291
 6292
 6293
 6294
 6295
 6296
 6297
 6298
 6299
 6300

BIBLIOGRAPHY

BIBLIOGRAPHY

- Agrawal, K. K., B. L. Clary and G. L. Nelson. 1969. Investigation into the theories of desorption isotherms for rough rice and peanuts - I. ASAE Paper No. 69-890.
- American Association of Cereal Chemists (AACC). 1975. 1975 Revisions to AACC Approved Methods 45-05:1-9, St. Paul, Minnesota.
- Association of Official Analytical Chemists (AOAC). 1970. Official methods of analysis, 11th ed. 26.051-26.055, Washington, DC.
- Association of Official Analytical Chemists (AOAC). 1975. Official methods of analysis. 12th ed. 26.044-26.047. Washington, DC.
- Anderson, H. W., E. W. Nehring and W. R. Wichser. 1975. Aflatoxin contamination of corn in the field. J. of Agric. and Food Chem. 23:775-782.
- Aris, R. and N. R. Amundson. 1973. Mathematical Methods in Chemical Engineering. Vol. 2. Prentice Hall, Englewood Cliffs, N. J.
- Bakker-Arkema, F. W. and W. G. Bickert. 1966. A deep bed computational cooling procedure for biological products. Trans. ASAE 9:834-836, 845.
- Bakker-Arkema, F. W. and W. G. Bickert. 1967. Computer simulation of the cooling of a deep bed of cherry pits. Mich. Agric. Exp. Sta. Quart. Bull. 50:204-211.
- Bakker-Arkema, F. W., W. G. Bickert and R. V. Morey. 1968. Gekoppelte Wärme und Stoffaustausch während des Trocknungsvorgangs in einem Behälter mit Getreide. Landwirt. Forsch. 17:175-180.
- Bakker-Arkema, F. W., T. W. Evans and L. E. Lerew. 1970. Michigan State University grain drying models. ASAE Paper No. 70-832.
- Bakker-Arkema, F. W., L. E. Lerew, S. F. DeBoer and M. G. Roth. 1974. Grain dryer simulation. Mich. State Univ., Agric. Exp. Sta. Res. Report 224.
- Bakker-Arkema, F. W., D. B. Brooker and M. G. Roth. 1977. Feasibility study of in-bin corn drying in Missouri using solar energy. Proc. Solar Grain Drying Conference, Univ. of Ill., Champaign, Ill.
- Bakker-Arkema, F. W., R. C. Brook and L. E. Lerew. 1978. Cereal Grain Drying. In: "Advances in Cereal Science and Technology", Vol. II. ed. by Y. Pomeranz. American Assoc. of Cereal Chem., Inc., St. Paul, Minnesota.

- Barabolak, R., C. R. Colburn and R. J. Smith. 1974. Rapid screening method for examining corn and corn-derived products for possible aflatoxin contamination. *J. Assoc. Offic. Anal. Chem.* 57:764.
- Bard, Y. 1974. *Nonlinear Parameter Estimation*. Academic Press, N.Y.
- Beckwith, A. C., R. F. Vesonder and A. Ciegler. 1975. Action of weak bases upon aflatoxin B₁ in contact with macromolecular reactants. *J. Agric. Food Chem.* 23:582-587.
- Beckwith, A. C., R. F. Vesonder and A. Ciegler. 1976. Chemical methods investigated for detoxifying aflatoxins in foods and feeds. *Adv. in Chem. Series* 149:58-67.
- Bird, R. B., W. E. Steward and E. N. Lightfoot. 1960. *Transport Phenomena*. John Wiley & Sons, Inc., New York, N.Y.
- Black, L. T. 1979. Personal communication.
- Bothast, R. J., E. B. Lancaster and C. W. Hesseltine. 1973. Ammonia kills spoilage molds in corn. *J. Dairy Sci.* 56:241-245.
- Bothast, R. J., G. H. Adams, E. E. Hatfield and E. B. Lancaster, 1975. Preservation of high-moisture corn: a microbiological evaluation. *J. Dairy Sci.* 58:386-391.
- Bothast, R. J., M. L. Goulden, O. L. Shotwell and C. W. Hesseltine. 1976. *Aspergillus flavus* and aflatoxin production in acid-treated maize. *J. Stored Prod. Res.* 12:177-183.
- Bottini, E. 1927. Sulla conservazione della frutta. Ricerche sperimentali eseguite sulle arancie. *Ann. Chim. Appl.* 17:129.
- Boyce, D. S. 1965. Grain moisture and temperature changes with position and time during through drying. *J. Agric. Eng. Res.* 10:333-341.
- Brekke, O. L., A. J. Peplinski and E. B. Lancaster. 1975a. Aflatoxin inactivation in corn by aqua ammonia. ASAE Paper No. 75-3507.
- Brekke, O. L., A. J. Peplinski and E. L. Griffin, Jr. 1975b. Cleaning trials for corn containing aflatoxin. *Cereal Chem.* 52:198-204.
- Brekke, O. L., A. J. Peplinski, G. E. N. Nelson and E. L. Griffin, Jr. 1975c. Pilot-plant dry milling of corn containing aflatoxin. *Cereal Chem.* 52:205-211.
- Brook, R. C. 1977. Design of Multistage Grain Dryers. Unpublished Ph.D. dissertation, Michigan State Univ., E. Lansing, MI.
- Brooker, D. B., F. W. Bakker-Arkema and C. W. Hall. 1974. *Drying Cereal Grains*. The AVI Publishing Co., Inc. Westport, CT.

- Brooker, D. B., B. A. McKenzie and H. K. Johnson. 1978. The present status of on-farm grain drying. ASAE Paper No. 78-3007.
- Brunauer, S., P. H. Emmett and E. Teller. 1938. Adsorption of gases in multimolecular layer. J. Amer. Chem. Soc. 60:309.
- Brunauer, S., L. S. Deming, W. E. Deming and E. Teller. 1940. On a theory of the van der Waals adsorption of gases. J. Amer. Chem. Soc. 62:1723.
- Bullerman, L. B., J. M. Baca and W. T. Stott. 1975. An evaluation of potential mycotoxin-producing molds in corn meal. Cereal Foods World 20:248-250, 253.
- Chilton, T. H. and A. P. Colburn. 1934. Mass transfer (absorption) coefficients, prediction from data on heat transfer and fluid friction. Ind. Eng. Chem. 26:1183.
- Chu, S. T. and A. Hustrulid. 1968. Numerical solution of diffusion equations. Trans. ASAE 11:705-708.
- Copeland, L. O. 1976. Principles of Seed Science and Technology. Burgess Publishing Co., Minneapolis, Minnesota.
- Cucullu, A. F., L. S. Lee, W. A. Pons, Jr. and J. B. Stanley. 1976. Ammoniation of aflatoxin B₁: Isolation and characterization of a product with molecular weight 206. J. Agric. Food Chem. 24:408-410.
- Dam, R., S. W. Tam and L. D. Satterlee. 1977. Destruction of aflatoxins during fermentation and by-product isolation from artificially contaminated grains. Cereal Chem. 54:705-714.
- Danziger, M. T., M. P. Steinberg and A. I. Nelson. 1971. Storage of high-moisture field corn. Illinois Res., Fall, p.8.
- del Giudice, P. M. 1959. Exposed-layer wetting rates of shelled corn. Unpublished M. S. thesis, Agric. Eng. Dept., Purdue Univ.
- Dollear, F. G. 1969. Detoxification of aflatoxins in foods and feeds. In : Aflatoxin - Scientific Background, Control and Implications, ed. by L. A. Goldblatt. Academic Press, New York, N. Y.
- Donald, J. O. 1977. Controlling mold damage and aflatoxin problems in corn. Circular R-70, Alabama Coop. Ext. Ser., Auburn, Alabama.
- Dubin, M. M. 1972. Fundamentals of the theory of physical adsorption of gases and vapors in micropores. In : Adsorption-Desorption Phenomena. ed. by F. Ricca. Academic Press, New York, N. Y.
- Eckhoff, S. R., J. E. Cauwenberge, R. J. Bothast, G. W. Nofsinger and E. B. Bagley. 1978. Sulfur dioxide supplemented ambient air drying of high-moisture corn. ASAE Paper No. 78-3518.

- Eno, C. F. W. G. Blue and Y. M. Good, Jr. 1955. The effect of anhydrous ammonia on nematodes, fungi, bacteria and nitrification in some Florida soils. *Soil Sci. Soc. Amer. Proc.* 19:55.
- Eppley, R. M., L. Stoloff, M. W. Trucksess and C. W. Chung. 1974. Survey of corn for *Fusarium* toxins. *J. Assoc. Offic. Anal. Chem.* 57:632.
- Faith, W. L., D. B. Kayes and R. L. Clark. 1975. *Industrial Chemicals*. 4th ed., Wiley, New York, N. Y.
- Farmer, D. M. and F. W. Bakker-Arkema. 1970. Use of digital computer for efficient drying of high-moisture cereal grain dough. *Trans. ASAE* 13:61-63, 66.
- Fedewa, D. J., S. J. Pscodna and E. Molenda, Jr. 1978. Michigan Corn Harvesting and Marketing Statistics. 1977. *Mich. Crop Rep. Serv.*, Lansing, Mich.
- Fedewa, D. J. and S. J. Pscodna. 1978. Michigan Agricultural Statistics. 1978. Michigan Department of Agriculture, Lansing, Mich.
- Felkel, C., J. Tuite and R. C. Brook. 1978. Storability of high moisture corn when stored at simulated post-harvest temperatures of three locations in Indiana. *ASAE Paper No. 78-3515*.
- Fennell, D. I., R. J. Bothast, E. B. Lillehoj and R. E. Peterson. 1973. Bright greenish-yellow fluorescence and associated fungi in white corn naturally contaminated with aflatoxin. *Cereal Chem.* 50:404.
- Fennell, D. I., E. B. Lillehoj and W. F. Kwolek. 1975. *Aspergillus* and other fungi associated with insect-damaged field corn. *Cereal Chem.* 52:314-321.
- Fennell, D. I., W. F. Kwolek, E. B. Lillehoj, G. A. Adams, R. J. Bothast, M. S. Zuber, O. H. Calvert, W. D. Guthrie, A. J. Bockholt, A. Manwiller and M. D. Jellum. 1977. *Aspergillus flavus* presence in silks and insects from developing and mature corn ears. *Cereal Chem.* 54:770-778.
- Flood, C. A. Jr., M. A. Sabbah, D. Meeker and R. M. Peart. 1972. Simulation of a natural-air corn drying system. *Trans. ASAE* 15: 156-159, 162.
- Foster, G. H. 1953. Minimum air flow requirements for drying grain with unheated air. *Agric. Eng.* 34:681-684.
- Foster, G. H. 1976. Grain drying - reflections and perspectives. *ASAE Paper No. 76-3005*.

- Gilatrack, J. D. 1969. Role of ammonia in the control of avocado root rot with alfalfa meal soil amendment. *Phytopathology* 59:973.
- Glueckauf. 1955. Theory of chromatography. Part 10. *Trans. Faraday Soc.* 51:1540.
- Goering, H. K. and C. H. Gordon. 1973. Chemical aids to preservation of high moisture feeds. *J. Dairy Sci.* 56:1347.
- Goldblatt, L. A. ed. 1969. Aflatoxin - Scientific Background, Control and Implication. Academic Press, New York, N.Y.
- Gregg, S. J. and K. S. W. Sing. 1967. Adsorption, Surface Area and Porosity. Academic Press, London.
- Gustafson, R. J. and G. E. Hall. 1972. Density and porosity changes of shelled corn during drying. *Trans. ASAE* 15:523-526.
- Hall, G. E., L. D. Hill, E. E. Hatfield and A. H. Jensen. 1974. Propionic-acetic acid for high-moisture corn preservation. *Trans. ASAE* 17:379-382, 387.
- Hall, K. R., L. C. Eagleton, A. Acrivos and T. Vermeulen. 1966. Pore- and solid- diffusion kinetics in fixed-bed adsorption under constant-pattern conditions. *Ind. Eng. Chem. Fundamentals.* 5:212.
- Hayes, A. W., N. D. Davis and U. L. Diener. 1966. Effect of aeration on growth and aflatoxin production by *Aspergillus flavus* in submerged culture. *Appl. Microbiol.* 14:1019.
- Henderson, S. M. and R. L. Perry. 1955. Agricultural Process Engineering. John Wiley & Sons, Inc., New York, N.Y.
- Herting, D. C. and E. E. Drury. 1974. Antigungal activity of volatile fatty acids on grains. *Cereal Chem.* 51:75.
- Hesseltine, C. W. 1976. Conditions leading to mycotoxin contamination of foods and feeds. In : Mycotoxin and Other Fungal Related Food Problems. ed. by J. V. Rodricks. *Adv. in Chem. Ser. Vol.149.* Amer. Chem. Soc., Washington DC.
- Hesseltine, C. W., O. L. Shotwell, W. F. Kwolek, E. B. Lillehoj, W. K. Jackson and R. J. Bothast. 1976. Aflatoxin occurrence in 1973 corn at harvest. II. Mycological studies. *Mycologia* 68:341-353.
- Holaday, C. E. and J. Lansden. 1975. Rapid screening method for aflatoxin in a number of products. *J. Agric. Food Chem.* 23:1134.
- Hougen, O. A., K. M. Watson and R. A. Ragatz. 1960. Industrial Chemical Calculations. John Wiley & Sons, Inc., New York, N.Y.

- Huber, J. T., R. E. Lichtenwalner and J. W. Thomas. 1973. Factors affecting response of lactating cows to ammonia-treated corn silages. *J. Dairy Sci.* 56:1283.
- Huber, J. T. 1975. Protein and non-protein nitrogen utilization in practical dairy rations. *J. Anim. Sci.* 41:954.
- Hukill, W. V. 1954. Drying of grains. In : *Storage of Cereal Grain and Their Products*. ed. by J. A. Anderson and A. W. Alcock. Amer. Assoc. of Cereal Chem., St. Paul, Minnesota.
- Hunt, W. H., R. C. Semper and E. B. Liebe. 1976. Incidence of aflatoxin in corn and a field method for aflatoxin analysis. *Cereal Chem.* 53:227-232.
- Jones, G. M., D. N. Mowat, J. I. Elliot and E. T. Moran, Jr. 1974. Organic acid preservation of high moisture corn and other grains and the nutritive value : a review. *Can. J. Anim. Sci.* 54:499-517.
- Karger, B. L., L. R. Snyder and C. Horvath. 1973. *An Introduction to Separation Science*. John Wiley & Sons, New York, N.Y.
- Katz, S. M. 1949. Permanent hysteresis in physical adsorption. A theoretical discussion. *J. Phys. Chem.* 53:1166.
- Kenyon, E., C. A. Hines and S. J. Pscodna. 1976. Michigan Corn Harvesting and Marketing Statistics, 1975. Mich. Crop Rep. Ser., Lansing, Mich.
- Knapp, W. R., D. A. Holt and V. L. Lechtenberg. 1974. Anhydrous ammonia and propionic acids as hay preservatives. *Agron. J.* 66:823.
- Kraemer, E. O. 1931. In : *A Treatise on Physical Chemistry*. ed. by H. S. Taylor. p.1661. MacMillan, New York, N. Y.
- Lai, F. S. and D. F. Aldis. 1978. Comparison of grain quality and efficiency of three methods of grain drying. ASAE Paper No. 78-3528.
- Lancaster, E. B., A. C. Stringfellow and O. L. Brekke. 1975. Treating shelled corn with ammonia-application via ammonia-air mixture. *Trans. ASAE* 18:1158-1164.
- Langmuir, I. 1918. The adsorption of gases on plane surfaces of glass, mica and platinum. *J. Amer. Chem. Soc.* 40:1361.
- Ledoux, E. 1948. Dynamic cooling of adsorbent beds. *Ind. Eng. Chem.* 40:1970.
- Lee, L. S. 1974. Ammoniation of aflatoxin B₁. *J. Assoc. Offic. Anal. Chem.* 57:626-631.

- Liley, P. E. and W. R. Gambill, 1973. Physical and chemical data. In: The Chemical Engineers' Handbook, ed by R. H. Perry and C. H. Chilton. 5th ed. McGraw-Hill Publishing Co., New York, N.Y.
- Lillehoj, E. B., O. L. Shotwell and C. W. Hesseltine. 1973. Aflatoxin: new mold-produced poison plagues food and feed. *Crops and Soil* 25:12-14.
- Lillehoj, E. B., W. F. Kwolek, D. I. Fennell and M. S. Milburn. 1975A. Aflatoxin incidence and association with bright greenish-yellow fluorescence and insect damage in a limited survey of freshly harvest high-moisture corn. *Cereal Chem.* 52:403.
- Lillehoj, E.B., W. F. Kwolek, G. M. Shannon, O. L. Shotwell and C. W. Hesseltine. 1975B. Aflatoxin occurrence in 1973 field corn. I. A limited survey in the southeastern U.S. *Cereal Chem.* 52:603.
- Lillehoj, E. B., W. F. Kwolek, E. E. Vandergraft, M. S. Zuber, O. H. Calvert, N. Widstrom, M. C. Futrell and A. J. Bockholt. 1975C. Aflatoxin production in *Aspergillus flavus* inoculated ears of corn grown at diverse locations. *Crop Sci.* 15:267.
- Lillehoj, E. B., W. F. Kwolek, A. Manwiller, J. A. DuRant, J. C. LaPrade, E. S. Horner, J. Reid and M. S. Zuber. 1976A. Aflatoxin production in several corn hybrids grown in South Carolina and Florida. *Crop Sci.* 16:483-485.
- Lillehoj, E. B., W. F. Kwolek, R. E. Peterson, O. L. Shotwell and C. W. Hesseltine. 1976B. Aflatoxin contamination fluorescence and insect damage in corn infected with *Aspergillus flavus* before harvest. *Cereal Chem.* 53:505-512.
- Lillehoj, E. B., D. I. Fennell and W. F. Kwolek. 1977. Aflatoxin and *Aspergillus flavus* occurrence in 1975 corn at harvest from a limited region of Iowa. *Cereal Chem.* 54:366-372.
- Lin, M. T. and J. C. Dianese. 1976. A coconut-agar medium for rapid detection of aflatoxin production by *Aspergillus* spp. *Phytophthology* 66:1466-1469.
- Marsh, P. B., K. Bollinbacher, J. P. San Antonio and G. V. Merola. 1955. Observations on certain fluorescent spots in raw cotton associated with the growth of microorganisms. *Texas Res. J.* 24:1007.
- Marsh, P. B., M. E. Simpson, R. J. Ferretti, T. C. Campbell and J. Donoso. 1969. Relation of aflatoxins in cotton seeds at harvest to fluorescences in the fiber. *J. Agric. Food Chem.* 17:462.
- Masri, M. S., H. L. E. Vix and Goldblatt. 1969. Process for toxifying substances contaminated with aflatoxin. U.S. Patent No. 3,429,709.

- Matz, S. A. 1969. Cereal Science. The AVI Publishing Co., Westport, Connecticut.
- McBain, J. W. 1935. An explanation of hysteresis in the hydration and dehydration of gels. J. Amer. Chem. Soc. 57:699.
- McCallan, S. E. A. and C. Setterstrom. 1940. Toxicity of ammonia, chlorine, hydrogen cyanide, hydrogen sulfide and sulfur dioxide gases. I. General methods of correlations. Contrib. Boyce Thompson Inst. 11:325.
- Miller, B. S. 1979. The U.S. Grain Marketing Research Laboratory. Personal communication.
- Neal, D. C., R. E. Wester and K. C. Gunn. 1933. Growth of the cotton root-rot fungus in synthetic media, and the toxic effect of ammonia on the fungus. J. Agric. Res. 47:107.
- Ngoddy, P. O. 1969. A Generalized Theory of Sorption Phenomena in Biological Material. Ph.D. dissertation. Michigan State Univ. E. Lansing, Michigan.
- Nofsinger, G. W., R. J. Bothast, E. B. Lancaster and E. B. Bagley. 1976. Ammonia-supplemented ambient temperature drying of high moisture corn. Trans. ASAE 20:1151-1154, 1159.
- Nofsinger, G. W., R. J. Bothast and R. A. Anderson. 1978. Extending the allowable drying time for ambient conditioned high-moisture corn. Paper presented at the ASAE annual summer meeting at Logan, Utah.
- Nogotov, E. F. 1978. Applications of Numerical Heat Transfer. McGraw-Hill Publishing Co., New York, N.Y.
- O'Dell, W. T. 1975. Information on aflatoxins. South Carolina Ext. Ser. Clemson Univ. Information Note 1.
- Özisik, M. N. 1968. Boundary Value Problems of Heat Conduction. International Textbook Co., Scranton, Pennsylvania.
- Park, S. W. 1974. A theoretical investigation of sorption kinetic models and its application to the sorption kinetics of water vapor and carbon tetrachloride. A Ph. D. dissertation, Kansas State Univ., University Microfilm International, Ann Arbor, Mich.
- Park, S. W. and B. G. Kyle. 1975. Sorption kinetics and equilibria of carbon tetrachloride on wheat. Cereal Chem. 52:611.
- Peplinski, A. J., O. L. Brekke, R. J. Bothast and L. T. Black. 1978. High moisture corn - an extended preservation trial with ammonia. Trans. ASAE 21:773-776, 781.

- Perry, R. H. and C. H. Chilton. 1973. *Chemical Engineers' Handbook*. 5th ed. McGraw-Hill Publishing Co., New York, N.Y.
- Pfost, H. B., S. G. Maurer, D. S. Chung and G. A. Milliken. 1976. Summarizing and reporting equilibrium moisture data for grains. ASAE Paper No. 76-3520.
- Pierce, R. O. and T. L. Thompson. 1978. Management of solar and low-temperature grain drying systems - Part I: Minimum airflow rates: supplemental heat and fan operation strategies with full bin. ASAE Paper No. 78-3515.
- Pierce, R. O. and T. L. Thompson. 1978. Management of solar and low-temperature grain drying systems - Part II: Layer drying and solution to the overdrying problem. ASAE Paper No. 78-3514.
- Pons, W. A. Jr., A. F. Cucullu, A. O. Franz, Jr., L. S. Lee and L.A. Goldblatt. 1973. Rapid detection of aflatoxin contamination in agricultural commodities. *J. Assoc. Offic. Anal. Chem.* 56:803.
- Pons, W. A. Jr. 1976. Resolution of aflatoxins B₁, B₂, G₁ and G₂ by high-pressure liquid chromatography. *J. Assoc. Offic. Anal. Chem.* 59:101-105.
- Przybylski, W. 1975. Formation of aflatoxin derivatives on thin layer chromatographic plates. *J. Assoc. Offic. Anal. Chem.* 58:163-164.
- Rambo, G., J. Tuite and G. L. Zachariah. 1975. Fluorescence associated with corn infected with *Aspergillus flavus* and *A. parasiticus* in storage. *Cereal Chem.* 52:757-764.
- Rambo, G. W., J. Tuite and R. W. Caldwell. 1974. *Aspergillus flavus* and aflatoxin in preharvest corn from Indiana in 1971 and 1972. *Cereal Chem.* 51:848.
- Ranz, W. E. and W. R. Marshall, Jr. 1952. Evaporation from drops. Part II. *Chem. Eng. Prog.* 48:141-146, 173-180.
- Rao, K. S. 1941. Hysteresis in sorption. Parts I, II, III, IV, V and VI. *J. Phys. Chem.* 45:501.
- Reynolds, T. M. 1963. Chemistry of nonenzymatic browning. I. The reaction between aldose and amine. *Adv. Food Res.* 12:1-52.
- Roberts, D. E. and D. B. Brooker. 1975. Grain drying with a recirculator. *Trans. ASAE* 18:181-184.
- Robinson, R. A. and R. H. Stokes. 1959. *Electrolyte Solutions*. 2nd ed., Academic Press, New York, N.Y.

- Rodriguez-Arias, J. H. 1956. Desorption isotherms and drying rates of shelled corn in the temperature range of 40 to 140°F. Ph.D. dissertation, Michigan State University. Department of Agricultural Engineering, E. Lansing, Michigan.
- Romer, T. R. 1975. Screening method for the detection of aflatoxins in mixed feeds and other agricultural commodities with subsequent confirmation and quantitative measurement of aflatoxins in positive samples. *J. Assoc. Offic. Anal. Chem.* 58:500-506.
- Romer, T. R. and A. D. Campbell. 1976. Collaborative study of a screening method for the detection of aflatoxins in mixed feeds, other agricultural products, and foods. *J. Assoc. Offic. Anal. Chem.* 59:110-117.
- Ross, I. J., O. J. Loewer and G. M. White. 1978. Potential for aflatoxin development in low temperature drying systems. ASAE Paper No. 78-3516.
- Rugumayo, E. W. and F. W. Bakker-Arkema. 1978. Solar grain drying : low temperature corn drying and absorption equations. ASAE Paper No. 78-3511.
- Sabbah, M. A. 1968. Prediction of batch drying performance with natural air. Unpublished M. S. thesis, Agric. Eng. Dept., Purdue Univ.
- Sargent, K., R. B. A. Carnaghan. 1963. Groundnut toxicity in poultry : experimental and chemical aspects. *Brit. Vet. J.* 119:178-184.
- Satterfield, C. N. 1970. *Mass Transfer in Heterogeneous Catalysis.* M.I.T. Press, Cambridge, Mass.
- Sauer, D. B. 1973. Grain preservatives for high-moisture feed grains. A report from the U.S. Grain Marketing Research Center, Agric. Res. Serv., USDA, Manhattan, Kansas.
- Sauer, D. B. and R. Burroughs. 1974. Efficacy of various chemicals as grain mold inhibitors. *Trans. ASAE* 17:557-559.
- Sauer, D. B., T. O. Hodges, R. Burroughs and H. H. Converse. 1975. Comparison of propionic acid and methylene bis-propionate as grain preservatives. *Trans. ASAE* 18:1162-1164.
- Saul, R. A. and J. L. Steele. 1966. Why damaged shelled corn costs more to dry. *Agric. Eng.* 47:326-329, 337.
- Saul, R. A. 1970. Deterioration rate of moist shelled corn at low temperatures. ASAE Paper No. 70-302.

- Schroeter, L. C. 1966. Sulfur dioxide application in foods, beverages, and pharmaceuticals. Pergamon Press, Oxford, England.
- Schumann, T. E.W. 1929. Heat transfer : A liquid flowing through a porous prism. J. of Franklin Institute 208:405-416.
- Seitz, L. M. and H. E. Mohr. 1976. A new method for quantitation of aflatoxin in corn. Cereal Chem. 54:179-183.
- Shannon, G. M., R. D. Stubblefield and O. L. Shotwell. 1973. Modified rapid screening method for corn. J. Assoc. Offic. Anal. Chem. 56:1024.
- Shannon, G. M. and O. L. Shotwell. 1975. A quantitative method for determination of aflatoxin B₁ in roasted corn. J. Assoc. Offic. Anal. Chem. 58:743-745.
- Shotwell, O. L., C. W. Hesseltine, H. R. Burmeister, W. F. Kwolek, G. M. Shannon and H. H. Hall. 1969. Survey of cereal grains and soybeans for the presence of aflatoxin. II. corn and soybeans. Cereal Chem. 46:454-463.
- Shotwell, O. L., C. W. Hesseltine, M. L. Goulden and E. E. Vandegraft. 1970. Survey of corn for aflatoxin, zearalenone and ochratoxin. Cereal Chem. 47:700-707.
- Shotwell, O. L., C. W. Hesseltine, E. E. Vandegraft and M. L. Goulden. 1971. Survey of corn from different regions for aflatoxin, ochratoxin and zearalenone. Cereal Sci. Today 16:266-273.
- Shotwell, O. L., M. L. Goulden and C. W. Hesseltine. 1972. Aflatoxin contamination : Association with foreign material and characteristic fluorescences in damaged corn kernels. Cereal Chem. 49:458.
- Shotwell, O. L., C. W. Hesseltine and M. L. Goulden. 1973. Incidence of aflatoxin in southern corn, 1969-1970. Cereal Sci. Today 18: 192-195.
- Shotwell, O. L. and R. D. Stubblefield. 1973. Collaborative study of three screening methods for aflatoxin in corn. J. Assoc. Offic. Anal. Chem. 56:808-812.
- Shotwell, O. L., W. F. Kwolek, M. L. Goulden and L. K. Jackson. 1975A. Aflatoxin occurrence in some white corn under loan. 1971. I. Incidence and level. Cereal Chem. 52:373-380.
- Shotwell, O. L., G. M. Shannon and C. W. Hesseltine. 1975B. Aflatoxin occurrence in some white corn under loan. 1971. II. Effectiveness of rapid tests in segregating contaminated corn. Cereal Chem. 52:381-387.

- Shotwell, O. L., M. L. Goulden, A. M. Jepson, W. F. Kwolek and C. W. Hesseltine. 1975C. Aflatoxin occurrence in some white corn under loan. 1971. III. Association with bright greenish-yellow fluorescence in corn. *Cereal Chem.* 52:670-677.
- Shotwell, O. L., M. L. Goulden, R. J. Bothast and C. W. Hesseltine. 1975D. Mycotoxin in hot spots in grains. I. Aflatoxin and zearalenone occurrence in stored corn. *Cereal Chem.* 52:687-697.
- Shotwell, O. L., G. M. Shannon and M. L. Goulden. 1976. Confirmation of results of rapid screening test for aflatoxins performed at corn elevator. *J. Assoc. Offic. Anal. Chem.* 59:1419-1421.
- Shotwell, O. L. 1977. Aflatoxin in corn. *J. Amer. Oil Chemists' Society* 54:216A-224A.
- Shove, G. C. and F. W. Andrew. 1968. Cooling, chilling and dehydration of stored shelled corn. *ASAE Paper No.* 68-334.
- Shove, G. C. 1973. New techniques in grain conditioning. In : *Grain Storage: Part of a System*, ed. by R. N. Sinha and W. E. Muir. The AVI Publishing Co., Westport, Conn.
- Shove, G. C. 1974. Low temperature drying of shelled corn. Paper presented at the Grain Conditioning Conference, Univ. of Illinois.
- Shove, G. C. 1976. Efficient energy management with low temperature grain drying. *Farm Electrification Council, Columbia, Missouri.*
- Sinha, R. N. and W. E. Muir. 1973. *Grain Storage : Part of a System.* The AVI Publishing Co., Westport, Conn.
- Smith, H. E. 1977. Aflatoxin in corn and other commodities. ESC-587 Ext. Ser. USDA, Washington, D.C.
- Smith, J. M. 1970. *Chemical Engineering Kinetics.* 2nd ed. McGraw-Hill Publishing Co., New York, N.Y.
- Speck, M. L. ed. 1976. *Compendium of methods for microbiological examination of foods.* Amer. Public Health Assoc., Washington, D.C.
- Stack, M. E. and A. E. Pohland. 1975. Collaborative study of a method for chemical confirmation of the identity of aflatoxin. *J Assoc. Offic. Anal. Chem.* 58:110-113.
- Steele, J. L. and R. A. Saul. 1962. Laboratory measurements of the rate of deterioration of grain during drying. Paper presented at Mid-central Regional ASAE meeting at Lincoln, Nebraska.
- Steele, J. L. 1967. Deterioration of damaged shelled corn as measured by carbon dioxide production. Unpublished Ph.D. dissertation, Iowa State Univ.

- Steele, J. L., R. A. Saul and W. V. Hukill. 1969. Deterioration of shelled corn as measured by carbon dioxide production. *Trans. ASAE* 12:685-689.
- Sterling, C. 1964. Starch-primulin fluorescence. *Protoplasma* 59:180.
- Stoloff, L. 1972. Molds and Mycotoxins. What FDA is doing about the mycotoxin problem. In : Master manual on molds and mycotoxins. *Farm Technology Agri-Fieldman* 28:60a.
- Stoloff, L. 1976. Occurrence of mycotoxins in foods and feeds. In: *Mycotoxins and Other Fungal Related Food Problems. Adv. in Chem. Ser. Vol. 149. Amer. Chem. Soc., Washington, D.C.*
- Stoloff, L., S. Henry and O. J. Francis, Jr. 1976. Survey for aflatoxins and zearalenone in 1973 crop corn stored on farms and in country elevators. *J. Assoc. Offic. Anal. Chem.* 59:118-121.
- Taubenhaus, J. J. 1920. A study of the black and the yellow molds of ear corn. *Texas Agric. Sta. Bull.* 270:3-10.
- Thomas, H. C. 1944. Heterogeneous ion exchange in a flow system. *J. Amer. Chem. Soc.* 66:1664.
- Thomas, F., R. M. Eppley and M. W. Trucksess. 1975. Rapid screening method for aflatoxins and zearalenone in corn. *J. Assoc. Offic. Anal. Chem.* 58:114-116.
- Thompson, T. L., R. M. Peart and G. H. Foster. 1968. Mathematical simulation of corn drying - a new model. *Trans. ASAE* 11:582-586.
- Thompson, T. L. 1972. Temporary storage of high-moisture shelled corn using continuous aeration. *Trans. ASAE* 15:333-337.
- Treybal, R. E. 1968. *Mass-Transfer Operations.* McGraw-Hill Publishing Co., New York.
- Tuite, J. 1961. Fungi isolated from unstored corn seed in Indiana in 1956-1958. *Plant Dis. Rep.* 45:212-215.
- Tuite, J., G. H. Foster and R. A. Thompson. 1970. Moisture limits for storage of corn aerated with natural and refrigerated air. *ASAE Paper No.* 70-306.
- Tuite, J. and R. W. Caldwell. 1971. Infection of corn seed with *Helminthosporium maydis* and other fungi in 1970. *Plant Dis. Rep.* 55:387-389.
- USDA, ARS, NRRC. 1977. Aflatoxin : detection and determination in corn. CA-NRRC-37(Rev. 3) Oct. 1977, Peoria, Illinois.

- USDA, Economic Research Service. 1974. Feed situation 253. U. S. Dept. of Agric.
- Vandegrift, E. E., C. W. Hesseltine and O. L. Shotwell. 1975. Grain preservatives : Effect on aflatoxin and ochratoxin production. *Cereal Chem.* 52:79-84.
- Velasco, J. 1972. Detection of aflatoxin using small columns of florisil. *J. Amer. Oil Chem. Soc.* 49:141-142.
- Vermeulen, T. 1953. Theory of irreversible and constant-pattern solid diffusion. *Ind. Eng. Chem.* 45:1664.
- Vermeulen, T. and N. K. Hiester. 1954. Ion-exchange and adsorption column kinetics with uniform partial presaturation. *J. Chem. Phys.* 22:96.
- Vermeulen, T. G. Klein and N. K. Hiester. 1973. Adsorption and ion exchange. In : *The Chemical Engineers' Handbook*. ed. by Perry and Chilton. McGraw-Hill Publishing Co., New York, N.Y.
- Vesonder, R. F., A. C. Beckwith, A. Ciegler and R. J. Dimler. 1975. Ammonium hydroxide treatment of aflatoxin B₁. Some chemical characteristics and biological effects. *J. Agric. Food Chem.* 23:242.
- Warren, K. S. 1962. Ammonia toxicity and pH. *Nature* 195:47.
- Watson, S. A. and K. R. Yahl. 1971. Survey of aflatoxin in commercial supplies of corn and grain sorghum used for wet-milling. *Cereal Sci. Today* 16:153.
- Weyde, E. and E. Wicke. 1940. Die Gestalt der Sorptionsflächen bei der Ad- und Desorption unter verschiedenen Bedingungen. *Kolloid Z.* 90:156.
- Wheeler, A. 1951. Reaction rates and selectivity in catalytic pores. In : *Adv. in Catalysis*, Vol. III, p. 249. Academic Press, New York.
- Wheeler, C. A., Jr. 1976. The energy crisis : Where farm field and oil field meet. *Corn Annual* prepared by Corn Refiners Assoc., Inc., Washington D. C.
- Wilke, C. R. and O. A. Hougen. 1945. Mass transfer in the flow of gases through granular solids extended to low modified Reynolds numbers. *Trans. Amer. Inst. Chem. Eng.* 41:445.
- Williams, E. E., M. Fortes, D. G. Colliver and M. R. Okos. 1978. Simulation of stirred bin low temperature corn drying. *ASAE Paper No. 78-3012*.

- Wogan, G. N. 1973. *Methods in Cancer Research*, ed. by H. Busch. Academic Press, New York. Chapter VII. pp 309-344.
- Yaciuk, G. W. E. Muir and R. N. Sinha. 1975. A simulation model of temperatures in stored grain. *J. Agric. Eng. Res.* 20:245-258.
- Yoshida, F., D. Romaswami and O. A. Hougen. 1962. Temperatures and partial pressures at the surfaces of catalyst particles. *AIChE J.* 8:5-11.
- Young, L. A., R. G. Brown and B. A. Sharp. 1970. Propionic acid preservation of corn for pigs. *Can. J. Anim. Sci.* 50:711.
- Zink, H., R. C. Brook and R. M. Peart. 1978. Engineering analysis of energy source for low temperature drying. *ASAE Paper No.* 78-3517.

MICHIGAN STATE UNIV. LIBRARIES



31293100642770